Fabrication of Molecular Imprinted Polymer based Sensors for the Detection of Mono and Disaccharides

PhD Thesis

By

NAZIA ASGHAR

Sulaiman Bin Abdullah Aba Al-Khail - Center for Interdisciplinary Research in Basic Sciences (SA-CIRBS),

Faculty of Basic and Applied Sciences,

International Islamic University, Islamabad

2020

I Chemistry, Organic
II Diabetes mellitus
III Disaccharides

Fabrication of Molecular Imprinted Polymer based Sensors for the Detection of Mono and Disaccharides

PhD Thesis

By

NAZIA ASGHAR

23-FBAS/PHDNS/F-15

Supervisor

Dr. Ghulam Mustafa

Sulaiman Bin Abdullah Aba Al-Khail - Center for Interdisciplinary Research in Basic Sciences,

(SA-CIRBS),

Faculty of Basic and Applied Sciences

International Islamic University, Islamabad

2020

Fabrication of Molecular Imprinted Polymer based Sensors for the Detection of Mono and Disaccharides

Researcher:

Nazia Asghar

Reg. No. 23-FBAS/PHDNS/F-15

Supervisor:

Dr. Ghulam Mustafa

Assistant Professor

Sulaiman Bin Abdullah Aba Al-Khail - Center for Interdisciplinary Research in Basic Sciences

(SA-CIRBS),

Faculty of Basic and Applied Sciences,

International Islamic University, Islamabad

2020


بسم الله الرحمن الرحيم

Sulaiman Bin Abdullah Aba Al-Khail-Center for Interdisciplinary Research in Basic Sciences (SA-CIRBS),

International Islamic University Islamabad

Dated: 17-08-2020

FINAL APPROVAL

It is to certify that we have read the thesis submitted by Ms. Nazia Asghar and it is our judgement that this thesis is of sufficient standard to warrant its acceptance by the International Islamic University, Islamabad for the PhD degree in Chemistry.

COMMITTEE

1. **External Examiner**
Prof. Dr. Amin Badshah
Professor,
QAU, Islamabad.

2. **External Examiner**
Dr. Imran Shahid
Associate Professor,
IST, Islamabad.

3. **Internal Examiner**
Dr. Ikram Ullah
Assistant Professor,
SA-CIRBS, FBAS, IIUI.

4. **Supervisor**
Dr. Ghulam Mustafa
Assistant Professor,
SA-CIRBS, FBAS, I IUI.

5. **Chairman SA-CIRBS.**
Prof. Dr. Muhammad Riaz
Chairman/Head, SA-CIRBS,
FBAS, IIUI.

Dean, FBAS
Name
International Islamic University, Islamabad.

A thesis is submitted to Sulaiman bin Abdullah Aba Al-Khail - Center for Interdisciplinary Research in Basic Sciences (SA-CIRBS), International Islamic University, Islamabad as a partial fulfillment of requirement for the award of the degree of PhD Chemistry.

DECLARATION

I hereby declare that this thesis, neither as a whole nor as a part thereof has been copied out from any source. It is further declared that I have prepared this thesis is entirely on the basis of my personal efforts made under the sincere guidance of my supervisor.

Dated: 27-08-2020

Nazia

Nazia Asghar

23-FBAS/PHDNS/F-15

FORWARDING SHEET BY RESEARCH SUPERVISOR

The thesis entitled "Fabrication of Molecular Imprinted Polymer Based Sensors for the Detection of Mono and Disaccharides" submitted by **Nazia Asghar, registration no. 23/FBAS/PHDNS/F-15** in partial fulfillment of PhD degree in Chemistry at Sulaiman Bin Abdullah Aba Al-Khail - Center for Interdisciplinary Research in Basic Sciences (SA-CIRBS), has been completed under my guidance and supervision. I am satisfied with the quality of student's research work and allow her to submit this thesis for further process to graduate with Doctor of Philosophy degree from Sulaiman Bin Abdullah Aba Al-Khail-Center for Interdisciplinary Research in Basic Sciences (SA-CIRBS), as per IIUI rules and regulations.

Dr. Ghulam Mustafa
Assistant Professor,
Sulaiman Bin Abdullah Aba Al-Khail - Center for Interdisciplinary Research in Basic Sciences (SA-CIRBS),
International Islamic University,
Islamabad.

Dated: 27-08-2020

DEDICATION

Dedicated to My Beloved

"Parents"

CONTENTS

ACKNOWLEDGEMENTS

All the virtues and praise for ***ALLAH*** Almighty, the most Gracious, the most Merciful, who created us as a Muslim in the Sacred Ummah of the ***Holy Prophet Mohammad*** ﷺ. Lots of Salaam and gratitude to the ***Holy Prophet Mohammad*** ﷺ whose teachings are the guiding star in the time of dark and despair. I am grateful to ALLAH, the ALMIGHTY for giving me this magnificent life and utmost courage to follow the path of knowledge, discovery and to achieve the milestone of my Doctoral Thesis.

I am the most thankful to my research supervisor, Dr. Ghulam Mustafa, who has been my inspiration and the role model for my PhD research. I am incredibly fortune to have him as my supervisor. Without his inspiration, guidelines and continuous support, this thesis would not have been possible.

It was not easy to start this big endeavour at the beginning. I am obliged to all my teachers and friends who gave me stimulation for going ahead with my Doctorate and for moral and technical support during the course of my studies. I am also incredibly fortune to have Professor Dr. Abdul Hameed as Incharge, SA-CIRBS. I owe my thanks to him for his guidance and encouragement. I am also thankful to all faculty members of SA-CIRBS, Professor Dr. Muhammad Riaz, Dr. Ikram Ullah and Dr. Syada Aaliya Shahzadi for his help, prayers. I am cordially thankful to Dr. Mehwish Taneez whose continuous moral support always put me ahead.

I would like to thank my friends i.e. Sidra Saeed, Asia Naureen, Aqsa Aslam, Maimoona Yasinzai, Safia, Ayesha Naveed, Madiha Saeed, Aqsa Javed, Khunsa Saeed and My juniors at SA-CIRBS, that I had the privilege to work with the fruitful discussions and for creating such a nice working environment and all those who supported me in writing and incanted me to strive towards my goal.

Special thanks to my dearest brother Dr. Guftaar Ahmed Sardar Sidhu whose care and affection always strengthen me and your guidance always put me on the right way. My PhD is never gonna to be done without your continuous courage and endless support. I am heartily thankful to you. I also be grateful to my dearest sisters Sajida Guftaar and Shazia Mohsin for their love, help and support. I also want to thank my sweet and lovely brothers Muhammad Nafees Asghar, Muhammad Nadeem Asghar and Mohsin Rasheed. At the end, I would say special thanks to very specials my dearest Ammi Jan

and Abou Je for their sacrifices just to improve my life, all their prayers were what sustained me this far.

Nazia Asghar August 27th, 2020

LIST OF ABBREVIATIONS

Ag	Silver
AIBN	N-N, Azo-Bisisobutyronitrile
Au NP/RGO	Gold Nanoparticles/Reduced Graphene Oxide
Au	Aurum (Gold)
CE	Carbon Electrode
Cerium Dioxide	CeO_2
Cm	Centimeter
CuO	Copper Oxide
EGDMA	Ethylene Glycol Dimethacrylate
FTIR–ATR Reflectance	Fourier Transform Infrared- Attenuated Total
FTIR	Fourier Transform Infrared Spectroscopy
GCE	Glassy Carbon Electrode
GE	Glassy Electrode
GO	Graphene Oxide
GO-MIP	Graphene Oxide Molecular Imprinted Polymer
GO-MIP-MAA	Graphene Oxide-Molecularly Imprinted Polymer-Methacrylic Acid
GO-MIP-NVP	Graphene Oxide-Molecularly Imprinted Polymer-N-Vinyl Pyrolidone
GO-MIP-PS	Graphene Oxide-Molecularly Imprinted Polymer-Polystyrene
GO-MIP-PU	Graphene Oxide-Molecularly Imprinted Polymer-Polyurethane
Gr-AuNP	Graphene-Gold Nanoparticles
Gr-AuNP-C-Dots	Graphene-Gold Nanoparticles-Carbon-Dots
IDEs	Inter Digital Electrodes
Ir	Iridium
Khz	Kilohertz
LCR	Inductance, Capacitance and Resistance

LoD	Limit of Detection
MAA	Methyl Acrylic Acid
MIPs	Molecularly Imprinted Polymers
MnO_2	Manganese Oxide
MnO_2-MWCNTs	Mangnese Oxide-Multiwalled Carbon
Nf	Nano Faraday
Ni NPs@MWCNTs	Nickel Nanoparticles Coreshell Multiwalled Carbon Nanotubes
NIPs	Non-Imprinted Polymers
nm	Nano Meter
NVP	N-Vinylpyrolidone
Pd	Palladium
Pt	Platinum
PPm	Parts Per Million
PPb	Parts Per Billion
QCM	Quartz Crystal Microbalance
Rd	Rhodium
Rh	Rhudenium
Ru	Ruthenium
SEM	Scanning Electron Microscope
Sty	Styrene
TGA/DTA	Thermogravimetric Analysis/Differential Thermal Analysis
TiO_2	Titanium Dioxide
UV	Ultraviolet
ZnO	Zinc Oxide
µl	Micro Liter

LIST OF FIGURES

LIST OF TABLES

ABSTRACT

Diabetes mellitus is a life threatening issue and imparts its major role in death. A close monitoring of mono and disaccharides show pivotal role for the diagnosis, prevention and other sugar related diseases. It is of substantial interest to develop cost effective, easy to use, simple, highly sensitive, specific devices for the real-time and online monitoring of sugars. Sensors are the promising candidates for identification and quantification of saccharides. Electrochemical sensors are assumed as excellent analytical devices for easy, quick and inexpensive saccharide detection. Among these different types of sensors, non-enzymatic electrochemical sensors are of substantial importance because of their simple instrumentation, easy operation based on which high selectivity and good sensitivity can be achieved for sugars detection.

In second chapter, molecularly imprinted polymer based sensors were designed for the glucose detection. Different polymer systems were used to achieve optimised sensitivity and selectivity response. (1) Vinyl pyrolidone system was used and LoD was ~136 ppb and its highest detection limit was ~500 ppm. (2) Polyacrylate based receptors were synthesized and LoD was ~115 ppb with maximum limit of detection was ~500 ppm. (3) Polyurethane based receptors were developed for glucose detection and measured LoD was ~71 ppb and its range of detection was ~71 ppb to 500 ppm. (4) Polystyrene based receptors were used and measured LoD was ~15 ppb and ~590 ppm was its upper detection limit. The polystyrene based MIPs were merged with GO to synthesize GO-MIPs nanocomposite to enhance the sensitivity and selectivity of fabricated sensors. The measured lower limit of detection of GO-MIP composite based sensor was ~ 6 ppb and detection range was ~ 6 ppb to 600 ppm.

In third chapter of this thesis, initally MIPs based sensors were developed for the estimation of β-fructose. (1) Polyvinyl pyrolidone receptors were prepared and their lower limit of detection was ~300 ppb having upper limit of ~500 ppm. (2) Polyurethane based receptors were developed with LoD of ~107 ppb with highest detection limit of ~520 ppm. (3) Styrene based receptors were synthesized and measured LoD was ~96 ppb and its detection range was ~96 ppb to 500 ppm. (4) Acrylate based receptors were synthesized and its LoD was ~ 60 ppb having maximum detection limit of ~525 ppm. Furthermore, fructose imprinted polyacrylate in

combination with GO were used as receptors to achieved enhanced sensitivity and selectivity and fabricated sensor bears LoD of ~46 ppb towards fructose and highest detection range from ~46 ppb to 600 ppm .

In fourth chapter, MIPs based receptors were synthesized for the detection of diaccharide i.e. β-maltose. (1) Styrene based receptors were developed and its sensitivity range was 150 ppb to 507 ppm with lower limit of detection of ~150 ppb. (2) Polyurethane based β-maltose imprinted receptors were prepared and measured LoD was ~115 ppb with its detection range of ~115 ppb to 525 ppm. (3) Polyvinyl pyrolidone based receptors were synthesized and LoD of ~68 ppb was measured by signal to noise ratio (S/N = 3) with range of detection of 68 ppb to 529 ppm. (4) Polyacrylate based maltose imprinted receptors were synthesized and LoD of ~39 ppb was found with sensitivity range of 39 ppb to 530 ppm. To enhance the sensor response, nanocomposite was prepared by using functionalized graphene and its LoD was enhanced upto ~16 ppb with estimation range ~ 16 ppb to 600 ppm. At the end of this chapter, we can conclude that 40:60 ratio between monomer to cross-linker, polyacrylate based imprinted receptors were fond the most appropriate for maltose detection.

In fifth chapter of my thesis, molecularly imprinted polymer based receptors were synthesized for the estimation of α-sucrose. (1) Polystyrene based imprinted receptors were prepared firstly, limit of detection of ~83 ppb was calculated with its detection range of 83 ppb to 520 ppm. (2) Polyvinyl pyrolidone based sensor was developed and an LoD of ~68 ppb with its detection range of ~68 ppb to 525 ppm towards sucrose. (3) ~39 ppb of LoD was found towards sucrose with its wide detection range of 39 ppb to 520 ppm by polyacrylate based sucrose imprinted receptors. At the end of this chapter, (4) polyurethane receptors were synthesized for sucrose detection and its lowest limit of detection ~31 ppb with its detection range ~31 ppb to 528 ppm for sucrose. Functionalized graphene and MIPs based nanocomposite was prepared to improve the lowest limit of detection. The LoD of ~16 ppb and maximum LoD of ~600 ppm was presented by GO–MIP–PU showed that nano-composite based sensors enhance the sensor characteristics due to the excellent properties of graphene oxide. From this chapter, we can conclude that 45:55 ratio of monomer to cross-linker, polyurethane

based imprinted sensors were found highly sensitive, selective and reproducible for sucrose detection.

1 Chapter 1 INTRODUCTION

1.1 Introduction

Carbohydrates, the building blocks and nutritive elements are termed as monosaccharide and their polymers such as oligosaccharides and polysaccharides, the most abundant organic stuff present on earth (Röckendorf and Lindhorst 2004, Bennett and Forster 2009, Berg et al. 2015, Wang and Lee 2015). Carbohydrates are digested by humans to simpler forms of sugars such as glucose, a monosaccharide which is the primary carbohydrate energy source used by the body (Fareed et al. 2017).

Monosaccharides, the most important and basic unit of carbohydrates and serve as energy fuel and for life, it is considered as basic component e.g. 5-carbon, saccharides play an important role of information carrier, in DNA is deoxyribose and in RNA as ribose sugars, furthermore, the six carbon sugar mostly termed as D-glucose either blood sugar or grapes sugar, D-fructose is known as fruit sugar; and D-galactose, which is present in milk in combination with glucose (Zhu et al. 2017, Qian et al. 2018). Monosaccharides, the mostly are naturally present having same configuration at five-carbon termed as D-glyceraldehyde. The linear and cyclic forms of glucose are present in equilibrium in aqueous solutions (figure.1.1).

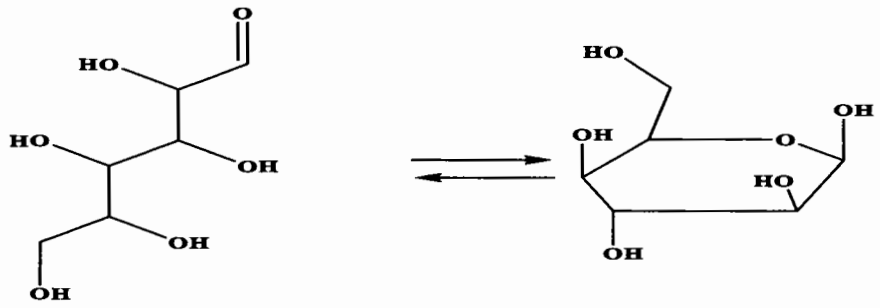

Figure 1.1: Linear and cyclic forms of Glucose

D-glucose is of substantial importance in metabolic homeostasis in humans, it serves as energy source for human beings and helps in the proper functioning of when used or in the formation of vital carbohydrates through biosynthesis. Glucose may change and help to produce energy when it is consumed by human body (Wang et al. 2018). Disaccharides are the simplest and biologically essential oligosaccharides. Maltose, sucrose and lactose are the naturally occurring abundant sugars. Maltose, which is present in the form of malt, Lactose, a sugar naturally found in mammalian milk, is a combination of glucose and galactose. Sucrose, also named as table sugar, mixture of

fructose and glucose (figure 1.2). Oligosaccharides and their derivatives are of highly significant in pharmaceutical industry (Liu et al. 2018). For example, streptomycin is the oligosaccharide, have chemotherapeutic effect extracted in 1943, also used for the cure of tuberculosis. an antidiabetic "Acarbose" used for the treatment of type II diabetes mellitus. Cyclodextrin as cyclic oligosaccharide is produced by starch hydrolysis (Poonthiyil et al. 2018).

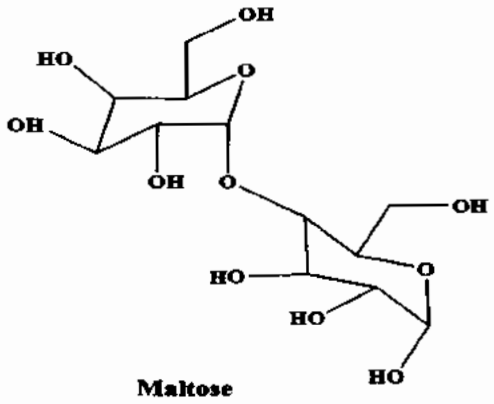

Maltose

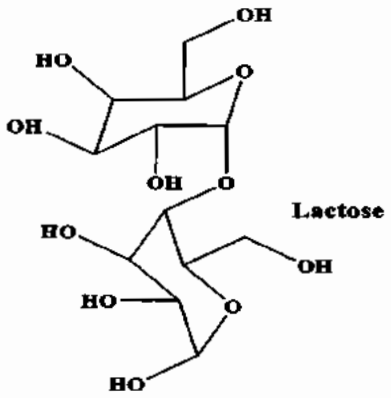

Lactose

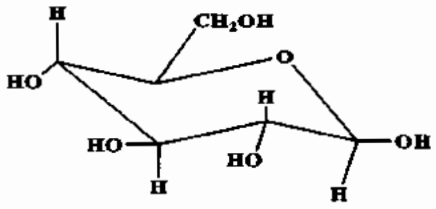

Glucose

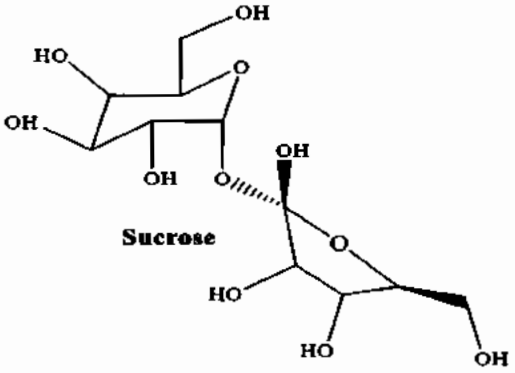

Sucrose

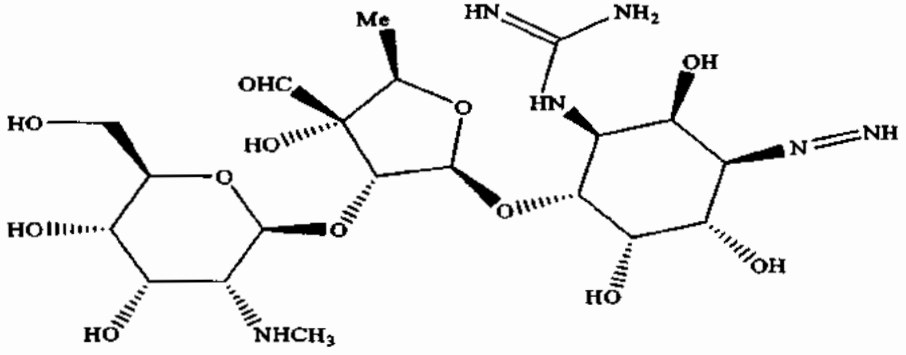

Streptomycin

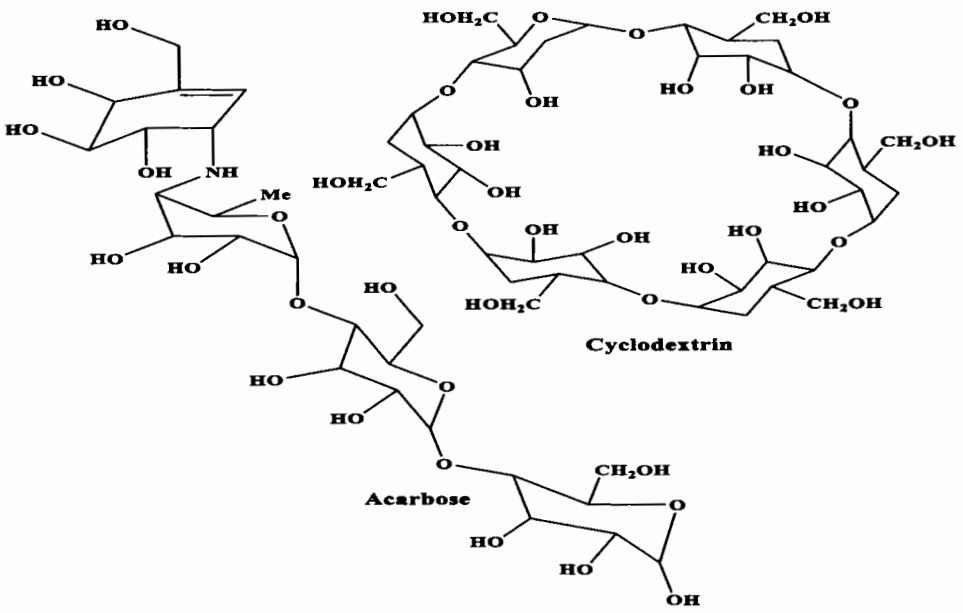

Figure 1.2: Common oligosaccharides and their analogues

Hyperglycemia or hypoglycemia depends on the amount of glucose present in blood (Ciuk et al. 2018). When glucose level is lower than normal in blood is hypoglycemia (Al-Zubaidi et al. 2018, Chattopadhyay, George et al. 2018). Normal person has glucose in their blood in the range of 80-100 mg/dL. Low blood sugar levels have the following symptoms such as confusion, nervousness, feebleness, starvation, dizziness, difficulty speaking and shakiness. Higher blood glucose level than normal is termed as hyperglycaemia. Hyperglycaemia causes frequent urination, elevated glucose thirst level (Bangen et al. 2018, Tatulashvili et al. 2018).

1.2 Saccharides detection

Due to the mentioned reasons, carbohydrates detection is very essential for human beings. For the determination of glucose concentration, various detection methods such as HPLC (Choi et al. 2016), polarimetry (Cote et al. 2018, Liu et al. 2018), Raman spectroscopy (Fraden et al. 2016, Chen et al. 2018), laser photoacoustic spectroscopy (Tanaka et al. 2018), near infrared spectroscopy (Ren et al. 2018, Tajima et al. 2018), optical coherence tomography (Chen et al. 2018, Chen et al. 2018) and electrochemistry (Long and Phong 2018, Sun et al. 2018) have been used. These above mentioned methods, electrochemical methods have been applied for the detection of saccharides because of their excellent selectivity, good sensitivity, reliability, reproducibility and

easy handling, easy maintenance as well as low cost (Kim et al. 2018, Li et al. 2018). Detection of saccharides is an important analytical task. It has been studied from literature that 40 % of blood tests are related to it. Furthermore, glucose determination is important in many other respects such as in biotechnology, in the food and feed processing and in biochemistry etc. The continuous blood glucose monitoring is a basic need due to the fact that about 4–5 % of population suffer from diabetes mellitus (Ho, Rumsfeld et al. 2006, Silveira, Pokhvisneva et al. 2018). Marvelous efforts have been made over the last few decades to detect sugars in real samples, including chromatography (Huang et al. 2018), colorimetry (Jia et al. 2017, Tanaka et al. 2017), spectrophotometric assay (Alijanpour, Akhoondi et al. 2017), electrochemiluminescence (Sojic et al. 2017) and electrochemical detection (Liu et al. 2018, Meng et al. 2018, Shan et al. 2018, Zhu et al. 2018). Amongst these methods, electrochemical biosensors got famous because of simple operation, elevated sensitivity, very low limit of detection, and low cost (Babu et al. 2018, Shan et al. 2018, Xie et al. 2018).

1.3 Chemical sensors

Due to the pivotal role of saccharides in physiological processes, sugar detection is of substantial importance in food products, biological and clinical processes (Chaiyo et al. 2018, Lin et al. 2018, Shan et al. 2018). Diabetes mellitus is one of the largest health problem to worldwide. It is studied that number of diabetes patients may be double to 300million by 2025 (Wu et al. 2018, Zhang et al. 2018). It can be concluded from these studies that there is an ever-growing demand synthesize a sensitive, selective, reliable and low-cost glucose sensors to determine the glucose level on regular basis (Zhang et al. 2018).

Sensors have many advantages over classical instruments because they are very cheap, small in size, simple to operate, and can be fabricated easily. Due to their miniaturization, several different sensors can be fabricated on one device to make a multi sensor array and can be used for remote measurements of different analytes unlike the classical instruments. Due to these characteristics, sensors can be used for online monitoring of some specific analytes and appropriate for all types of applications (Huang et al. 2018, Ling et al. 2018). Chemical and bio-sensors are of substantial

importance and getting famous in the arena of modern analytical chemistry. Increased interest and demands are essentially due to particularly in diagnostics, environmental investigation, food analysis and for monitoring purpose and detection of chemical warfare agents (Haupt and Mosbach 2000, Alexander et al. 2017).

The first decade of the 21st century was celebrated as "Sensor decade". A sensor is a small sized device which transforms a physical change into an analytically useful electrical signals. Sensor actually considered as a part of interface between the world of analytical electrical devices like computers and physical world (Pluhar et al. 2013). In this modern era, sensors have gotten substantial importance in research world because it is significant in electronic devices and enormous capability for information processing have been synthesized within the electronics. Various saccharide measurements have motivated the development of miniaturized devices for the online and real time detection (Lee et al. 2019). A chemical sensor changes chemical information of the concentration of a particular sample part and total composition analysis, into analytically useful electrical signals as shown in figure 1.3. The chemical information generated due to the chemical reaction of an analyte (template) and also from physical property of any system investigated. Chemical sensing is a process of getting information about the concentration of a specified analyte or the composition of target analyte in real time (Lakshmi et al. 2009). So a chemical sensor is used to recognize and measure the specific analyte in the mixture more precisely and an ideal chemical sensor should be selective and sensitive.

A chemical sensor is composed of three major parts,

- Sensitive layer
- Transducer
- Electronics and data storage system

1.3.1 Recognition layer (Receptors)

The recognition layer is a chemically synthesized layer containing either a polymer or an antibody (natural or synthetic) that is used to selectively monitor the chemical constituents within the environment of the sensor. When this recognition layer is exposed to the analyte of interest, it interacts with it. Upon this interaction, change in

the physical properties of the sensitive layer (Bennett and Forster 2009) i.e. mass, optical absorbance, reflectance, polarity, impedance, voltage, fluorescence behavior and these changes are detected by the transducer system.

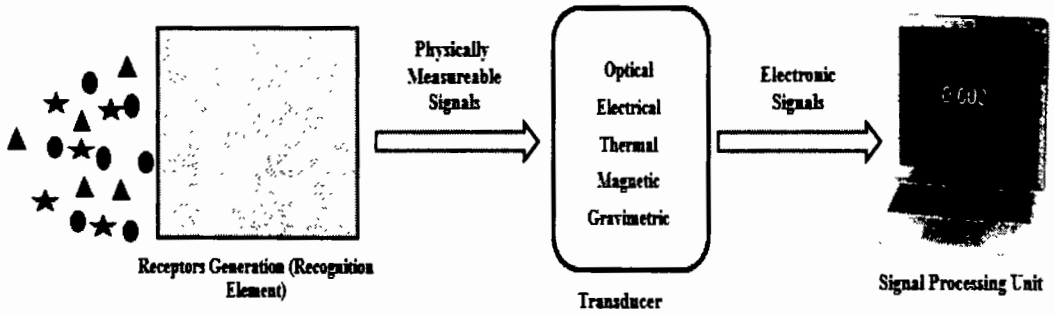

Figure 1.3: General layout of a chemical sensor

Different chemicals and their combinations are frequently used for sensing purpose so sensors can be developed by using any type of chemical. Three major types of recognition layer are as follow:

i. Ion selective layer is based on measuring any change in the concentration of ions such as ion exchange polymers and ion selective IDEs.
ii. Molecular recognition based sensitive layers which follows the host-guest chemistry, spectroscopic methods, molecular size interactions and most commonly molecular imprinting etc.
iii. Bio-recognition layer i.e. biologically sensitive species e.g. enzymes, nucleic acids, antibodies, proteins which interact with biological molecules to generate biosensors.

1.3.2 Transducers (Electrochemical)

A transducer is an electronic device that transforms energy from one type to another (Xing et al. 2017). Different types of transducers are in practice for the fabrication of molecularly imprinted polymer based sensors such as optical, electrochemical, thermal and mass sensitive transducers. In optical sensors, spectroscopic methods are mostly used for analysis. Absorption, fluorescence and scattering are the techniques used in optical transducers. Electrochemical sensors are further divided into three types (Silva et al. 2017).

(a) Potentiometric transducers measure the change in electrical potential.

(b) Voltammetric and Amperometric transducers which apply some potential and measure the current produced.

(c) Conductometric transducers which depend on measuring the change in the conductance with changing in the composition of the analyte.

Figure 1.4: IDE used as transducer for the electrochemical measurements of sensitive layer. The desired structure of IDE (gold) was fabricated via screen printing on the glass substrate. Transducer has 9 fingers with equal gaps and width (300*300).

Thermal transducers are the devices which convert the chemical changes into heat to some detectable electrical quantity such as resistance, capacitance and inductance. Thermistors, pellistors and other thermal detectors are frequently used. Mass sensitive transducers are based on piezoelectric effect i.e. the change in the frequency of oscillating crystal with the change of mass loaded onto it. Most common examples of mass sensitive transducers are surface acoustic wave devices (SAW) and quartz crystal microbalances (QCM). In this work, electrochemical transducers have been used.

1.3.3 Electronics and data storage systems

The electronics and softwares are required to convert the signal produced by the transducer into a readable form, so that the data obtained can be analyzed further. These are specifically designed or selected for that particular application. But in most of the cases, it is an electronic circuit used to amplify the signals produced and suitable software to change it into a presentable form.

1.4 Molecular imprinting technology

Molecular imprinting technique is a process in which monomers and cross-linkers in the presence of template (imprinted) molecule are polymerized together. Initially template molecule and functional monomer forms a complex after which polymerization take place (Cecchini, et al. 2017). After polymerization highly cross-linked polymer is formed which held their functional groups in position. Template removal from polymer leaving behind empty spaces which is similar in shape and size to the template molecule. Thus molecular memory with very high specificity is introduced in to the highly crossed-linked polymer. Now this polymer has the ability to bind with target molecule (Malik et al. 2018). The synthesized MIP may be polymeric or oligomeric or 2D surface assemblies. MIPs have a wide range of advantages with comparison to natural biomolecules (table 1.2). This technology has many promising features and many benefits including easy synthesis, similar structure based recognition cavities, a highly stabilized and mechanical backbone of polymer matrix and large number of applications to different molecules, metalloids and metal ions (Gui et al. 2018). The technique of molecular imprinting has different advantages such as it is used in purification, isolation, chiral separation, catalysis and in biosensor.

Three important features of the MIPs are:

I. Their selectivity and optimum affinity, is analogous to the natural receptors (Bossi et al. 2007).
II. Their exceptional stability, which is higher than that of natural biomolecules (Chen et al. 2020).
III. Their simplest preparation and easy to use to different applications (Saylan et al. 2019).

Molecular imprinting technology has a wide range of applications such as small molecules such as drugs and large ones as proteins and cells have been imprinted successfully. The best imprinted results were obtained with biological molecules having molecular weight in the range of 200 to 1200Da. The resultant molecular imprinted polymers are low price, robust, with high affinity and selectivity that is proper for their industrial applications (Gui et al. 2018). The increased speficity and stability

of MIPs made them favorable substituents to anti-bodies, enzymes and natural receptors for its use in sensors applications (Cecchini, et al. 2017).

Table 1.1: Comparison of molecular imprinted polymers and natural molecules used for the synthesis of sensors.

Molecular Imprinted Polymers (MIPs)	Natural biomolecules
Imprinted polymers are more stable at low pressure, pH and temperature i.e. <180◦C.	Less stable.
Easy to prepare, easy to handle, and inexpensive.	Enzymes and receptors are higher in price.
Imprinted polymers can work efficiently in organic solvents.	Natural biomolecules show commonly poor performance on non-aqueous medium.
Due to easy operation and easy handling, MIP based sensors are relatively easy to synthesize.	Various natural molecules have different working conditions such as, ionic strength, temperature, pH and substrate etc.
Generally, MIPs of any chemical compound could be synthesized.	Enzymes and natural biomolecules may be used for limited number of analytes.
Imprinted polymers are highly compatible with micromachining technology.	Enzymes and natural receptors have poor compatibility with micromachining technology and miniaturization.

Molecular imprinting is of two main types i.e. bulk imprinting and surface imprinting.

1.4.1 Bulk imprinting

The technique of bulk imprinting is successful for low molecular weight compounds. For imprinting of macromolecule, MIPs are the simplest method. For the whole protein 3D binding sites are formed in this method (Kryscio and Peppas 2012). The target molecule is wholly imprinted in the molecular imprinted polymer and it must be

removed wholly from the polymer matrix after polymerization. The next step is the formation of small particles from the bulk polymers. The polymer is mechanically crushed to form small particles. In this way molecular imprinted polymer is formed having 3D interaction sites specific to the template molecule. Usually bulk imprinting is chosen to imprint small molecules. The advantage of this method is that the imprint molecules are easily adsorbed and release and this process is reversible and faster due to which imprinted support can be utilized for several rounds of analyses (Ertürk and Mattiasson 2017).

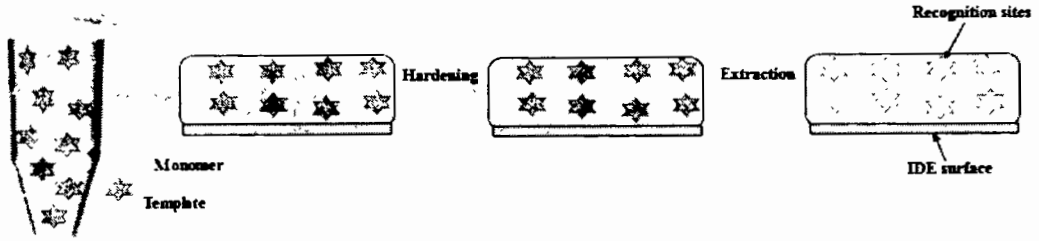

Figure 1.5: Schematic presentation of bulk imprinting

Bulk imprinting is used for various organic compounds such as volatile organic compounds, polycyclic aromatic compounds, environmental contaminants, pharmaceutically active compounds etc. The desired template is added to functional monomer during polymerization (Zamora-Gálvez et al. 2017). A schematic protocol for bulk imprinting is shown in Figure 1.4. Due to molecular imprinting, binding sites are generated not only the surface of synthesized receptors, but also distributed over the whole bulk of the polymer matrix, hence, it is termed as "bulk imprinting." Consequently, the newly developed recognition layer holds large number of cavities, most of them may be assessable by diffusion onto the polymer matrix. The presence of interaction sites may help to increase the sensor signals, e.g. small template molecules confirms the sensitivity (Pan et al. 2018).

1.4.2 Surface imprinting

In surface imprinting, surface of the solid substrate is required for the imprinting of MIP. In this technique, obtained MIPs have abundant cavities and sites.

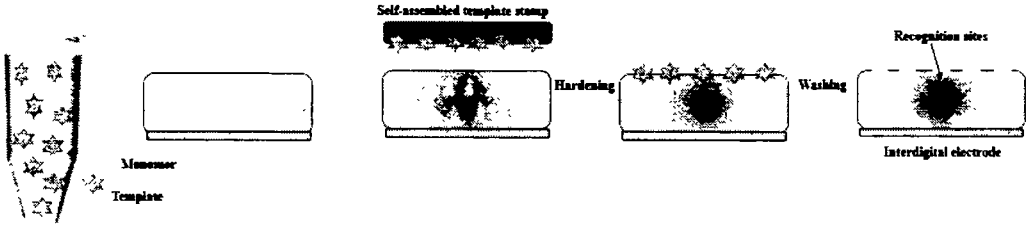

Figure 1.6 : Schematic presentation of surface imprinting.

In this technique binding sites are present only at the surface instead of whole matrix. Surface imprinting is used for macromolecule (Devkota et al. 2017). The main drawback of this method is the reduced number of the binding sites, as binding sites are present only at the surface. Surface imprinting methodology is mostly used for large template including microorganisms, proteins and cells, which is the major drawback of this method (Frasco, Truta et al. 2017).

1.5 Basic feature of molecularly imprinted polymers (MIPs)

1.5.1 Covalent approach

Covalent imprinting was the first approach for realizing the affinity of molecule in organic polymer networks. In this imprint technique, template is covalently bonded with polymerizable groups in bond formation and the process of rebinding (Speltini et al. 2017). After polymerization the target molecule is removed from matrix and binding sites are left which are identical in shape to the target molecule, having the ability to rebind with target molecule in future covalently. The benefit of this method is functional groups are related to the template molecule (Chen et al. 2016). However, there are some short-comings such as diols, aldehydes, amines, carboxylic acids, ketones led to the synthesis for other imprinting methodologies (Viveiros et al. 2018).

1.5.2 Non-covalent approach

Non covalent approach, is now most commonly used methodology to create molecularly imprinted binding sites. This method is based on non-covalent interaction of functional monomer with template molecule before polymerization, free radical polymerization with a cross-linking monomer and then subsequent removal of template. The non-covalent interactions are hydrogen bonging, Vander Waals forces, and π-π interactions. In this method, rebinding of template is also achieved using non-

covalent interaction. This method has very simple and cheap method of MIP preparation sites (Meier et al. 2012). The success of this method depend on the stabilization of non-covalent interaction between monomer and analyte, which results the binding of functional groups of monomer into the cavities generated by the template. The imprinted materials can be prepared within a reasonable time in any well-equipped laboratory. Some of the non-covalently bonded MIPs show high selectivity and binding affinities (Sellergren 2001) such as methyl methacrylic acid is the best monomer which binds with template via hydrogen bond.

1.5.3 Semi-covalent imprinting

Semi-covalent approach is a combination of both covalent and non-covalent approach. This method uses covalent interaction by using a template with polymerizable groups and non-covalent interaction during the process of rebinding. The advantage of this method is that the binding sites have narrower distribution and other kinetics restrictions do not exist (Viveiros et al. 2018). This technique was used to eliminate the shortcomings of non-covalent interactions (Whitcombe et al. 2014). This technique comprises the covalent bonding template and monomer and later, the removal of analyte molecule by a process termed as hydrolysis. At the end, the imprinted cavities by template molecule are ready for their interaction with analyte through non-covalent interactions.

The following advantages of semi-covalent approach are

I. All the monomers with specific functional groups interact with the specific analyte.
II. Stoichiometric ratios of both monomer and template molecule are used,
III. Analyte rebinding is simplistic with binding cavities.

However, semi-covalent approach has some limitations because of limited number of suitable monomers availability. For the synthesis of any MIP, a monomer, cross-linker, a template molecule, a free radical initiator and an appropriated solvent as porogen are the basic components required for molecular imprinting.

1.6 Chemicals required for MIPs

1.6.1 Template

Template and functional monomer are backbone of the molecularly imprinting process. The interaction between monomer and template determines the success of any MIPs. Ideally strong interactions enhance the recognition mechanism of synthetic receptors (Yang et al. 2018). Appropriately selected species as a template can produce maximum recognition sites (Figueiredo et al. 2016). Analyte and functional monomer must have non covalent approach. For the selection of template, stability, capability of hydrogen bonding establishment and absence of polymerized groups prevent the newly synthesized free radicals (Chen et al. 2016). In this proposed research work, the template molecules will be the mono and disaccharides.

1.6.2 Functional monomer

Functional monomer imparts vital role in cavities generation for the analyte of interest (Iacob et al. 2018). The interactions between monomer and template may be covalent or noncovalent. Most commonly used monomer are meth-acrylic acid (MAA), acrylic acid (AA), 2- or 4-vinyl pyridine, sulphonic acids, carboxylic acids (acrylic acid, methacrylic acid, vinyl benzoic acid), hetero-aromatic bases (vinyl pyridine, vinyl imidazole). Methacrylic acid, most frequently used due to covalent and noncovalent interaction with template (He et al. 2018). Monomer to template ratio is significant because analyte decides the exact number of monomer molecule to be attached. The functionality of template and monomer molecule matching is important to increase the complex formation and the imprinting effect (Liang et al. 2018).

1.6.3 Cross-linker

The amount and nature of cross-linker used for the synthesis of molecular imprinted polymer impart a vital role to enhance the selectivity of a sensor. The responsibility of cross-linker is to maintain structure of polymer matrix (gel-type, macrosporous or a microgel powder), stabilization of active sites and enhance the strength to the polymer imprinting binding sites (Vasapollo et al. 2011). Ethylene glycol dimethacrylate (EGDMA), trimethylo propane trimethacrylate (TRIM) and divinely benzene (DVB)

are most commonly used cross-linkers in MIPs. For PCPs analysis, EGDMA is a frequently used cross-linker. For triclosan analysis, DVB and TRIM have been used to prepare imprinted nano beads. For polymerization process, high cross-linker to functional monomer ratio is preferred for the material with suitable mechanical strength and access permanently porous materials to maintain the stability of recognition sites. After the removal of template, it is the responsibility of high cross-linker to maintain three dimensional structure (chemical functionality and shape to that of template cavities). Polymers with cross-link ratios in excess of 80 % will be often used (Liang et al. 2018).

1.6.4 Porogenic solvents

Porogenic solvents have significant role for porous structure of MIPs. Strength of non-covalent interactions is determined by the nature and amount of solvents. It also helps to influence the morphology of polymer, which is directly related to the efficiency of MIPs. Following points are important to consider during the selection of solvent,

- Firstly, all the polymer ingredients such as template, free radical initiator, functional monomer and cross-linker should be soluble in the selected porogenic solve.
- Secondly, porogenic solvents must have the ability to develop pores into the resulting polymer.
- Thirdly, porogenic solvents must be of lower polarity results in lower interference at complex formation stage.

1.6.5 Initiators

Different chemicals having different physical and chemical properties can perform as free radical initiator. Usually, initiators are required in relatively small quantity as compare to the concentration of functional monomer. The decomposition rate of initiator can be controlled and triggered by different methods such as heat, light and electrochemical and chemical ways, based on its chemical nature. Most commonly used initiator is azobisisobutyronitrile (AIBN). AIBN as free radical initiator can be suitably degraded by sunlight (UV) or thermolysis (heat) to produce stabilized, carbon

centered radicals having ability to start the growth of a number of vinyl monomers (Phan et al. 2014).

1.6.6 Polymerization conditions

Molecular imprinted polymers (MIPs) of higher selectivity are made at low temperature as compared to polymerization at increased temperature. Usually 60 °C is referred to as an appropriate polymerization temperature. Elevated temperature imparts negative effect on the stability of MIPs which leaves bad impact on the reproducibility of monolithic stationary phases and produced high column pressure drops. Therefore, comparatively low temperature for a long reaction time will be selected to provide a reproducible polymerization.

1.6.7 Immobilization of MIPs onto transducer surfaces

MIP-based chemical sensors will be constructed by immobilizing MIPs onto the transducer surface. MIP-based recognition elements will be prepared on transducer platform either as thin films or layers by deposition or grafting. The film or layer coated onto the transducer is important for useful response of a sensor.

In-situ polymerization is an excellent immobilization process and comprises of in-situ electro synthesis of molecular imprinted polymer (MIPs) onto the transducing surface. In-situ polymerization has the substantial benefit of integrating the immobilization step into an automatic mass-production process and technique will be applied to appropriate template molecules.

Immobilization by surface coating is another important method of coating and immobilizing molecular imprinting polymer (MIPs) onto the selected transducer (QCM, IDEs) surface. Spin and spray coating will help in the synthesis of thin film of MIPs (if prepared in a suitable dissolved solvent). MIPs deposition can be performed manually at different times to prepare sensors.

Another important method is entrapment of MIP particles into gels or membranes will also be used for electrochemical or mass sensitive transducers for immobilization. Then these polymerized material will be deposited onto the surface of transducer.

1.7 Properties of chemical sensors

1.7.1 Limit of detection (LoD)

LoD helps to enhance the number of imprinted binding sites. In electrochemical sensors, we should prefer the most sensitive transduction type. In all cases, the LoD is a combined form of transduction type and basic feature related to the binding sites.

1.7.2 Selectivity

Selectivity is an important parameter for the development of a sensor. For selectivity analysis, different interferents with same structure, functional group and geometry were selected and then sensor response can be measured by their electrochemical behavior (Dai et al. 2014). By changing the composition of binding medium and measurement medium, detection of any template molecule can be optimized in case of voltammetry detection (Yang et al. 2018). Electrochemical transduction also uses the similar medium for the detection and binding. Interfering species related on the basis of structure can be detected by electrochemical potential (Lian et al. 2012).

1.7.3 Reproducibility and reversibility

Preferably, molecularly imprinted polymer based sensors should be reversible with irregular washing and binding cycles to recover the identification properties. Sometimes, full extraction of template requires large washing time i.e. 12 hours (Whitcombe et al. 2011). Furthermore, partial removal of template is not a serious problem because molecular imprinted polymer based sensors can be fused into device that use an in-expensive and fresh inexpensive component every time (Dai et al. 2014, Yang et al. 2018). Electro-polymerization is an important source for the development of reproducible and easily prepared sensors.

1.7.4 Response time and long-term stability

Generally, response time of molecular imprinted polymer based sensors have been longer than thin films. The smallest response time was obtained from grafting polymerization (Fernández-Cori et al. 2015, Kajisa, Li et al. 2018). Sensors developed by using acrylic or vinyl as monomers have reported that MIPs have excellent stability

during prolonged storage (more than six months in many cases), as expected for a highly cross-linked polymer.

1.8 Problem statement

The determination of mono and disaccharides is very important for scientific research purposes, like food industries, pharmaceutics and clinical chemistry. Diabetes mellitus is chronic disease and worldwide health issue. It is abnormal metabolic condition due to insulin deficiency, elevated level of glucose i.e. hyperglycemia and is result of increased or decreased glucose level than the normal range 80-120 mg/dL (4.4-6.6 mM). Increased concentration of glucose is the major reason for death and disability in the world. Problems of attacking diabetes are important to consider, including increased threats of heart diseases, severe renal issues and blindness. These complications can be significantly decreased by controlled release of blood glucose. The measurement of glucose and supervision of diabetes mellitus thus needs a regular checking of blood glucose concentration. Credible determinations have been done over the last few years to test glucose in blood samples through Chromatography, Calorimetry, Spectrophotometric assay, Electrochemiluminescence and Electrochemical detection. Many conventional methods for glucose measurement work based on electrochemical or calorimetric analysis. Commonly used glucose detection methods are glucometer, performed by using a little sample of blood which is taken by pricking the finger of a patient, following the introduction of blood to a disposable glucometer strip through capillary action. These techniques require off-site analysis grab samples, costly and time-consuming. Due to these reasons, innovative methods that should be selective and effective for the determination of different sugars are needed on urgent basis. For the monitoring of glucose, electrochemical instruments have been used for many decades (pH, dissolved oxygen, conductivity). Molecularly imprinted polymers (MIPs) based chemical sensors are compact robust devices with increased sensitivity and selectivity towards analyte of interest. These help in large number of clinical applications. The chemical sensors are highly sensitive and selective for specific saccharide in the presence of other saccharides such as oligosaccharides and polysaccharides with almost identical molecular masses, atomic radii, functional groups and oxidation states. These

unique properties of chemical sensors make them as promising tools for the online and real-time monitoring of mono and disaccharides.

1.9 Aim and objectives

Aim

Fabrication of molecular imprinted polymer based sensors for the detection of mono and disaccharides.

Objectives

I. To screen out suitable polymer system for the molecular imprinting of monosaccharides and disaccharides.
II. To analyze optimization of molecular imprinted polymer (MIPs).
III. To study characterization of MIPs (spectroscopic, microscopic etc.).
IV. To immobilize receptors onto transducer surface.
V. To enhance the selectivity and sensitivity of the different saccharides by generating NPs of MIPs and their composites with functionalized graphene.
VI. To achieve real time and online analysis of sugars with fabricated sensors.

1.10 Scope and significance of the study

Molecular imprinting technology has the potential in the selective removal, extraction of a wide range of small to large species (molecules, ion, metal ions and metalloids). The MIPs technique has numerous features and advantages i.e. pre-designed recognition, high thermal and mechanical stability, robust, reproducible, easy to operate, regeneratable and miniature size devices, excellently sensitive and selective in their response. Therefore, MIPs are getting substantial attention to detection purposes. The applications of MIPs are increasing and extending into different research fields such as enzyme catalysis, solid phase, chromatographic sciences, bio/chemo sensors and computational modeling of imprinted polymers.

1.11 Literature review

Advanced techniques that are both productive and selective for the detection of sugars are of substantial interest for analytical chemists and scientists. More recently, molecularly imprinted polymers (MIPs) are gaining widespread attention due to their notable sensitivity and selectivity based recognition property (Li et al. 2011). MIPs are synthetic polymers that generate sieves or cavities on the surface of polymer matrix having affinity to target molecules. The template molecule binds with the monomer through covalent or noncovalent bonding and then adding the cross-linking agent, a complex is formed around functional monomers through co-polymerization (Vasapollo et al. 2011). Removal of the imprint template leaves specific cavities whose size, shape, and functional groups are matching to the template molecule (Auriol et al. 2011). The history of molecular imprinting technology seems to be a bit complicated. The first appearance of molecularly imprinted technique (MIT) reportedly found in literature during early 1930s.

MIPs can be used for a wide range of analytes. Dickert and Lieberzeit for the first time introduced surface imprinting techniques in combination with mass-sensitive devices for recognizing (viruses, enzymes and cells), coating the sensor surface with polyurethane layers using sol-gel technologies (Alexander et al. 2006; Baghayeri et al. 2016). Evidently, the application of piezoelectric sensors using MIPs as recognition interface provides sufficient mass change for the effective detection of large molecules and entire organisms. Recently, the combination of QCM and MIPs has been applied in selective sensing of analyte of interest. Using gravimetric piezoelectric sensors with recognition layers based on MIPs for the detection of small molecules (i.e., molecular weight < 600 Da) results in an increase of the analytical signal in liquid during binding events, which is affected by the density, viscosity and three dimensional (3D) structure of the surface layer (Ye & Mosbach, 2008). Analytical methods that enable continuous monitoring of blood glucose have thus been sought. Continuous glucose monitoring (CGM) provides real-time information on trends whether the glucose levels are increasing or decreasing, magnitude, duration, and frequency of glucose fluctuations during the day. Ideally, analytically functional continuous glucose monitoring devices

could be linked to an insulin delivery pump, creating an artificial pancreas (Ramanavicius et al. 2013).

Typical probes for oxygen include luminescent complexes of ruthenium, platinum or palladium which are strongly quenched by oxygen. The probes usually are immobilized in a sensor layer with a thickness of typically 2 mm, and the enzyme is immobilized in- or on-such a sensor layer. Alternatively, and in particular context with intracellular sensing, the components have been immobilized on nanoparticles. The numerous sensors described in the literature differ from each other mainly in the kind of fluorescent probe, the type of polymer matrix, and the way of immobilizing the enzyme (Satoshi et al. 2013; Chung & Hur, 2016; Dhara et al. 2016). Various kinds of polymers have been used including hydrogels, chitosan, proteins from silk worm, egg shell membranes, various kinds of sol-gels, but also hydrophobic polymers such as polystyrene where the enzyme has to be immobilized on its surface. Numerous technical layouts have been reported for such sensors. Many are of the planar sensor layer type. These can be placed, for example, in a microwell or a microfluidic flow cell. Others are based on the use of optical fibres with the sensor material fixed at its tip (Singh et al. 2011).

Till today, a number of effective techniques have been developed to measure glucose, and among these, the electrochemical method has attracted much attention due to the high sensitivity of the resulting devices, ease of operation, and low cost (Mustafa et al. 2012). The glucose detection is performed by two methods i.e. one involving glucose oxidase and other method is enzyme free. The conventional glucose biosensors are fabricated by using glucose oxidase which favours the selective oxidation of glucose in the presence of O_2 to produce hydrogen. The biological activity of enzyme sensors is susceptible to inactivation for the change of temperature and pH values. However, the development of the enzymatic biosensor systems faces two major challenges: insufficient loading of immobilized enzyme and poor bio-stability due to the nature of enzymes. Enzymes exposed to the thermal (relatively high temperature above 40 °C) or chemical (e.g. strongly basic or acid environment) during fabrication, storage, and use procedures could denature and lose their bioactivity. Therefore, non-enzymatic glucose sensors have received keen interest and have been developed rapidly due to the advantages of the thermal and chemical stability. For instance, noble metals and noble

metal based materials, such as Pt, Pd, Au and their metal alloy have been explored as catalysts for non-enzymatic glucose detection. Transition metal (Ni and Cu) and their oxide (NiO, CuO, Cu_2O) also showed improved performance of the direct electrocatalytic oxidation (Basabe-Desmonts et al. 2007; Joo and Brown, 2008).

Tyrosinase was also determined by MIPs based sensors. A MIP based sensor was developed by electropolymerization of o-phenylenediamine of tyrosinase from mushrooms. The template was extracted by proteinase K and sensor showed a linear sensor response range of 50 nM with LoD of 3.9 nM with linear regression co-efficient (R^2) value of 0.99 (Yarman. 2018). Vitamin K serve as co-factor to prevent the blood from clotting. Therefore, the detection of vitamin K is of substantial importance. Molecularly imprinted polymer based sensors provide the solution for its detection. To develop a sensor, a synthetheic compound i.e. menadione (vitamin K_3) was used as a template molecule. MIPs based sensor provides a good detection range with LoD of 700nM by the heat transfer method (Eersels et al. 2018).

Molecularly imprinted polymer based sensors were used for the detection of lipoproteins i.e. low density lipoprotein (LDL) and high density protein (HDL) by using bimonomer mixtures such as methacrylic acid and vinylpyrolidone in ratio of 3:2 and 2:3 respectively. The fabricated sensor exhibited the LoD towards LDL and HDL in the range of 3-400 mg/dL and 8-200 mg/dL respectively (Chunta et al. 2019). Molecular imprinting technique is a versatile method for the separation of analyte from a sample mixture and also for determination purpose. A MIPs based sensor was prepared for the detection of *Escherichia coli* bacteria in food samples and their fluids etc. The recognition receptors were synthesized by employing polyurethane thin layer on stain less steel chip. The transducer measures the thermal resistance which showed linear response with increased number of captured bacteria. The findings from these experiments indicated that thermal conductivity increases. The reference (*Enterobacterae*) was also used to cross-check the sensitivity of sensor at the proposed signal/noise ratio (Cornelis et al. 2019).

2 Chapter 2 FABRICATION OF MOLECULARLY IMPRINTED POLYMERS AND NANOCOMPOSITE BASED SENSORS FOR THE DETECTION OF GLUCOSE

2.1 Introduction

Glucose is an exceptional energy source for the human beings (Foltynski et al. 2018) and a preliminary energy source for brain; therefore, its accessibility affects biological processes (Muscogiuri et al. 2018). The blood glucose level between 4.4-6.1 mMol/L considered being normal during fasting and the exceeding of glucose level from this range alarms the medical issues (Martin et al. 2018). A continuous increased level of blood glucose leads to hyperglycemia (Anunciação et al. 2018, Dash et al. 2018). Diabetes Miletus is World known health issue among the other problems related to hyperglycemia (Rush and Yan 2017, Nikbakht et al. 2018). Major cause of hyperglycemia may be the laziness, lack of exercise, obesity and genetic susceptibility (Micha et al. 2017, Mielgo-Ayuso et al. 2017). Glucose is a monosaccharide with both an aldehyde and polyalcohol groups. It bears four chiral carbon atoms; C_2, C_3, C_4 and C_5. Glucose has five hydroxyl groups which imparts characteristics of hydrogen bond donor and hydrogen bond acceptor shown in figure 2.1 (Shendurse and Khedkar 2016). Function of Insulin on muscle and adipose tissues are (i) carbohydrate metabolism, it enhances the glucose transport rate within cell membrane. (ii) protein metabolism, helps to increase transfer of different amino-acids (Dimitriadis et al. 2011). Beta cells of pancreas release insulin, a basic hormone that maintains glucose level from blood to cells (Alduraywish et al. 2017, Radwan et al. 2018). Insulin level (increase/ decrease) may be the result of insistent hyperglycemia, which alternatively cause the diabetes (Radwan et al. 2018). People with fasting glucose level (100 mg/dL to 125 mg/dL) is considered as prediabetes , those with increased blood glucose level (140 mg/dL to 200 mg/dL) at considerable risk for developing diabetes mellitus as well as cardiovascular diseases (Tuladhar et al. 2012, Protheroe et al. 2017).

2.1.1 Type 1 diabetes mellitus

5-10 % of people suffers from Type 1 diabetes mellitus (T1DM), it was termed as insulin dependent diabetes. It is produced by a cellular-mediated autoimmune destruction of the beta cells, finally leading to insulin deficiency which can occur at any age. People with T1DM usually require daily insulin treatment to sustain life (Griffin et al. 2018).

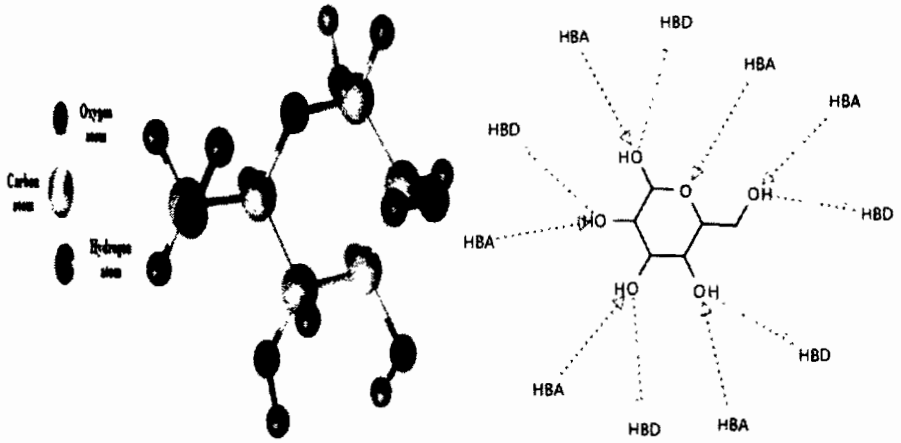

Figure 2.1: 3D structure of Glucose (HBA = Hydrogen bond acceptor, HBD = Hydrogen bond donor.

2.1.2 Type 2 diabetes mellitus

90-95 % diabetic patients belongs to Type 2 diabetes mellitus, it was termed as non-insulin dependent diabetes, it affects the persons who bears insulin resistance and these individuals do not require insulin treatment to survive (Castedal et al. 2018, Muñoz, Valdés et al. 2018). The persons with this type of diabetes are insulin resistance and may be obese (Perreault 2018, Wan, Fung et al. 2018). These types of patients mostly go undiagnosed for several years because hyperglycemia rises slowly, at early stages of diabetes and mostly it is not very severe (Maruo, Mori et al. 2018). Physical activeness, dietary habits and life style factors are major causes of type 2 diabetes mellitus (Griffin, Wall et al. 2018, Yaiyiam and Suthutvoravut 2018).

2.1.3 Gestational diabetes mellitus

This type of diabetes mostly associated with elevated blood glucose diagnosed during pregnancy. This does not mean that the woman will have diabetes after baby birth or that she had it before she conceived but it is a risk factor for type 2 diabetes in the future (Trautwein, Koppenol et al. 2018).

The increased level of glucose causes severe diseases such as nervous, cardiac, renal, cerebral, ocular and peripheral vascular diseases in diabetic patients. Diabetes mellitus is a serious health issue; this causes 4 million deaths every year and 171 million people suffering from diabetes worldwide. It has been estimated that number of diabetic

patients would be more than double of the existing patients globally (Sharma, Kaur et al. 2018, Zimmermann-Schlegel, Wild et al. 2018). To avoid future complications, diabetic patients should examine their blood glucose level firmly though no cure for diabetes (Iacovazzo, Flanagan et al. 2018).

Glucose is an uncharged, low molecular weight molecule of substantial importance. Anomalous glucose concentration in blood, if not properly observed, can cause serious life-threatening difficulties to patients that can result in diabetes or other related diseases (Behera, Rai et al. 2018, Karst, Lammer et al. 2018, Steinarsson, Rawshani et al. 2018). Furthermore, the deficiency or efficiency of glucose level in human blood can be fatal and can cause numerous life-threatening diseases therefore, the determination of blood glucose is of potent importance and for this purpose hand-in and simple in use detection tools are of substantial interest (Vargas, Ruiz et al. 2016, Shen, Sun et al. 2018). Currently numerous analytical techniques such as, spectrophotometry (Leotério, Silva et al. 2015), colorimetry (Emran, Mekawy et al. 2018), spectrofluorometry (de Falco and Lanzotti 2018), gas chromatography (GC) (Ma, Sun et al. 2014), mass spectrometry (MS) (Wang, Yu et al. 2018), flow injection analysis, and high-performance liquid chromatography (Liao, Lu et al. 2016, Emran, Khalifa et al. 2017) are in practice for the quantification of glucose contents. Therefore, there is always an ever-growing demand of highly sensitive, selective, reliable and cost effective glucose contents monitoring device (Yuan, Li et al. 2018, Zhang, Luo et al. 2018) and hence, substantial efforts have been made in this field. Various sensor systems have been reported based on glucose oxidase and enzyme free sensing strategies (Dai, Cao et al. 2018, Boobphahom, Rattanawaleedirojn et al. 2019). However, certain factors including pH, temperature, humidity, toxic chemicals, denaturation by environmental changes, time consuming and cost-effectiveness indeed limit their real-time applications (Saraf, Natarajan et al. 2018). To address these issues, many attempts have been made to detect glucose by non-enzymatic receptors and are mostly based on the electrochemical oxidation of glucose at the electrode surface (Chatterjee, Das et al. 2018). The molecular imprinting provides a straightforward strategy for the generation of highly selective receptors having specific recognition sites for the desired template (Emran, Shenashen et al. 2018). Molecular imprinted polymers

(MIPs) based sensor receptors offer substantial sensitivity, selectivity, storage stability, mechanical strength and cost effectiveness, reversibility, limit of detection and selective behavior of sensor in complex media. In this chapter, we have reported optimized molecular imprinting of glucose molecules by using 30:70 of functional monomer and cross-linker, then the MIPs based electrochemical sensor was fabricated by utilizing stretchable interdigital electrode (IDE) as transducer and exposed to different concentrations of glucose. Furthermore, the sensitivity, selectivity, response time, reproducibility and life time spam of the fabricated sensor has been improved by using molecular imprinted polymers-functionalized graphene nanocomposite as receptors.

2.2 Experimental section

2.2.1 Chemicals and materials

Glucose (99.5 %), sucrose (99 %), maltose (99 %), fructose (99 %), dimethyl sulphoxide (DMSO, 99.7%), n-vinyl pyrolidone (99 %), 4, 4′-diphenylmethanediioscyanate (DPDI 98 %), phloroglucinol (PG 99 %), bisphenol A (BPA ≥99 %), chloroform, methacrylic acid (MAA 99 %), styrene and 2,2′-azobisisobutyronitrile (AIBN 99 %) and ethylene glycol dimethacrylate (EGDMA 98 %), acetone (≥ 99 %), methanol (99.8 % anhydrous), ethanol (99.8 % anhydrous) were purchased from Merck and Sigma Aldrich with the maximum available purity.

2.2.2 Synthesis of n-vinyl pyrolidone based molecularly imprinted polymer (VP-MIP)

Poly(vinylpyrolidone) MIP was synthesized by following the method (Yasinzai, Mustafa et al. 2018) with few alterations. 2.7×10^{-4} mM of Vinylpyrolidone, 3.5×10^{-4} mM of EGDMA was mixed into an eppendorf having 500 µL (4 mmole) of glucose solution in DMSO. Mixture was homogenized by vortex and then 4 mg of AIBN was used as free radical initiator. Vortex this resultant solution and heated at 60 °C for 45minutes in water bath till a transparent gel point was attained.

2.2.3 Synthesis of non-imprinted polyvinyl pyrolidone polymer (VP-NIP)

A non-imprinted monolith (NIP-monolith) was prepared for reference experiment using the similar experimental procedure without adding template (glucose). Poly(vinylpyrolidone) MIP was synthesized by following the method (Yasinzai, Mustafa et al. 2018) with few alterations. 2.7 $\times 10^{-4}$ mM of Vinylpyrolidone, 3.5 $\times 10^{-4}$ mM of EGDMA was mixed into an eppendorf having 500 µL DMSO. Mixture was homogenized by vortex and then 4 mg of AIBN was added as free radical initiator. Vortex this resultant solution and heated at 60 ℃ for 45 minutes in water bath till a transparent gel point was attained.

2.2.4 Synthesis of methacrylic acid based molecularly imprinted polymer (MAA-MIP)

Imprinted polymer was synthesized by mixing 3.4×10^{-4} of methacrylic acid (MAA) as functional monomer, 3.5 $\times 10^{-4}$ mM of EGDMA as cross linker, 5 mg of AIBN as free radical initiator and 500 µL of DMSO as solvent. 2 mg (4 mM) of glucose was added to mixture as template. The mixture was vortex for 5 minutes to homogenize and then place in water bath at 60 °C for 45 minutes to polymerize.

2.2.5 Synthesis of non-imprinted polymer (MAA-NIP)

Non-Imprinted polymer was synthesized by the same method as MAA-MIP without addition of template (glucose) molecule. Glucose imprinted polymer was synthesized by adding 3.4×10^{-4} mM of methacrylic acid (MAA) as functional monomer, 3.5 $\times 10^{-4}$ mM of EGDMA as cross linker, 5 mg of AIBN as free radical initiator and 500 µL of DMSO as solvent. The mixture was vortex for 5 minutes to homogenize and then place in water bath at 60 °C for 45 minutes to polymerize.

2.2.6 Synthesis of polyurethane based molecularly imprinted polymer (PU-MIP)

Polyurethane based maltose imprinted receptors were synthesized using 40 to 60 ratio between monomer and cross-linker. Urethane based receptors were synthesized by 1.9×10^{-6} mM of phloroglucinol (PG), 8×10^{-4} mM of bisphenol A and 3.6×10^{-4} mM of DPDI was vortexed in 1 mL of DMSO. Glucose (2 mmole) was added and homogenized by vortex. The resultant solution was heated for 30 minutes at 45 °C in water bath till gel point was obtained which indicated the synthesis of maltose imprinted polymer.

2.2.7 Synthesis of non-imprinted polymer (PU-NIP)

Non-imprinted polyurethane (PU-NIP) was synthesized using the same procedure without adding glucose. Polyurethane based maltose imprinted receptors were synthesized using 40 to 60 ratio between monomer and cross-linker. Urethane based receptors were synthesized by 1.9×10^{-4} mM of phloroglucinol (PG), 8×10^{-4} mM of bisphenol A and 3.6×10^{-4} mM of DPDI was vortexed in 1 mL of DMSO and homogenized by vortex. The resultant solution was heated for 30 minutes at 45 °C in water bath till gel point was obtained which indicated the synthesis of maltose imprinted polymer.

2.2.8 Synthesis of polystyrene based molecularly imprinted polymer (PS-MIP)

Styrene (2.8×10^{-4} mM), 3.5×10^{-4} mM of ethylene glycol dimethacrylate (EGDMA), 2 mg of AIBN as free radical initiator were mixed into an eppendorf tube. To the above solution, 500 µL of dimethyl sulfoxide (DMSO) as solvent and 2 mg of glucose (4 mM) were solubilized by vortex. Then mixture was polymerized into water bath at 70 °C for 45 minutes till transparent gel point is reached. Non-imprinted polymer (reference) was also synthesized exactly in the same way without adding template (glucose).

2.2.9 Synthesis of non-imprinted polymer (PS-NIP)

For the synthesis of non-imprinted polymer (reference), performed the same procedure as above mentioned, without adding the template (glucose). Styrene (2.8×10^{-4} mM), 3.5 $\times10^{-4}$ mM of ethylene glycol dimethacrylate (EGDMA), 2 mg of AIBN as free radical initiator were mixed into an eppendorf tube. To the above solution, 500 µL of dimethyl sulfoxide (DMSO) as solvent and vortex it. Then mixture was polymerized into water bath at 70 °C for 45 minutes till transparent gel point is reached.

2.2.10 Synthesis of polystyrene graphene oxide based molecularly imprinted composite (PS-GO-MIP)

Polystyrene graphene oxide based molecularly imprinted composite was synthesized by adding graphene oxide (0.5 mg) and mixed through sonication (prepared by oxidation of graphite according to the modified Hammer's method as shown in figure 2.2) (Meng et al. 2019) in 600 µl of imprinted polymer. Then this suspension was sonicated till a homogeneous solution achieved.

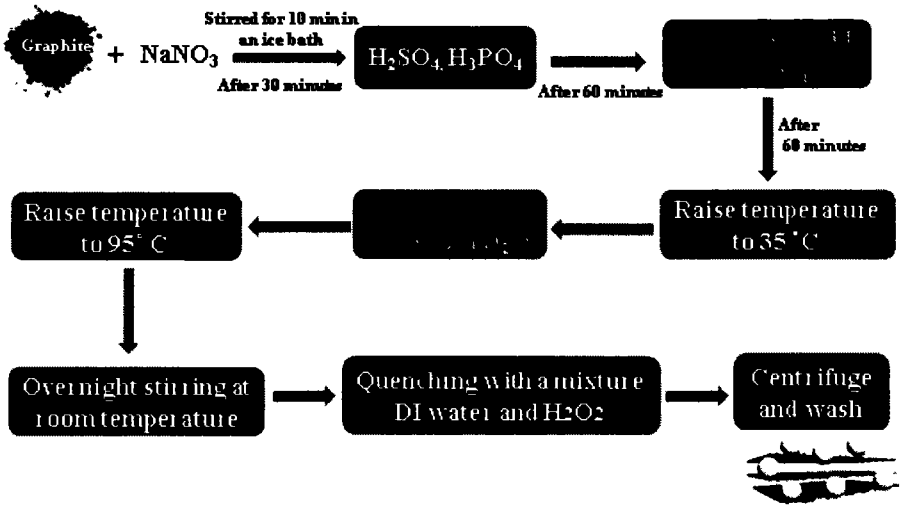

Figure 2.2: A schematic diagram for the synthesis of graphene oxide.

2.2.11 Immobilization of receptors onto interdigital electrodes (IDEs)

Interdigital electrode (IDE) with electrodes spacing (l= 0.5' and number of fingers = 18) was used as transducing surface, for sensor measurements. IDEs were cleaned by washing with de-ionized water followed by methanol. 15 µL of imprinted polymer

(MIP) was coated onto IDEs by spin coating at a speed of 2500 rpm as shown by figure 2.3.

Figure 2.3: Synthesized receptors were coated onto interdigital electrode by spin coating.

The IDEs were dried in oven overnight to achieved dry and compact polymer thin film.

2.2.12 Removal of template from MIPs thin films

To remove the template from imprinted polymer matrix, IDEs washed with deionized water by continuous stirring for 90 minutes using magnetic stirrer at room temperature. After washing out the template molecules from polymer thin films, template size identical cavities were achieved.

2.2.13 Characterization of receptors with fourier transform infra-red (FTIR)

FTIR spectra of thin films of all molecular imprinted polymers (MIPs), non-imprinted polymer (NIPs) and graphene oxide based composite (GO-composite) were recorded by using Shimdazu-1800S FTIR in the range of 4000-500 cm^{-1}.

2.2.14 Characterization of receptors with scanning electron microscope (SEM)

SEM images of receptor's thin films were attained by scanning electron microscope (LEO DSM 892 Gemini) equipped with energy dispersed X-ray EDX analyzer

2.2.15 Differential thermal and thermogravimetric (DTA/TGA) analysis of sensor receptors

Differential thermal and thermogravimetric analysis was studied by using STA PT1000 TG-DSC (STA Simultaneous Thermal Analysis) STA (TGDSC/DTA)

Thermogravimetric Analyzer (Linseis Thermal Analysis, Germany) with detector DTG-60H (detector serial number C30574700276TK) at a heating rate of 10 °C/min under air atmosphere. The temperature range was fixed from 0 °C to 600 °C. The amount of sample 5.33 g was taken for analysis.

2.3 Results and discussion

2.3.1 Characterization and sensor measurements of vinylpyrolidone system based receptors

2.3.1.1 Characterization of synthesized receptors by FTIR spectroscopy and scanning electron microscope

To study the chemical structure of thin films of imprinted and non-imprinted polymers, FTIR was plotted between wave number and % transmittance. A peak was observed at 2980 cm^{-1} as shown by figure 2.3, due to stretching vibrations of sp^3 (CH), while C-O-C stretching vibration was found at 1160 cm^{-1}. The ester group of EGDMA showed a characteristic stretching band at 1734 cm^{-1}. The peak at 1425 cm^{-1} was found a representative peak of C=N, C=C due to the stretching of pyridine group present in n-vinylpyrolidone. These major peaks in spectra showed that the polymerization occurred and imprinted polyvinyl pyrolidone were achieved by free radical polymerization of EGDMA and VP.

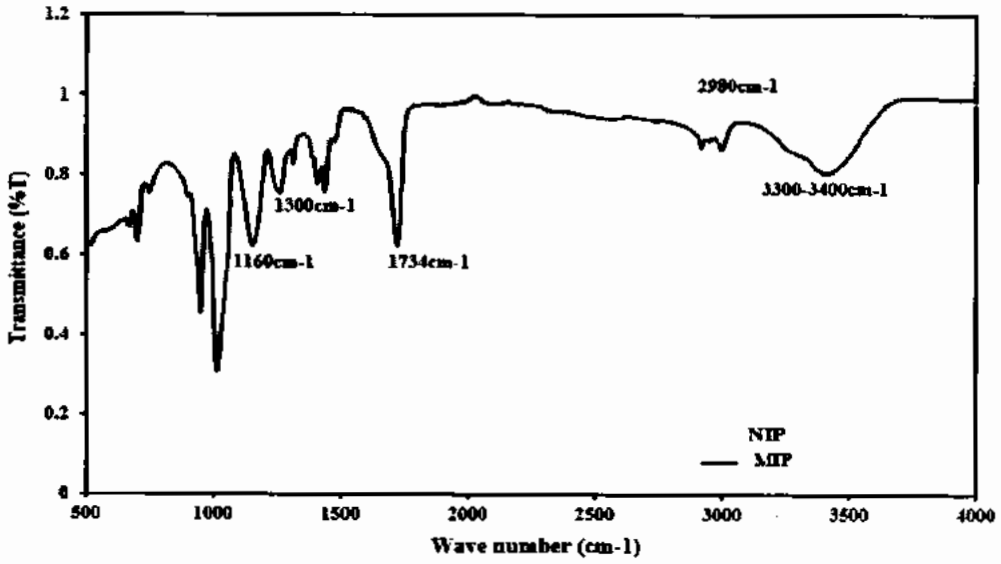

Figure 2.4: FTIR spectra of non- imprinted and imprinted polyvinyl pyrolidone based glucose receptors.

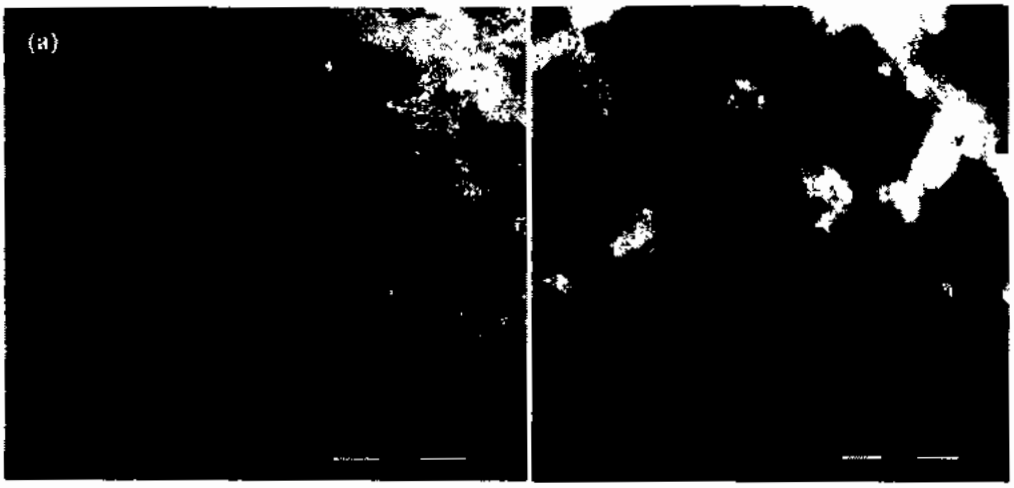

Figure 2.5: SEM images of (a) NIP and (b) MIPs of polyvinyl pyrolidone based glucose receptors.

To assess the surface morphology of synthesized receptors, scanning electron microscopy (SEM) was used. Thin films of the MIPs and NIPs were generated onto a glassy substrate and the SEM images of MIPs and NIPs are shown in figure 2.5. A homogenous, interconnected, porous and uniform skeleton with symmetrical distribution can be observed from the morphological view of obtained images. Different surface topography represented by thin films were clearly noticed, more suitable for permeability and a reduced mass transfer resistance.

2.3.1.2 Sensitivity measurements of fabricated sensor

The fabricated sensor was exposed to various concentrations of analyte ranging from 1-50 ppm to assess the sensor responses against these concentrations.

Figure 2.6: Sensor measurements of polyvinyl pyrolidone based glucose receptors by LCR meter.

At zero concentration (pure water only) of template molecule, capacitance was 0 nF. The sensor showed a response of 11 nF, 23 nF, 37 nF, 54 nF, 73 nF, 97 nF and 138 nF at 1 ppm, 5 ppm, 10 ppm, 20 ppm, 30 ppm, 40 ppm and 50 ppm of glucose as shown in figure 2.7 (a) where the dark black lines represents the sensor response IDEs coated with glucose imprinted polymers while non-imprinted polymer (NIP) as reference, for different concentrations ranging from 0-50 ppm. In contrast to MIP, the NIP exhibited very slight signals of 2-16 nF for the same concentrations, which is negligible as compared to that of imprinted polymer because of availability of cavities/selective molecular imprints present on the imprinted polymer surface. By increasing the concentration of analyte (glucose), conductance was increased which shows the concentration dependent linear response of fabricated sensor. The increase of conductance might be due to the -OH (hydroxyl) group present in glucose which was trapped within the molecular cavities present in polymeric matrix coated onto IDEs. Furthermore, the regression analysis of sensor responses depicts the linear behavior of sensor against the various concentrations of glucose ranging from 1-50 ppm with a correlation co-efficient (R^2) of value 0.98 as shown in figure 2.7 (b).

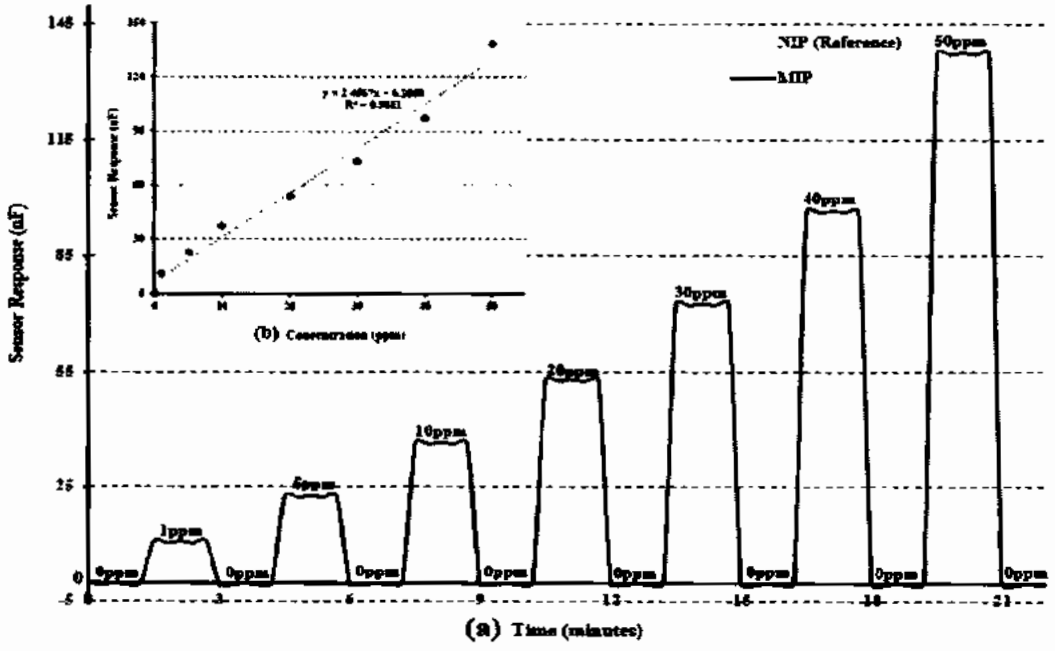

Figure 2.7: (a) Sensitivity response of NIP and MIP of polyvinyl pyrolidone based glucose sensor at different concentrations (0-50 ppm) and (b) Linear regression analysis of glucose sensor.

As can be seen in figure 2.7 (a) that at a concentration of 1ppm, the sensor signal was 11 nF with noise signal of 0.5 nF and the lower limit of detection (LoD) was calculated by signal to noise ratio (S/N = 3) method. The sensor exhibits very good LoD of ~136 ppb to 500 ppm towards its analyte of interest. Hence, the sensor responds very efficiently for the concentration range 1-50 ppm, which relates to the essential clinical amount of glucose for human beings. Obviously, the results of glucose sensor presented here showed very lower limit of detection, broad dynamic range and excellent response time i.e. ~2 seconds.

It is important for the synthesis of an efficient molecular imprinted polymer that there should be strong interactions between the functional monomer and analyte. The number of hydrogen bond acceptor and hydrogen bond donor groups present in glucose which has a vital role in the development of non-covalent interactions between glucose and polymeric matrix. Another reason for the substantial sensor signal changes of glucose imprinted VP polymer on exposing to glucose could be that glucose is selectively adsorbed in the polymer matrix that produces the potential change or greater in response with the increase in concentration even at very minute concentration of glucose. Ideally sensor should be concentration dependent and should be reversible. This newly fabricated sensor follows the same pattern and upon increasing the concentration of template, conductance increases in a linear manner which depicts the linear relation between template molecule and conductance. When the sensor was exposed to zero concentration of glucose after tacking sensor response of each concentration, the sensor reaches its initial value which represents the reversible and regeneratable behavior of fabricated sensor. The non-covalent interactions between the template molecules and polymeric matrix may base on the interaction of monomer and glucose molecules and the OH group present on glucose interacts with vinyl pyrolidone while methylene group of EGDMA provides support to imprinted polymer skeleton to generate cavities within polymer matrix. These possible interactions between template molecules and polymeric matrix can be seen in figure 2.8 where dipole-dipole force and hydrogen bonding cause the interaction between template molecule and imprinted cavities.

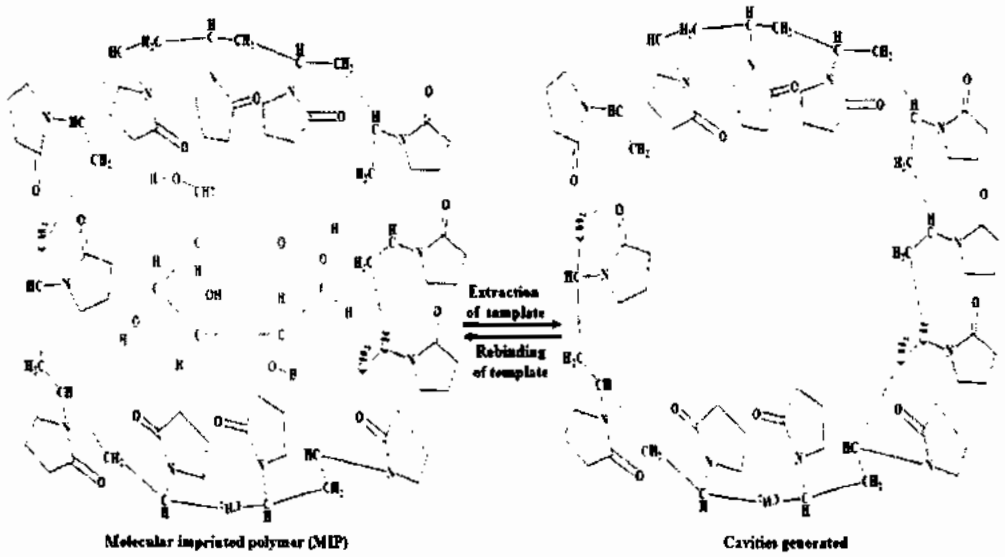

Figure 2.8: The rebinding and removal of template from polyvinyl pyrolidone based glucose receptors.

The ability of a template molecule to discriminate the other interfering species, which have a similar electro activity to the target analyte, same shape and similar oxidizing potential is considered as one of the most significant factors in electrochemical sensor design. Superior response of any sensor towards specific analyte may be due molecular imprinting because molecular imprinting shows key and lock mechanism.

2.3.1.3 Selectivity analysis of fabricated sensor

Selectivity is an important parameter for a fabricated sensor. It is very essential to check the selectivity of imprinted sensor by exposing it against various competing molecules based on structure, functional group and geometry of the imprinted analogue. Fructose, maltose, sucrose and n-hexane were selected as interfering species to evaluate the specificity of a sensor. Selectivity analysis was performed by exposing the fabricated sensor to 50 ppm concentration of glucose. At 50 ppm, conductance of glucose was 138nF while at same concentration, conductance value for fructose, sucrose, maltose and n-hexane was 8, 9, 7 and 4 nF respectively as shown in figure 2.8. The sensor response towards glucose is higher by the factor of 17 as compared to fructose while both have a similar number of carbon atoms and their molecular weight are also same. Glucose and fructose differ only in their structure and the spatial arrangements of

functional groups and this substantial difference between the sensor responses against both confirm the governing of key-lock rule exhibit by molecular imprinted polymers.

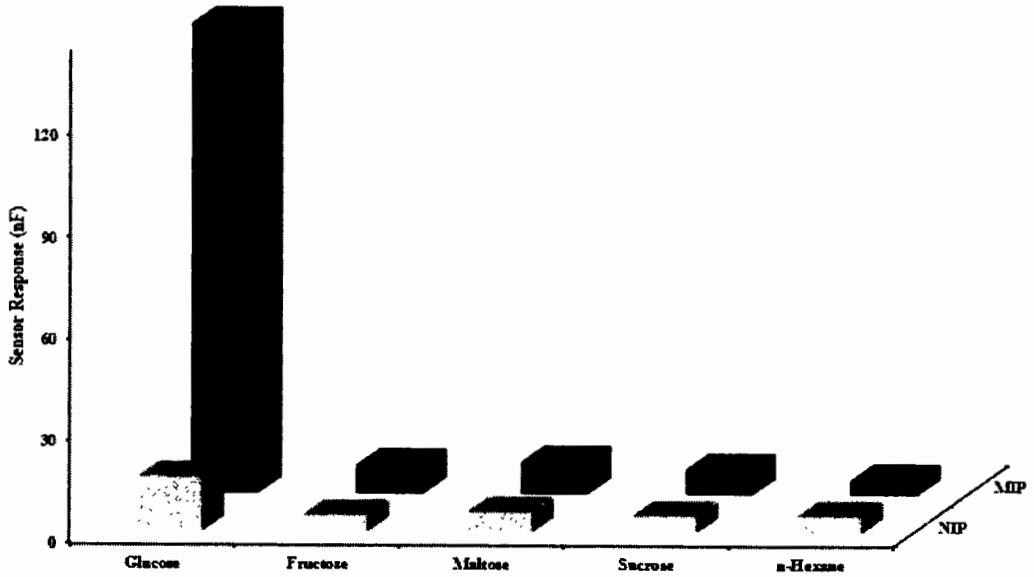

Figure 2.9: Selectivity of polyvinyl pyrolidone based glucose sensor against different competing molecules at 50 ppm.

It is also confirmed from the sensor behavior against these two highly identical species that molecular cavities are size and shape specific and the interactions are more dependent on size and geometry of the molecule showed higher selectivity response than other interfering species. Maltose exhibited a sensor response of 7 which is 15 folds less than glucose. Maltose and glucose have same structure and spatial arrangement, while maltose is a disaccharide, a combination of two glucose molecules. It showed a very negligible sensor response due to structural resemblance of cavities generated by glucose imprinted polymer. The sensor response showed by sucrose is 9 which is less by a factor of 20. During polymerization process, n-vinylpyrolidone and EGDMA rearranges themselves around the imprinted molecule in a very effective way towards the template molecule i.e. glucose. n-Hexane has six carbon atoms similar to glucose but differ on the basis of structural formula and functional group. The sensor response showed by n-hexane is 4 nF which is highly negligible than glucose (34 times). This is because both glucose and n-hexane differ from each other. There is no similarity between them except the same number of carbon atoms. Selectivity response of MIP is

also very high than NIP. Lower response of NIP is due to the absence of cavities onto the fabricated transducer.

2.3.1.4 Reproducibility, reusability and stability

An ideal sensor must be reproducible, highly stable and reusable for pharmaceutical and food industries.

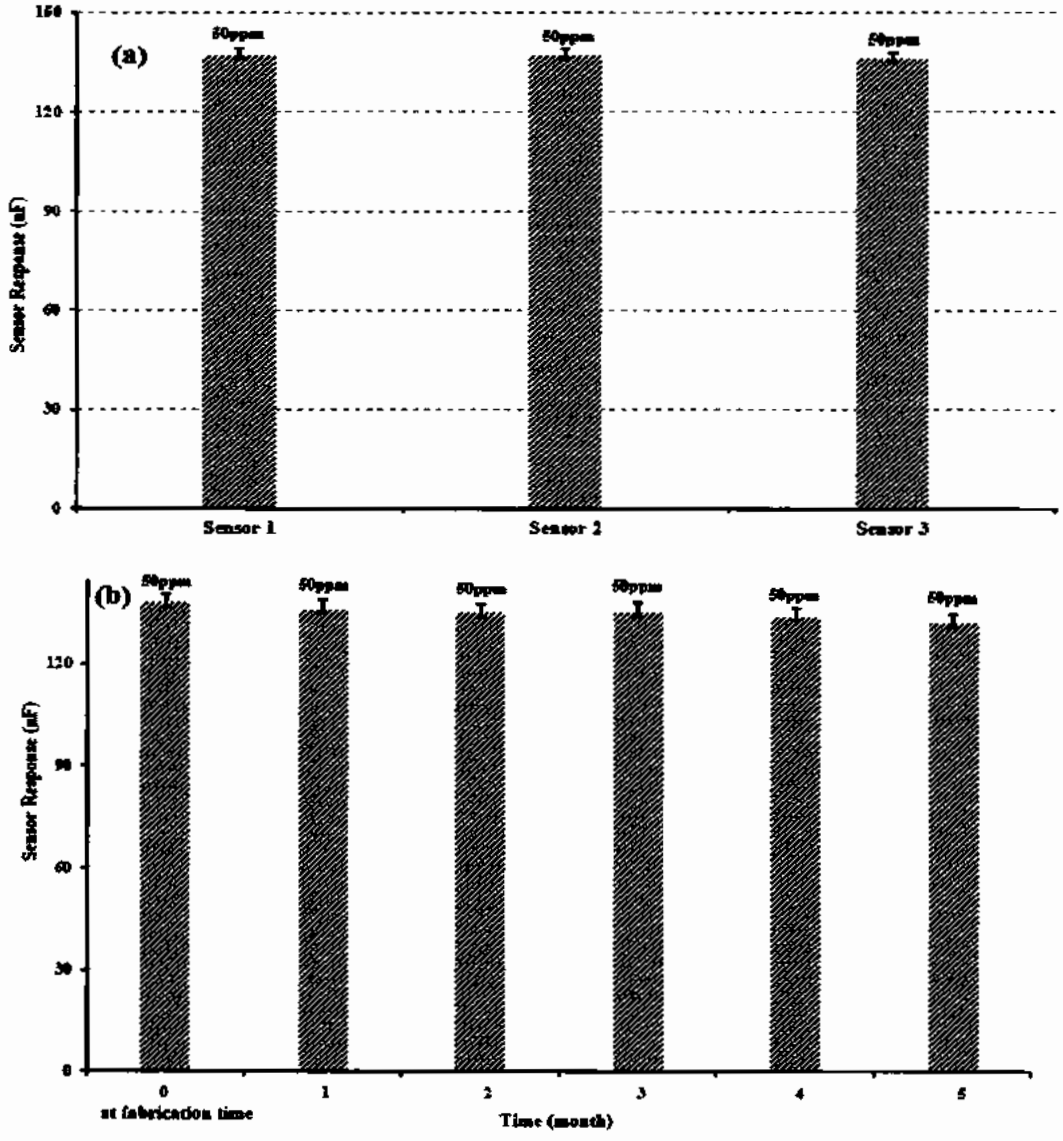

Figure 2.10: Reproducibility and reusability of three polyvinyl pyrolidone based glucose sensors prepared in the same manner (b) Stability profile of glucose sensor over the period of six months.

Reproducibility of a fabricated sensor is determined by measuring the sensor response repeated under same experimental conditions while at different time. To investigate the

reproducibility of a fabricated sensor, the sensitivity profile of sensor was assessed every month. The reproducibility of three different glucose imprinted sensors was measured using relative standard deviation of conductance (nF). The sensor signals of sensor 1 was 137 nF, sensor 2 showed sensor signals of 136 nF whereas for sensor 3, it was 136 nF. At different time, three different sensors showed different response under same experimental conditions as depicted in figure 2.10 (a). These observations confirmed the reproducibility of fabricated glucose sensor by 0.5 % RSD value (n=3). Stability of a sensor is a parameter that takes into account the reducibility of a fabricated device measurements after a long use. For stability profile, a glucose sensor was synthesized following the above mentioned procedure and stored it for six months. At every month, sensor response was assessed by exposing the sensor at 50 ppm concentration of template (glucose) molecule. The measured sensor response at zero month was 138 nF whereas after one month, sensor response was decreased to 136 nF. In third and fourth months, sensor signals were reduced upto 135 nF. Furthermore, the sensor cycle was repeated for fifth month, sensor signals of 134 nF were found respectively. These repeated sensor measurements were close to each other and were not observed any significant change in its response. This negligible reduction in sensor response might be due to minute thin film loss, swelling and shrinkage of fabricated receptor and number of effective collisions etc. This newly developed sensor showed highly efficient results (%age efficiency = 0.98 %) with maximum retained sensor response of 98.4 % as can be seen in figure 2.10 (b).

2.3.2 Characterization and sensor measurements of methacrylic acid system based receptors

2.3.2.1 Characterization of synthesized receptors by FTIR spectroscopy and scanning electron microscope

To assess functional group changes during the polymerization of methacrylic acid (MAA) and ethylene glycol dimethacrylate (EGDMA), ATR-FTIR analysis of receptors was performed.

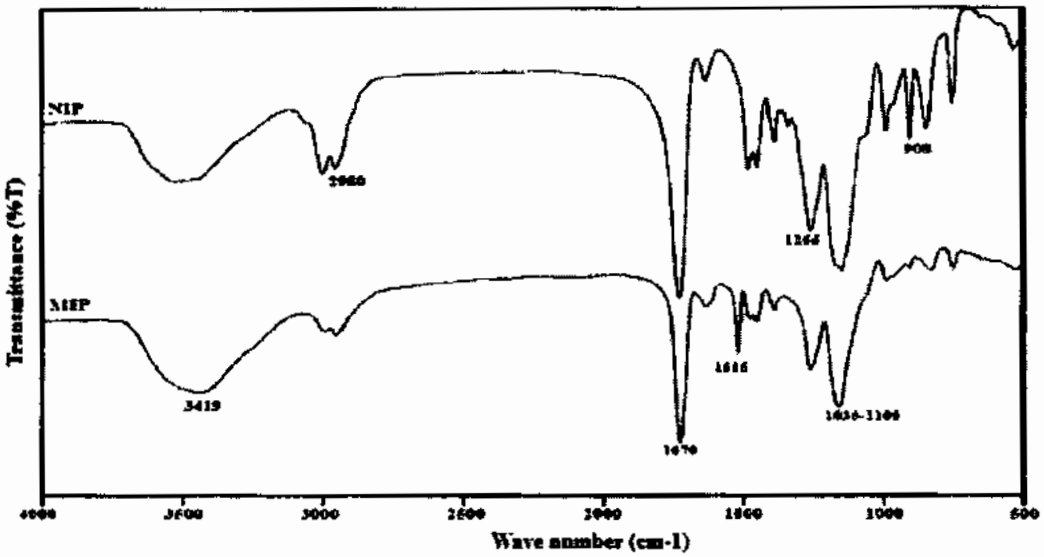

Figure 2.11: FT-IR spectra of NIP and MIP polyacrylic acid based glucose receptors.

FTIR spectra for acrylate based receptors was obtained in the range of 700-3900 cm^{-1} as shown in figure 2.11. Spectra of MAA and EGDMA showed –C=C stretching frequency at 1650 cm^{-1}. The peaks at 1670-1515 cm^{-1} are vibrational peaks indicating C-H stretching and C-H bending of polymer chains. The characteristics peaks centered at 1035-1149 cm^{-1} indicated the presence of polysaccharides in MIP. The absorption peak at 3200-3400 cm^{-1} was attributed to stretching vibrations of -OH of glucose. The peak at 1702 cm^{-1} shows the presence of ester group in the matrix and the other extra peaks are attributed to free radicle polymerization.

To assess the surface morphology of synthesized receptors, scanning electron microscope (SEM) was used. For this purpose, thin films of the MIPs and NIPs were generated onto a glassy substrate and the SEM images of MIPs and NIPs are shown in figure 2.12. SEM images showed granular topography of the coated thin films. Difference in the topography of both MIP and NIP indicated the extraction of template molecule.

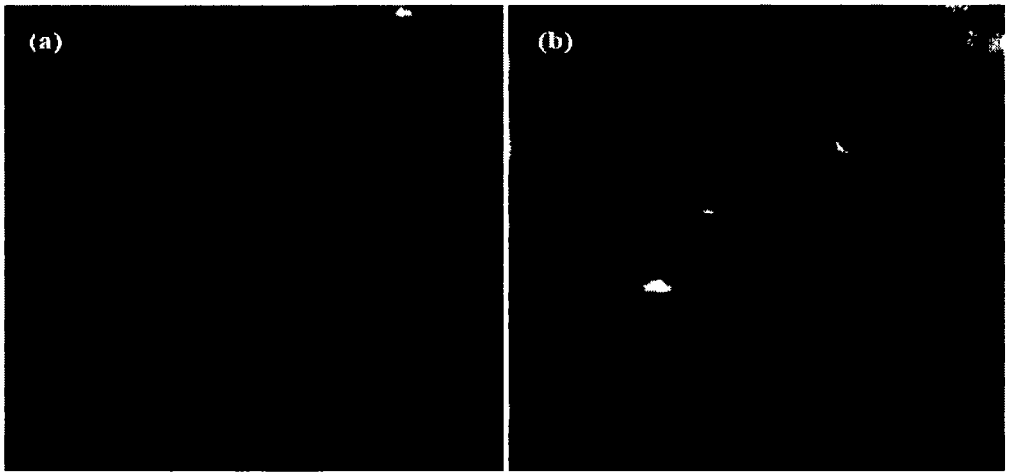

Figure 2.12: SEM images of (a) NIP and (b) MIP of methacrylic acid based glucose receptors.

2.3.2.2 Sensitivity analysis of fabricated sensor

After coating of glucose imprinted polymer onto IDEs and washing to generate cavities within polymeric matrix, the sensor was exposed to various concentrations of glucose to assess its sensitivity profile. The MIPs coated sensor yields substantially higher response as compared to its counterpart NIPs that can be seen in figure 2.13 (a). The obtained electrochemical results demonstrate that newly developed sensor was highly sensitive even at very low concentration of 1 ppm. At 0 ppm, the observed capacitance was 0 and as for 1, 5, 10, 20, 30, 40 and 50 ppm, measured response was 15 nF, 41 nF, 59 nF, 87 nF, 119 nF, 155 nF and 206 nF respectively with the lowest limit of detection ~115 ppb and highest detection limit of 500 ppm. Non-imprinted polymer was also exposed to the same concentrations of analyte and sensor signals were very less. The increase of conductance might be due to the -OH (hydroxyl) group present in glucose which was trapped within the molecular cavities present in polymeric matrix coated onto IDEs. Furthermore, the regression analysis of sensor responses depicts the linear behavior of sensor against the various concentrations of glucose ranging from 1-50 ppm with a correlation co-efficient (R^2) of value 0.99 as shown in figure 2.13 (b).

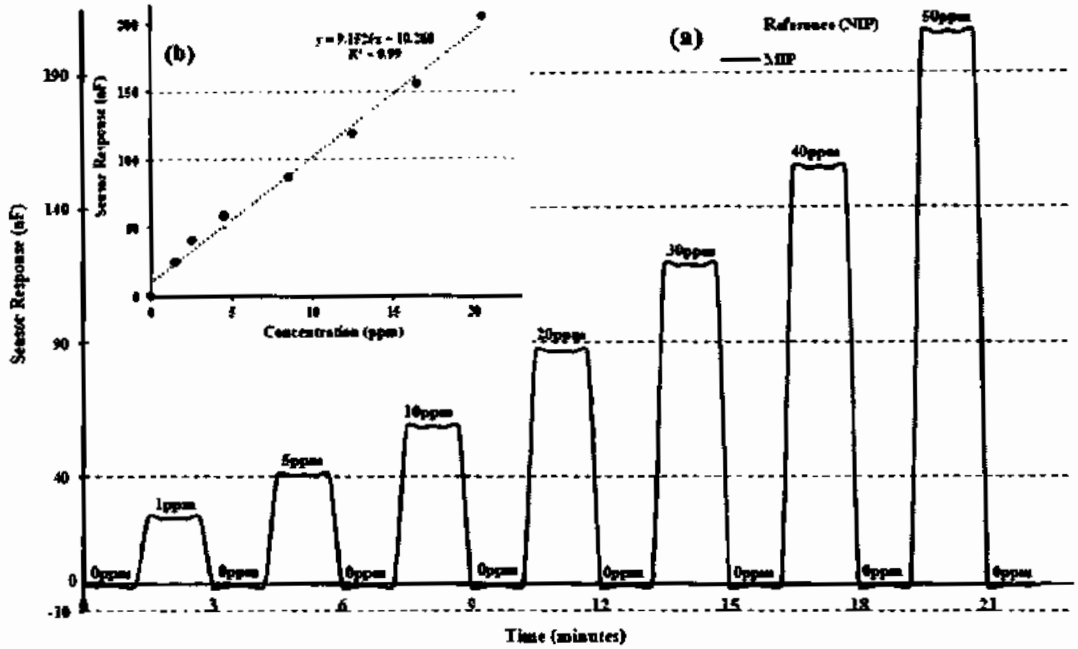

Figure 2.13: (a) Sensitivity response of NIP and MIPs of methacrylic acid based glucose sensor at different concentration (0-50 ppm) (b) Linear regression analysis of glucose sensor.

It is important for the synthesis of an efficient molecular imprinted polymer that there should be strong interactions between the functional monomer and analyte. The number of hydrogen bond acceptor and hydrogen bond donor groups present in glucose which has a vital role in the development of non-covalent interactions between glucose and polymeric matrix. Another reason for the substantial sensor signal changes of glucose imprinted acrylate polymer on exposing to glucose could be that glucose is selectively adsorbed in the polymer matrix that produces the potential change or greater in response with the increase in concentration even at very minute concentration of glucose. Ideally sensor should be concentration dependent and should be reversible. This newly fabricated sensor follows the same pattern and upon increasing the concentration of template, conductance increases in a linear manner which depicts the linear relation between template molecule and conductance. When the sensor was exposed to zero concentration of glucose after tacking sensor response of each concentration, the sensor reaches to its initial value which represents the reversible and regeneratable behavior of fabricated sensor.

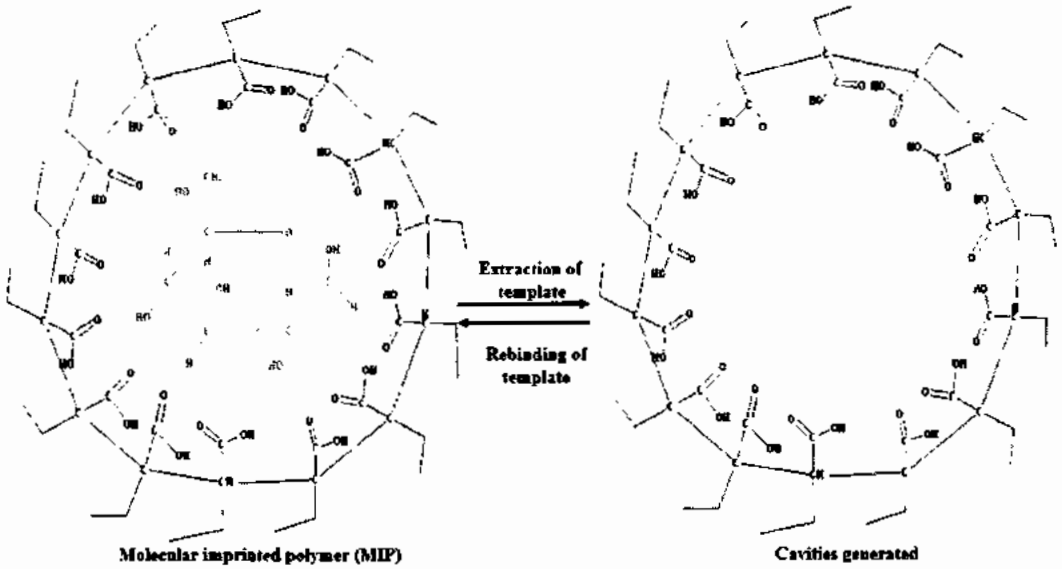

Figure 2.14: The rebinding and removal of template from methacrylic acid based glucose receptors.

On the other hand, if we consider the interaction between the template molecules and molecular binding sites within MIPs which are absent in NIPs then the higher sensor of MIPs can easily be explained. NIP does not show any significant change in its response due to lack of binding capacity towards analyte. Methacrylic acid provides support in generation of cavities within polymer matrix whereas, non-covalent interactions between OH group of glucose and -COOH functional group of functional monomer may develop. These possible interactions between template molecules and polymer matrix can be seen in figure 2.14 where dipole-dipole force and hydrogen bonding cause the interaction between template molecule and imprinted cavities. The capability of MIP to remove template molecule from other interfering species (having similar electro activity to the targeted molecule, same structure and similar oxidizing potential) is supposed the most important parameter in electrochemical sensor. Pronounced sensor response towards specific analyte is attributed to molecular imprinting which was generated by key and lock mechanism.

2.3.2.3 Selectivity analysis of sensor

Selectivity is an important parameter of chemical sensor. Sensitivity analysis, alone is not sufficient, therefore, it is important to check the selectivity by exposing it against different competing molecules based on structural and functional analogues. Fructose,

maltose, sucrose, n-hexane were selected as interfering species to evaluate the selectivity performance of the sensor. At 50ppm, conductance of glucose and other interfering molecules were checked as shown in figure 2.15. Glucose sensor showed signals (conductance) of 206 nF whereas fructose, maltose, sucrose and n-hexane were 15 nF, 15 nF, 10 nF and 10 nF respectively.

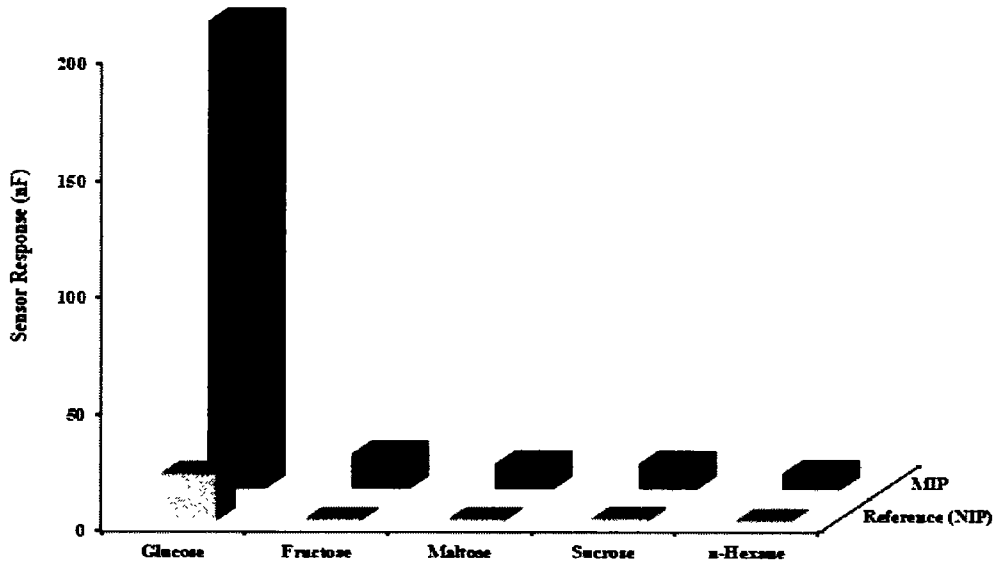

Figure 2.15: Selectivity analysis of methacrylic acid based glucose sensor against different competing molecules at 50 ppm.

Glucose showed 14 times increased sensor response than fructose, 19 folds higher than maltose and sucrose and very negligible response was found by n-hexane. From these observations, it is confirmed that thin film of receptors bears highly selective cavities related to glucose than other competitors. During polymerization, methacrylic acid and EGDMA rearrange themselves in a very effective way around the imprinted specie results in a high number of recognition sites which is highly selective towards the respective analyte.

2.3.2.4 Reproducibility, reusability and stability

To assess the reproducibility of fabricated sensor, three different sensors were synthesized thrice under normal temperature and pressure.

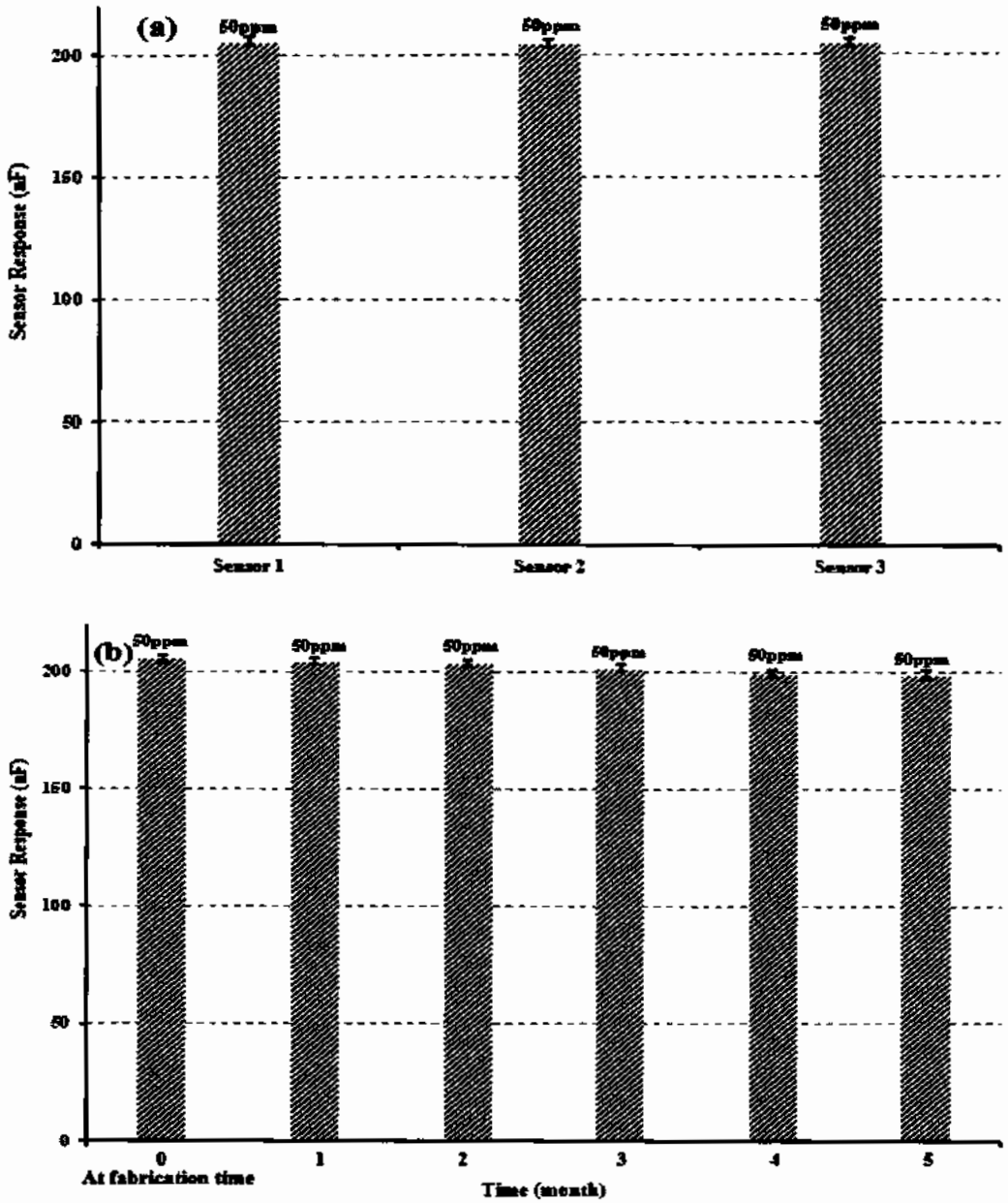

Figure 2.16: (a) Reproducibility and reusability a of three methacrylic acid based glucose sensors prepared in the same manner (b) Stability profile of glucose sensor over the period of six months.

These fabricated sensors were exposed to 50 ppm concentration of analyte after one month and sensor response was measured. The obtained relative standard deviation (RSD) of 0.4 % signifies the effective repeatability of 50 ppm with continuous use as shown in figure 2.16 (a). In addition, 99 % sensor response was maintained which also indicates that glucose MIP based sensor possesses excellent repeatability and reproducibility.

For stability measurents, a glucose imprinted polyacrylate sensor was synthesized using the same recipe and stored for six months under normal temperature and pressure. The fabricated sensor was exposed to 50 ppm concentration of glucose solution and capacitance was measured thrice. From these measurements, relative standard deviation (RSD) of 1.25 % indicated that the fabricated glucose sensor is highly stable at above mentioned conditions as shown in figure 2.16 (b).

2.3.3 Characterization and sensor measurements of urethane system based receptors

2.3.3.1 Characterization of synthesized receptors by FTIR spectroscopy and scanning electron microscope

To study the chemical changes during polymerization of MIP and NIP, FTIR analysis in ATR mode was performed.

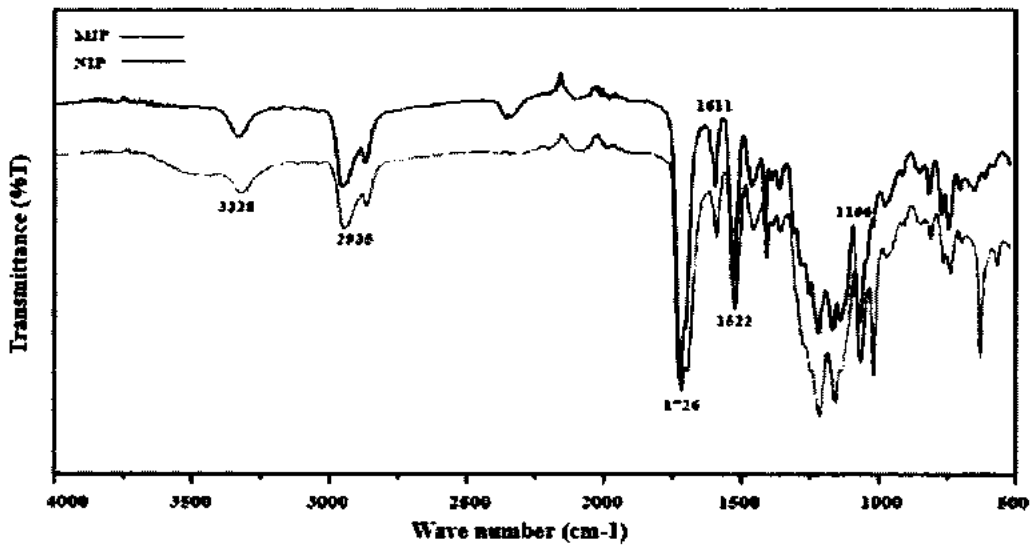

Figure 2.17: FT-IR spectra of non-imprinted and imprinted polyurethane based glucose receptors.

In this polymer matrix, N-H characteristic absorption peak was found at 3328 cm^{-1} due to the presence of hydrogen bond in the urethane linkage and urea groups. Carbonyl group showed stretching vibrations at 1726 cm^{-1}. The stretching vibrations of ester (C(O)-C) was present at 1126 cm^{-1}. The carbonyl peak (C=O) around 1700 cm^{-1} due to ester-polyols and urethane.

To assess the surface morphology, synthesized receptors were coated onto the glassy medium to achieve thin films of receptors. Surface morphology of thin film receptors (NIP and MIP) was examined by scanning electron microscope (SEM) shown in figure 2.18.

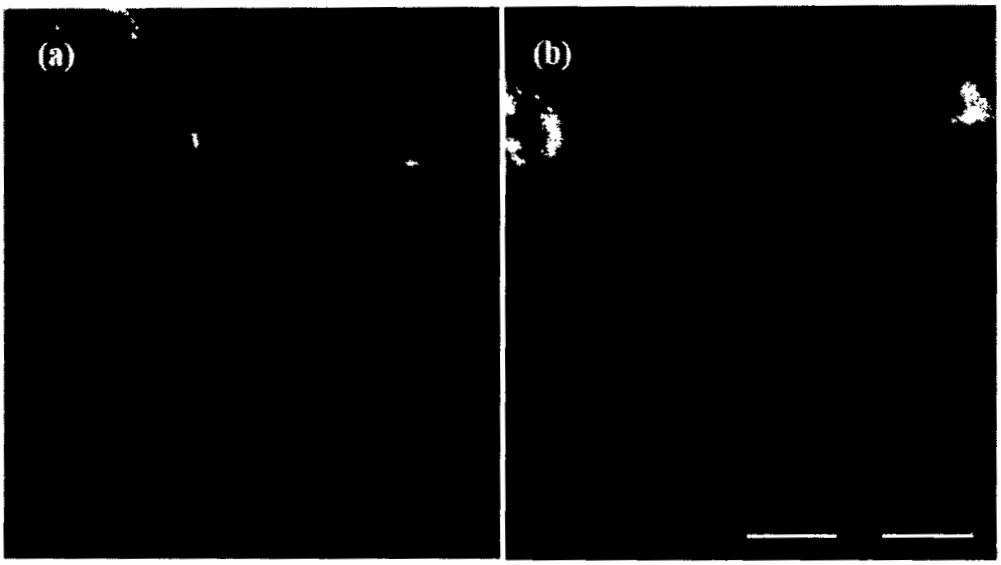

Figure 2.18: SEM images of (a) NIP and (b) MIP of polyurethane based glucose receptors.

The thin film of MIPs showed swollen and rough morphology while NIP exhibited highly porous structure while NIP shows smooth and non-porous surface. Difference in the topography indicated the presence of template molecule in MIPs within the polymer matrix whereas in NIP, there is no template molecule which proves the successful polymerization.

2.3.3.2 Sensitivity measurements of fabricated sensor

The sensor shows the response of both MIP and NIP containing different amounts of template, both layers are roughly 100 nm high on IDEs. The sensitivity profile of fabricated IDEs was checked by LCR meter. IDEs were connected to LCR meter (figure 2.5) and exposed it into various concentrations of template ranging from 0-50 ppm. The effect of imprinting is obvious; both IDEs respond to signals even at lower concentrations of analyte. At 0 ppm concentration of glucose (analyte), the observed conductance was 0 and at 1 ppm, 5 ppm, 10 ppm, 20 ppm, 30 ppm, 40 ppm and 50 ppm, conductance was 21 nF, 34 nF, 41 nF, 86 nF, 141 nF, 197 nF and 275 nF respectively

shown in figure 2.19 (a). While NIP response at these concentrations was found 15 nF at 50 ppm concentration, which is negligible as compared to MIP response. However, on the imprinted IDE, its response is substantially greater, by a factor of at-least eighteen than on the non-imprinted polymer matrix.

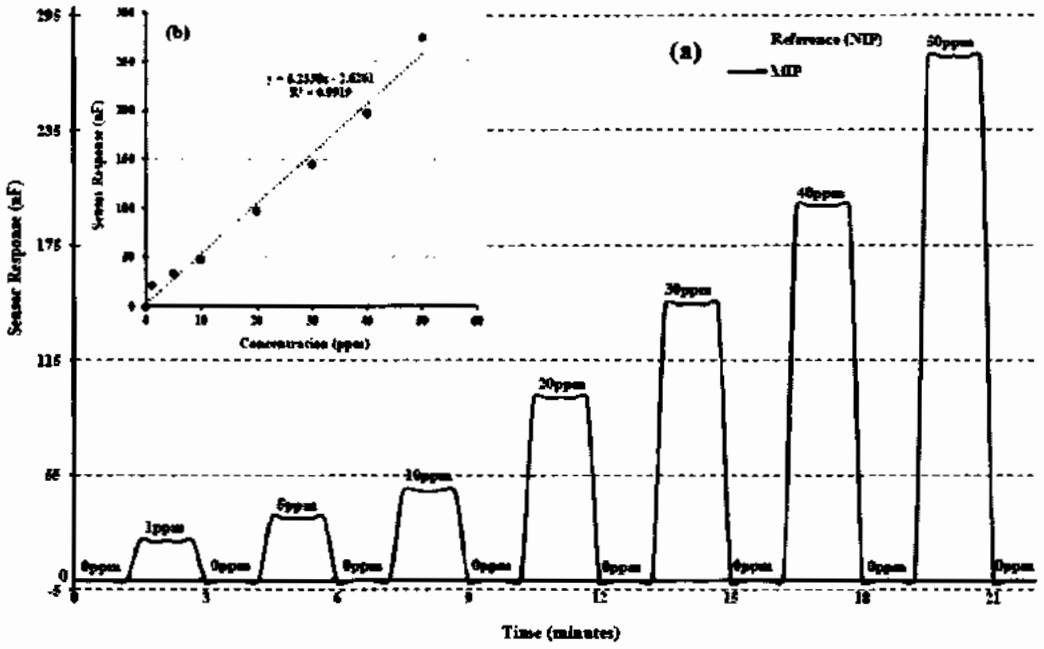

Figure 2.19: (a) Sensitivity response of NIP and MIPs of polyurethane based glucose sensor at different concentration (0-50 ppm) (b) Linear regression analysis of glucose sensor.

The significant difference between the responses of NIP and MIP is because of availability of molecular imprints/cavities present on the surface of imprinted polymer. Moreover, it can also be assessed the affinity interactions between the analyte and polymer matrix, the change in sensor response indicates that template molecule is inserted into the cavities of sensitive layer which is present on the whole of imprinted polymer. Furthermore, low noise level (0.5 nF) allows for limit of detection as low as 71 ppb and maximum detection limit ~500 ppm which is surprising for glucose detection. All the proposed sensors are reversible in nature, in case of long term stability, no extra care was required during their operation. The sensor response was measured in the range of 22-275 nF.

Sensitivity response is directly related to analyte concentration, therefore the figure 2.19 (a) shows that as the concentration of analytes increases, the conductance was also increased which indicates a linear response of the fabricated sensor.

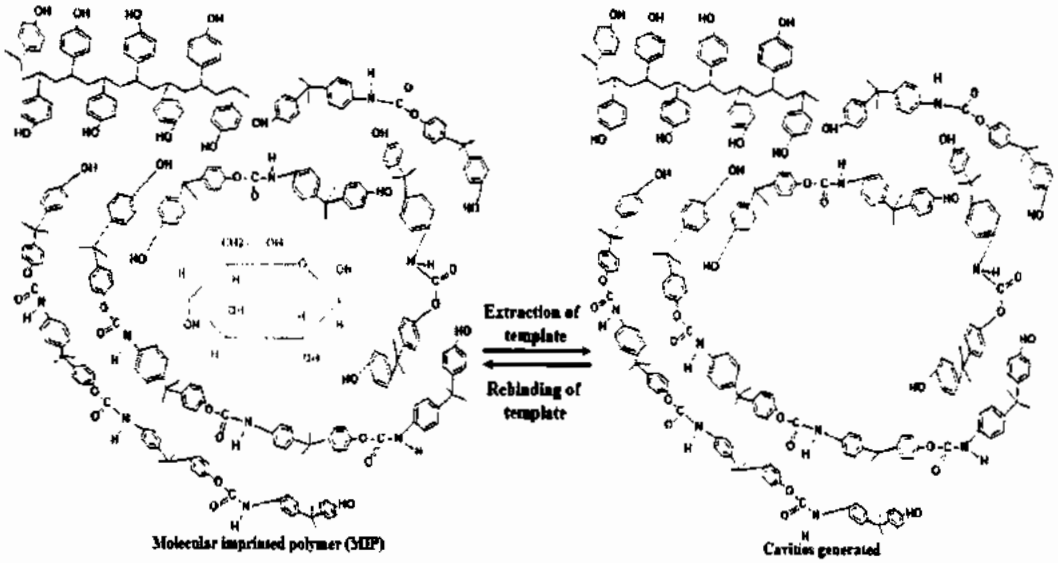

Figure 2.20: The rebinding and removal of template from polyurethane based glucose receptors

This might be the reason that the glucose bears OH groups which have negative charge act as an electroactive species. Hydrogens present in DPDI can act as both hydrogen donor / acceptor. Hydroxyls of glucose show hydrogen bonding and it is important for the synthesis of an excellent imprinted polymer that there should be appropriated interactions between template and functional monomer. The sensor produced linear response with linearity co-efficient (R^2) = 0.99 as shown in figure 2.19 (b). It may also be possible that strong interactions developed between DPDI and template (figure 2.20).

2.3.3.3 Selectivity analysis of sensor

Selectivity is a crucial analytical parameter used for the chemical sensor for the detection of template molecule (glucose). Selectivity of glucose sensor was performed against fructose, sucrose, maltose and n-hexane at 50 ppm as shown in figure 2.21. These molecules are competing species for glucose, have structural and functional group similarities with glucose. Glucose exhibited highest sensor response than other competing species. The results showed that glucose response was 21 times higher

response than fructose, 22 times than maltose, 39 times from sucrose and 55 times higher than n-hexane respectively. It shows that glucose is highly selective and specific for imprinted sensor. The comparison of selective behavior of glucose sensor with other competing species showed that fructose has higher selectivity co-efficient than others. The greater selectivity co-efficient of fructose might be because it is also a monosaccharide sugar such as glucose therefore, it has maximum structural resemblance. Sucrose and maltose both are disaccharide, due to same functional group, selectivity co-efficient is also higher than n-hexane.

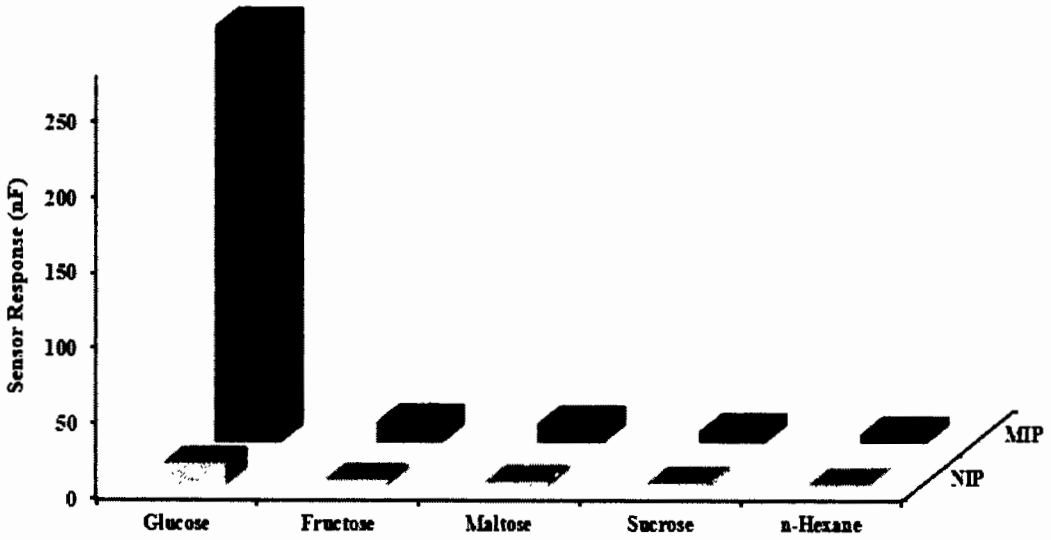

Figure 2.21: Selectivity analysis of polyurethane based glucose sensor against different competing molecules at 50 ppm.

2.3.3.4 Reproducibility, reusability and stability

To evaluate the reproducibility, reusability and longer term stability of the fabricated sensor, repeatability tests were performed at 50 ppm concentration of glucose, where the same sensor was washed with de-ionized water and stored at room temperature when it was not in use. Reproducibility of sensor data showed RSD =1.36 % where n=6 and with maximum retained sensor response was 98.9 %. Furthermore, stability of sensor was evaluated after an interval of 1month upto 6months. sensor was stored at optimized conditions upto 6months, the sensor retained its more than 98.9 % efficiency to its initial response as shown in figure 2.22.

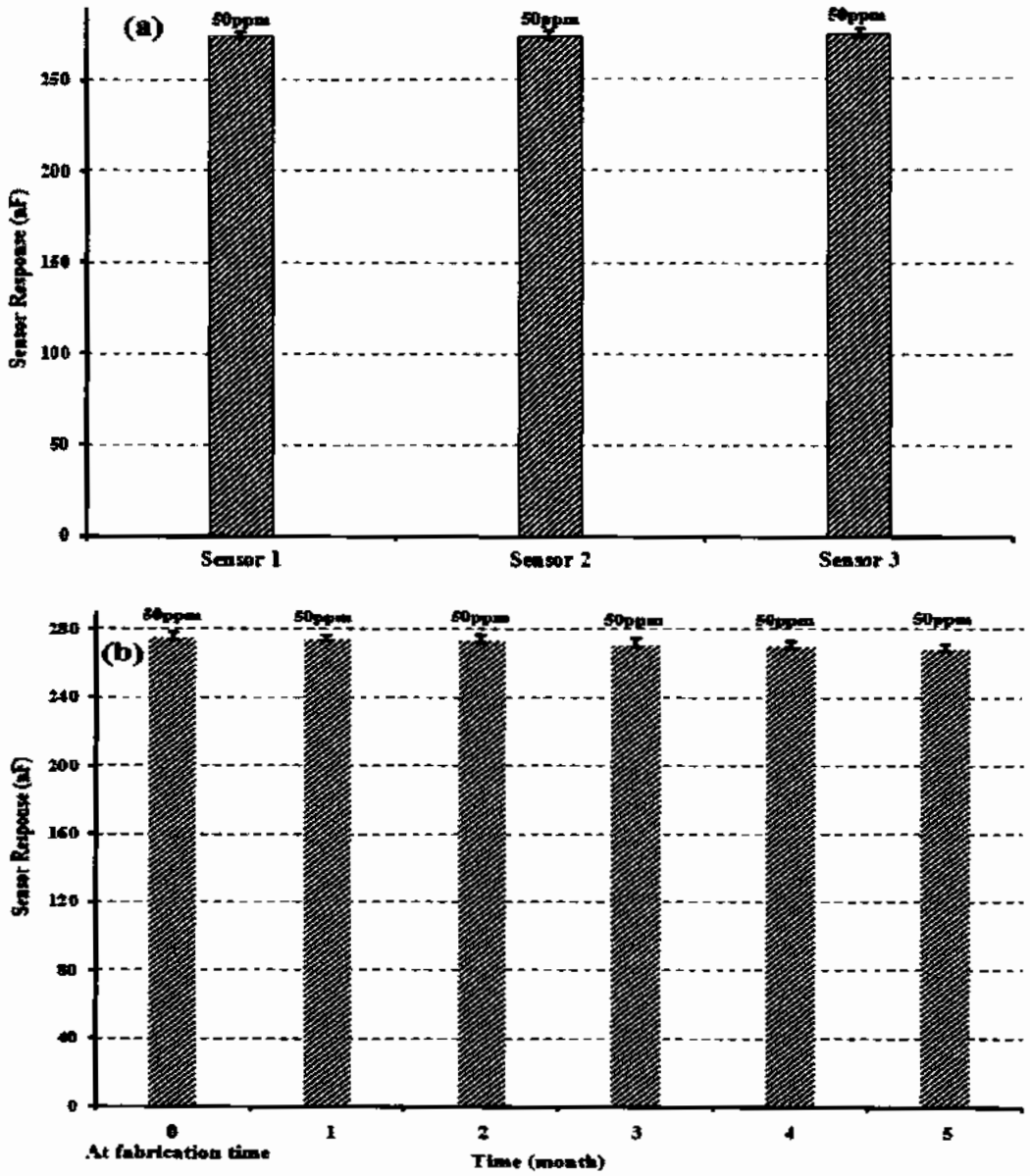

Figure 2.22: (a) Reproducibility and reusability of three polyurethane based glucose sensors prepared in the same manner (b) Stability profile of glucose sensor over the period of six months.

2.3.4 Characterization and sensor measurements of styrene system based receptors

2.3.4.1 Characterization of synthesized receptors by FTIR spectroscopy and scanning electron microscope

To understand the changes in the functional group of NIP, MIP and GO-MIP (graphene composite), FTIR analysis (ATR mode) was performed. FTIR spectra for polystyrene

system was observed in the range from 600-4000 cm^{-1}. The characteristic peak at 900-1100 cm^{-1} indicates the presence of glucose in case of both MIP and GO-MIP whereas absence of this peak in NIP spectra confirms the removal of glucose. The absorption peak at 3000-3400 cm^{-1} was attributed to stretching vibrations of –OH of glucose and confirms the hydrogen bond formation which is absent in NIP. The peak at 2800-2900 cm^{-1} were assigned to the sp^2 (CH) aromatic rings. By comparing the peaks present with MIP and GO-MIP, were found absent in NIP.

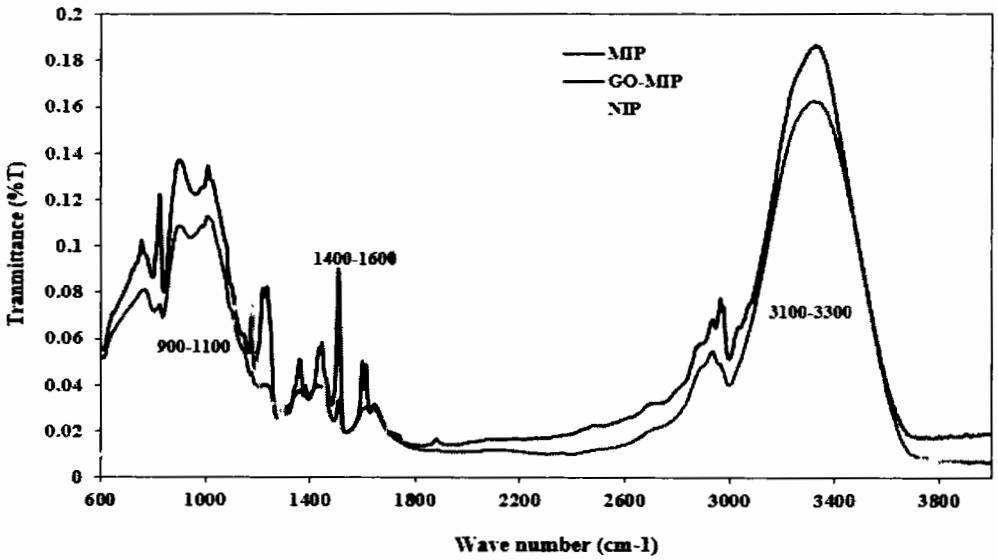

Figure 2.23: FT-IR spectra of non- imprinted and imprinted polystyrene based glucose receptors.

The surface morphology of generated NIP, MIPs and GO-MIPs thin films was assessed by scanning electron microscopy (SEM) and microscopic images of the molecular imprinted polymer and non-imprinted polymer (NIPs) shown in figure 2.24. After the polymerization, template (glucose) molecules were extracted by washing with water which leads to the creation of the template identical moieties within the styrene based polymeric matrices. The micrograph of imprinted polymer showed the surface changes during template molecules removal from polymer matrix and porogenic effect during polymerization while such structures have not been seen in NIP.

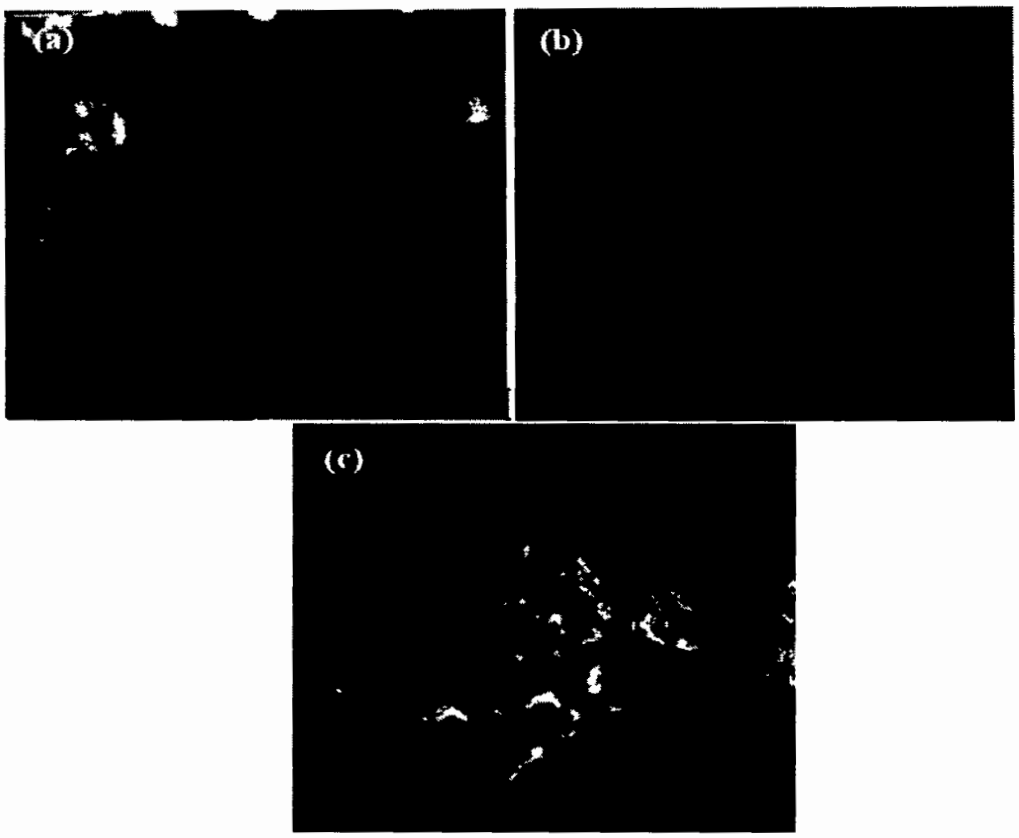

Figure 2.24: SEM images of (a) MIP (b) NIP and (c) GO-MIPs composite of polystyrene based glucose receptors.

2.3.4.2 Thermogravimetric and differential thermal analysis (TGA/DTA)

To determine the stability of non-imprinted, imprinted and GO-MIPs composite, the weight loss and derivative weight loss of NIP, MIPs and GO-MIPs was examined by thermogravimetric and differential thermal analysis (TGA/DTA). In case of 2.25 (a) NIP, weight loss in TGA curve was observed in temperature range of 25 to 600 °C. During the first stage, temperature change starts from 23.22 °C and ends at 302.75 °C with weight loss of -1.579 mg while in the second is -4.007/5.33 mg weight loss. Temperature changes start from 305.10 °C and end at 591.69 °C. The total weight loss in case non-imprinted TGA curve is -5.586/5.33 mg (-104.5 %). In case of 2.25 (b) MIPs, during the first stage, temperature changes start from 29.05 °C and end at 595.63 °C with weight loss of -5.359/5.33 mg (-100.5 %). In case of 2.25 (c) GO-MIPs composite, temperature change starts from 14.52 °C and ends at 596.80 °C with weight loss of -5.462/5.34 g (-102.3 %).

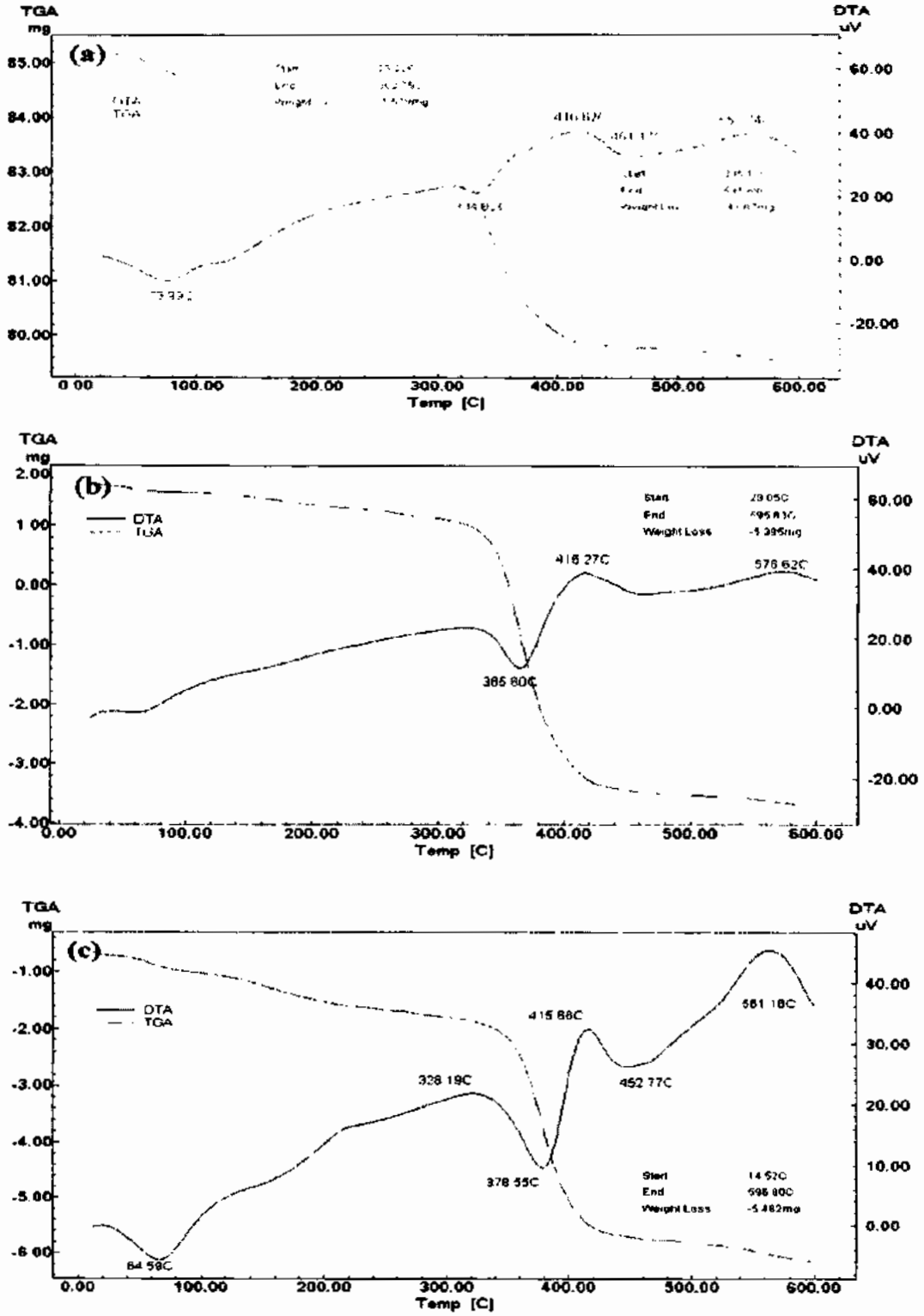

Figure 2.25: TGA and DTA curves of (a) NIP (b) MIPs and (c) GO-MIPs composite of polystyrene based glucose receptors.

These findings from TGA curves indicate that styrene based polymers and their composites are highly stable and can be used for the molecular imprinting of glucose to generated highly selective receptor for sensing purposes.

2.3.4.3 Sensitivity measurements of fabricated sensor

Molecular imprinted polymers (MIPs), coated onto stretchable transducer (IDE) surface bears size identical recognition cavities to bind selectively with template molecules in non-ionic and non-covalent linkages. The incorporation of glucose into cavities from sample solution results in changing the electrical properties of the MIPs layer onto transducer surface. The conductivity of MIPs thin film varies with the variation of incorporation of glucose molecules into recognition sites. Thus, conductance of the MIPs layer is directly related to the incorporated glucose molecules concentration within the polymeric matrix. In order to assess the sensor response towards template molecules, it was exposed to various concentration of glucose solution and sensor responses were observed by measuring sensor signals with the help of high precision LCR meter (IET 7600 Plus precision LCR meter).

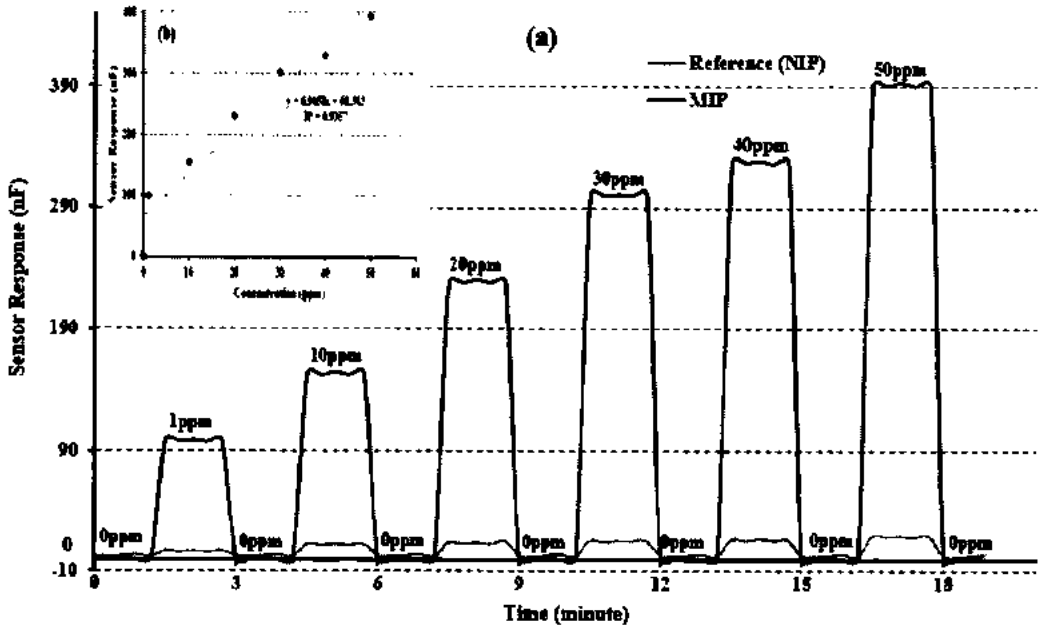

Figure 2.26: (a) Sensitivity response of NIP and MIPs polystyrene based glucose sensor at different concentrations (0-50ppm) and (b) Linear regression analysis of glucose sensor.

The sensor behavior towards the various concentration of glucose in aqueous solution has been shown in figure 2.26 (a). At a concentration of 50 ppm, sensor showed a change in response of 393 nF while the sensor response gradually enhances with the increases in glucose concentration showing the linear behavior. The sensor exhibits an excellent reversibility when subjected to zero concentration of glucose solution. Sensor response of styrene system has been recorded from 1-50 ppm concentration of glucose with lowest limit of detection ~15 ppb and detection range ~15 ppb to 590 ppm. The sensor showed a change in signals from 99.9 nF to 393 nF towards 1 ppm to 50 ppm concentrations of glucose which indicates the concentration dependent linearity of sensor signals which is due to the change in number of glucose molecules incorporated in sensor moieties. Styrene monomer is hydrophobic with no particular functionality and the role it may assist in formation of glucose imprint within polymer matrix where it could exactly fix and organize with the crosslinking agent, EGDMA. It thus induces shape and geometrically fit holes in MIPS that make it capable of selective incorporation of template molecules. While the behavior of sensor with NIPs as recognition materials is not influenced by the change in concentration as can be depicted by figure 2.26 (a). The conductance measurements of sensor responses are performed at pH 7 while the effect of pH can be removed by subtracting NIPs based sensor responses from MIPs based glucose sensor.

To improve the performance and sensitivity of a fabricated sensor, optimizing the structure of imprinted polymer was designed in such a way that recognition cavities should be situated in close proximity and at the surface of polymer material. In order to achieve above goal, the surface area of receptors and interactions between the analyte and sensor receptors were enhanced by combining the MIPs with functionalized graphene. For this purpose, functionalized graphene was added during polymerization. The sensitivity of graphene oxide based composite substantially enhance towards analyte due to the excellent electrical and mechanical properties of functionalized graphene.

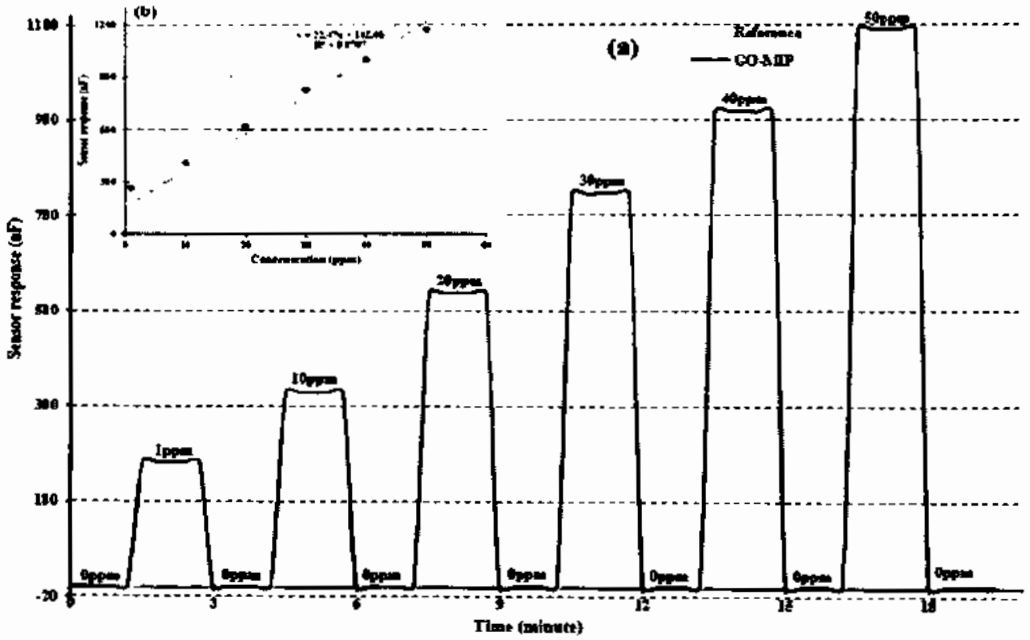

Figure 2.27: (a) Sensitivity response of NIP and GO-MIPs composite of polystyrene based glucose sensor at different concentrations (0-50 ppm) and (b) Linear regression analysis of glucose sensor.

Figure 2.27 shows the sensor response between non-imprinted polymer (NIP) and Graphene oxide composite. Graphene composite enhances the sensor signals ~3 folds with a very lowest limit of detection of 6 ppb and highest detection limit of 600 ppm. It is because of the electrical conductance nature of graphene and excellent increase in surface area of imprinted polymer.

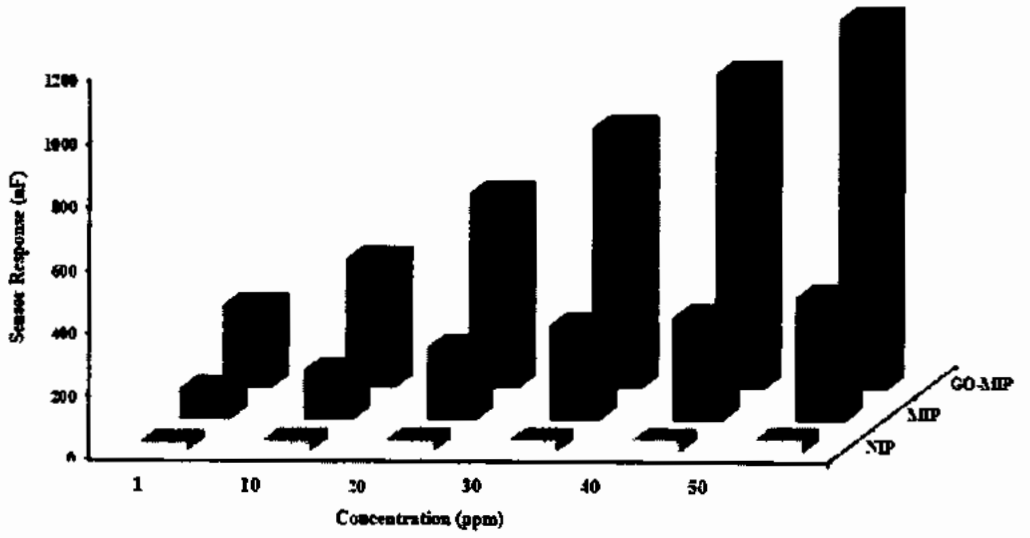

Figure 2.28: Comparison of NIP, MIPs and GO-MIPs composite of polystyrene based glucose sensor at different concentrations (0-50 ppm).

The surface morphological studies showed availability of the high surface area as compared to other polymers which leads to the high sensor response because of glucose-styrene interactions which leads to the maximum adsorption of template molecules. The non-covalent interactions between the template molecules and polymeric matrix may base on the interaction of crosslinking agent and glucose molecules and the OH group present glucose interact with EGDMA while the styrene provides support in form of polymerization to generate cavities within polymer matrix. The possible interactions between template molecules and polymer matrix can be seen in figure 2.28 where dipole-dipole force and hydrogen bonding cause the interaction between template molecule and imprinted cavities.

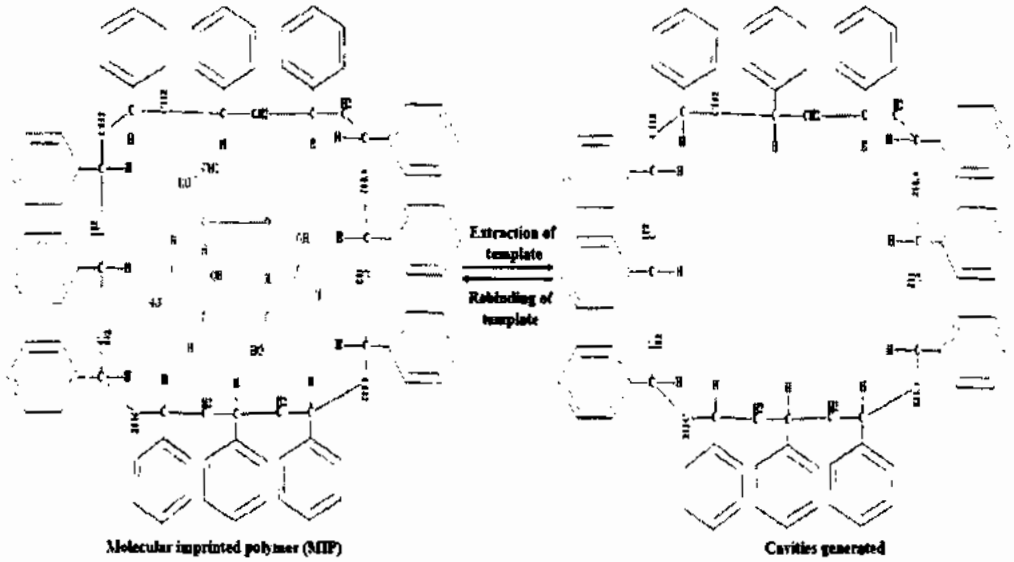

Figure 2.29: The rebinding and removal of template from polystyrene based glucose receptors.

The capability of an analyte to discriminate the other competing molecules having the same size, same structure and similar electro-activity are considered to be an important parameter. Superior response towards specific analyte may be due to molecular imprinting which was generated by key and lock mechanism.

2.3.4.4 Selectivity analysis of sensor

Selectivity analysis is a characteristic feature of bulk imprinting polymer; this is the reason this technique is applied to impart selectivity to polymer towards the template molecules. The cavities synthesized after the removal analyte are complementary to the

imprinting species in size, shape and coordination geometries which leads to substantial selectivity of fabricated sensor. The sensor selectivity response demonstrates whether a fabricated sensor is suitable for the sample, in which number of competing molecules with highly identical mass, structure and chemical properties are present along with the analyte of interest. Therefore, it is important to analyze if the sensor is selective for the molecule of interest or not.

Polystyrene based molecular imprinted glucose sensor was exposed to the complex mixture of different molecules which are also present in blood such as amino acid, lipids, globulin, fibrinogen, defense compounds such as lysozymes (polysaccharide), urea, uric acid, glycerol and an anti-coagulant heparin. It shows the highly selective and sensitive behavior against these competing molecules. There was no marked difference between the results obtained by different concentrations of analyte and complex mixture (blood). Furthermore, the selectivity behavior of glucose sensor was assessed by exposing the sensor towards the different competing agents which have almost identical molecular mass or similar number of carbon chain or functionalities i.e. maltose, sucrose, n-hexane etc.

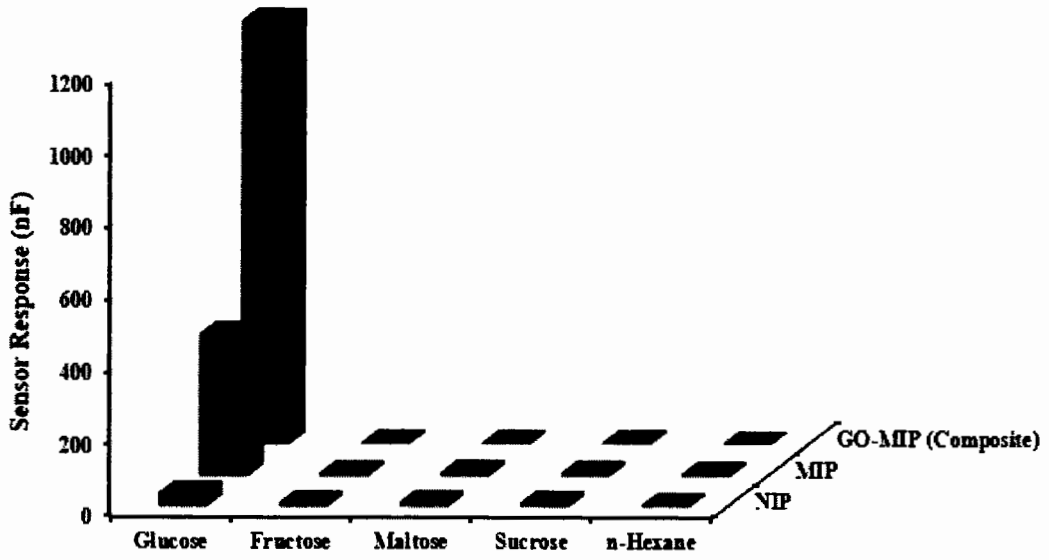

Figure 2.30 : Selectivity of imprinted polystyrene based glucose sensor against different competing molecules at 50 ppm.

The fabricated sensor showed the sensor signals of 393nF for MIP and 1171 nF for GO-MIP composite. Graphene composite based sensor was observed as highly sensitive

and selective for the interfering molecules, 5 nF, 5 nF 6 nF and 3 nF towards glucose, maltose, sucrose and n-hexane respectively. The glucose and maltose both are monosaccharide but differ in their structures but the sensor signal of sensor towards glucose is higher by the factor of almost 234 while n-hexane with similar number of carbon atoms differ by factor of 390. On the other hand, sucrose being disaccharide with double number of carbon atoms have negligible influence on the sensor signals. It could be clearly seen from the figure 2.30 that the sensor is highly selective for glucose and shows many folds more selective signals as compared to other competing species.

2.3.4.5 Reproducibility, stability and reusability

To further investigate the repeatability and long term stability of a graphene oxide based sensor, the sensor sensitivity profile was assessed every three months for a period of six months by exposing the sensor to similar concentration of glucose as shown by figure 2.31 (a). The obtained relative standard deviation (RSD) of 0.32 % signifies the effective repeatability of 50ppm concentration with continuous usage. In addition, 99.5 % of sensor response was maintained which also indicate that glucose GO/MIP based sensor possesses excellent repeatability and reproducibility.

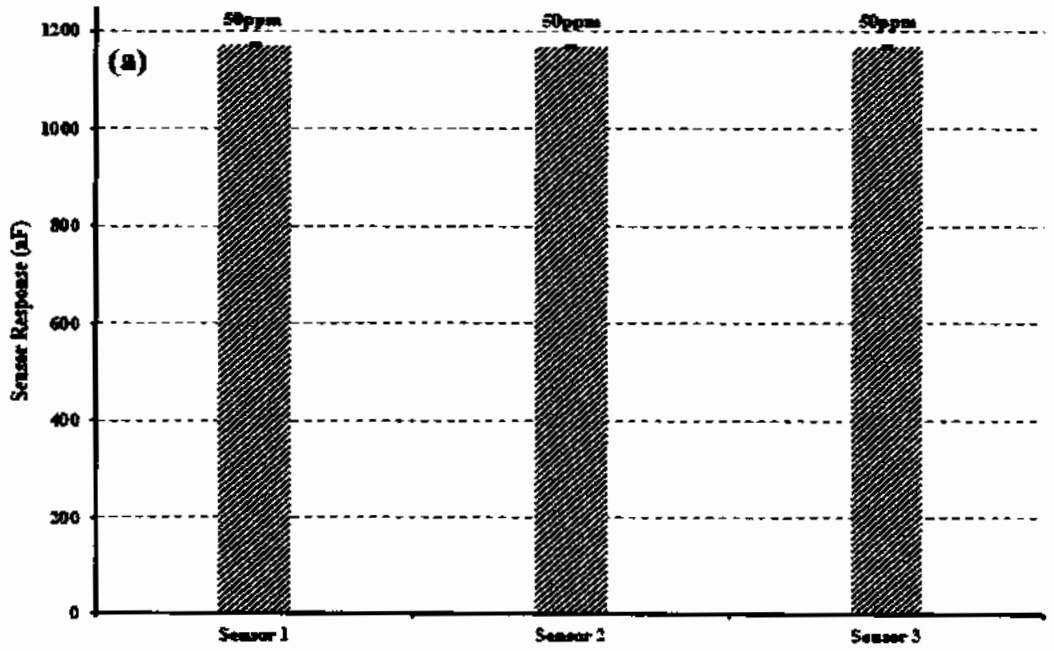

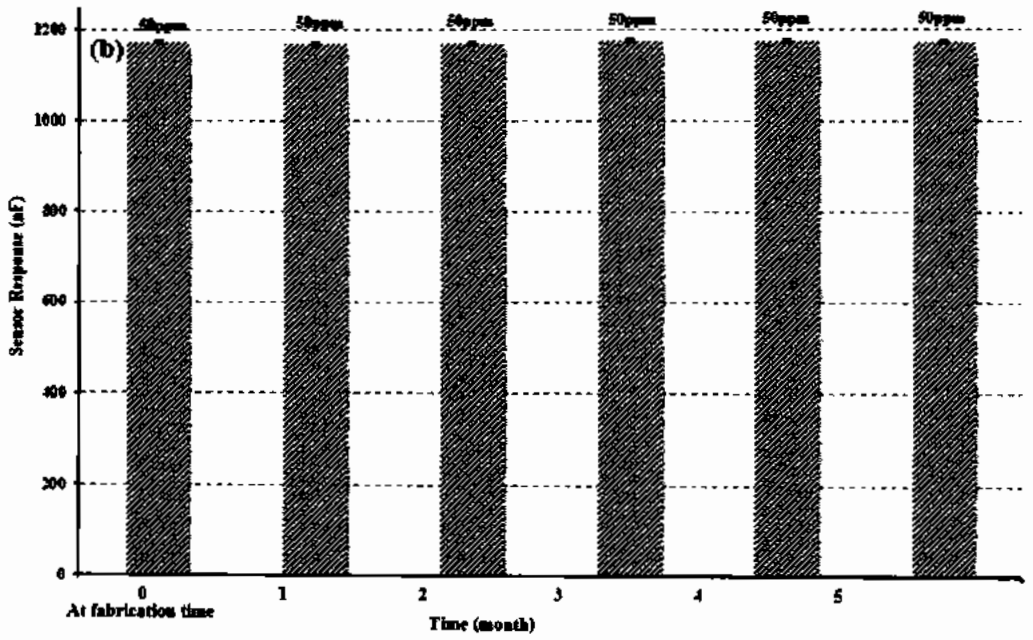

Figure 2.31: (a) Reproducibility and reusability of three polystyrene based glucose sensors prepared in the same manner (b) Stability profile of glucose sensor over the period of six months.

The sensitivity response of these different electrochemical sensors was estimated with 50 ppm concentration of glucose. The calculated relative standard deviation of 0.18 % indicated that the reproducibility response of currently designed sensors was not significantly different as can be seen in figure 2.31 (b).

2.4 Comparison of sensor receptors (imprinted vinyl pyrolidone, methacrylic acid, urethane and styrene)

Different molecularly imprinted polymer systems such as polyvinyl pyrolidone, polyacrylic acid, polyurethane and polystyrene were fabricated and used as sensor receptors to enhance the sensor efficiency. NVP as monomer showed lower sensor response which might be due to insufficient incorporation tendency of template molecules in NVP system that results in less number of cavities present on the bulk of polymer matrix. Methacrylic acid exhibited efficient imprinting using MAA monomer, had a strong influence on adsorption of the template used to prepare hydrophobic polymer matrix. When template is a polyhydroxy molecule, then there might be the possibility of stronger hydrogen bonding interactions with methacrylic acid as

monomer, a major reason for the increased sensor response. Polyurethane system was also assessed to enhance the sensor signals. Polyurethane as monomer has proton donor groups (N-H or O-H) as well as the lone pair donor groups (C=O). The proton donor group in this polymer matrix may interact with template molecule by forming H-bonding with electron donor groups (C=O). while the electron pair donor groups of polymer as well as template may interact with each other and enhances the sensor signals.

The highest sensor response was noted with polystyrene based system as shown in figure 2.32. On the basis of the polystyrene structure and functionalities it might be assumed that cavities generated in polystyrene system are more stable due to stronger interactions between template and polystyrene than other monomers. The stability of styrene system based polymer might be higher due to the aromatic nature of benzene ring present in styrene. The sensor response of GO-MIP composite based sensor was found ~3 folds higher than simple MIPs of styrene due to the excellent mechanical and electrical properties of functionalized graphene.

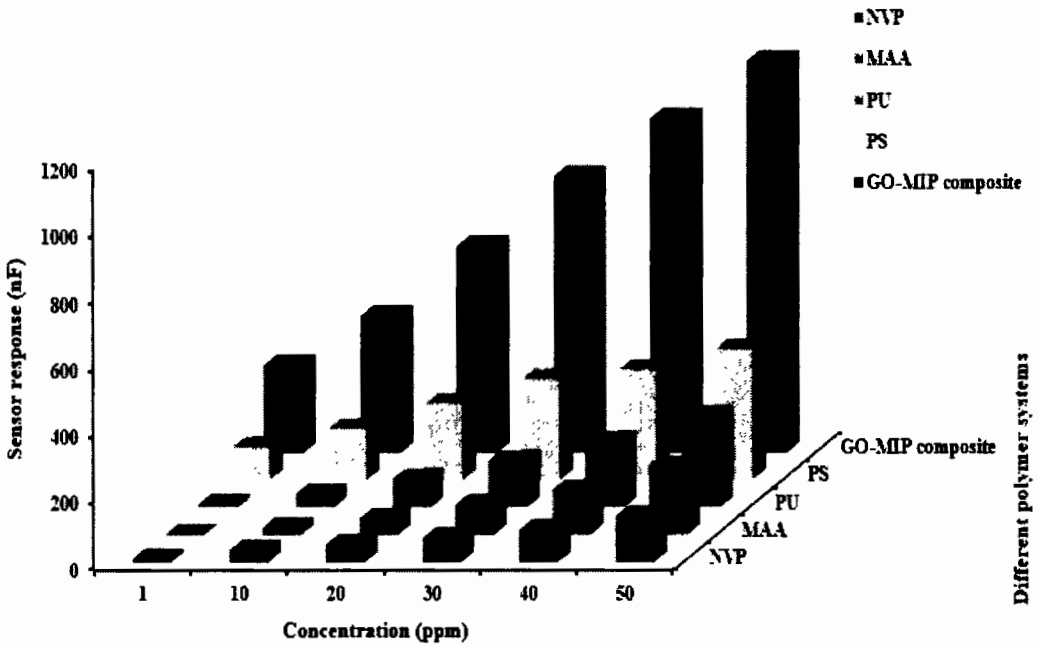

Figure 2.32: Comparison of different systems used for the detection of glucose at different concentrations.

Due to the hydrophobic nature of styrene, it may impart an important role in polymer synthesis to form an imprinted polymer of glucose where it could be helpful to

specifically fix and co-ordinate with the cross-linker i.e. EGDMA. It thus induces the geometric key and lock geometry of imprinted polymer which enables the polymer matrix for selective adsorption of templated molecule. It is also of substantial importance from the above mentioned results that polystyrene based polymer showed the higher sensor effect as compared to other monomers because of its aromaticity and functionality. Table 2.1 shows the results of different polymer systems discussed in chapter 2.

Table 2.1: Comparison of results with previous reported literature.

Analyte	Detection method	Technique	Range of detection	Reproducibility (RSD)	Reference
Glucose	Non-enzymatic	Cyclic voltammetry (CV)	1 µM-25 mM	5 %	(Cho, Noh et al. 2018)
Glucose	Non-enzymatic	Electrosensor cyclic voltammetry	0.5-4.4 mM	≤6 %	(Farid, Goudini et al. 2016)
Glucose	Non-enzymatic	Cyclic voltammetry (CV)	0.1-6 mM	1.8 % (95.5 % RSR)	(Alexander, Baraneedharan et al. 2017)
Glucose	Non-enzymatic	CV and Electrochemical impedance spectroscopy (EIS)	0.8-4 mM	14.57 % (84.11 % RSR)	(Wu, Tian et al. 2019)
Glucose	Non-enzymatic	CV and Electrochemical impedance spectroscopy (EIS)	50-600 µM	2.7 % (87.8 % RSR)	(Zheng, Wu et al. 2018)
Glucose	Non-enzymatic	CV	1-15 mM	2.29 % (96.93 % RSR)	(Xu, Niu et al. 2018)
Glucose	Non-enzymatic (NVP as monomer)	Conductance	136 ppb-500 ppm (~2 seconds)	1.5 % (98.4 % RSR)	Present work

Glucose	Non-enzymatic (MAA as monomer)	Conductance	115 ppb-500 ppm (~2 seconds)	1.38 % (98.8 % RSR)	Present work
Glucose	Non-enzymatic (DPDI as monomer)	Conductance	71 ppb-500 ppm (~2 seconds)	1.36 % (98.3 % RSR)	Present work
Glucose	Non-enzymatic (styrene as monomer)	Conductance	15 ppb-590 ppm (~2 seconds)	-	Present work
Glucose	Non-enzymatic (Styrene + GO as monomer)	Conductance	6 ppb-600 ppm (~2 sec)	0.32 % (99.5 % RSR)	Present work

2.5 Conclusion

In this chapter, MIPs and their composites have been synthesized using different monomers and the measured sensor responses of n-VP, MAA, urethane and styrene imprinted polymer systems were in the following order: n-VP < MAA < PU < Styrene. The surface morphology of styrene based glucose imprinted receptors depicts the uniform generation template identical cavities as compared to other polymers. Furthermore, to enhance the sensor response, graphene oxide composites of styrene based receptors were synthesized. It was found that graphene oxide based sensor responses are many folds higher as compared to that of imprinted polymers. We can conclude that styrene system is most suitable for the imprinting of glucose and bears high sensitivity and selectivity. While the composite of imprinted polystyrene with functionalized graphene induces higher incorporation and moieties for the template molecules and produced substantial higher sensor response. Hence the sensitivity, selectivity, limit of detection and stability of the fabricated sensor is improved by using MIPs-GO composite and it can have potential technological applications in field of chemical sensors and material science.

3 Chapter 3 FABRICATION OF MOLECULARLY IMPRINTED POLYMERS AND NANOCOMPOSITE BASED SENSORS FOR THE DETECTION OF FRUCTOSE

3.1 Introduction

Fructose, a monosaccharide that is naturally present in fruits, vegetables and other foods e.g. honey, sugar cane, beet root etc. Fructose was discovered by a French Chemist; Augustin Pierre Dubruntfaut in 1947 and is also known as ketose that mostly crystalizes as β-fructopyranose possess five hydroxyls as hydrogen bond acceptor and six hydrogen bond donors as shown in figure 3.1. Due to its sweetness and low cost, glucose syrup is termed as high fructose corn syrup (HFCS). Since 1970s, it was used for synthetic products in which liquid sugar was required and 42 % fructose was used on the first generation of HFCS. The second generation was developed in 1976, fructose percentage was between 55 % and 90 % of the compounds (Carvalho, Souza et al. 2018).

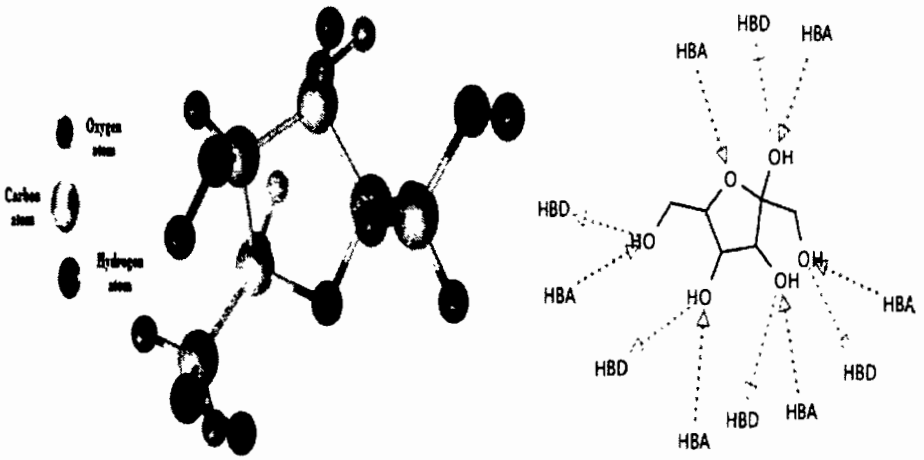

Figure 3.1: 3D structure of Fructose (HBA = Hydrogen bond acceptor, HBD = Hydrogen bond donor)

Since 1960s, fructose intake is increasing fastly and presently, individual intake is assessed to be 50 to 70 g of fructose daily accounting for 10 to 15 % of the total dietary caloric intake. High consumption of fructose is resulted in severe public health issues such as several metabolic disorders, including obesity, non-alcoholic fatty liver disease, and cardiovascular diseases (Villegas, Rivard et al. 2018). Therefore, rapid and efficient quantification of fructose in urine and blood is of great importance from diagnostic point of view for the diagnosis of different diseases related to blood and urine fructose level in body. Numerous methods are in practice for the detection of fructose in diet, beverages, urine and blood namely; chromatography (Kirchert and Morlock 2018),

spectrophotometry (de Souza Costa, de Paula et al. 2019), surface enhanced raman scattering (Perumal, Balasundaram et al. 2015), colorimetry (Xiong, Zhang et al. 2015, Liu, He et al. 2016) and electrochemical methods (Barman, Hossain et al. 2018; Dhara and Mahapatra 2018, He, Tian et al. 2018). These methods are complicated, costly and involve several steps during sample preparation and analysis therefore, among these methods, electrochemical sensor become more popular owing to its fast response, high sensitivity, easy operation, portability and due to miniature size. Sensor receptors play key role for the selective detection of analyte of interest and molecular imprinted polymer (MIPs) owning high sensitivity and selectivity (Kubo, Tachibana et al. 2018) properties, are of great worth due to high stability, specificity and reusability. Molecular imprinted polymer based electrochemical sensors (MIECS), a combination of molecular imprinted technique (MIT) and electrochemical sensors which are widely favored in chemistry field (Zheng, Wu et al. 2018). In this chapter, different MIPs based electrochemical sensors were fabricated by using n-vinyl pyrolidone (VP), urethane (DPDI), methacrylate (MAA) and styrene (Sty) polymer systems as sensor receptors and their sensitivity, selectivity, response time, stability, LoD, regeneratability etc. were assessed at room temperature and pressure conditions by exposing to various concentrations of fructose and other competing agents. Furthermore, composite of most suitable imprinted polymer system (acrylate system) with functionalized graphene was also synthesized to achieve the high sensitivity of fabricated sensor.

3.2 Experimental section

3.2.1 Chemicals and materials

Glucose (99.5 %), sucrose (99 %), maltose (99 %), fructose (99 %), dimethyl sulphoxide (DMSO, 99.7 %), n-vinyl pyrolidone (99 %), 4, 4′diphenylmethanediioscyanate (DPDI; 98 %), phloroglucinol (PG; 99 %), bisphenol A (BPA; ≥99 %), chloroform, methacrylic acid (MAA; 99 %), styrene and 2,2′-azobisisobutyronitrile (AIBN; 99 %) and ethylene glycol dimethacrylate (EGDMA; 98 %), acetone (≥ 99 %), methanol (99.8 %, anhydrous), ethanol (99.8 %, anhydrous) were purchased from Merck and Sigma Aldrich with the maximum available purity.

3.2.2 Synthesis of n-vinyl pyrolidone based molecularly imprinted polymer (VP-MIP)

Poly(vinylpyrolidone) MIP was synthesized by adding 3.1×10^{-4} mM of Vinyl pyrolidone, 3.3×10^{-4} mM of EGDMA were mixed into an eppendorf having 500 µL (4 mmole fructose solution in DMSO) of fructose solution. After homogenizing 4 mg of AIBN was added to above mixture and vortex. The resultant solution was heated to 60 °C for 45 minutes in water bath till a transparent gel point was attained.

3.2.3 Synthesis of non-imprinted polymer (NVP-NIP)

NVP-NIP was prepared without adding template (fructose) molecule in the same way as MIP was synthesized. Fructose NIP was synthesized by adding 3.3×10^{-4} mM of Vinyl pyrolidone, 3.3×10^{-4} mM of EGDMA were mixed into an eppendorf having 500 µL DMSO. After homogenizing 4 mg of AIBN was added and vortex the above mixture. The resultant solution was heated to 60 °C for 45 minutes in water bath till a transparent gel point was attained.

3.2.4 Synthesis of polyurethane based molecularly imprinted polymer (PU-MIP)

Polyurethane based maltose imprinted receptors were synthesized using 40 to 60 ratio between monomer and cross-linker. Urethane based receptors were synthesized by 1.9×10^{-6} mM of phloroglucinol (PG), 8×10^{-4} mM of bisphenol A and 3.6×10^{-4} mM of DPDI was vortexed in 1 mL of DMSO. Fructose (2 mmole) was added and homogenized by vortex. The resultant solution was heated for 30 minutes at 45 °C in water bath till gel point was obtained which indicated the synthesis of maltose imprinted polymer.

3.2.5 Synthesis of non-imprinted polymer (PU-NIP)

PU-NIP was also prepared in the same way without adding fructose as template molecule. Polyurethane based maltose imprinted receptors were synthesized using 40 to 60 ratio between monomer and cross-linker. Urethane based receptors were synthesized by 1.9×10^{-4} mM of phloroglucinol (PG), 8×10^{-4} mM of bisphenol A and 3.6×10^{-6} mM of DPDI was vortexed in 1 mL of DMSO and homogenized by vortex.

The resultant solution was heated for 30 minutes at 45 °C in water bath till gel point was obtained which indicated the synthesis of maltose imprinted polymer.

3.2.5 Synthesis of styrene based imprinted polymer (PS-MIP)

Styrene Styrene (3.4×10^{-4} mM), 3.3×10^{-4} mM of ethylene glycol dimethacrylate (EGDMA), 2 mg of AIBN as free radical initiator were mixed into an eppendorf tube. To the above solution, 500 µL of dimethyl sulfoxide (DMSO) as solvent and 2 mg of fructose (2 mM) were added and homogenized by vortex. Then mixture was polymerized into water bath at 70 °C for 45 minutes till transparent gel point is reached.

3.2.6 Synthesis of non-imprinted polymer (PS-NIP)

Non-imprinted polymer (reference) was also synthesized exactly in the same way without adding template (fructose). Styrene (3.4×10^{-4} mM), 3.3×10^{-4} mM of ethylene glycol dimethacrylate (EGDMA), 2 mg of AIBN as free radical initiator were mixed into an eppendorf tube. To the above solution, 500 µL of dimethyl sulfoxide (DMSO) as solvent and homogenized by vortex. Then mixture was polymerized into water bath at 70 °C for 45 minutes till transparent gel point is reached.

3.2.7 Synthesis of methacrylic acid based molecularly imprinted polymer (MAA-MIP)

Imprinted polymer was synthesized by mixing 4.1×10^{-4} mM of methacrylic acid (MAA) as functional monomer, 3.3×10^{-4} mM of EGDMA as cross linker, 4 mg of AIBN as free radical initiator and 500 µL of DMSO as solvent. Fructose (2 mM) was added to the above mixture as template. The mixture was vortex for 5 minutes to homogenize and then place in water bath at 60 °C for 45 minutes to polymerize.

3.2.8 Synthesis of non-imprinted polymer (MAA-NIP)

MAA-NIP was also prepared in the same way without adding template (fructose) molecule same as above mentioned. Imprinted polymer was synthesized by mixing 4.1×10^{-4} mM of methacrylic acid (MAA) as functional monomer, 3.3×10^{-4} of EGDMA as cross linker, 4 mg of AIBN as free radical initiator and 500 µL of DMSO as solvent. The mixture was vortex for 5 minutes to homogenize and then place in water bath at 60 °C for 45 minutes to polymerize.

3.2.9 Synthesis of methacrylic acid graphene oxide based molecularly imprinted composite (MAA-GO-MIP)

Graphene oxide composite of molecularly imprinted methacrylic acid was synthesized by adding 0.5 mg of graphene oxide in 600 µl of imprinted MAA and a suspension of composite was prepared by sonication.

3.2.10 Immobilization of receptors (MIPs, NIPs and Composite) onto IDEs

Interdigital electrode (IDE) with electrodes spacing (l= 0.5' and number of fingers=18) was used as transducing surface for sensor measurements. IDEs were cleaned by washing with de-ionized water followed by methanol. 15 µL of imprinted polymer (MIP) was coated onto IDEs by spin coating at a speed of 2500 rpm as shown in figure 2.2. The IDEs were dried in an oven overnight to achieve dry and compact polymer thin film.

3.2.11 Removal of template from MIPs

To remove the template molecule (fructose) from imprinted polymeric matrix, IDEs were washed with deionized water with continuous stirring for 90 minutes by using magnetic stirrer at room temperature. After washing out the template molecules from polymer thin films, template size identical cavities were achieved.

3.2.12 Characterization of receptors with fourier transform infra-red (FTIR)

FTIR spectra of thin films of all molecular imprinted polymers (MIPs), non-imprinted polymer (NIPs) and graphene oxide based composite (GO-composite) were recorded by using Shimdazu-1800 S FTIR in the range of 4000-500 cm^{-1}.

3.2.13 Characterization of receptors with scanning electron microscope (SEM)

SEM images of receptor's thin films were attained by scanning electron microscope (LEO DSM 892Gemini) equipped with energy dispersed X-ray EDX analyzer.

3.2.14 Differential thermal and thermogravimetric (DTA/TGA) analysis of receptors

Differential thermal and thermogravimetric analysis was carried out by using STA PT1000 TG-DSC (STA Simultaneous Thermal Analysis) STA (TGDSC/DTA) Thermogravimetric Analyzer (Linseis Thermal Analysis, Germany) with detector DTG-60 H (detector serial number C30574700276TK) at a heating rate of 10 °C/min under air atmosphere. The temperature range was fixed from 0 °C to 600 °C.

3.3 Results and Discussions

3.3.1 Characterization and sensor measurements of n-vinyl pyrolidone system based receptors

3.3.1.1 Characterization of synthesized receptors by FTIR spectroscopy and scanning electron microscope

To study the functional group modification of receptor thin films, FTIR analysis of MIP (molecular imprinted-VP) based receptors was performed as shown in figure 3.2. FTIR spectra was found in the range from 700-3700 cm^{-1} and major peaks in spectra confirmed that MIP receptors of fructose were synthesized by free radical polymerization of EGDMA and VP.

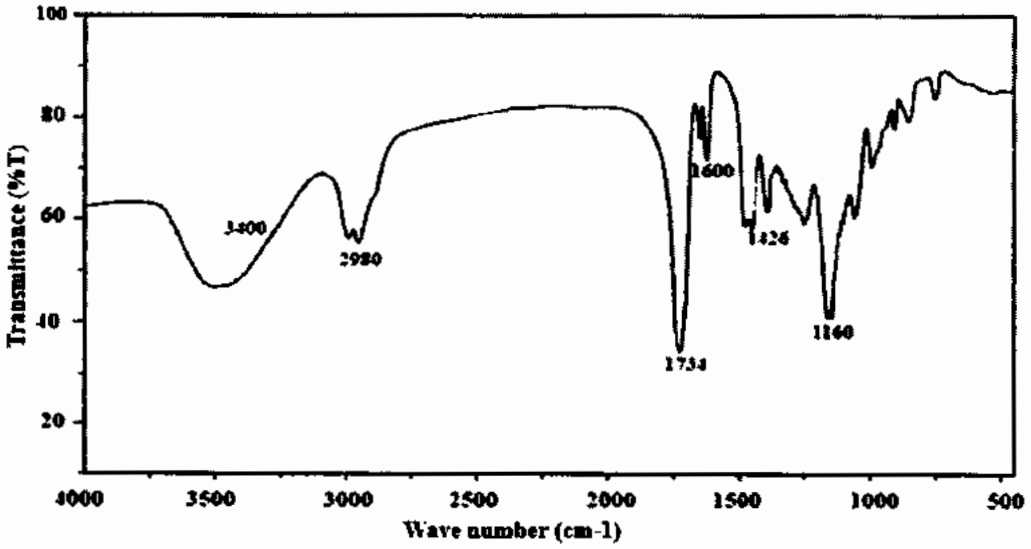

Figure 3.2: FT-IR spectra of imprinted polyvinyl pyrolidone based fructose sensor.

In imprinted-VP spectra, the characteristic peak occurs at 2980 cm^{-1} due to stretching of sp^3 CH and stretching of C-O was found at 1160 cm^{-1}. The peaks obtained at 1600 cm^{-1} and 1425 cm^{-1} are due to C=N, C=C corresponded to stretching of pyridine group present in n-vinylpyrolidone.

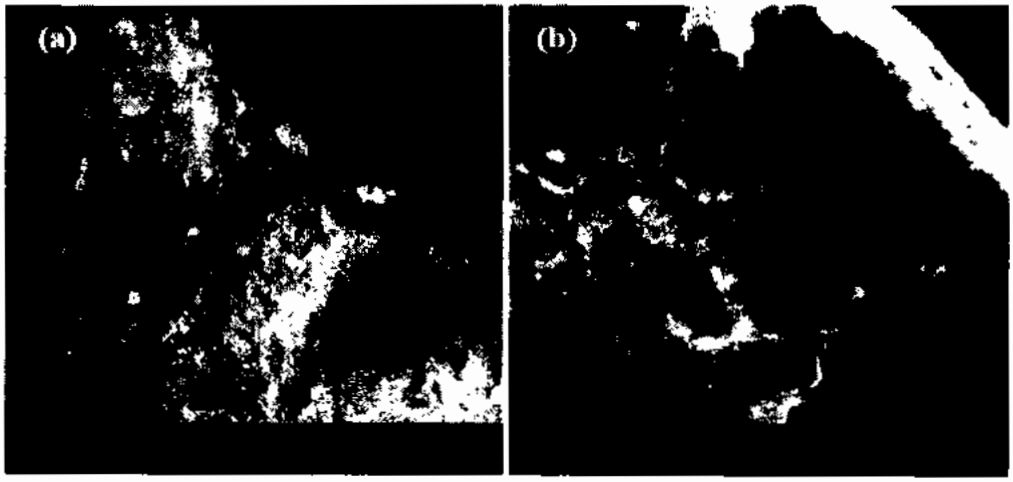

Figure 3.3: SEM images of (a) NIP and (b) MIP of polyvinyl pyrolidone based fructose receptors.

To assess the surface morphology of thin films of imprinted and non-imprinted receptors, scanning electron microscope was used. For this purpose, thin films of the MIPs and NIPs were generated onto a glassy substrate and the SEM images of MIPs and NIPs are shown in figure 3.3. A homogeneous, porous and rough morphology with uniform distribution can be observed from the topographical view of MIPs images. These images showed that both NIP and MIP have different morphology due to the presence and absence of template molecule. Different morphology of both MIP and NIP indicated the successful polymerization of polymers.

3.3.1.2 Sensitivity measurements of fabricated sensor

After coating of fructose imprinted polymer onto IDEs and washing to generate cavities within polymeric matrix, the sensor was exposed to various concentrations (0, 1, 5, 10, 20, 30, 40 and 50 ppm) of fructose to assess its sensitivity profile.

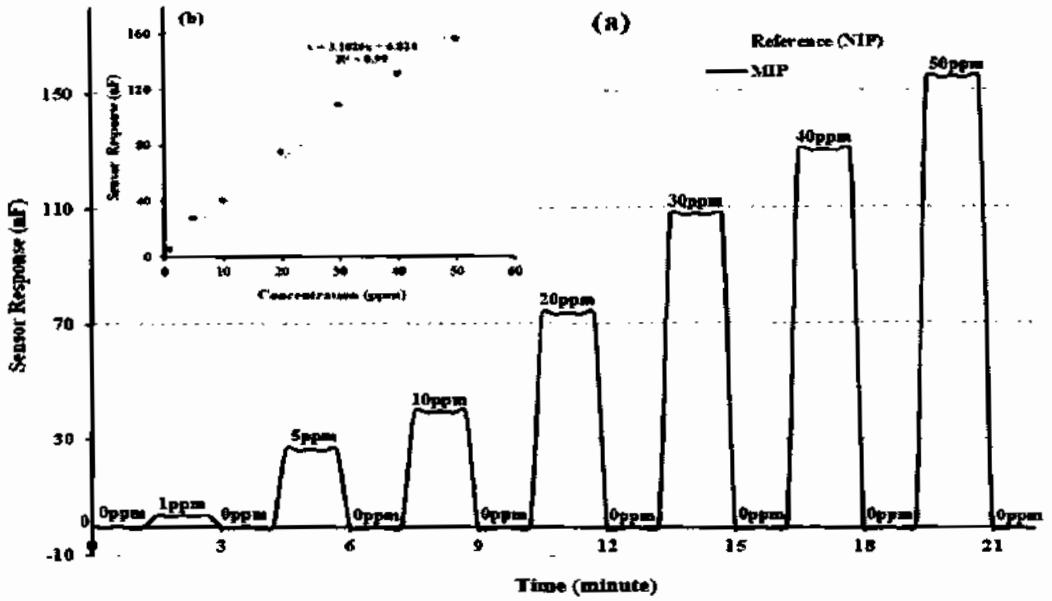

Figure 3.4: (a) Sensitivity response of NIP and MIP of polyvinyl pyrolidone based fructose sensor at different concentration (0-50 ppm) and (b) Linear regression analysis of fructose sensor.

After washing the sensor with water, its response again reaches to its initial value which means the sensor shows complete reversibility and regeneratability. While the sensor possesses the lower limit of detection (LoD) of 300 ppb towards the fructose. At 0 ppm, the observed capacitance was 0 and at 1 ppm, 5 ppm, 10 ppm, 20 ppm, 30 ppm, 40 ppm and 50 ppm of maltose the sensor responses of 5 nF, 28 nF, 41 nF, 75 nF, 109 nF, 131 nF and 156 nF have been observed respectively. The obtained electrochemical results demonstrated that newly fabricated sensor was highly sensitive even at very low concentration of 1 ppm as shown in figure 3.4 (a). The NIP was also exposed to the same concentrations of analyte and sensor signals were found very less. The linearity of sensor was assessed by linear regression analysis of obtained sensor responses at different concentrations of analyte (0-50 ppm) with range of detection ~300 ppb to 500 ppm and the sensor showed linear response with a linear co-efficient of regression (R^2) of value 0.99 as can be seen in figure 3.4 (b).

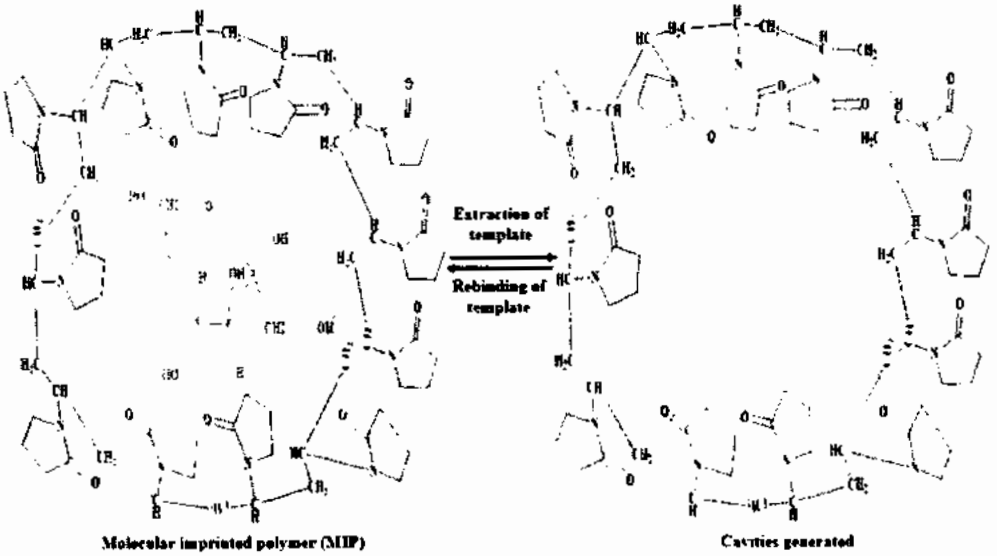

Figure 3.5: The extraction and rebinding of template from n-vinylpyrolidone based imprinted polymer.

The non-covalent interactions between the template molecules and polymeric matrix may be on the basis of interaction between functional monomer and fructose, the OH group present on fructose interact with carbonyl group of n-vinyl pyrolidone while EGDMA provides support for polymerization to generate cavities within polymer matrix. The possible interactions between template molecules and polymer matrix can be seen in figure 3.5 where dipole-dipole force and hydrogen bonding cause the interaction between template molecule and imprinted cavities.

3.3.1.3 Selectivity analysis of sensor

Selectivity is a fundamental parameter of chemical sensor for the detection of analyte of interest. Selectivity response of fructose sensor was checked against different competing molecules such as glucose, maltose, sucrose and n-hexane at 50 ppm concentration of each as can be seen in figure 3.6. The cavities present in MIPs bear structural resemblance with fructose molecules thus showed highest affinities towards fructose due to key-lock phenomenon as compared to other competing species.

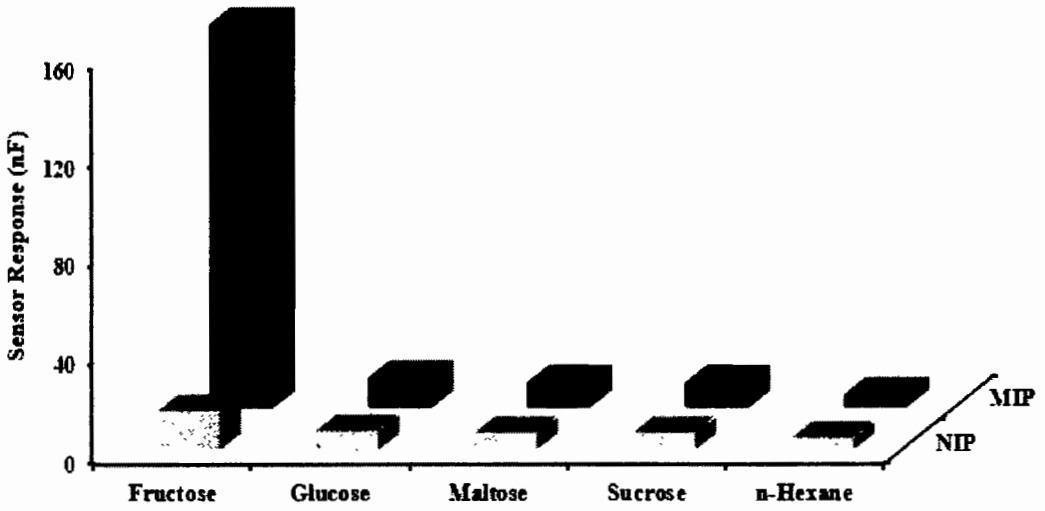

Figure 3.6 : Selectivity analysis of n-vinyl pyrolidone based fructose sensor against different competing molecules at 50 ppm.

While the other competing species have no structural and 3-dimensional resemblance with cavities present in sensor receptors therefore these molecules were unable to fit-in MIPs cavities. It showed that fabricated sensor is highly selective towards template molecule as compared to other competing species. The sensor response showed by fructose is higher by the factor of 13 as compared to glucose while both have the similar number carbon atoms and their molecular weight is also same. Glucose and fructose differ only in their structure and the spatial arrangements of functional groups and this substantial difference between the sensor responses against both confirm the governing of key-lock rule exhibit by molecular imprinted polymers. In the case of maltose and sucrose, sensor response is 16 folds lower due to the structural difference and conductivity of interfering molecules. Sucrose and maltose are bulky molecules than fructose because these are the disaccharides. Fructose sensor also has high selectivity co-efficient as compare to n-hexane which is attributed by structural resemblance. Hexane molecules may also be entrapped in the selective cavities of template i.e. fructose due to its smaller size.

3.3.1.4 Reproducibility, reusability and stability

An ideal sensor must be reproducible, highly stable and reusable for pharmaceutical and food industries. Reproducibility of a fabricated sensor is determined by measuring

the sensor response repeated under same experimental conditions while at different time.

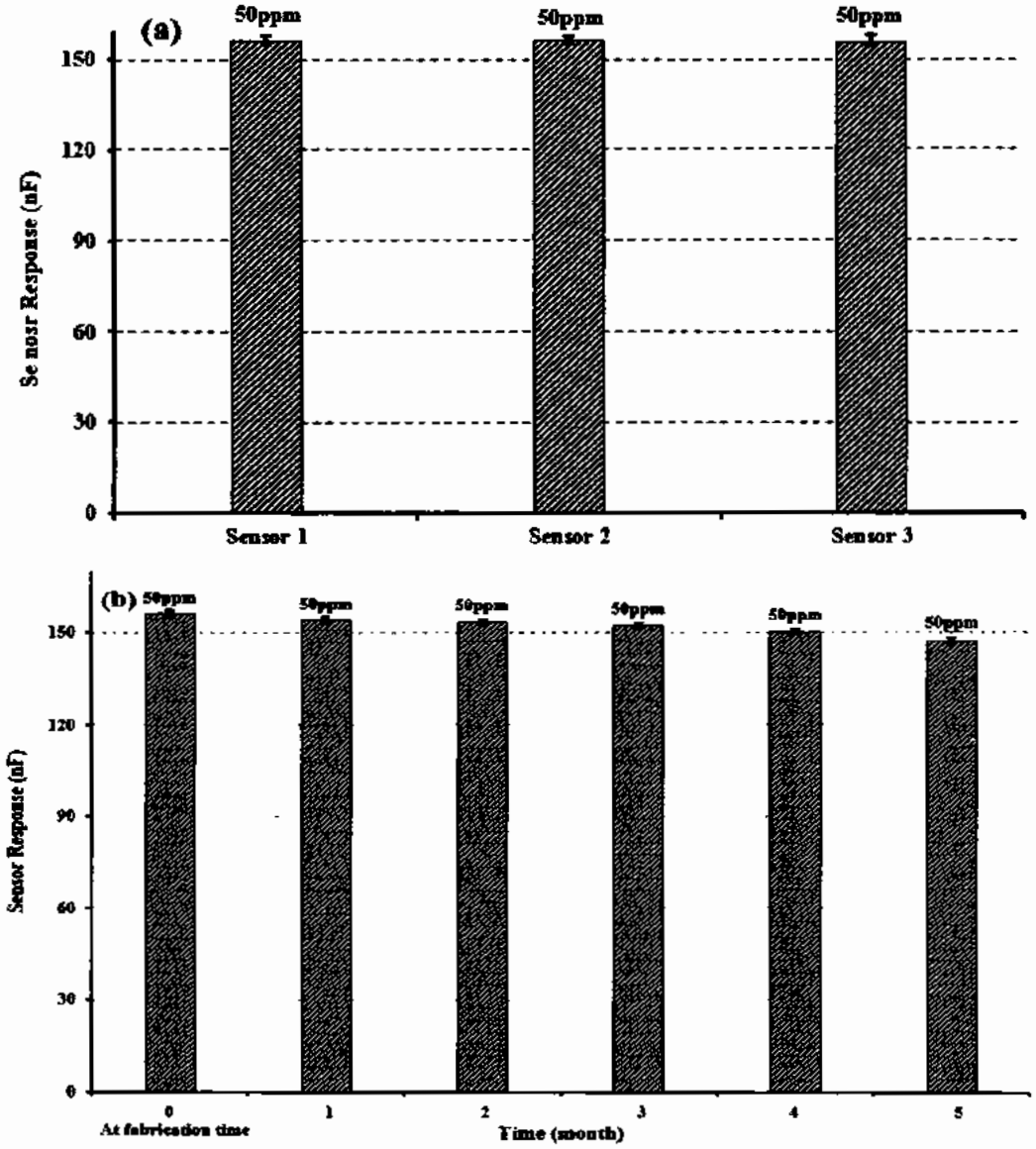

Figure 3.7: (a) Reproducibility and reusability of three vinyl pyrolidone based sensors prepared in the same manner (b) Stability profile of sensor over the period of six months.

Stability of a sensor is a parameter that measures the reproducibility of a fabricated device measurements after long use. Reproducibility and stability are the most important parameters for chemical sensor practical applications. The regeneratability and reproducibility was also checked for the fructose sensor. To assess reproducibility, three different sensors were developed by using the same procedure and exposed them to 50 ppm concentration of analyte (fructose). At different time, three different sensors

showed different response under same experimental conditions as depicted in figure 3.7 (a).

These observations confirmed the regeneratability and reproducibility of proposed glucose sensor by 2 % RSD value (n= 6) with retained sensor response of 97 % indicating that MIP based fructose sensor possesses excellent stability, reproducibility and regeneratability. Furthermore, the stability of six different fructose imprinted sensors was checked using relative standard deviation of conductance (nF). At zero month, the sensor signals were 156 nF, after one month, sensor showed signals of 154nF whereas after two months, it was 153 nF, for third and fourth months, sensor signals were 152 and 150 nF, at fifth months, the noted sensor signals were 147 nF as shown in figure 3.7 (b). After six months, these observations confirmed the stability of fabricated fructose sensor by 2 % RSD value (n=6) and maintained sensor response upto 96 %.

3.3.2 Characterization and sensor measurements of urethane system based receptors

3.3.2.1 Characterization of synthesized receptors by FTIR spectroscopy and scanning electron microscope

To study the functional group changes of receptor thin films, FTIR analysis in ATR mode was performed. FTIR spectra of imprinted and non-imprinted thin films were examined to find out the structural changes in molecular interactions between the heteroatoms present in polyurethane and template molecule (fructose).

In this polymer matrix, N-H characteristic absorption peak was found at 3328 cm^{-1} due to the presence of hydrogen bond in the urethane linkage and urea groups. Carbonyl group showed stretching vibrations at 1726 cm^{-1}. The stretching vibrations of ester (C(O)-C) was present at 1126 cm^{-1}. The carbonyl peak (C=O) around 1700 cm^{-1} due to ester-polyols and urethane as shown in figure 3.8.

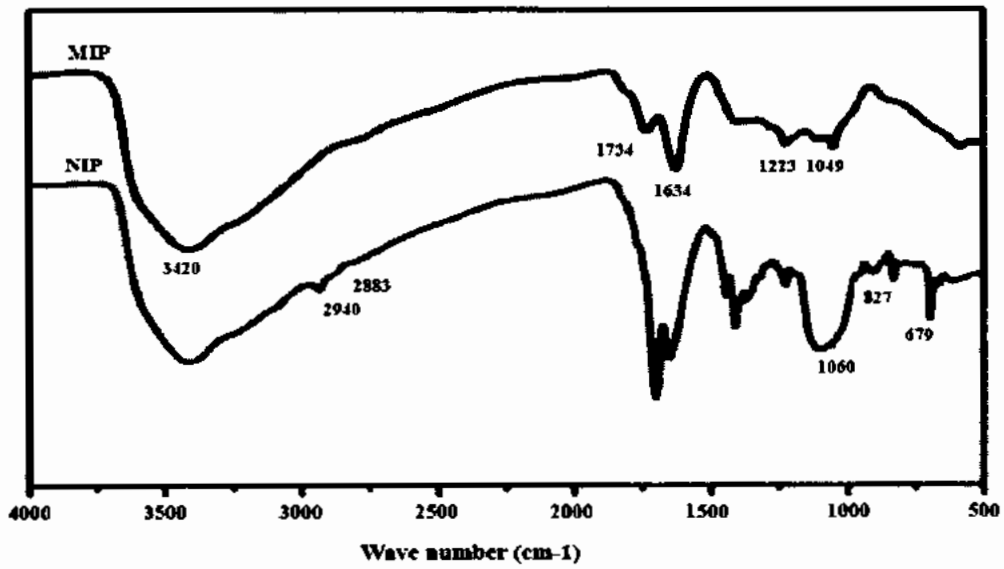

Figure 3.8: FTIR spectra of imprinted and non-imprinted polyurethane based fructose receptors.

To study the surface morphology, scanning electron microscope (SEM) was used. For this purpose, synthesized receptors were coated onto the glassy medium to achieve the thin films of MIPs and NIPs. NIP particles showed different size with surface roughness. However, MIP had porous surface with cloud appearance as shown in figure 3.9.

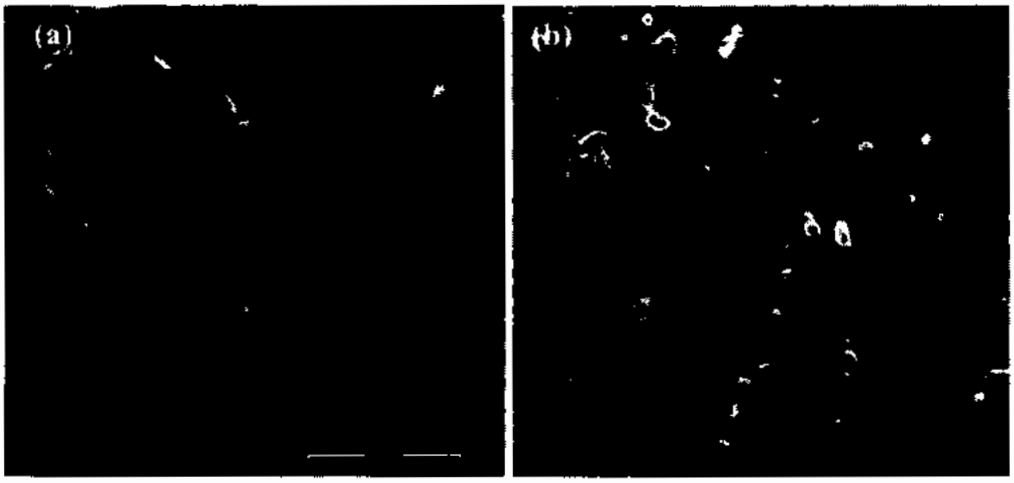

Figure 3.9: SEM images of (a) NIP and (b) MIP of polyurethane based fructose receptors.

This process confirms that the template molecule plays an important role in the synthesis of imprinted polymer by free radical polymerization. In this method, synthesis of NIP without template, the monomer forms dimers due to intermolecular hydrogen bond. However, in case of MIP, there is an additional molecular interaction between

monomer and template specie i.e. fructose which might increase the growth of cross-linked polymer.

3.3.2.2 Sensitivity analysis of fabricated sensor

The conductance of sensitive layer coated onto the transducer surface (IDE) was measured by exposing it against different concentrations of analyte (fructose). IDEs were dipped into different ppm solutions, attached to LCR meter and measurements were carried out at 20 Hz in AC mode. At concentration of 1 ppm, the sensor response was 14 nF which increases with increasing the concentration of analyte. At 1 ppm, 5 ppm, 10 ppm, 20 ppm, 30 ppm, 40 ppm and 50 ppm, the sensor showed a response of 14 nF, 57 nF, 108 nF, 179 nF, 221 nF, 289 nF and 340 nF respectively with lower detection limit (LoD) ~107 ppb. It is revealed in figure 3.10 (a) that by increasing the concentration of analyte, fabricated sensor showed higher sensor response due to molecular imprinting. By increasing the concentration of analyte response was increased which mean that response is linear and its saturation point is 520 ppm.

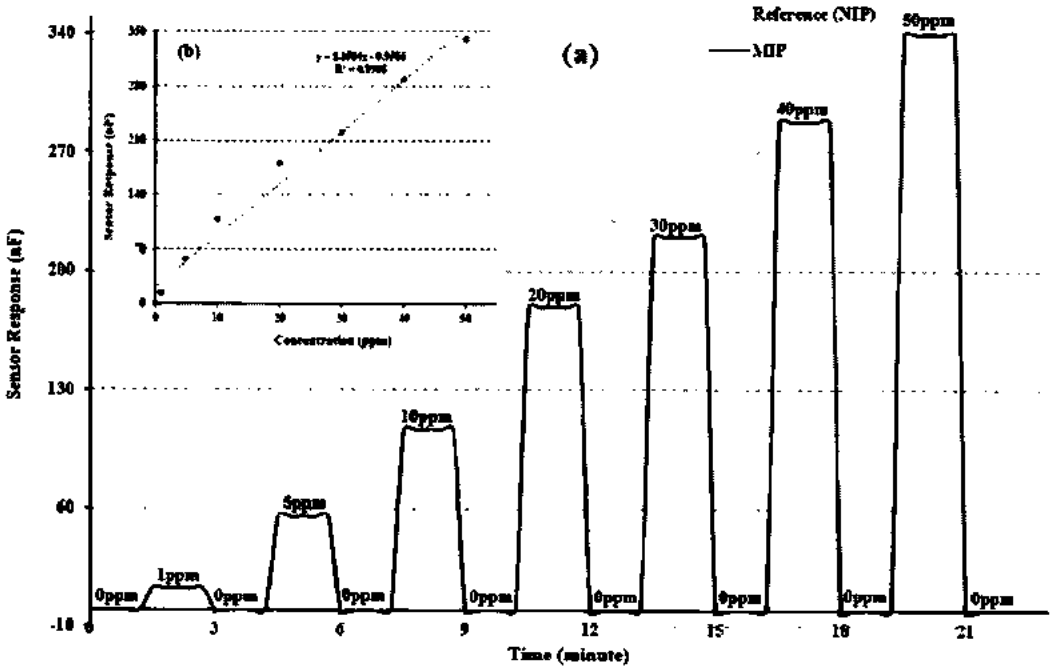

Figure 3.10: Sensitivity response of MIP and NIP of polyurethane based fructose receptors at different concentrations (0-50 ppm) and (a) Linear regression analysis of fructose sensor.

On the other hand, reference electrode shows negligible response at all the respective concentration of fructose. The sensitivity and selectivity of molecular imprinted polymer can be increased by increasing the number of binding sites. The non-covalent interactions between the template molecules (fructose) and polymeric matrix may base on the interaction of crosslinking agent and fructose molecules and the OH group present in fructose interact with NH-CO group of DPDI while the Bisphenol A provides support in form of polymerization to generate cavities within polymer matrix. The fabricated sensor exhibits an excellent reversibility when subjected to zero concentration of fructose solution. By increasing the concentration of analyte, sensor response was increased which mean that response is linear with linear regression coefficient (R^2) value of 0.99 as shown in figure 3.10 (b).

The possible interactions between template molecules and polymer matrix can be seen in figure 3.11 where dipole-dipole force and hydrogen bonding (between N-H group of DPDI and -OH group of fructose) cause the interaction between template molecule and imprinted cavities.

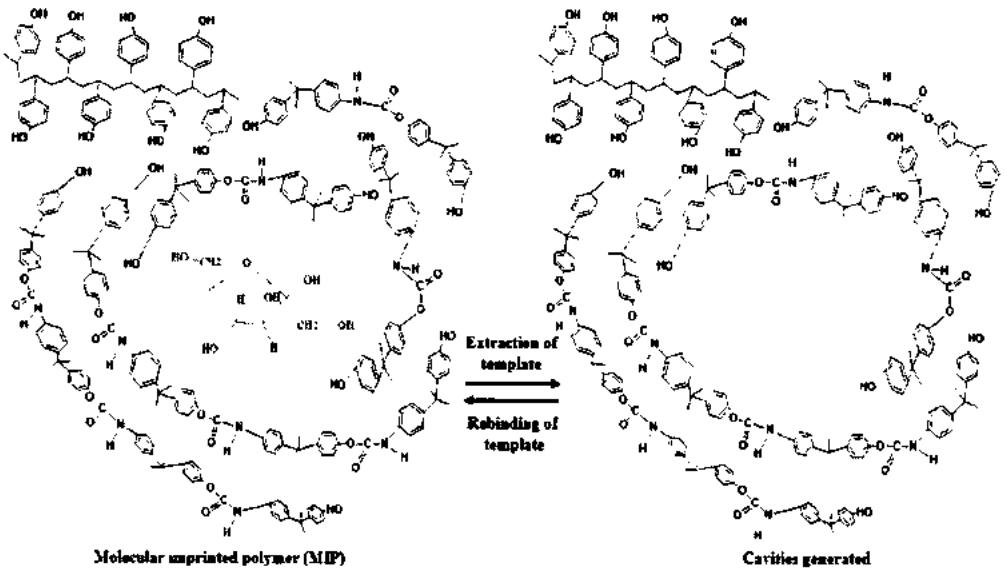

Figure 3.11: The extraction and rebinding of template from urethane based fructose receptors.

3.3.2.3 Selectivity analysis of sensor

Selectivity of sensor can be measured by exposing the sensor to different interfering species of same concentration against template molecule. Although the polymer was

not prepared for structurally related competing molecules but their sensing was checked with imprinted membrane prepared for fructose. Sensor showed response towards competing species but the response of template was higher than other molecules. Selectivity response was checked against different competing molecules i.e. glucose, maltose, sucrose and n-hexane. Fructose shows 23 times higher sensor signals than glucose and furthermore, maltose and sucrose show 28 times less response as compared to fructose. n-Hexane also gives the least response than the above mentioned interfering species. From figure 3.12, we can see that there was a drastic change in the selectivity of the MIP film in comparison to other interfering molecules at the same concentration as fructose. The study of selectivity of fructose and remaining interfering species is due to possible interactions exhibits negligible influence on fructose detection. This selective response is because of existence of active sites on the MIP surface, layer, which identify the fructose template molecules via spatial structure complementation and group interaction.

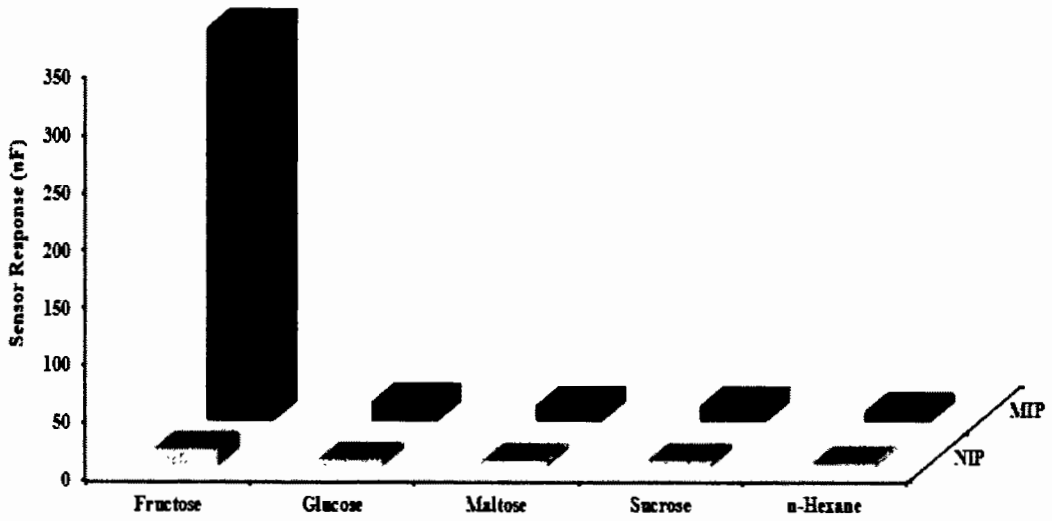

Figure 3.12: Selectivity analysis of polyurethane based fructose sensor against different competing molecules at 50 ppm.

The results concluded that fructose sensor bears high selectivity for fructose determination. Sensor showed high response towards template in the presence of other competing species with same molecular geometry conforming that molecular imprinted polymer is highly selective towards target molecule.

3.3.2.4 Reproducibility, reusability and stability

In the case of reproducibility, three different sensors were developed by following the same method and exposed to the fixed concentration of template molecule.

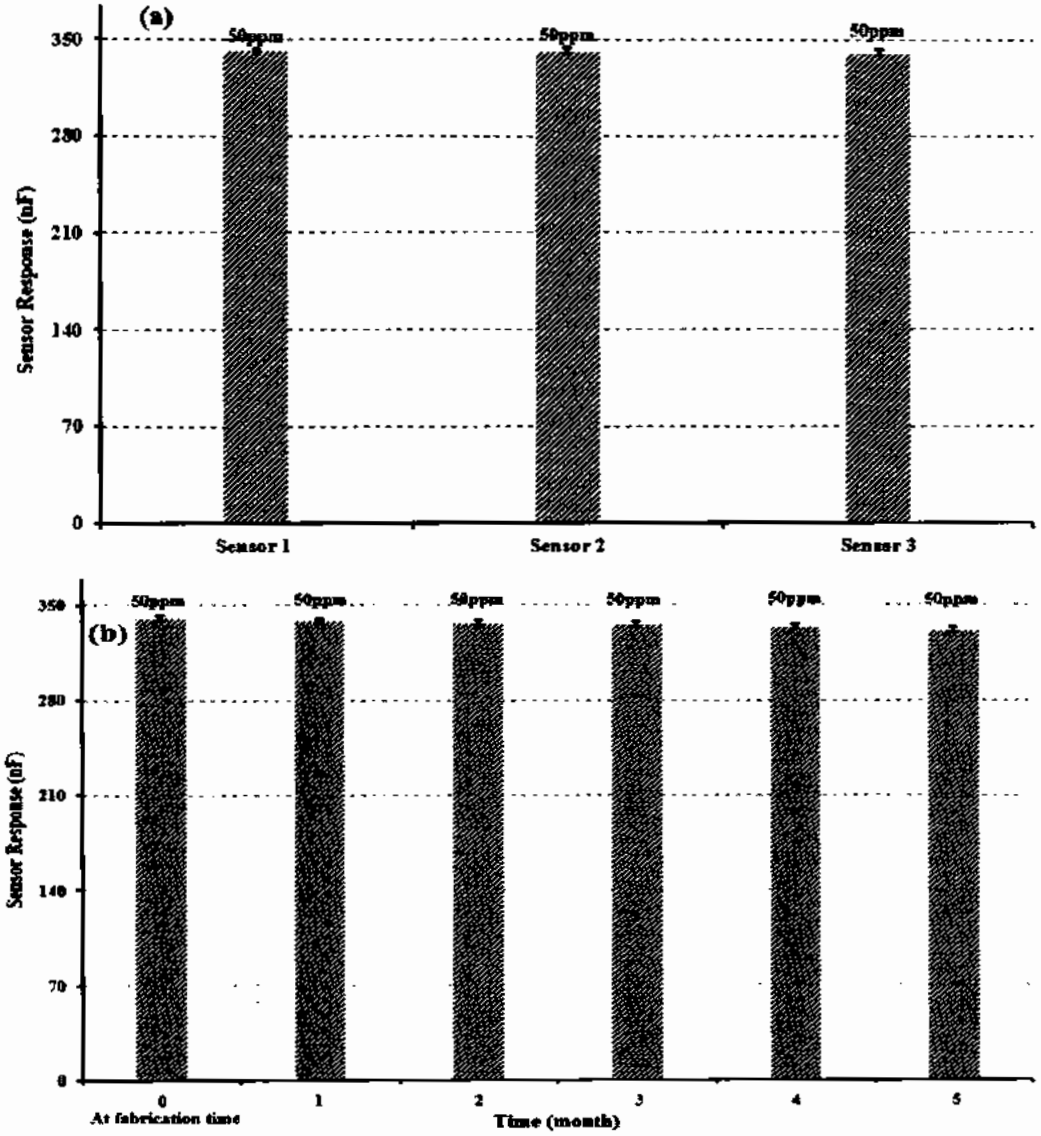

Figure 3.13: (a) Reproducibility and regeneratability of three sensors prepared in the same manner (b) Stability of sensor over the period of six months.

After measuring the sensor response of these fabricated sensors, relative standard deviation (RSD) value was found to be 0.17 %. These sensors were also stored at room temperature and pressure and retained 99.5 % of its initial sensor response after six months indicating that MIP based fructose sensors possess an excellent regeneratability

and reproducibility. To investigate the stability of fabricated fructose sensor, six replicative measurements were performed using the same sensor for six months.

For stability, the fabricated sensor was stored at room temperature and pressure for a period of six months and sensor response was measured after every month and calculated RSD value was 0.98 % with retained sensor response of 98.9 % as shown in figure 3.13 (b).

3.3.3 Characterization and sensor measurements of styrene system based receptors

3.3.3.1 Characterization of synthesized receptors by FTIR spectroscopy and scanning electron microscope

To understand the functional group changes in the structure of NIP and MIPs, FTIR analysis (ATR mode) was performed.

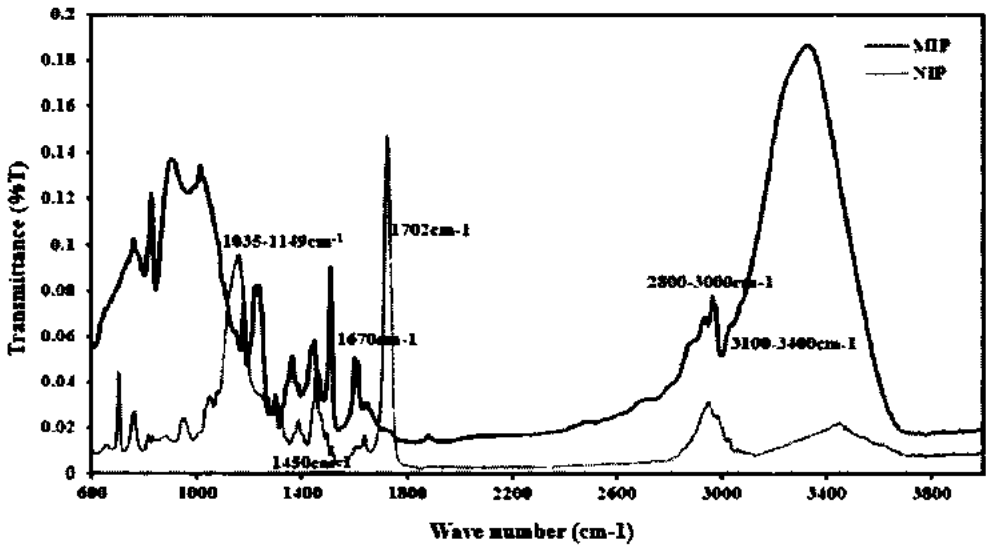

Figure 3.14 : FTIR spectra of MIP and NIPs of polystyrene based fructose receptors.

FTIR spectra for polystyrene system was observed in the range from 600-4000 cm^{-1}. The characteristic peak at 900-1100 cm^{-1} indicates the presence of glucose in case of both MIP and GO-MIP whereas absence of this peak in NIP spectra confirms the removal of glucose. The absorption peak at 3000-3400 cm^{-1} was attributed to stretching vibrations of –OH of glucose and confirms the hydrogen bond formation which is absent in NIP. The peak at 2800-2900 cm^{-1} were assigned to the sp^2 (CH) aromatic

rings. By comparing the peaks present with MIP and GO-MIP, were found absent in NIP.

The surface morphology of generated MIPs thin films was assessed by scanning electron microscopy (SEM) and microscopic images of the molecular imprinted polymer and non-imprinted polymer (NIPs) showed in figure 3.15.

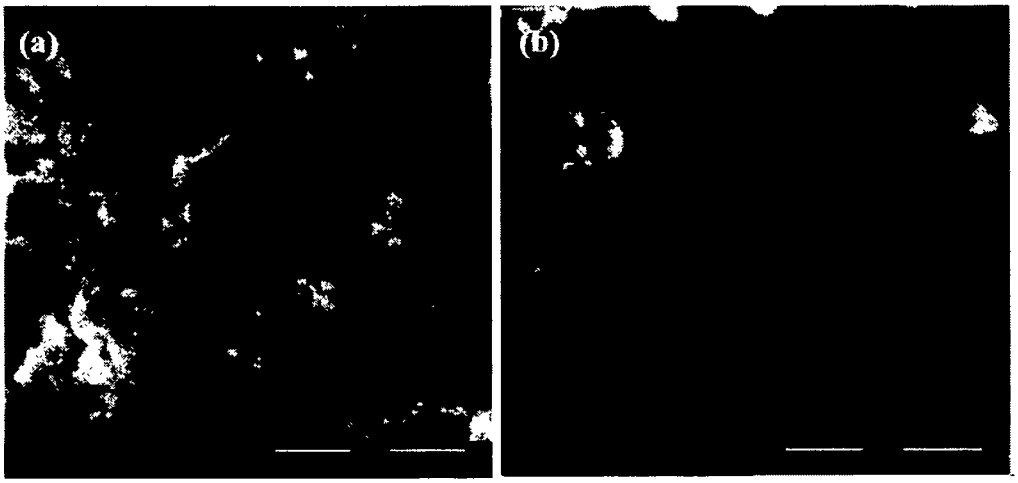

Figure 3.15: SEM images of (a) NIP and (b) MIPs of polystyrene based fructose receptors.

After the extraction of template (fructose) molecules by washing with water which leads to the creation of the template identical moieties within the styrene based polymeric matrices. The micrographs of SEM showed that micro and nanostructures have been produced in the imprinted polymer surface due the removal of template observed in the micrographs of non-imprinted polymer which indicates the surface changes of polymer surface during template molecules removal from polymer matrix molecules and porogenic effect during polymerization while such a structures have not been seen in NIP.

3.3.3.2 Sensitivity analysis of fabricated sensor

To assess the sensor response towards template molecule, the fabricated sensor was exposed to various concentrations of fructose solution and sensor response was observed by measuring capacitance with the help of high precision LCR meter (IET 7600 Plus precision LCR meter). The sensor behavior towards the various concentration of fructose in aqueous solution has been shown in figure 3.16 (a). At

concentration of 1ppm, the sensor response was 26 nF which increases with increasing the concentration of analyte. At 1 ppm, 5 ppm, 10 ppm, 20 ppm, 30 ppm, 40 ppm and 50 ppm, the sensor showed a response of 16 nF, 58 nF, 108 nF, 183 nF, 367 nF, 336 nF and 417 nF respectively with lower detection limit (LoD) ~96 ppb. It is revealed in figure 3.16 (a) that by increasing the concentration of the analyte, the fabricated sensor showed a higher sensor response due to molecular imprinting with a saturation point of 500ppm. The capacitance of MIPs thin film varies with the variation of incorporation of fructose molecules into recognition sites. Thus, conductance of the MIPs layer is directly related with the incorporated template molecule concentration within the polymeric matrix. Styrene as monomer is hydrophobic in nature with no particular specialty and the role it may assist in the formation of glucose imprinted polymer.

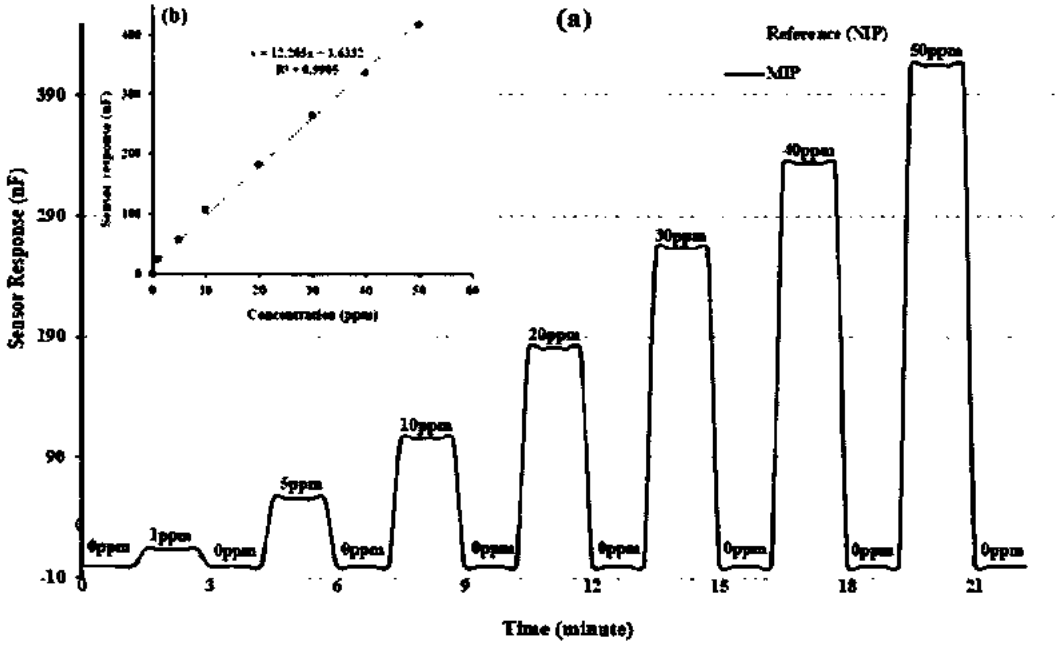

Figure 3.16: (a) Sensitivity response of MIP and NIP of polystyrene based fructose receptors at different concentrations (0-50 ppm) and (a) Linear regression analysis of fructose sensor.

The fabricated sensor exhibits an excellent reversibility when subjected to zero concentration of fructose solution. By increasing the concentration of analyte, sensor response was increased which mean that response is linear with linear regression co-efficient (R^2) value of 0.99 as shown in figure 3.16 (b). The response of non-imprinted (NIP) polymer was very low at the same concentrations of template (fructose) molecule

and significant difference of sensor response between MIPs coated IDE and NIPs coated IDE is because of availability imprinted cavities/selective molecular imprints on the surface of imprinted polymer based receptors. While the behavior of sensor with NIPs as recognition materials is not influenced by the change in concentration. The non-covalent interactions between the template molecules and polymeric matrix may base on the interaction of crosslinking agent and fructose molecules and the OH group present fructose interact with -CH of styrene while EGDMA provides the support in polymerization to generate cavities within polymer matrix. The possible interactions between template molecules and polymer matrix where weak dipole-dipole force and hydrogen bonding cause the interaction between template molecule and imprinted cavities.

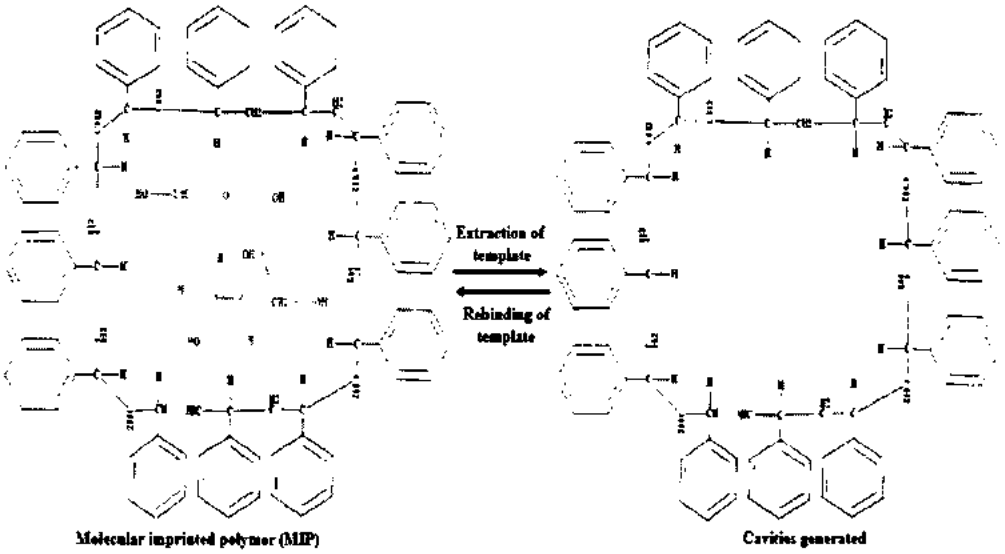

Figure 3.17: The extraction and rebinding of template from polystyrene based fructose receptors.

The capacity of template molecule to differ from other competing molecules is an essential factor for the designing of an electrochemical sensor. Superior sensor response towards specific analyte may be due to molecular imprinting which was based on key and lock mechanism shown in figure 3.17.

3.3.3.3 Selectivity analysis of sensor

Selectivity analysis is a characteristic feature of bulk imprinting polymer strategies which is why this technique is applied to impart selectivity to polymer towards the

template molecules. The moieties formed after extractions of the template molecules are complementary identical to the imprinting species in size, shape and coordination geometries which leads to substantial selectivity of fabricated sensor. The sensor selectivity response demonstrates whether a fabricated sensor is suitable for the sample, in which number of competing molecules with highly identical mass, structure and chemical properties are present along with the analyte of interest. Therefore, it is important to analyze if the sensor is selective for the molecule of interest or not.

Figure 3.18 : Selectivity analysis of fructose sensor against different competing molecules at 50ppm.

The selectivity behavior of fructose sensor was assessed by exposing the sensor towards the different competing agents which have almost identical molecular mass or similar number of carbon chain or functionalities i.e. glucose, maltose, sucrose, n-hexane etc. The fabricated sensor showed the sensor signals of 416nF for MIP based sensor and was observed as highly sensitive and selective for the interfering molecules, 10nF, 8nF, 5nF and 3nF towards glucose, maltose, sucrose and n-hexane respectively. The fructose and glucose both are monosaccharide but differ in their structures and sensor signal towards glucose is higher by the factor of almost 42 while n-hexane with similar number of carbon atoms differ by factor of 138. On the other hand, sucrose being disaccharide with double number of carbon atoms have negligible influence on the sensor signals. It could be clearly seen from the figure 3.18 that the sensor is highly

selective for fructose and shows many folds more selective signals as compared to other competing species.

3.3.3.4 Reproducibility, reusability and stability,

To assess the reproducibility and reusability of fabricated sensor, three different fructose sensors were synthesized thrice by following the same recipe. These fabricated sensors were stored at room temperature and pressure for a period of three months and their sensor response was measured by exposing them at 50 ppm concentration of template molecule.

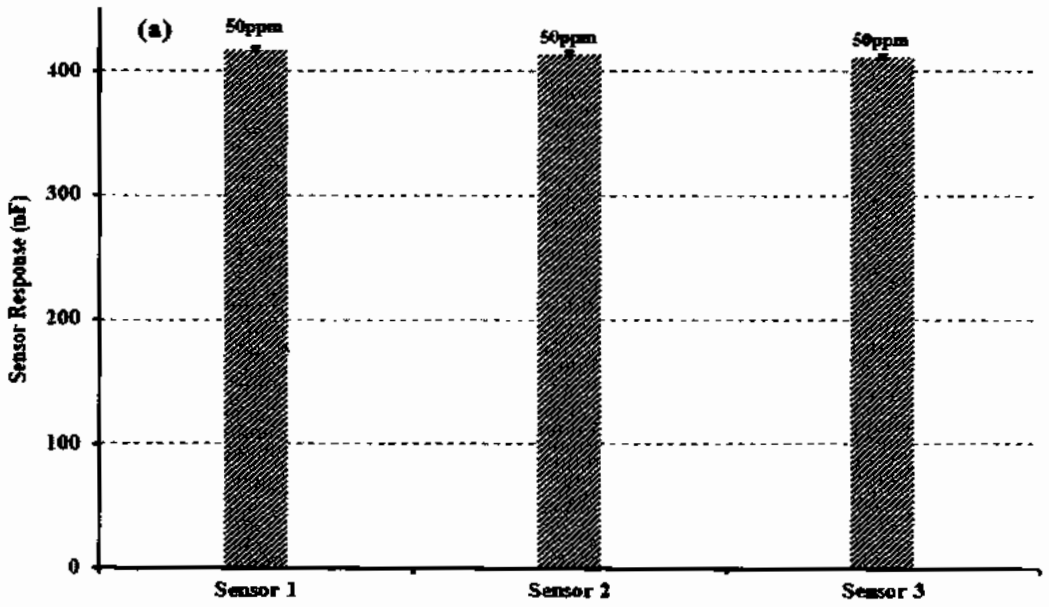

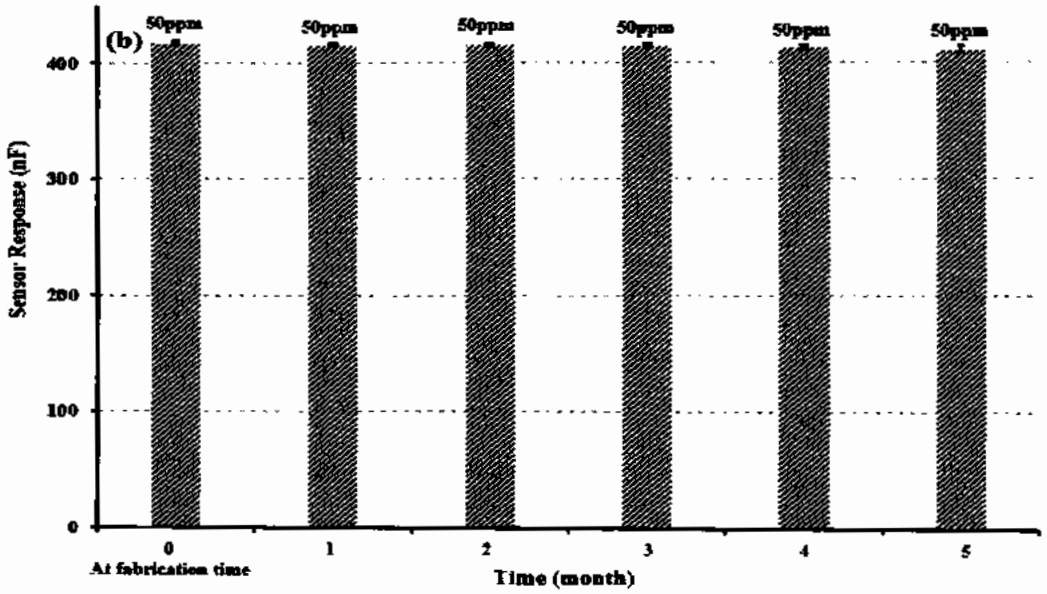

Figure 3.19: (a) Reproducibility and reusability of three sensors prepared in the same manner (b) Stability profile of sensor over the period of six months.

From these measurements, the calculated relative standard deviation of 0.15 % indicated that the reproducibility response of currently designed sensors was not significantly different as shown in figure 3.19 (a). It was found that 99.5 % of sensor response was maintained which also indicated that MIP based fructose sensor possesses excellent repeatability, regeneratability and reproducibility. To investigate the long term stability of a sensor, the sensor sensitivity profile was assessed every month for a period of six months by exposing the fabricated sensor to 50 ppm concentration of fructose as shown in figure 3.19. The obtained relative standard deviation (RSD) of 0.4 % signifies the effective repeatability of 50 ppm concentration with continuous usage (figure 3.19 b).

3.3.4 Characterization and sensor measurements of methacrylic acid based receptors

3.3.4.1 Characterization of synthesized receptors by FTIR spectroscopy and scanning electron microscope

To analyze the functional group modification of imprinted polymer and graphene oxide based receptors, FTIR analysis was performed in the range of 500-4000 cm^{-1} as shown in figure 3.20.

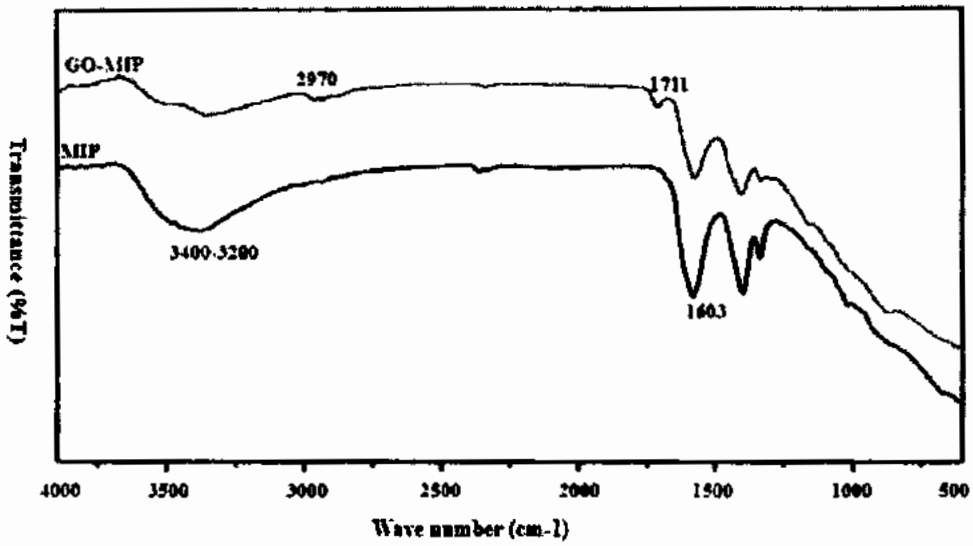

Figure 3.20: FT-IR spectra of MIP and GO-MIPs composite based methacrylic acid based fructose receptors.

FTIR spectra for acrylate based receptors was obtained in the range of 700-3900 cm^{-1} as shown in figure 3.20. Spectra of MAA and EGDMA showed –C=C stretching frequency at 1650 cm^{-1}. The peaks at 1670-1515 cm^{-1} are vibrational peaks indicating C-H stretching and C-H bending of polymer chains. The characteristics peaks centered at 1035-1149 cm^{-1} indicated the presence of polysaccharides in MIP. The absorption peak at 3200-3400 cm^{-1} was attributed to stretching vibrations of -OH of glucose. The peak at 1702 cm^{-1} shows the presence of ester group in the matrix and the other extra peaks are attributed to free radicle polymerization.

To assess the surface morphology of NIP, MIPs and GO-MIPs composite, scanning electron microscope was used and synthesized receptors were coated onto glass substrate to achieve thin films. Microscopic images showed that NIPs have very smooth surface while the images of MIPs showed high surface roughness due to the swelling of polymer on the incorporation of template molecules within the polymeric matrix.

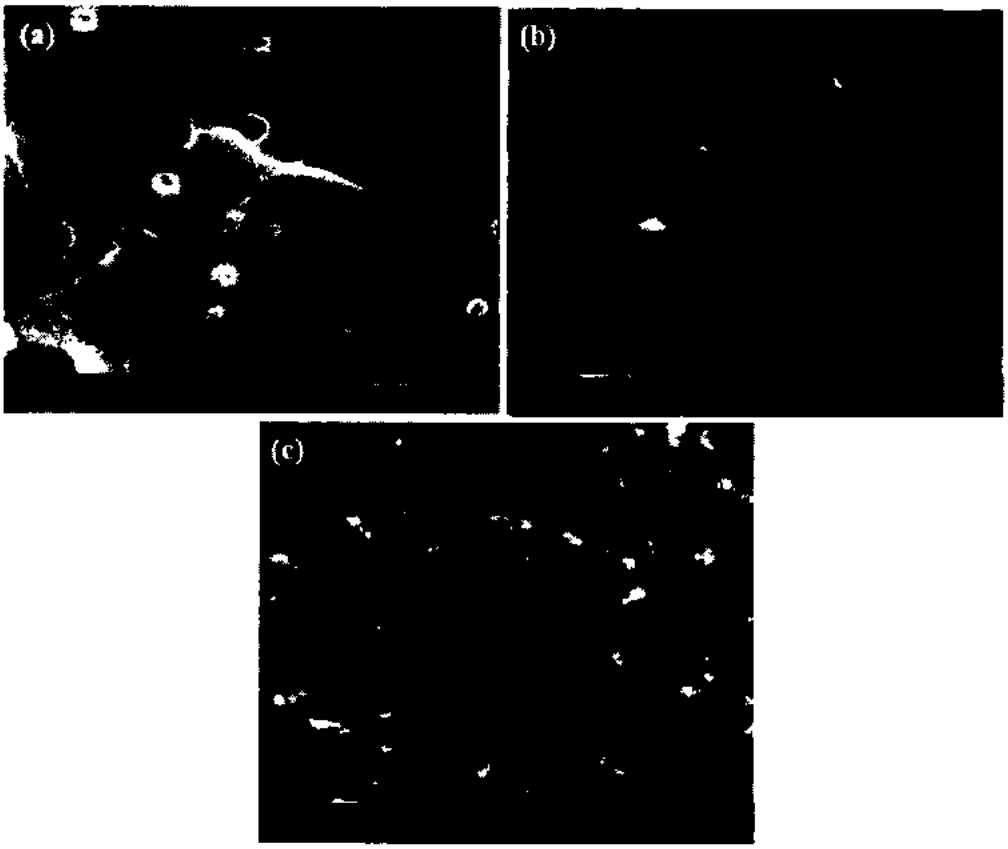

Figure 3.21: SEM images of (a) NIP (b) MIPs and (c) GO-MIPs composite of methacrylic acid based fructose receptors.

The SEM images also showed the microstructures in the imprinted polymer surface due to the removal of template as shown in figure 3.21. Topographical difference was observed in the imprinted polymer which indicated the surface changes during polymerization while such structures have not been seen in NIP. The SEM image of GO-MIP composite exhibited the completely embedded microstructures.

3.3.4.2 Thermogravimetric and differential analysis (TGA/DTA)

The thermogravimetric and derivative analysis (TGA/DTA) of NIP, MIP and GO-MIP composite were performed to assess the thermal stability at temperature range 0 °C to 600° C with a temperature change at rate of 10 °C/ minute. The initial weight loss of NIP occurs between 18.34 °C – 322.86 °C is -2.777/5.33 mg due to the loss of adsorbed water and crystal water as shown in Figure 3.22 (a). The second stage starts from 322.86 °C and ends at 596.34 °C with a weight loss of -2.797/5.33 mg and total weight loss is -2.777-2.797= -5.567 mg (-104.4 %). This weight loss contributes to the further

decomposition of chemical bonds present in NIP. Figure 3.22 (b) shows the TGA/ DTA curve of MIP in which temperature change starts from 15.99 °C and stopped at 58.09 °C with weight loss of -0.616/5.35 mg The next temperature shift starts from 59.55 °C – 338.20 °C with loss of weight -3.451/5.35 mg. The third shift in temperature change starts from 339.66 °C and ends at 596.67 °C.

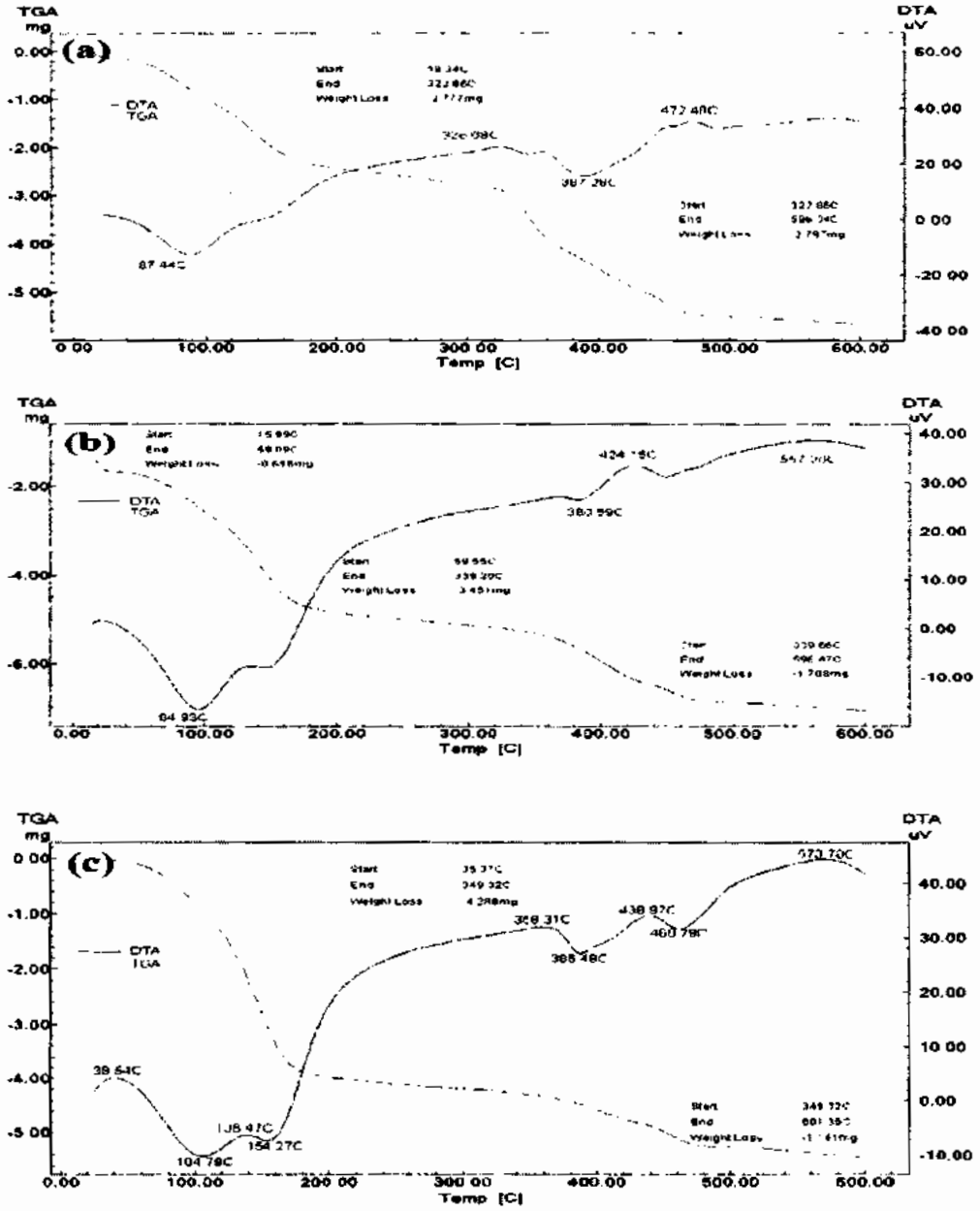

Figure 3.22 : TGA and DTA curves of (a) NIP (b) MIPs and (c) GO-MIPs composite of methacrylic acid based fructose receptors.

The total weight loss in MIP-TGA curve was -6.053/5.35 mg (-113.1 %). In this curve, temperature changes from 35.37- 349.32 °C with weight loss of -4.288 mg whereas second change ranges from 349.32 to 601.35 °C with loss of -1.141/ 5.36 mg. Overall weight loss in this curve was -5.429/5.36 mg (-101.3 %) as shown in figure 3.22 (c). These findings from TGA curves indicate that acrylate based polymers and their composites are highly stable and can be used for the molecular imprinting of fructose to generated highly selective receptor for sensing purposes.

3.3.4.3 Sensitivity analysis of fabricated sensor

After coating of fructose imprinted polymer onto IDEs and washing to generate cavities within polymeric matrix, the sensor was exposed to various concentrations of fructose to assess its sensitivity profile. The obtained electrochemical results demonstrate that newly fabricated sensor was highly sensitive even at very low concentration of 1 ppm as shown in figure 3.23 (a). At 0 ppm, the observed capacitance was 0 and as for 1 ppm, 5 ppm, 10 ppm, 20 ppm, 30 ppm, 40 ppm and 50 ppm, measured response was 19 nF, 48 nF, 90 nF, 188 nF, 330 nF, 489 nF and 626 nF respectively with the lowest limit of detection ~60 ppb having the highest estimation point of 525 ppm. Non-imprinted polymer was also exposed to the same concentrations of analyte and sensor signals were very less as compared to sensor signals of MIPs.

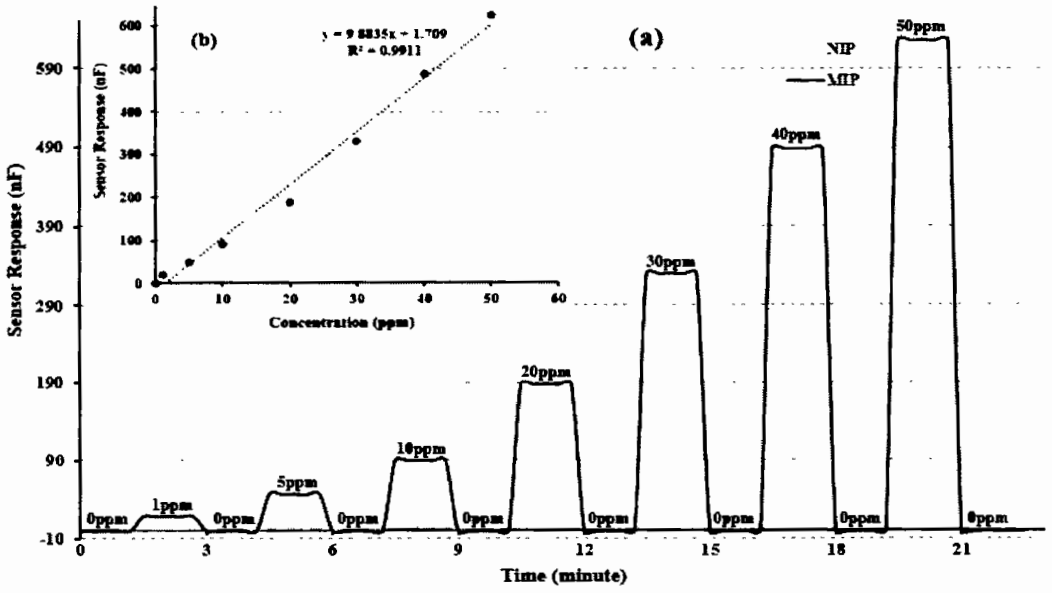

Figure 3.23 : (a) Sensitivity response of NIP and MIP of methacrylic acid based fructose sensor at different concentration (0-50 ppm) (b) Linear regression analysis of fructose sensor.

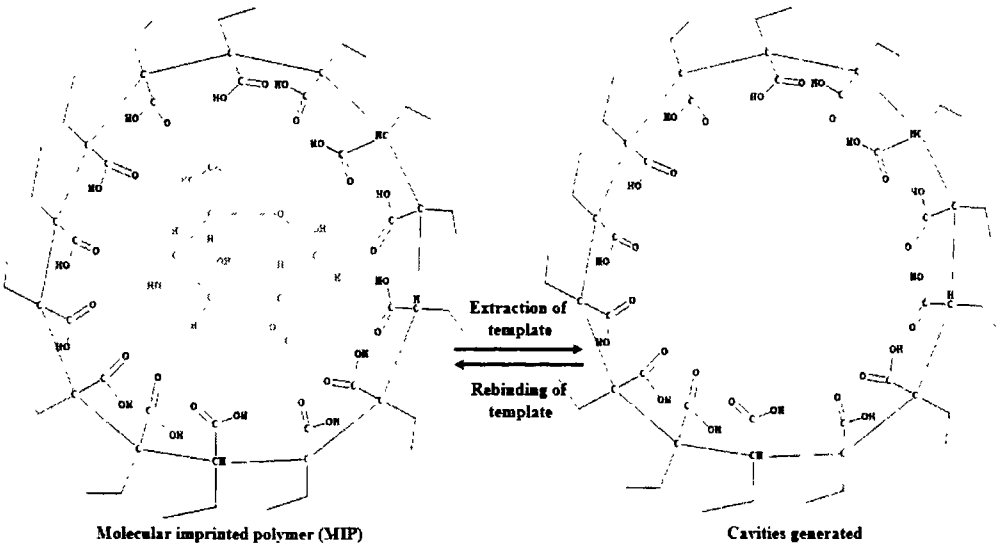

Figure 3.24: The extraction and rebinding of template from methacrylic acid based fructose receptors.

The linearity of sensor was assessed by linear regression analysis of obtained sensor responses (0-50 ppm) and the sensor showed linear response with a linear co-efficient of regression (R^2) of value 0.99 as can be seen in figure 3.23 (b). The increase of capacitance might be due to the -OH (hydroxyl) group present in fructose which was trapped within the molecular cavities present in polymeric matrix coated onto IDEs.

It is important for the synthesis of an efficient molecular imprinted polymer that there should be strong interactions between the functional monomer and analyte. The number of hydrogen bond acceptor and hydrogen bond donor groups present in fructose which has a vital role in the development of non-covalent interactions between fructose and polymeric matrix as shown in figure 3.24. Another reason for the substantial sensor signal changes of fructose imprinted acrylate polymer on exposing to fructose could be that fructose is selectively adsorbed in the polymer matrix that produces the potential change or greater in response with the increase in concentration even at very minute change in concentration of fructose. Ideally sensor should be concentration dependent and should be reversible. This newly fabricated sensor follows the same pattern and upon increasing the concentration of template, conductance increases in a linear manner which depicts the linear relation between template molecule and conductance. When

the sensor was exposed to zero concentration of fructose after tacking sensor response of each concentration, the sensor reaches its initial value which represents the reversible and regeneratable behavior of the fabricated sensor. On the other hand, if we consider the interactions between the template molecules and molecular binding sites within MIPs which are absent in NIPs then the higher sensor response of MIPs can easily be explained on the basis of molecular imprinting phenomenon. NIP does not show any significant change in its response due to lack of binding capacity towards analyte.

To enhance the sensor performance and sensitivity of the sensor, optimizing the structure of imprinted polymer was designed in such a way that recognition cavities should be situated nearby and at the surface of polymer material. In order to achieve above goal, the surface area of receptors and interactions between the analyte and sensor receptors were enhanced by combining the MIPs with functionalized graphene. For this purpose, functionalized graphene was added during polymerization. The sensitivity of graphene oxide based composite substantially enhance towards analyte due to the excellent electrical and mechanical properties of functionalized graphene.

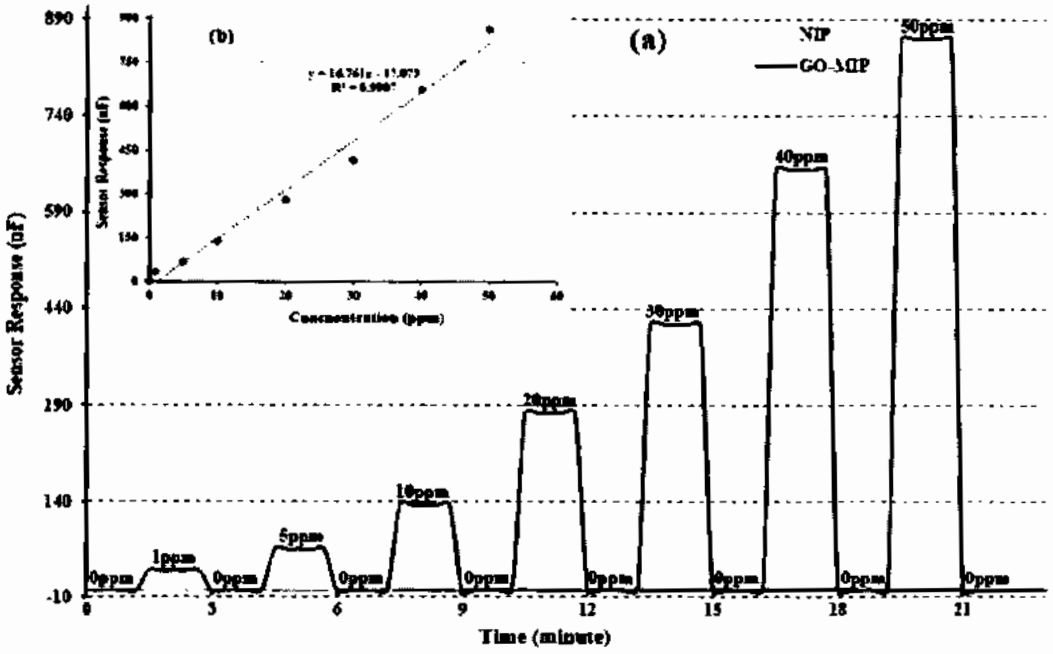

Figure 3.25: (a) Sensitivity response of GO- MIP composite and NIP of methacrylic acid based fructose receptors at different concentrations (0-50 ppm) and (b) Regression analysis of GO-MIP based fructose receptors.

At 50 ppm concentration of fructose, there is drastic increase in conductance which is 862 nF. The graph shows a linear response of 33 nF, 66 nF, 136 nF, 279 nF, 417 nF,

658 nF, and 862 nF while exposing to analyte concentrations i.e. 1 ppm, 5 ppm, 10 ppm, 20 ppm, 30 ppm, 40 ppm and 50 ppm respectively as shown in figure 3.25 (a).

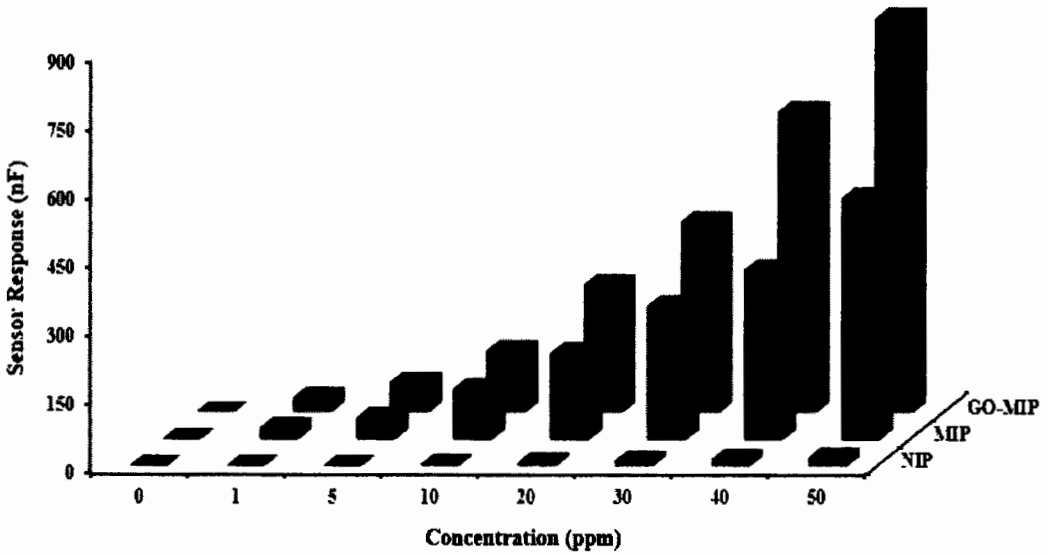

Figure 3.26: Comparison of sensor response of NIP, MIPs and GO-MIPs (composite) of methacrylic acid based fructose sensors at different concentrations (0-50 ppm).

The limit of detection of GO-MIPs composite was ~46 ppb and saturation of 600 ppm calculated from the calibration curve shown in figure 3.25. The linearity of fructose sensor response was measured by linear regression analysis which resulted in a linear co-efficient of value $R^2 = 0.99$ which shows highly linear and concentration dependency of sensor response as shown in figure 3.25 (b). Comparison of NIP, MIP and GO-MIP composite was shown in figure 3.26 by bar graph. This graph confirms the substantial worth of graphene sheets while comparing the sensor signals of MIP and GO-MIP composite, the response of GO-MIP composite was 1.4 folds higher than simple MIP. The surface morphological studies showed availability of the high surface area as compared to other polymers which leads to the high sensor response because of fructose-MAA interactions which leads to the maximum adsorption of template molecules.

3.3.4.4 Selectivity analysis of sensor

Selectivity is an important parameter of chemical sensor and sensitivity, alone is not sufficient, therefore, it is important to check the selectivity of MIPs and GO-MIPs

composite by exposing it against different competing molecules based on structural and functional analogues. Fructose, glucose, maltose, sucrose and n-hexane were selected as interfering species to evaluate the selectivity performance of the sensor.

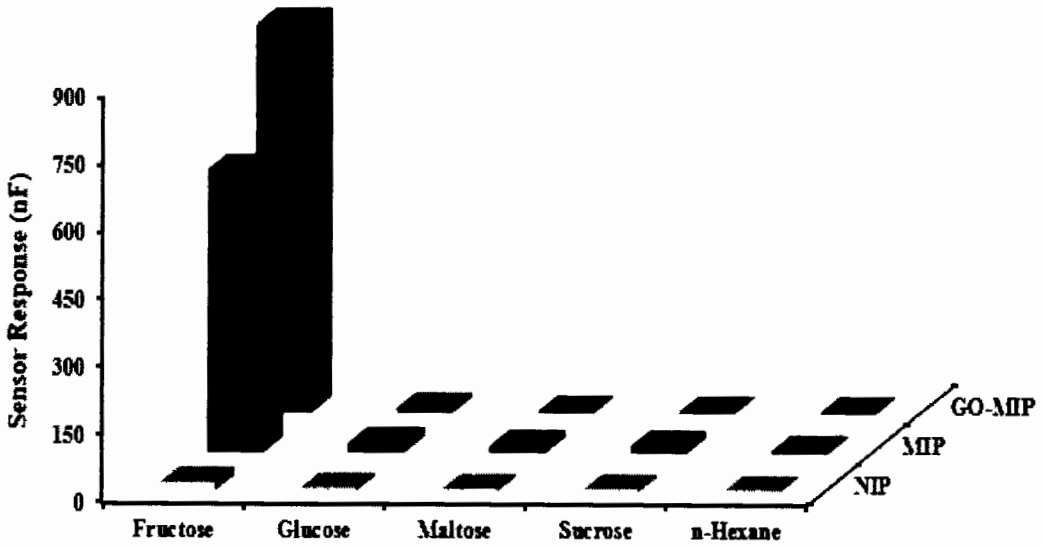

Figure 3.27: Selectivity analysis of methacrylic acid based fructose sensor against different competing molecules at 50 ppm.

At 50 ppm, conductance of fructose and other interfering molecules were checked as shown in figure 3.27. Fructose MIP based sensor show signals (conductance) 626 nF whereas fructose, maltose, sucrose and n-hexane were 20, 14, 14 and 5 nF respectively. Sensor response of GO-MIP composite based fructose was 862 nF and sensor signals of other competing molecules were 9, 3, 3 and 2 nF for glucose, maltose, sucrose and n-hexane. During polymerization, methacrylic acid and EGDMA rearrange themselves in a very effective way around the imprinted specie results in a high number of recognition sites which is highly selective towards the respective analyte.

Selectivity is far high for fructose (95 times) than glucose as interfering molecule, for maltose and sucrose, it was 287 folds, and also exhibits highly negligible response for n-hexane. This proves that GO-MIP (composite) sensor is highly sensitive as well as selective against competing species.

3.3.4.5 Stability, reusability and reproducibility

As the GO-MIPs composite showed high sensitivity and selectivity towards the fructose therefore, this composite was chosen to assess further sensor characteristics. First of all, for the analysis of reproducibility, three different sensors were synthesized thrice by following the same recipe and the fabricated sensors were exposed to the template solution of 50 ppm concentration. The calculated RSD value of 1.5 % demonstrated that the fabricated sensor is excellently reproducible. It can be seen from these results, molecular imprinted polymer layer responds in a stable way with only 0.5 % loss of initial sensor response.

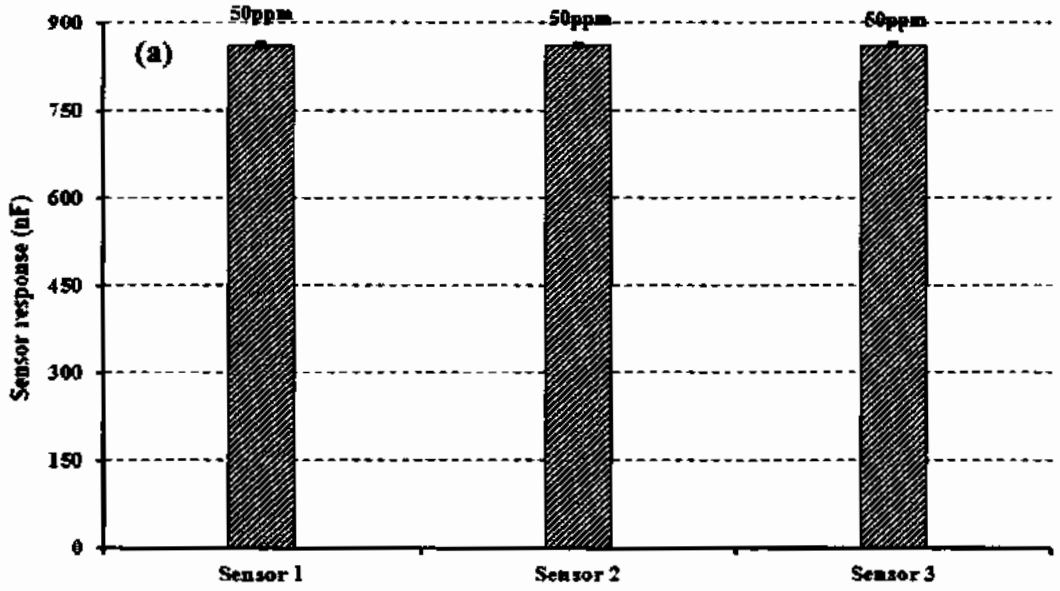

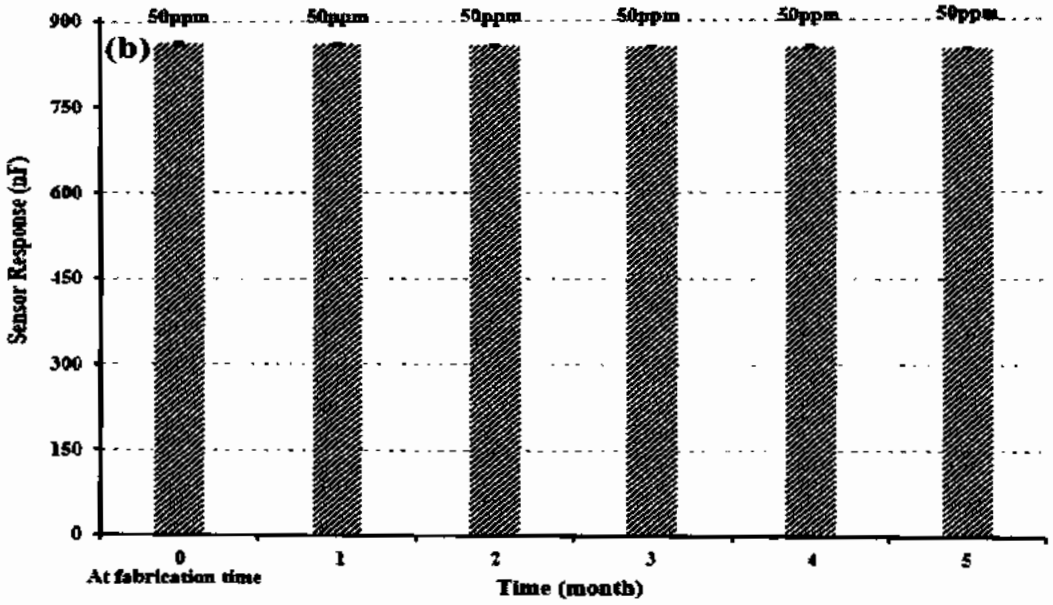

Figure 3.28: (a) Reproducibility of three GO-MIPs composite based sensors prepared in the same manner (b) Stability of GO-MIPs composite over the period of six months.

Secondly, for stability of GO-MIP composite, the fabricated sensor was stored for six months under room temperature and pressure. It was assessed by monitoring the sensor responses at 50 ppm concentration every month for a period of six months as shown in figure 3.28 (b). The obtained relative standard deviation (RSD) of 0.5 % signified the effective stability of 50 ppm with continuous use. In addition, 99.5 % sensor response was maintained and also indicated that fructose GO-MIP composite based sensor possesses excellent reproducibility, repeatability and stability.

3.4 Comparison of sensor receptors (imprinted vinyl pyrolidone, urethane, styrene and methacrylic acid)

Different molecularly imprinted polymer systems (vinyl pyrolidone, urethane, styrene and methacrylic acid) were fabricated and used as sensor receptors to achieve enhanced sensor efficiency. The sensor responses comparison of these three polymer systems is shown in figure 3.29. NVP based sensor receptors showed lower sensor response which might be due to insufficient incorporation tendency of template molecules that resulted in lesser number of cavities present on the bulk of polymer matrix.

Urethane system was also assessed to enhance the sensor signals. Polyurethane as monomer has proton donor groups (N-H or O-H) as well as the lone pair donor groups (C=O). The proton donor group in this polymer matrix may interact with template molecule by developing H-bonding with electron donor groups (C=O). While the electron pair donor groups of polymer as well as template may interact with each other and enhances the sensor signals.

Base on the polystyrene structure and functionalities, it might be assumed that cavities generated in styrene system are more stable due to stronger interactions between template and polystyrene than other NVP and PU as monomers. The stability of styrene system based polymer might be higher due the aromatic nature of benzene ring present in styrene structure. The most top sensor response was noted with methacrylate system as shown in figure 3.29. The functional monomer i.e. methacrylic acid exhibited the efficient imprinting due to a strong influence on adsorption of the template molecules due to hydrophobicity of acrylate polymer matrix.

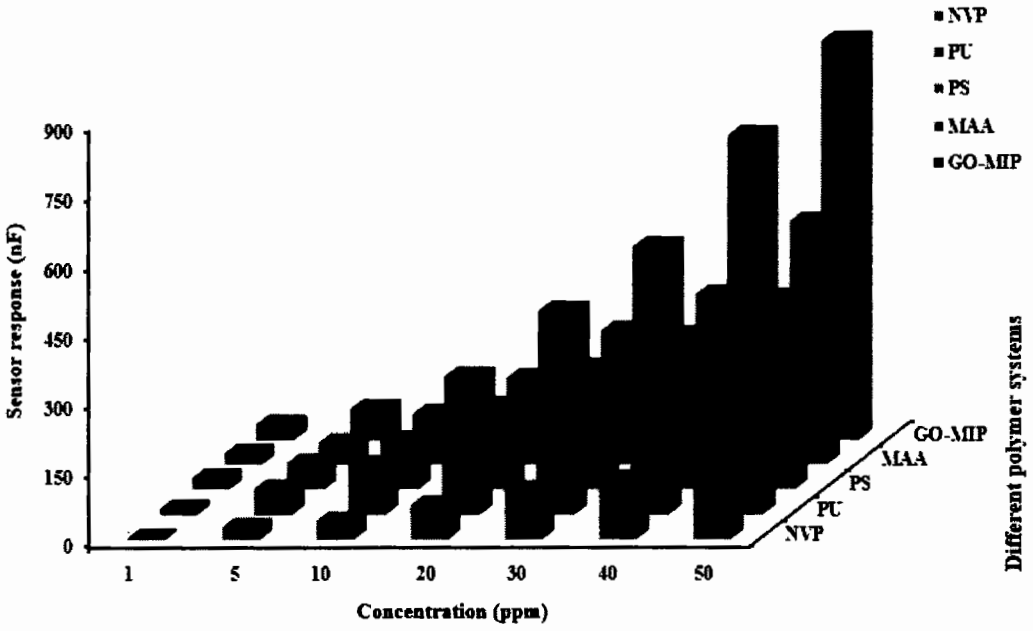

Figure 3.29: Comparison of sensor response of different polymer systems used for the detection of fructose.

When template is a polyhydroxy molecule, then there might be the possibility of stronger hydrogen bonding interactions with methacrylic acid as monomer, a major reason for the increased sensor response. Due to the structural and functionalities of

acrylate, it may impart an important role in polymer synthesis to form an imprinted polymer of fructose where it could be helpful to fix and co-ordinate with the cross-linker i.e. EGDMA specifically. It thus induces the geometric key and lock geometry of imprinted polymer which enables the polymer matrix for selective adsorption of templated molecule. It is also of substantial importance from the above mentioned results that acrylate based polymer showed the higher sensor effect as compare to other monomers because of its carboxylic group and functionality and methacrylic acid exhibits strong hydrogen bonding with fructose. Functionalized graphene based nanocomposite of acrylate was also used to measure the sensor response and found the sensor response many folds higher the simple acrylate MIP. The results obtained from different imprinted polymers were briefly reported in table 3.1 and compared these data with literature studies reporting fructose measurements using different electrochemical methods.

Table 3.1: Comparison of previously reported work with recently designed sensors.

Sr. No.	Analyte	Polymerization/ Technique	Monomer	LOD and detection range	Reference
1	Fructose, Glucose, Hypochlorite	Fluoride-assisted polymerization/ voltammetric detection	-	0.24 µM (240 ppb) for fructose and 0.36 µM (360 ppb) for glucose.	(Thiruppathi, Thiyagarajan et al. 2017)
2	Fructose	Cyclic voltammetry/ chronoamperometric	-	8 µM (8000 ppb)	(Nicholas, Pittson et al. 2018)
3	Fructose and glucose	Plasmonic detection	4- (Aminomethyl) phenylboronicacid hydrochloride	1 Mg/mL	(Muhammad, Liu et al. 2017)

4	Fructose and glucose	Differential pulse voltammetry (DPV)	o-phenylenediammine (o-PD)	0.137 µM (137 ppb) for fructose, 0.185 µM (185 ppb) for glucose	(Wang, Paim et al. 2014)
5	Fructose	Free radical polymerization	n-VP	300 ppb (300 ppb to 500 ppm)	Present work
6	Fructose	Free radical polymerization	DPDI	107 ppb (107 ppb to 525 ppm)	Present work
7	Fructose	Free radical polymerization	Styrene	96 ppb (96 ppb to 500 ppm)	Present work
8	Fructose	Free radical polymerization	MAA	60 ppb (60 ppb to 525 ppm)	Present work
9	Fructose	Free radical polymerization	MAA	46 ppb (46 ppb to 600 ppm)	Present work

From the above mentioned table, all sensors were found completely reversible, highly selective, sensitive, stable and reproducible than the reported sensors. Obviously, GO-MIP composite based fructose sensor presented very minute LoD and higher dynamic range than the simple MIP based fructose sensors along with very short detection time (~2 seconds).

3.5 Conclusion

In this chapter, MIPs and their composites have been synthesized using different monomers and the measured sensor responses of n-VP, urethane, styrene and MAA imprinted polymer systems are in the following order: n-VP < PU < Styrene < MAA. Furthermore, to enhance the sensor response, graphene oxide composites of acrylate based receptors are synthesized. It is found that graphene oxide composite based sensor responses are many folds higher as compared to that of imprinted polymers. We can conclude that methacrylate system is most suitable for the imprinting of fructose and bears high sensitivity and selectivity. While the composite of imprinted acrylate with functionalized graphene induces higher incorporation and moieties for the template molecules and produced substantial higher sensor response. Hence the sensitivity, selectivity, limit of detection and stability of the fabricated sensor is improved by using MIPs-GO composite and it can have potential technological applications in field of chemical sensors and material science.

4 Chapter 4 FABRICATION OF MOLECULARLY IMPRINTED POLYMERS AND NANOCOMPOSITE BASED SENSORS FOR THE DETECTION OF MALTOSE

4.1 Introduction

Carbohydrates have substantial significance in many fields such as pharmaceutical, biotechnology and food industry. Maltose is a well-known disaccharide used as sweetening agent in food (Xu, Gu et al. 2015) and comprises of two glucose subunits through α-(1-4)-D-glycosidic linkage. It is 12-20 % by composition of dry weight naturally present in different parts of plants such as seeds, leaves and malt (Xiaohong, Zhidong et al. 2017). Maltose has eleven hydrogen bond acceptors and eight hydrogen bond donors with one rotatable bond shown in figure 4.1.

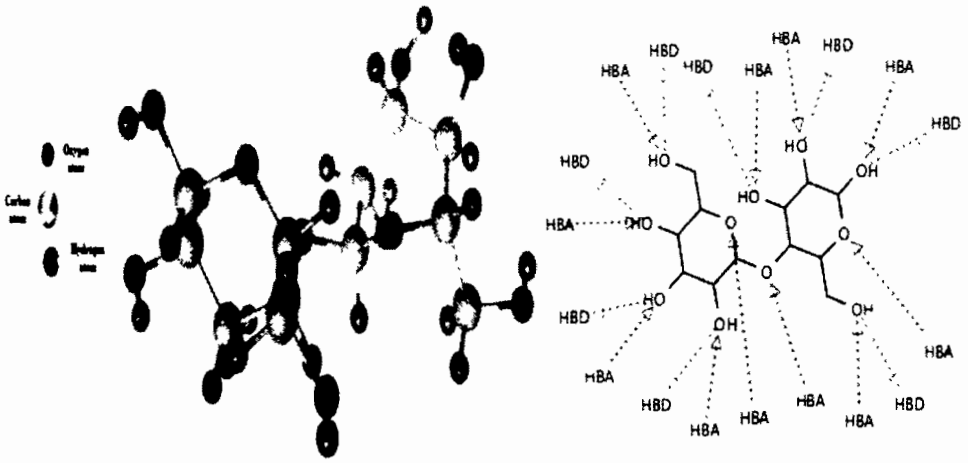

Figure 4.1: 3D structure of maltose (HBA = Hydrogen bond acceptor, HBD = Hydrogen bond donor)

High consumption of maltose causes serious health issues such as metabolic disorders, obesity, non-alcoholic fatty liver, and cardiovascular diseases. Therefore, rapid and efficient quantification of maltose in packed and bakery food items is of great importance. Numerous methods and techniques are in practice for the quantification of maltose such as high performance liquid chromatography (HPLC) (Elshaarawy, Mina et al. 2018), HPLC with evaporative light scattering detection (HPLC-ELSD) (Sun, Wang et al. 2016), gas chromatography coupled with mass spectrometry (GC-MS) (Lee, Shibamoto et al. 2019) and spectrophotometric methods. Since last decade electrochemical methods for the detection of maltose are getting substantial research interest among analytical chemist and material scientists due to their quick response, high sensitivity, highly selectivity (in many cases), cost effectiveness and repeatability

behavior. In 1962, Clark and Lyons designed the first enzymatic sensor for the detection of glucose with modified electrodes. Due to temperature, pH, and environmental factors, it was difficult to maintain the sensor response with enzymes. However, biosensors are highly dependent on the cultured enzymatic electrodes and a decrease in enzyme activity results in failure of detection processes. Recently, molecular imprinted polymers (MIPs) based sensors are used which are significantly beneficial to improve the analytical performance of electrochemical sensors. The MIPs based sensors as recognition elements are substantially important for selective recognition and a high sensitivity. The MIPs are artificially synthesized receptors with selectivity and higher affinity in their size, shape, molecular spation of functional groups towards the targeted molecule (analyte). In this chapter, we reported the fabrication of MIPs and MIPs-GO (nanocomposite) based sensors using different polymeric systems (styrene, vinyl-pyrolidone, urethane and acrylate) and cross-linker ratios. The synthesized receptors were characterized by FTIR, SEM and TGA. Furthermore, real-time sensor measurements have been performed to assess the various sensor parameters by exposing fabricated sensor to different concentrations of maltose and other competing species.

4.2 Experimental section

4.2.1 Materials and methods

For the synthesis of NIP, MIPs and GO-MIPs composite based maltose sensors, following chemicals such as glucose (99.5 %), sucrose (99 %), maltose (99 %), fructose (99 %), dimethyl sulphoxide (DMSO, 99.7 %), n-vinyl pyrolidone (99 %), 4, 4′diphenylmethanediioscyanate (DPDI; 98 %), phloroglucinol (PG; 99 %), bisphenol A (BPA; ≥99 %), chloroform, methacrylic acid (MAA; 99 %), styrene and 2,2′-azobisisobutyronitrile (AIBN; 99 %) and ethylene glycol dimethacrylate (EGDMA; 98%), acetone (≥ 99 %), methanol (99.8 %, anhydrous), ethanol (99.8 %, anhydrous) were purchased from Merck and Sigma Aldrich with the maximum available purity.

from Merck and Sigma Aldrich with the maximum available purity.

4.2.2 Synthesis of styrene based molecularly imprinted polymer (PS-MIP)

Styrene (3.4×10^{4} mM), 3.2×10^{4} mM of ethylene glycol dimethacrylate (EGDMA), 2 mg of AIBN as free radical initiator were mixed into an eppendorf tube. To the above solution, 500 µL of dimethyl sulfoxide (DMSO) as solvent and 2 mg of maltose (2 mM) were added and vortex it to obtain homogenized solution. Then mixture was polymerized into water bath at 70 °C for 45 minutes till transparent gel point is reached.

4.2.3 Synthesis of non-imprinted polymer (PS-NIP)

Non-imprinted polymer (reference) was also synthesized exactly in the same way without adding template (maltose). 3.4×10^{-4} mM of styrene, 3.2×10^{-4} mM of ethylene glycol dimethacrylate (EGDMA), 2 mg of AIBN as free radical initiator were mixed into an eppendorf tube. To the above solution, 500 µL of dimethyl sulfoxide (DMSO) as solvent and vortex it to obtain homogenized solution. Then mixture was polymerized into water bath at 70 °C for 45 minutes till transparent gel point is reached.

4.2.4 Synthesis of urethane based molecularly imprinted polymer (PU-MIP)

Polyurethane based maltose imprinted receptors were synthesized using 40 to 60 ratio between monomer and cross-linker. Urethane based receptors were synthesized by 1.9×10^{-6} mM of phloroglucinol (PG), 8×10^{-6} mM of bisphenol A and 3.6×10^{-6} mM of DPDI was vortexed in 1 mL of DMSO. Maltose (2 mmole) was added and homogenized by vortex. The resultant solution was heated for 30 minutes at 45 °C in water bath till gel point was obtained which indicated the synthesis of maltose imprinted polymer.

4.2.5 Synthesis of non-imprinted polymer (PU-NIP)

PU-NIP was also prepared in the same way without adding maltose as template molecule. Polyurethane based maltose imprinted receptors were synthesized using 40 to 60 ratio between monomer and cross-linker. Urethane based receptors were synthesized by 1.9×10^{-6} mM of phloroglucinol (PG), 8×10^{-6} mM of bisphenol A and 3.6×10^{-6} mM of DPDI was vortexed in 1 mL of DMSO and homogenized by vortex.

The resultant solution was heated for 30 minutes at 45 ℃ in water bath till gel point was obtained which indicated the synthesis of maltose imprinted polymer.

4.2.6 Synthesis of n-vinyl pyrolidone based molecularly imprinted polymer (VP-MIP)

Poly(vinylpyrolidone) based MIP was synthesized by following this method. 3.7×10^{-4} mM of vinyl pyrolidone, 3.2×10^{-4} mM of EGDMA were mixed into an eppendorf having 500 µL (4 mmole maltose solution in DMSO) of maltose solution. After homogenizing, 4 mg of AIBN was added to above mixture and vortex. The resultant solution was heated to 60 ℃ for 45 minutes in water bath till a transparent gel point was attained.

4.2.7 Synthesis of non-imprinted polymer (NVP-NIP)

NVP-NIP was prepared without adding template (maltose) molecule in the same way as MIP was synthesized. Poly(vinylpyrolidone) based MIP was synthesized by following this method. 3.7×10^{-4} mM of vinyl pyrolidone, 3.2×10^{-4} mM of EGDMA were mixed into an eppendorf having 500 µL of DMSO. After homogenizing, 4 mg of AIBN was added to above mixture and vortex. The resultant solution was heated to 60 ℃ for 45 minutes in water bath till a transparent gel point was attained.

4.2.8 Synthesis of methacrylic acid based molecularly imprinted polymer (MAA-MIP)

Maltose imprinted polymer was synthesized by mixing 4.7×10^{-4} mM of methacrylic acid (MAA) as functional monomer, 3.1×10^{-4} mM of EGDMA as cross linker, 4 mg of AIBN as free radical initiator and 500 µL of DMSO as solvent. 2 mM of maltose was added to the above mixture as template. The mixture was vortex for 5 minutes to homogenize and then place in water bath at 60 °C for 45 minutes to polymerize.

4.2.9 Synthesis of non-imprinted polymer (MAA-NIP)

MAA-NIP was also prepared in the same way without adding template (maltose) molecule same as above mentioned method. Maltose imprinted polymer was synthesized by mixing 4.7×10^{-4} mM of methacrylic acid (MAA) as functional

monomer, 3.1×10^{-4} mM of EGDMA as cross linker, 4 mg of AIBN as free radical initiator and 500 µL of DMSO as solvent. The mixture was vortex for 5 minutes to homogenize and then place in water bath at 60 °C for 45 minutes to polymerize.

4.2.10 Synthesis of polyacrylate graphene oxide based molecularly imprinted composite (MAA-GO-MIP)

Graphene oxide composite of molecularly imprinted methacrylic acid was synthesized by adding 0.5 mg of graphene oxide in 600 µL of imprinted MAA, sonicate and a suspension of composite was achieved.

4.2.11 Immobilization of MIPs, NIPs and Composite onto IDEs

Interdigital electrode (IDE) with electrodes spacing (L= 0.5' and number of fingers=18) was used as transducing surface for sensor measurements. IEDs were cleaned by washing with de-ionized water followed by methanol. 15 µL of imprinted polymer (MIP) was coated onto IDEs by spin coating at a speed of 2500 rpm (figure 2.2). The IDEs were dried in an oven overnight to achieve dry and compact polymer thin film.

4.2.12 Removal of template from MIPs

To remove the template molecule (maltose) from imprinted polymeric matrix, IDEs washed with deionized water with continuous stirring for 90 minutes by using magnetic stirrer at room temperature. After washing out the template molecules from polymer, thin films, template size identical cavities were achieved.

4.3 Results and discussion

4.3.1 Characterization and sensor measurements of styrene system based receptors

4.3.1.1 Characterization of synthesized receptors by FTIR spectroscopy and scanning electron microscope (SEM)

To study the functional modification of imprinted and non-imprinted thin film receptors, ATR-FTIR analysis was performed.

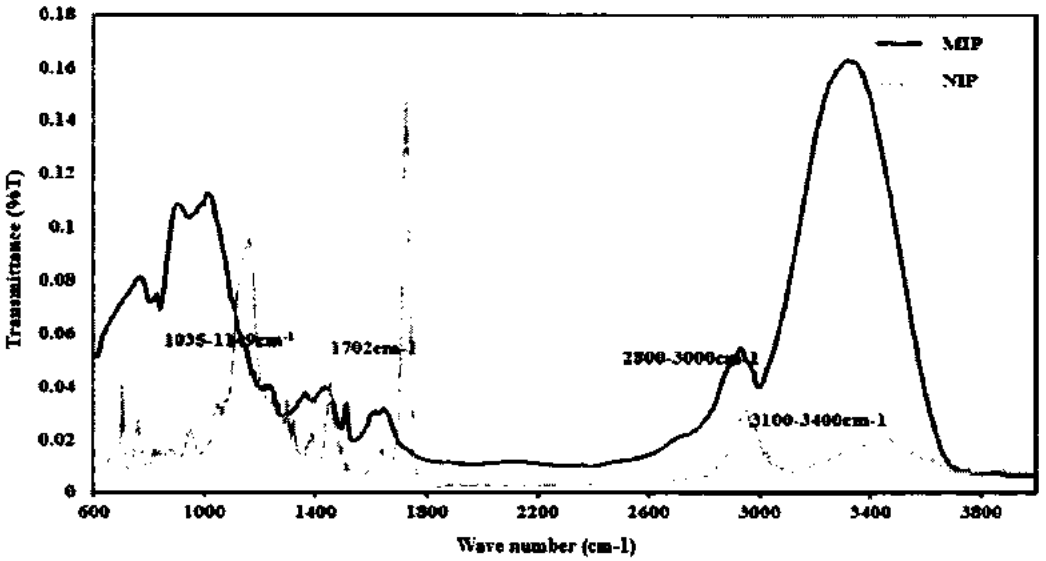

Figure 4.2: FT-IR spectra of non- imprinted and imprinted polystyrene based maltose receptors.

FTIR spectra for polystyrene system was observed in the range from 600-4000 cm^{-1}. The characteristic peak at 900-1100 cm^{-1} indicates the presence of glucose in case of both MIP and GO-MIP whereas absence of this peak in NIP spectra confirms the removal of glucose. The absorption peak at 3000-3400 cm^{-1} was attributed to stretching vibrations of –OH of maltose and confirms the hydrogen bond formation which is absent in NIP. The peak at 2800-2900 cm^{-1} were assigned to the sp^2 (CH) aromatic rings. By comparing the peaks present with MIP and GO-MIP, were found absent in NIP.

To examine the surface morphology, thin films of NIP and MIP were characterized by scanning electron microscope and receptors were coated onto the glass substrate to obtain thin films. Microscopic images showed that NIPs have very smooth surface while the images of imprinted polymers showed high surface roughness due to the swelling of polymer on the incorporation of template molecules within the polymeric matrix as shown in figure 4.3.

Figure 4.3: SEM images of (a) NIP and (b) MIPs of polystyrene based maltose receptors.

The SEM images showed that micro and nanostructures have been produced in the imprinted polymer surface due swelling of polymer surface and porogenic effect during polymerization while such structures have not been observed in the micrographs of NIPs. The appearance of pores and microscopic structures indicated the surface changes of MIPs due to extraction of template molecules from polymer matrix.

4.3.1.2 Sensitivity analysis of fabricated sensor

After coating of maltose imprinted receptors onto IDEs and washing to generate cavities within polymeric matrix, the fabricated sensor was exposed to various concentrations of maltose to assess its sensitivity profile. At 0 ppm, the observed capacitance was 0 and at 1 ppm, 5 ppm, 10 ppm, 20 ppm, 30 ppm, 40 ppm and 50 ppm of maltose the sensor responses of 10 nF, 21 nF, 44 nF, 75 nF, 119 nF, 138 nF and 186 nF have been observed respectively with the lowest limit of detection ~150 ppb. The obtained electrochemical results demonstrated that newly fabricated sensor was highly sensitive even at very low concentration of 1ppm as shown in figure 4.4 (a). The NIP was also exposed to the same concentrations of analyte and sensor signals were found very less. The linearity of sensor was assessed by linear regression analysis of obtained sensor responses at different concentrations of analyte (0-50 ppm) and the sensor showed linear response with a linear co-efficient of regression (R^2) of value 0.99 as can be seen in figure 4.4 (b). The increase of capacitance might be due to the -OH

(hydroxyl) group present in maltose which was trapped within the molecular cavities present in polymeric matrix coated onto IDEs.

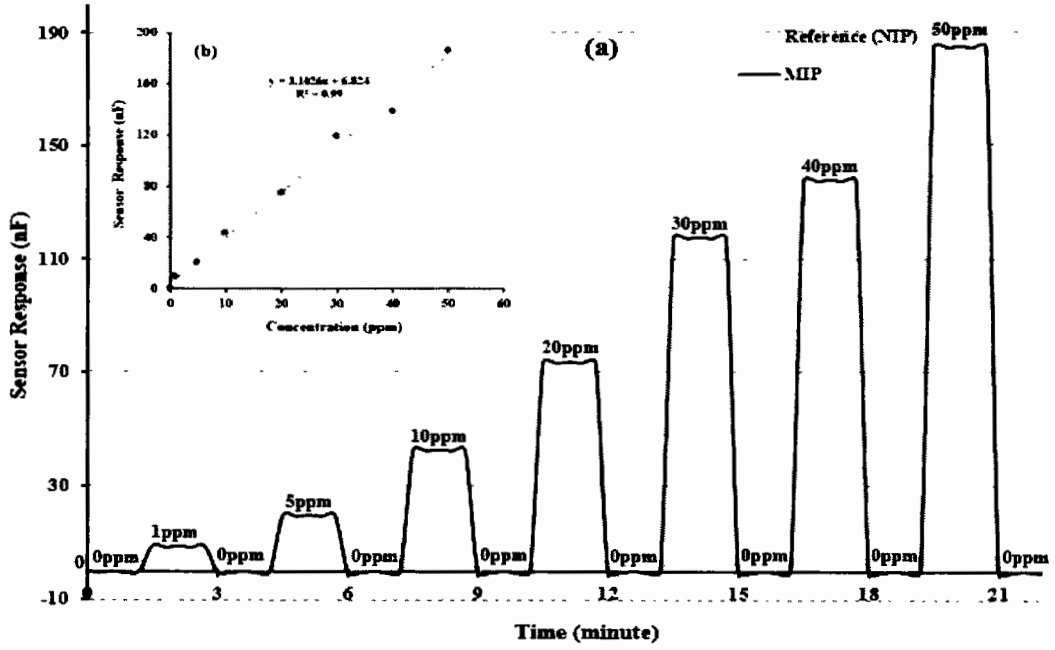

Figure 4.4: (a) Sensitivity response of NIP and MIPs of polystyrene based maltose sensor at different concentrations (0-50 ppm) and (b) Linear regression analysis of maltose sensor.

The MIPs coated sensor yields substantially higher response as compared to NIPs due to the presence of structural related cavities present on the surface of MIP. For the synthesis of an efficient molecular imprinted polymer, there must be robust interactions between the functional monomer and analyte. The hydrogen bond acceptor and hydrogen bond donor groups present in maltose played a vital role in the development of non-covalent interactions between maltose and polymeric matrix as shown in figure 4.5. Another reason for the sensor signal changes of maltose imprinted styrene polymer on exposing to maltose could be that maltose is selectively adsorbed in the polymer matrix. The selective absorption causes the potential change or greater in response with the increase in concentration even at very minute concentration of maltose and its saturation point is ~507 ppm. An ideal sensor should be concentration dependent and reversible. This newly fabricated sensor follows the same pattern and upon increasing the concentration of template, capacitance increases in a linear manner which depicts the linear relation between template molecule and capacitance.

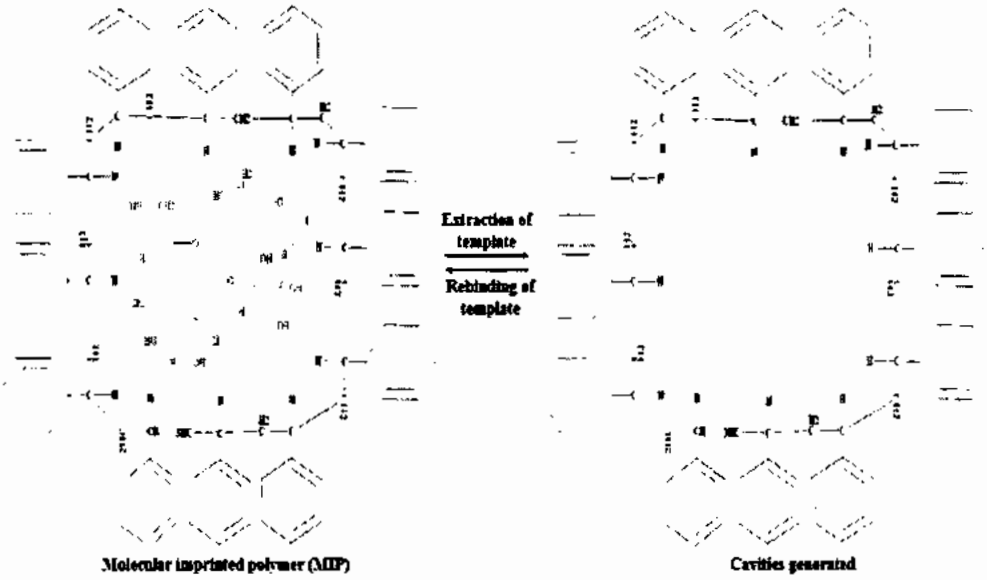

Figure 4.5: The rebinding and removal of template from polystyrene based maltose receptors.

When the fabricated sensor was exposed to zero concentration of maltose after taking sensor response of each concentration, the sensor approaches to its initial point which indicates the reversible response of fructose fabricated sensor. On the other hand, if we consider the interaction between the template molecules and molecular binding sites within MIPs which are absent in NIPs then the higher sensor of MIPs can easily be explained. NIP does not show any significant change in its response due to lack of binding capacity towards analyte. The surface morphology of imprinted polymer thin films is also another important parameter. Highly porous and rough surface morphology of MIP could be a reason to enhance the sensor response as compare to NIP due to its smooth surface.

4.3.1.3 Selectivity analysis of sensor

Besides sensitivity, reversibility and linearity, selectivity is an essential parameter of a sensor to assess its specific behavior in presence of other competing molecules.

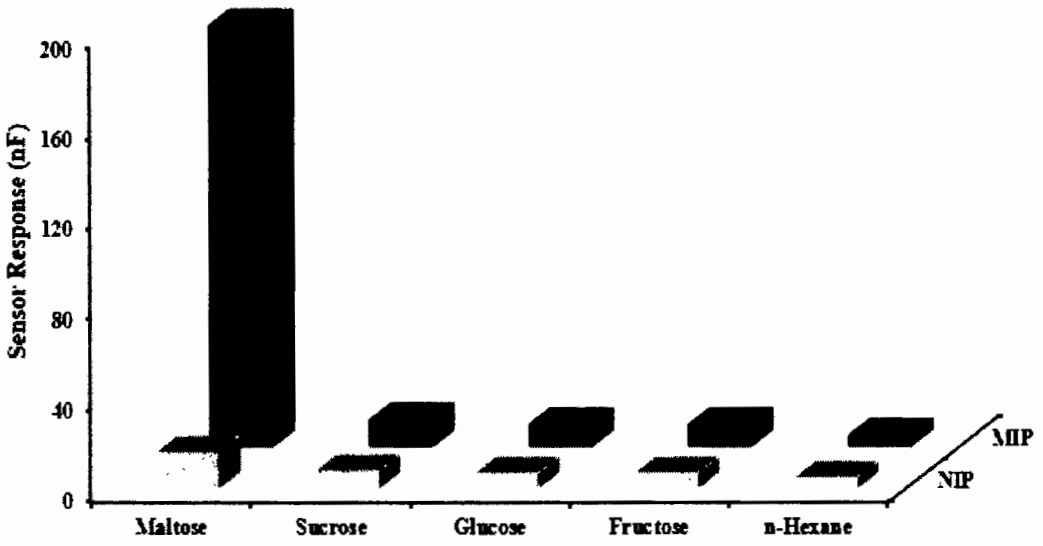

Figure 4.6: Selectivity of imprinted polystyrene based maltose sensor against different competing

For selectivity analysis, different structurally identical interfering molecules were used such as sucrose, glucose, fructose and n-hexane. The fabricated sensor was exposed to the similar concentrations (50 ppm) of maltose and above mentioned competing species and sensor responses towards each analyte were measured. As MIPs coatings specifically incorporates the respective template molecules i.e. maltose molecules, therefore the fabricated sensor showed higher sensor response towards maltose by the factor of 15 than sucrose, 19 folds higher than glucose and fructose respectively. This is because cavities generated at MIP surface not only size-selective but strongly distinguished from isomers and monosaccharides can be seen in figure 4.6. From these observations, we can say that molecular imprinted polymer based sensors are highly sensitive and selective. The reason for high selectivity is the presence of size and structurally dependent cavities synthesized by highly cross-linked polymer chains formed around the template molecule. During polymerization process, generation of non-covalent interactions networks between analyte and polymer matrix due to non-covalent means hydrogen bond, hydrophobic, dipole and π-π interactions. After the template removal, these interactions are retained within the polymer matrix which ideally leads to the adapted functionality, geometry and spatial of the resulting sieves.

This results in highly selective, stable matrices covering analytes ranging from molecules to entire cells.

4.3.1.4 Reproducibility, reusability and stability

To assess the reproducibility, three different sensors were synthesized thrice by following the same recipe and the fabricated sensors were exposed to the template solution (50ppm). These sensors were stored under normal conditions of temperature and pressure and their sensor responses were measured after one month thrice. The calculated RSD value of 0.38 % demonstrated that the fabricated sensor is excellently reproducible. It can be seen from these results, molecular imprinted polymer layer responds in a stable way for three months with only 0.5% loss of initial sensor response as shown in figure 4.7 (a).

For stability of MIP based maltose sensor, the fabricated sensor was stored for six months under room temperature and pressure.

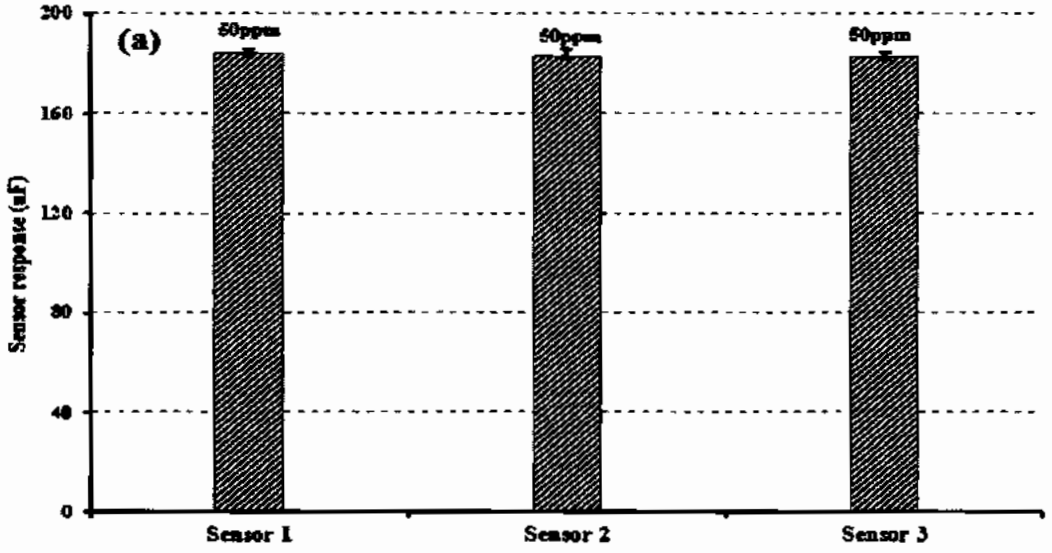

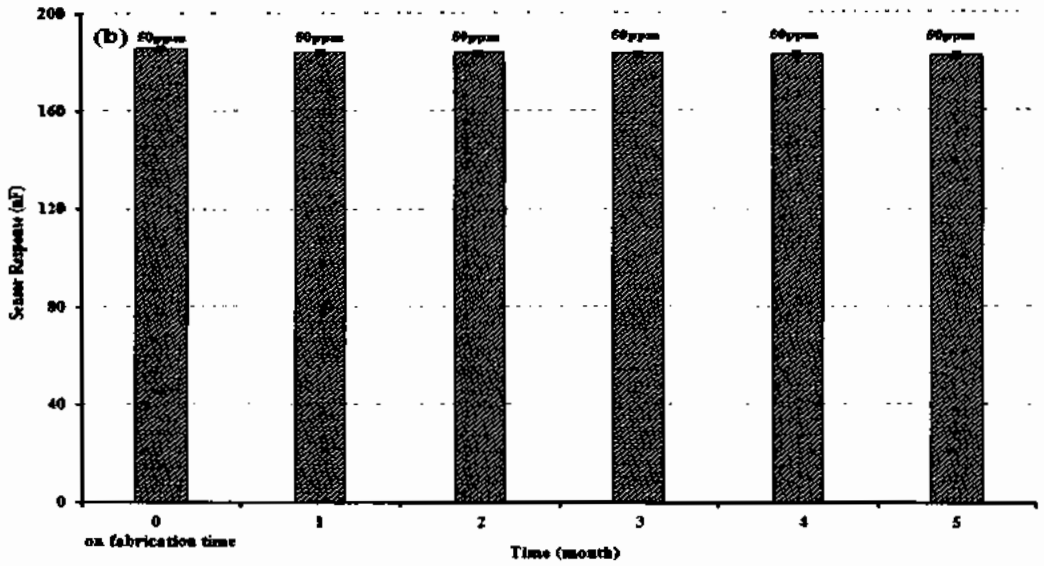

Figure 4.7: (a) Reproducibility and reusability of three polystyrene based maltose sensors prepared in the same manner (b) Stability profile of maltose sensor over the period of six months.

The sensor response as shown in figure 4.7 (b) showed that sensor signals were stable and the obtained relative standard deviation (RSD) of 0.8 % signifies the effective repeatability of 50 ppm concentration with continuous usage. In addition, 98.8 % of sensor response was maintained which also indicate that maltose MIP based sensor possesses excellent repeatability and high stability at the above mentioned conditions. Furthermore, after six months, only 0.5 % loss of sensor response, it might be due to swelling of imprinted polymer coated IDE in water over time. The imprinted layer maintained its integrity, as it is still effectively shielded the immediate IDE surface from changes in the surrounding.

4.3.2 Characterization and sensor measurements of urethane system based receptors

4.3.2.1 Characterization of synthesized receptors by FTIR spectroscopy and scanning electron microscope

To examine the functional group modification of NIP and MIP thin films, FTIR analysis was performed. For FTIR analysis, synthesized receptors were coated onto the glass substrate, dry and highly compact thin film of receptors was obtained.

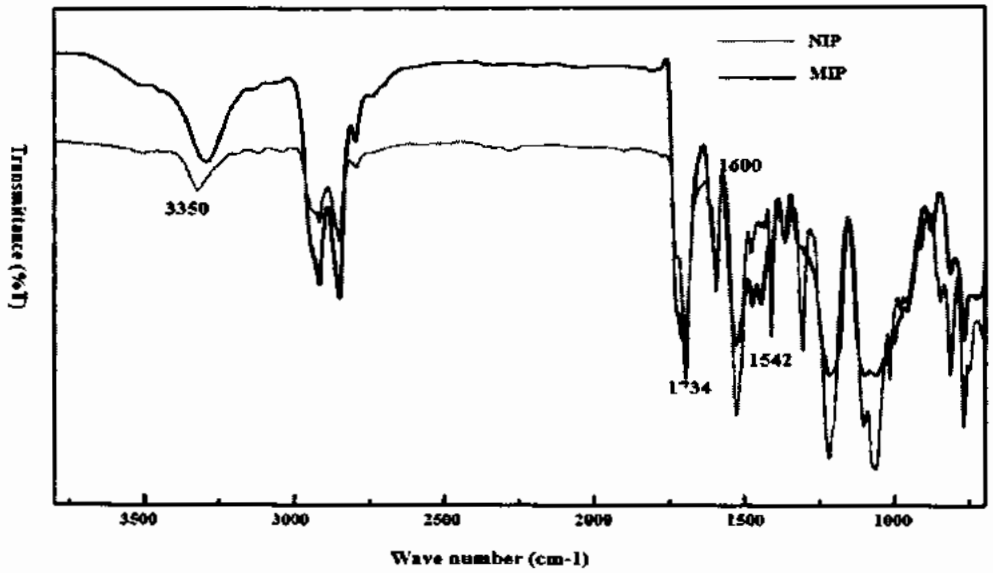

Figure 4.8: FT-IR spectra of non-imprinted and imprinted polyurethane based maltose receptors.

In this polymer matrix, N-H characteristic absorption peak was found at 3328 cm^{-1} due to the presence of hydrogen bond in the urethane linkage and urea groups. Carbonyl group showed stretching vibrations at 1726 cm^{-1}. The stretching vibrations of ester (C(O)-C) was present at 1126 cm^{-1}. The carbonyl peak (C=O) around 1700 cm^{-1} duc to ester-polyols and urethane as shown in figure 4.8.

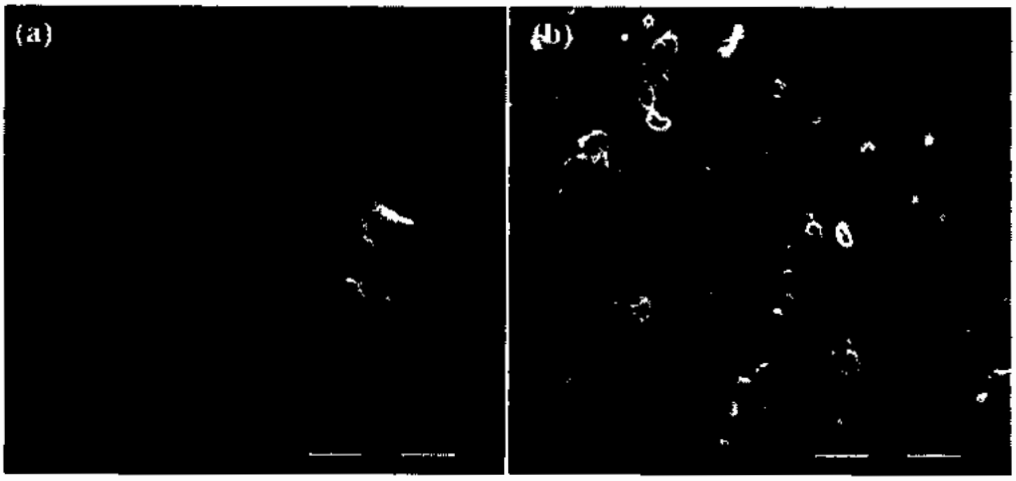

Figure 4.9: SEM images of (a) NIP and (b) MIP of polyurethane based maltose receptors.

To assess the surface morphology of MIP and NIP receptors, scanning electron microscope was used. The synthesized receptors were coated onto the glass substrate to obtain the thin films of fabricated receptors. The MIPs based receptors showed highly

porous and rough and non-imprinted polymer possess very smooth surface as shown in figure 4.9. The SEM images showed that microstructures on the imprinted receptor surface were due to the swelling of polymer on the incorporation of template within polymer matrix NIP has very smooth surface because such structures have not been seen on NIP thin film. Different morphology of both MIP and NIP indicated the successful polymerization of polymers.

4.3.2.2 Sensitivity analysis of fabricated sensor

To examine the sensor response of fabricated IDE towards analyte molecule (maltose), fabricated sensor was exposed to different concentrations of template molecule. The sensor response was measured against different concentrations ranging from 0-50 ppm and at 0 ppm, capacitance was 0 and as for 1 ppm, 5 ppm, 10 ppm, 20 ppm, 30 ppm, 40 ppm and 50 ppm, capacitance was 13 nF, 24 nF, 53 nF, 93 nF, 136 nF, 187 nF and 208 nF respectively as shown in figure 4.10 (a).

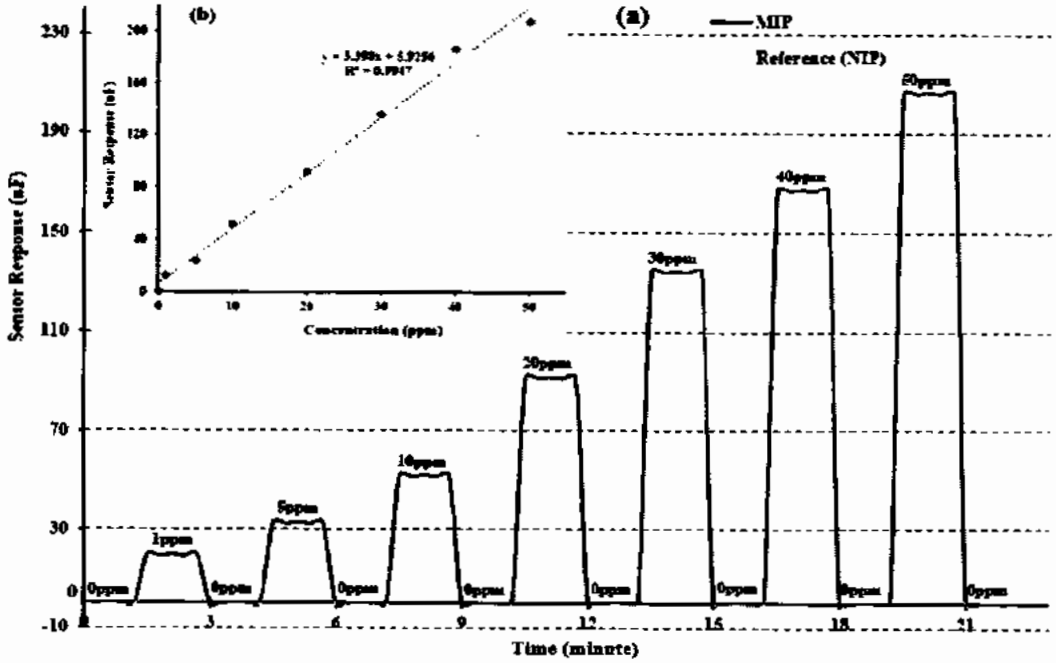

Figure 4.10 : (a) Sensitivity response of NIP and MIPs of polyurethane based maltose sensor at different concentration (0-50 ppm) (b) Linear regression analysis of maltose sensor.

While the response of NIP is 3 nF, 5 nF, 7 nF, 8 nF, 10 nF, 12 nF and 16 nF at 1 ppm, 5 ppm, 10 ppm, 20 ppm, 30 ppm, 40 ppm and 50 ppm concentration of template

(maltose) molecule which is very less as compared to the response of imprinted polymer and the significant difference of responses between MIPs coated IDEs and NIPs coated IDEs is because of the availability of selective molecular imprints/cavities in the molecular imprinted polymer. For measuring sensitivity of molecular imprinted polymer, different concentrations ranging from lower to higher were used. The conductance was increased in a linear manner so there is a linear relationship between concentration of template and conductance which means that sensor response is linear with linear regression co-efficient $R^2 = 0.99$ as shown in figure 4.10 (b). This might happen because -NH present in urethane molecule has a negative charge and maltose molecule acts as an electroactive specie. When this negatively charged atom interacts through electrostatic interaction with the -OH group of MIPs, the response of the sensor increases.

For the synthesis of a good sensor, it is important that there should be a reasonable amount of interaction between a template and functional monomer. Another reason could be that maltose is selectively adsorbed by the polymer matrix that creates potential change or increase in response to the change in concentration even at a minimal concentration of maltose. This confirms that the fabricated sensor is susceptible even at very low concentration of 1 ppm of template molecule (maltose) with a lower limit of detection (LoD) ~115 ppb and maximum detection point is ~525 ppm.

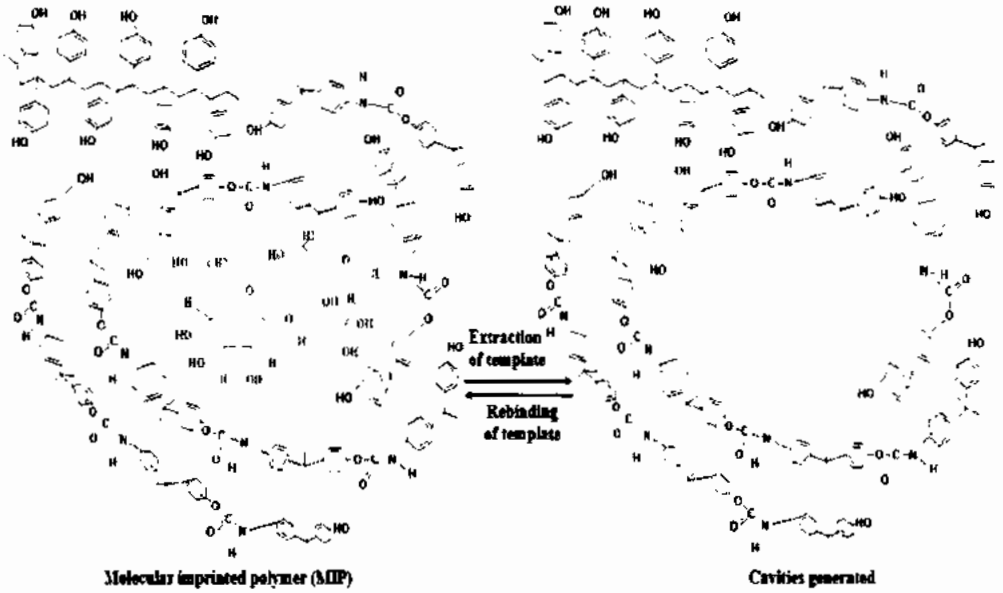

Figure 4.11: The rebinding and removal of template from polyurethane based maltose receptors.

After washing the sensor with water, its response again reaches to its initial value which means the sensor shows complete reversibility and regeneratability shown in figure 4.10 (a). On the other hand, if we see the interactions between the template and molecular imprinted binding sites, the sensitivity was enhanced as compared to non-imprinted polymer shown in figure 4.11. NIP does not show any significant change in its response due to lack of binding capacity towards analyte.

4.3.2.3 Selectivity analysis of sensor

For an ideal sensor, it should be highly selective towards its analyte of interest along with substantial sensitivity and linearity. To obtain a highly selective sensor, sucrose, fructose, glucose and n-hexane were chosen as interfering molecules. Selectivity was checked at 50 ppm, the conductance of maltose was 208 nF, in contrast at same concentration, this value for sucrose, fructose, glucose and n-hexane are 15 nF, 12 nF, 12 nF and 7 nF respectively. The difference between the sensor responses towards template molecules and other competing species proves the highly selective behavior of fabricated sensor.

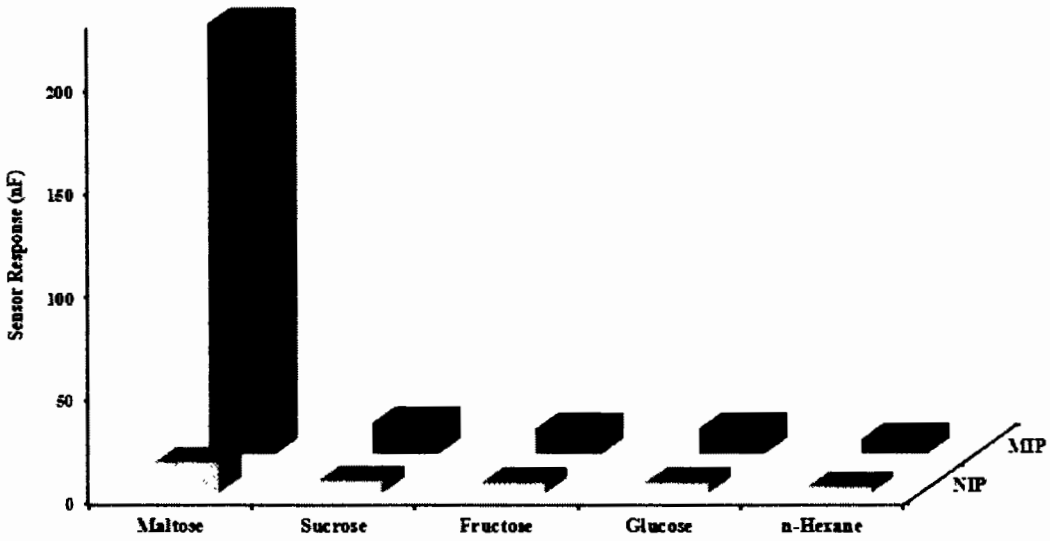

Figure 4.12: Selectivity analysis of polyurethane based maltose sensor against different competing molecules at 50 ppm.

This selectivity of the sensor was resulted due to the size identical cavities generation because during polymerization DPDI and Bisphenol A arrange themselves around the imprinted specie in a very effective way so they can produce highly effective recognition sites which is highly selective towards its template molecule i.e. maltose shown in figure 4.12. Selectivity coefficient for sucrose is greater in comparison to fructose which means that sucrose is strong interfering chemical specie for maltose than fructose due to same chemical structure. Greater selectivity coefficient of sucrose might be due to the resemblance of molecular structure and conductivity of analyte and interfering molecule.

4.3.2.4 Reproducibility, reusability and stability studies of fabricated sensor

Reproducibility, regeneratability, reversibility and stability of a sensor are important parameters to be addressed under normal conditions of temperature and pressure. For the analysis of reproducibility, three different sensors were synthesized following the same procedure and stored for a month at room temperature and pressure. These newly developed sensors were exposed to the template concentration (50 ppm) and sensor response was measured after one month for consecutive three times. Conductance was measured by LCR meter and figure 4.13 (a) described that at first, the sensor signals were stable, can be seen from error bars. The obtained relative standard deviation (RSD)

of <0.5 % signifies the effective reproducibility and regeneratability of the fabricated sensor at 50 ppm concentration with continuous usage.

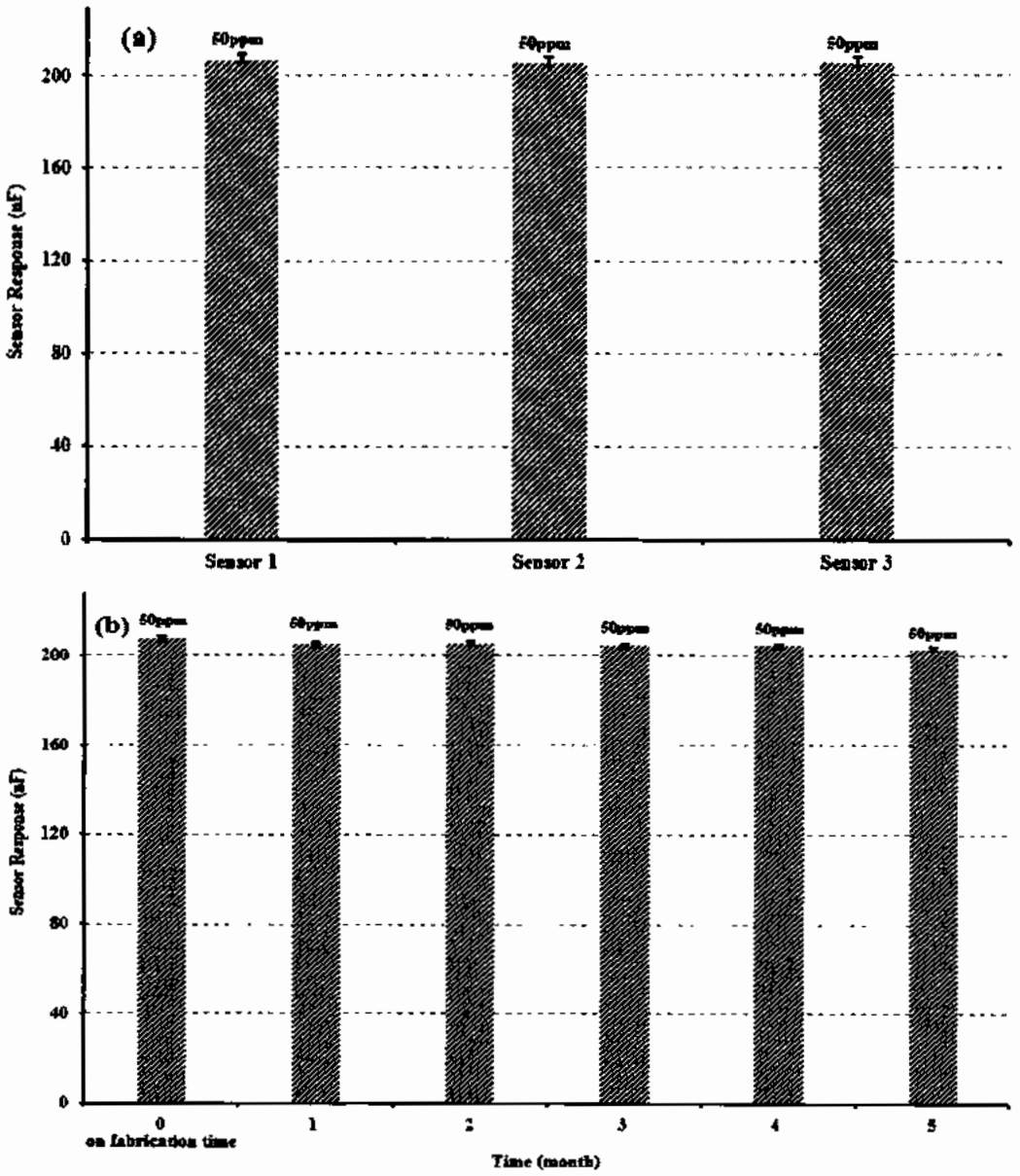

Figure 4.13: (a) Reproducibility and reusability of three polyurethane based maltose sensors prepared in the same manner (b) Stability profile of maltose sensor over the period of six months.

For stability of a fabricated sensor, a MIP based sensor was synthesized by the same recipe and stored under normal conditions of temperature and pressure. The above mentioned sensor was exposed to the 50 ppm concentration of template (maltose)

molecule and sensor response was measured after every month for a period of six months as shown in figure 4.13 (b).

From these observations, it was found that the fabricated maltose sensor didn't show any significant change in its response. In addition, 97 % of sensor response was maintained which also indicated that maltose MIP based sensor possesses excellent stability.

4.3.3 Characterization and sensor measurements of vinyl pyrolidone system based receptors

4.3.3.1 Characterization of synthesized receptors by FTIR spectroscopy and scanning electron microscope

To study the functional group modification during polymerization of n-vinyl pyrolidone and ethylene glycol dimethacrylate (EGDMA), FTIR analysis was performed. To study the chemical structure of thin films of imprinted and non-imprinted polymers, FTIR was plotted between wave number and % transmittance. A peak was observed at 2980 cm^{-1} as shown by figure 2.3, due to stretching vibrations of sp^3 (CH), while C-O-C stretching vibration was found at 1160 cm^{-1}. The ester group of EGDMA showed a characteristic stretching band at 1734 cm^{-1}. The peak at 1425 cm^{-1} was found a representative peak of C=N, C=C due to the stretching of pyridine group present in n-vinylpyrolidone. These major peaks in spectra showed that the polymerization occurred and imprinted polyvinyl pyrolidone were achieved by free radical polymerization of EGDMA and VP.

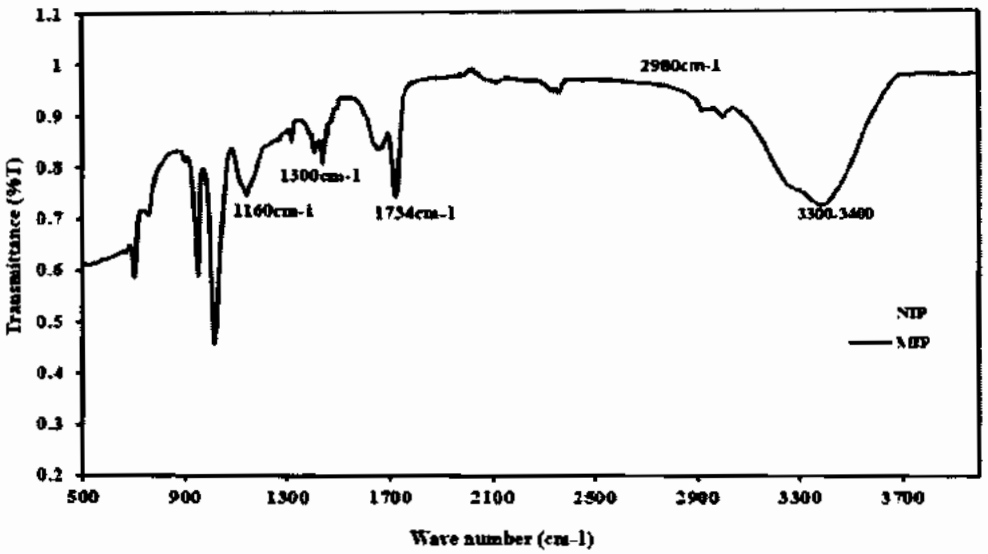

Figure 4.14: FT-IR spectra of non-imprinted and imprinted polyvinyl pyrolidone based maltose receptors.

To examine the surface morphology of molecular imprinted (MIP) and non-imprinted (NIP) receptors, scanning electron microscope was used. MIP and NIP receptors were coated onto glassy substrate to obtain thin films. SEM images showed that imprinted polymer bears highly rough and porous surface due to the swelling of polymer on the incorporation of template molecules within the polymeric matrix while non-imprinted receptors have smooth surface as shown in figure 4.15. The presence of these micro structures on the surface of MIP were due to the removal template molecule.

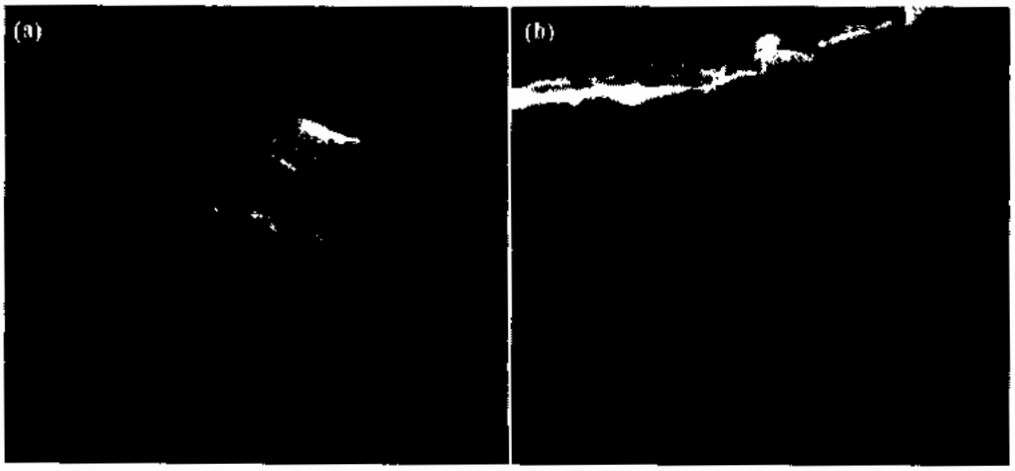

Figure 4.15 : SEM images of (a) NIP and (b) MIP of polyvinyl pyrolidone based maltose receptors

The topographical difference between MIP and NIP surfaces was observed which demonstrated the surface changes during polymerization of polymers.

4.3.3.2 Sensitivity analysis of fabricated sensor

For sensitivity measurement, synthesized maltose imprinted receptors were coated onto IDE and then washed to generate the imprints/cavities within the polymer matrix. The fabricated IDE was exposed to different concentrations i.e. 0- 50 ppm of maltose to examine the maltose sensitivity profile. When the fabricated sensor was exposed into the solution of 0ppm (de-ionized H_2O), the observed capacitance (Cs) was zero as shown in figure 4.16 (a). At 50 ppm concentration of analyte molecule, sensor exhibited the highest response i.e. 252 nF. Conductance was also measured at different concentration like 1 ppm, 5 ppm, 10 ppm, 20 ppm, 30 ppm, 40 ppm and 50 ppm, the observed sensor response was 22 nF, 37 nF, 72 nF, 123 nF, 172 nF, 207 nF and 252 nF respectively. On the other hand, reference electrode showed negligible response at all the respective concentrations of maltose. The number of binding sites present on the imprinted polymer surface are directly proportional to the sensitivity of sensor. Sensitivity response increases as the concentration of template (Maltose) increases which proves the highly linear behavior of fabricated sensor. Increase in the conductance upon increasing the template concentration leads to a certain where all available binding sites are completely occupied and further increase of analyte concentration will not influence the sensor response. This point or concentration will be higher limit of detection and this sensor showed saturation point at 529 ppm of maltose. It can be seen from figure that sensitivity is high for high concentration and upon increasing the concentration of template, conductance increases in a linear manner. This linear relationship between concentration of template and conductance with linear regression co-efficient $R^2 = 0.99$ can be seen figure 4.16 (b) and exhibited lower limit of detection ~68 ppb.

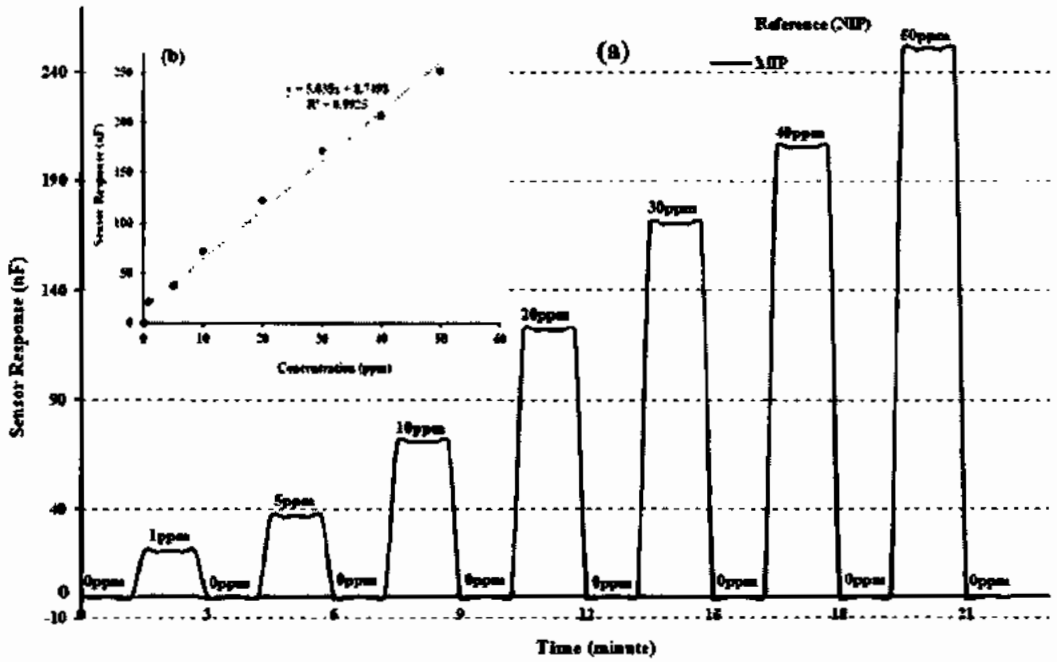

Figure 4.16 : (a) Sensitivity response of NIP and MIP of polyvinyl pyrolidone based maltose sensor at different concentrations (0-50 ppm) (b) Regression analysis of maltose sensor.

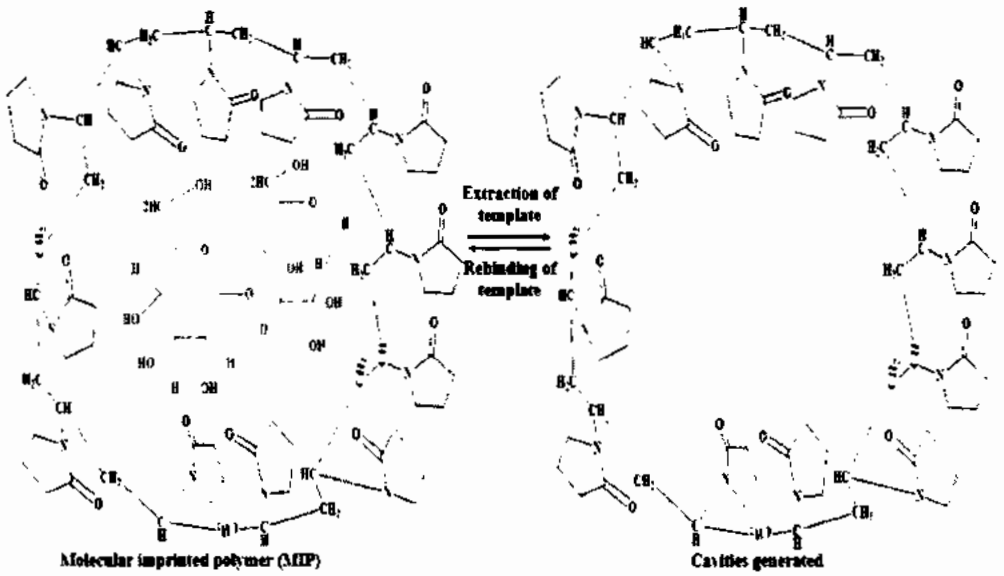

Figure 4.17: The rebinding and removal of template from polyvinyl pyrolidone based maltose receptors.

After treatment of the fabricated sensor with water, its response approaches to start point which indicates the sensor shows perfect reversibility and regeneratability. While the sensor possesses the lower limit of detection of 68 ppb towards the maltose. On the

other hand, NIP does not show any significant change in its response due to lack of binding capacity towards analyte. After washing the sensor with water, its response again reaches to its initial value which means the sensor shows complete reversibility and regeneratability shown in figure 4.16 (a). On the other hand, if we see the interactions between the template and molecular imprinted binding sites as shown in figure 4.17, the sensitivity was enhanced as compared to non-imprinted polymer. NIP does not show any significant change in its response due to lack of binding capacity towards analyte.

4.3.3.3 Selectivity analysis of sensor

Selectivity of a fabricated sensor can be measured by exposing the sensor to different interfering species including sucrose, fructose, glucose and n-hexane of same concentration against template (maltose) molecule. Although the polymer was not prepared for structurally related competing molecules, their sensing was checked with imprinted membrane prepared for maltose. The fabricated sensor showed response towards competing species while the response of template was higher than other molecules.

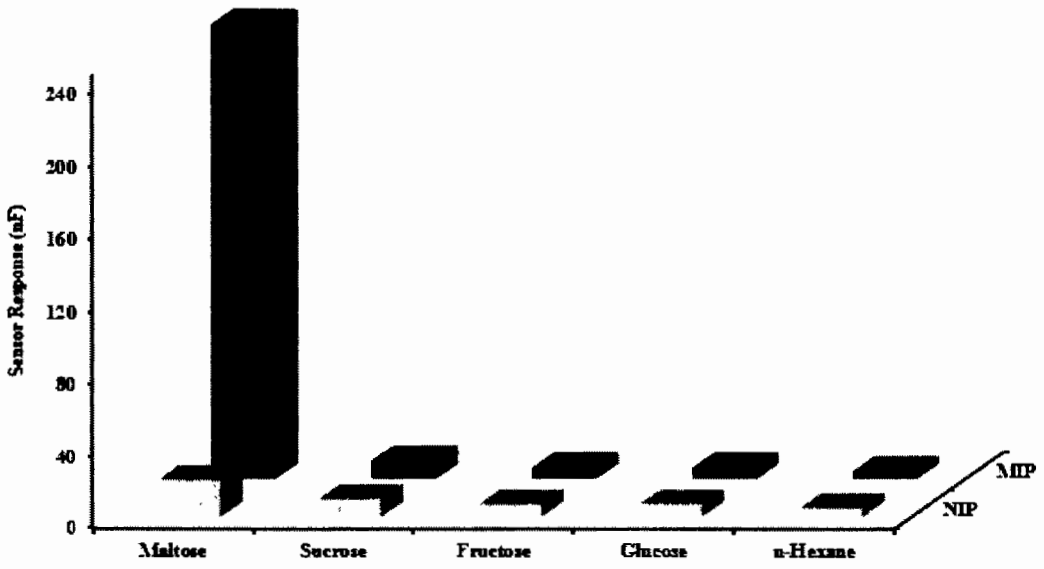

Figure 4.18: Selectivity analysis of polyvinyl pyrolidone based maltose sensor against different competing molecules at 50 ppm.

At 50 ppm, conductance of maltose and other interfering molecules were checked as shown in figure 4.18. Maltose MIP based sensor show signals (conductance) of 525 nF whereas sensor signals of sucrose, fructose, glucose and n-hexane were 10 nF, 6 nF, 6 nF and 4 nF respectively. Maltose sensor showed a response of 53 folds higher than sucrose, 88 times greater than glucose and fructose while for n-hexane, it was 131 folds higher for maltose. Sucrose showed higher selectivity response than other interfering molecules due to structure resemblance. They have same r geometry and bond angles due to which sucrose showed higher response than other competing species. Maltose and sucrose both are disaccharides have same functionalities. On the other hand, glucose and fructose are linear molecules due to which it showed negligible response. Sensor showed high response towards template in the presence of other competing species with same molecular geometry confirming that molecular imprinted polymer is highly selective towards target molecule.

4.3.3.4 Reproducibility, reusability and stability

For the success of newly developed sensor, it should be highly stable, reversible, regeneratable and reproducible when used for different applications. To assess the reproducibility and regeneratability of fabricated sensor, three different sensors were synthesized thrice using the same procedure and were stored at normal temperature and pressure. For the measurement of sensor response, the fabricated sensor was exposed to 50 ppm concentration of template molecule and stability profile was found by recording the signal responses of a sensor for a month under the room temperature and pressure (normal conditions). An acceptable accuracy was measured with relative standard deviation (RDS) ~0.25 % and indicated an excellent reproducibility as shown in figure 4.19 (a). To examine the stability, a sensor was synthesized thrice using the same synthesis process and stored for a period of six months under normal conditions. The sensor response was measured by exposing the fabricated sensor at 50 ppm concentration of maltose after every month upto six months as ca be seen in figure 4.19 (b).

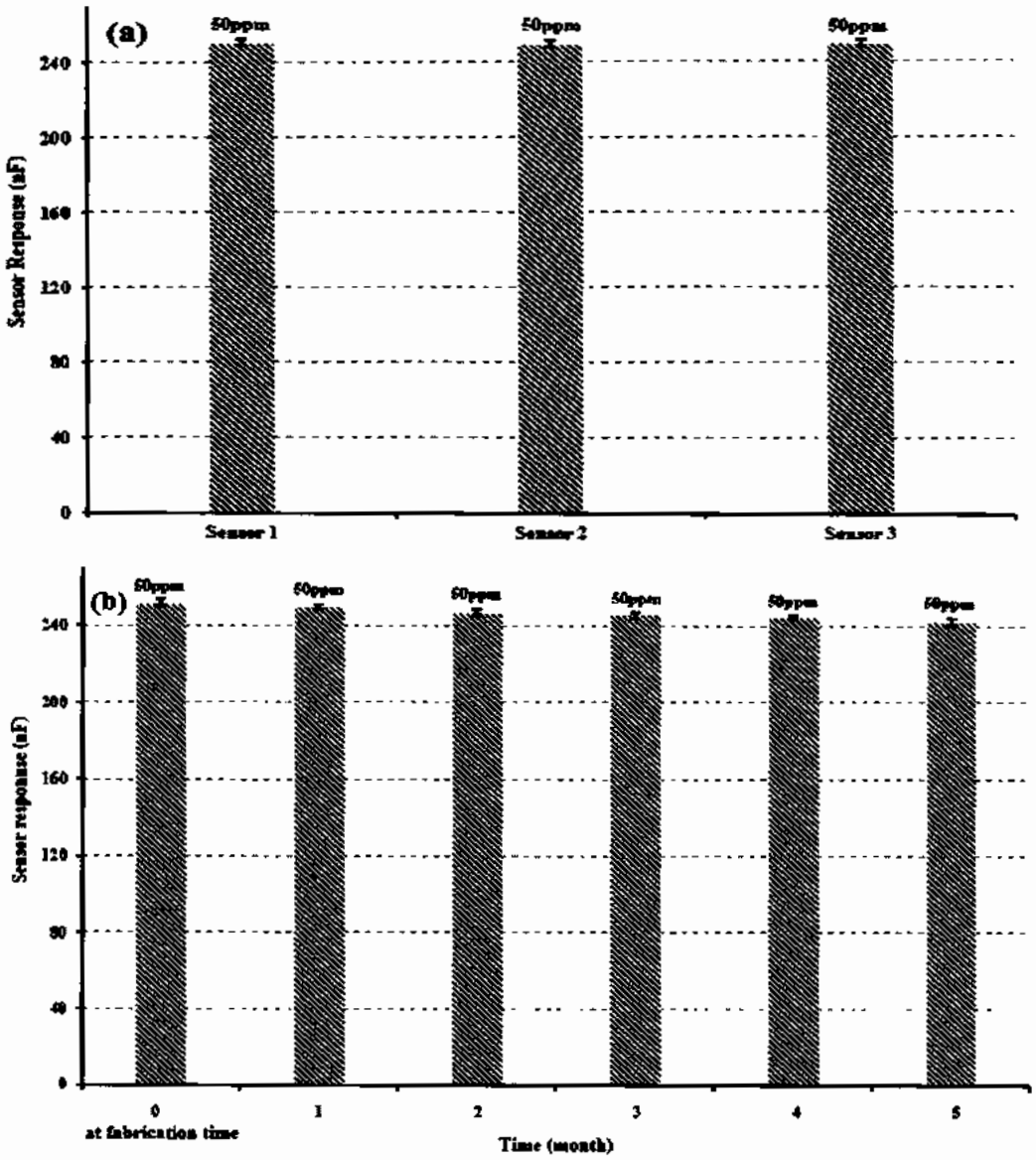

Figure 4.19: (a) Reproducibility and reusability a of three polyvinyl pyrolidone based maltose sensors prepared in the same manner (b) Stability profile of maltose sensor over the period of six months.

From these observations, it was found that senor didn't show any obvious change in sensor response. Moreover, the sensor response was analyzed after every month, maintained 99 % of the initial signals. The increased stability of electrochemical sensor is depending on the structural stability of highly cross-linked MIP complex.

4.3.4 Characterization and sensor measurements of imprinted methacrylic acid and its nanocomposite based receptors

4.3.4.1 Characterization of synthesized receptors by FTIR spectroscopy and scanning electron microscope

To study functional group changes during the polymerization of methacrylic acid (MAA) and ethylene glycol dimethacrylate (EGDMA), FT-IR analysis was performed.

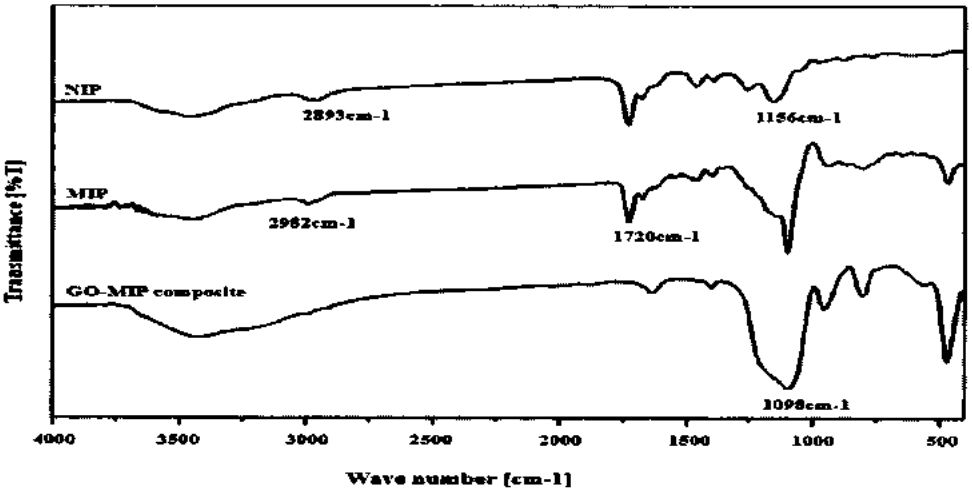

Figure 4.20 FT-IR spectra of NIP, MIPs and GO-MIPs composite methacrylic acid based maltose receptors.

FTIR spectra for acrylate based receptors was obtained in the range of 700-3900 cm^{-1} as shown in figure 4.20. Spectra of MAA and EGDMA showed –C=C stretching frequency at 1650 cm^{-1}. The peaks at 1670-1515 cm^{-1} are vibrational peaks indicating C-H stretching and C-H bending of polymer chains. The characteristics peaks centered at 1035-1149 cm^{-1} indicated the presence of polysaccharides in MIP. The absorption peak at 3200-3400 cm^{-1} was attributed to stretching vibrations of -OH of glucose. The peak at 1702 cm^{-1} shows the presence of ester group in the matrix and the other extra peaks are attributed to free radicle polymerization.

To examine the topography of the NIP, MIPs and GO-MIPs composite, Scanning Electron Microscope was used. For this purpose, the synthesized receptors were coated onto the glass substrate to achieve the thin films. Microscopic images showed that NIP

based receptors have smooth and non-porous surface while MIP based receptors showed highly rough and porous morphology as shown in figure 4.21.

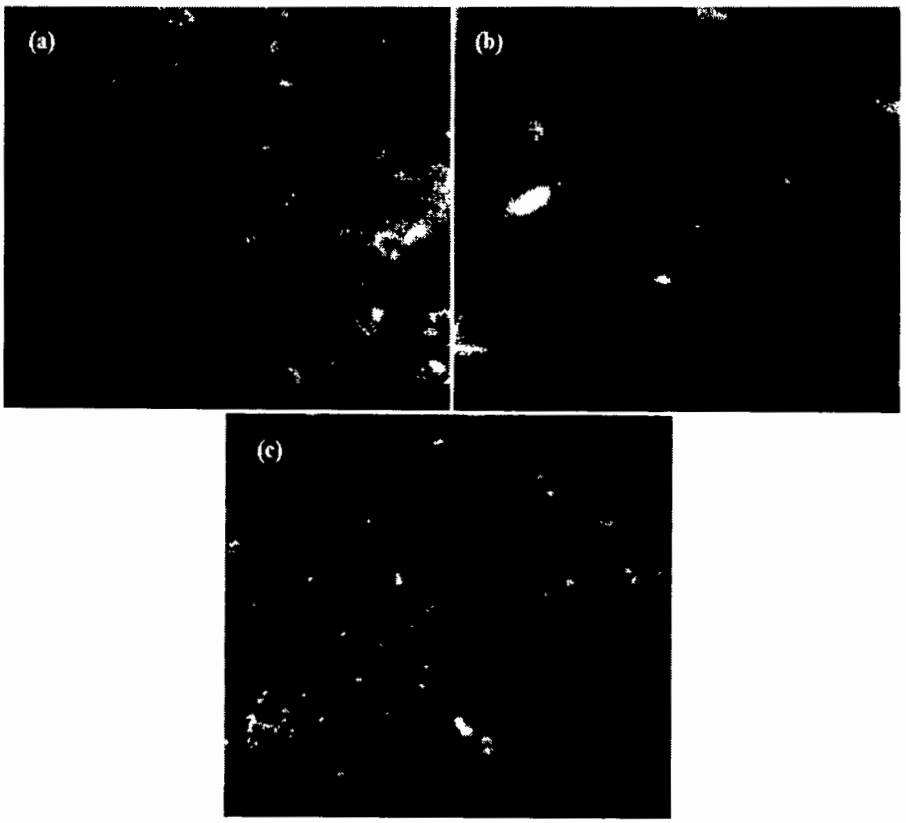

Figure 4.21: SEM images of (a) NIP, (b) MIPs and (c) GO-MIPs composite of methacrylic acid based maltose receptors.

The roughness of MIPs surface is due to the swelling of polymers on the incorporation of template molecule present within the polymeric complex. SEM image of GO-MIPs composite also showed completely embedded.

4.3.4.2 Thermogravimetric and differential thermal analysis (TGA/DTA)

Thermogravimetric analysis was performed to assess the mechanical and thermal stability of NIP, MIPs and GO-MIPs composite. TGA/ DTA profile was examined in the temperature range from 25 - 600 °C under nitrogen atmosphere. NIP has an initial negligible weight loss of -2.777/5.33 mg from 18.34 °C to 322.86 °C temperature related to the evaporation of solvent and water at first stage. The loss of mass between 322.86 °C and 596.34 °C is basically due to water removal from interior or condensation of

hydroxyl (OH) group. The obvious weight loss initiates from 400 ℃ is because of decomposition of imprinted polymer coatings (Li, Zhao et al. 2018). In second phase, mass loss was -2.797/5.797 mg and total mass loss is -5.574/5.797 mg (-100 %) shown in figure 4.22 (a). In case of molecular imprinted polymer (figure 5.22 b), a very small weight loss was noted (-3.430/5.33 mg) from temperature 35.38 ℃ – 272.36 ℃. In second shift, very minute mass loss of -1.781/5.33 mg was observed between a temperature of 287.4 ℃ - 577.35 ℃ and total weight loss was (-5.21/5.33 mg= -97.29 %). The thermogravimetric curve of GO-MIP composite showed mass loss in the temperature range of 28.43 ℃ to 367.2 ℃ was -4.054/5.3 mg while at second shift starts at 368.10 ℃ to 598.10 ℃ with weight loss of -1.38/5.3 mg can be seen in figure 4.22 c. The total mass loss in case of GO-MIP was -5.434/5.3 mg (-102.5 %).

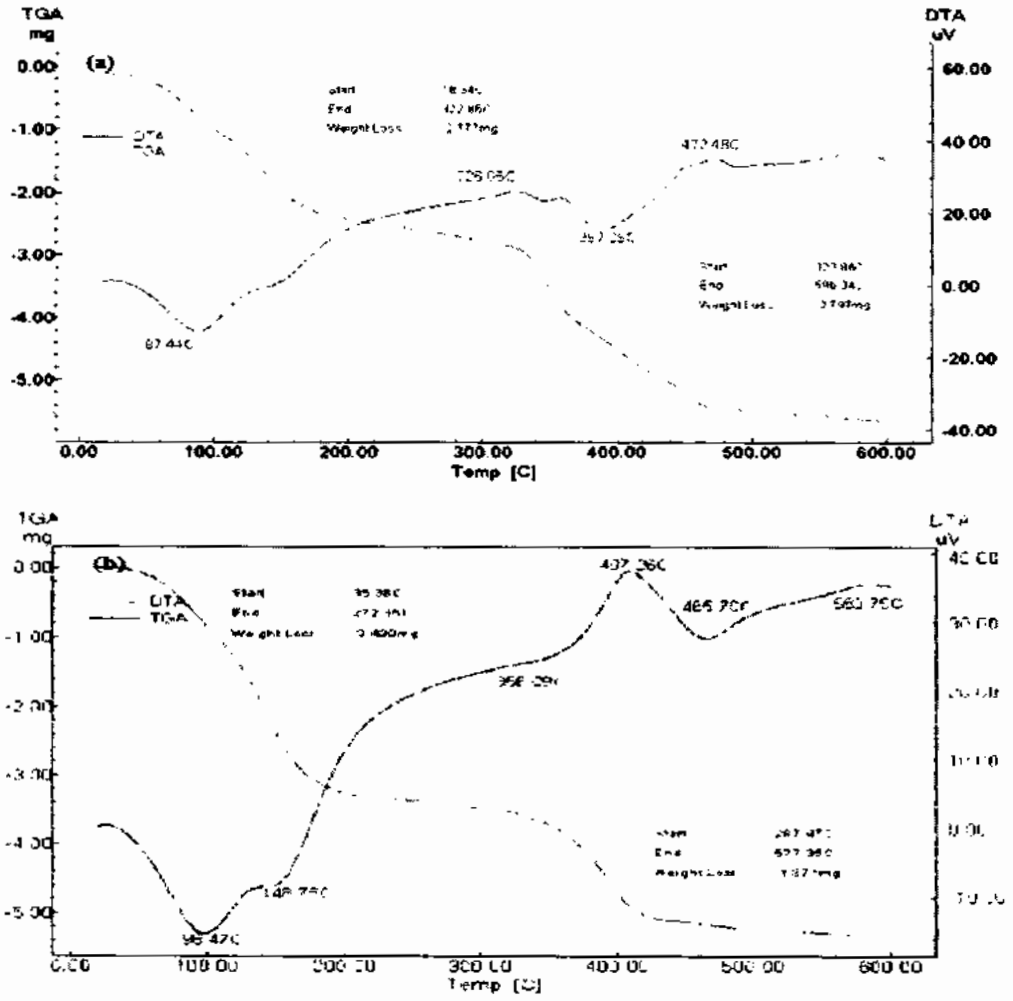

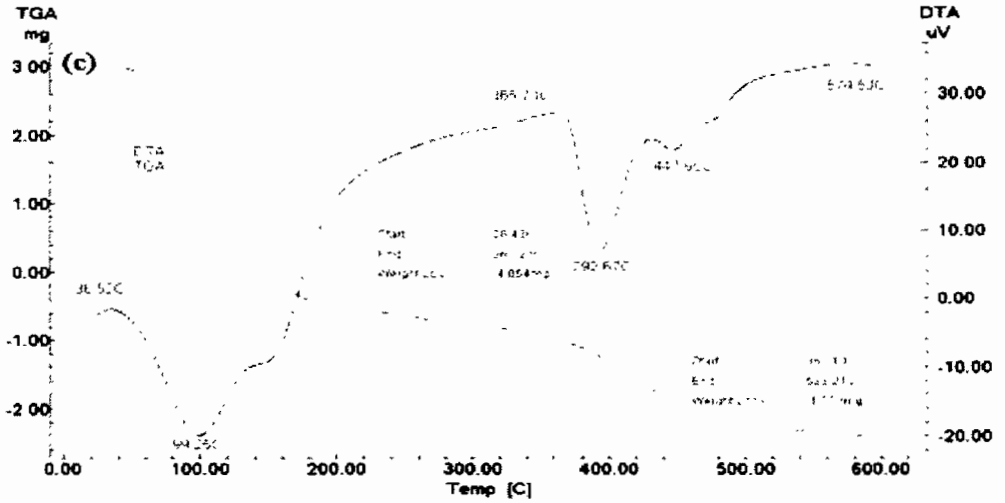

Figure 4.22 : TGA and DTA curves of (a) NIP (b) MIPs and (c) GO-MIPs composite of methacrylic acid based maltose receptors.

The different peaks present in DTG curve in temperature range of 25-600 ℃ are consistent with the weight losses of TG curve. The mass loss trend in NIP and MIPs was consistent with that of GO-MIP except the total loss is highly negligible in case of All NIP, MIPs and GO-MIPs composite. Furthermore, these results indicated that NIP, MIP and MIP/GO has been synthesized successfully with excellent thermal stability.

4.3.4.3 Sensitivity analysis of fabricated sensor

To assess the sensitivity of polyacrylate based maltose sensor, synthesized acrylate receptors were coated onto IDE and then washed to generate the imprints/cavities within the polymer matrix. The fabricated sensor was exposed to 0 ppm concentration (de-ionized H_2O) of template molecule, the observed capacitance (Cs) was zero as shown in figure 4.23 (a). At 50 ppm concentration of analyte (maltose) molecule, sensor exhibited the highest response i.e. 610 nF. Conductance was also measured at different concentration like 1 ppm, 5 ppm, 10 ppm, 20 ppm, 30 ppm, 40 ppm and 50 ppm, the observed sensor response was 38 nF, 111 nF, 181 nF, 232 nF, 328 nF, 455 nF and 610 nF respectively. On the other hand, the response of non-imprinted (NIP) was very low at the same concentrations of template (maltose) molecule and significant difference of sensor response between MIPs coated IDE and NIPs coated IDE is because of availability of template identical cavities/selective molecular imprints on the surface of

imprinted polymer based receptors. By increasing the concentration of maltose, conductance was increased which indicated that the sensor response is linear with linear regression co-efficient (R^2) value of 0.99 % as shown in figure 4.23 (b).

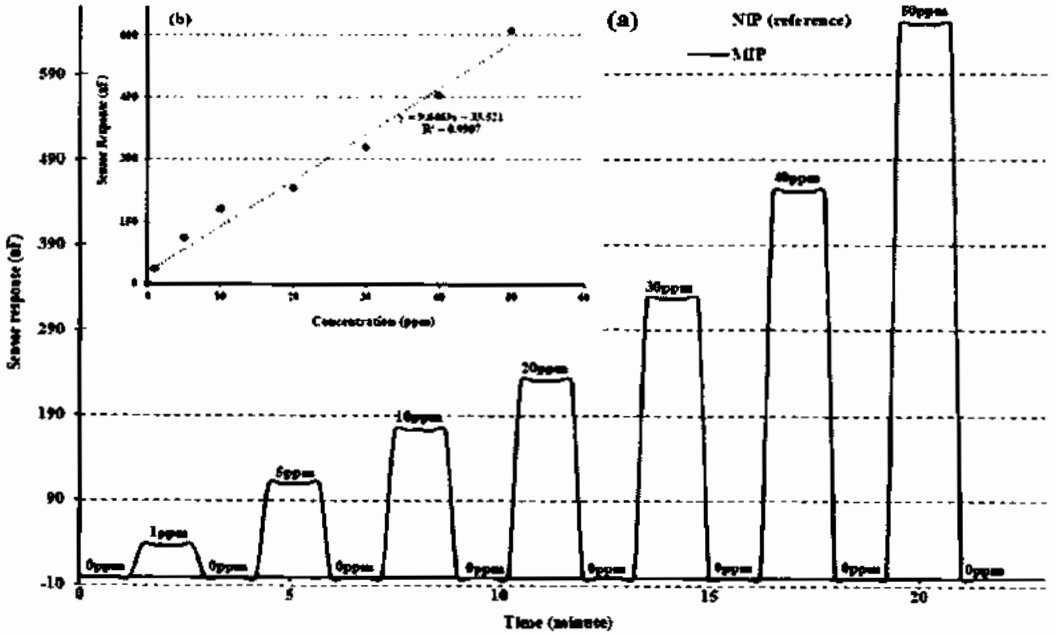

Figure 4.23: (a) Sensitivity response of NIP and MIPs of methacrylic acid based maltose sensor at different concentration (0-50 ppm) (b) Linear regression analysis of maltose sensor.

Increase in the conductance upon increasing the template concentration leads to saturation point at a higher concentration likely because of complete filling of cavities in the domain of polymer via adsorption of template molecule. For measuring sensitivity of maltose sensor, nanomolar (nM) concentration can be detected. By treating the maltose sensor with water, the sensor again exhibits the zero signals which confirms its reversibility behavior. While the sensor possesses the lower limit of detection (LoD) of 39 ppb with higher limit of 530 ppm towards the maltose, figure 4.23 shows the complete reversibility and regeneratability. The non-covalent interactions between the template molecules and polymeric matrix may base on the interaction of crosslinking agent and maltose molecules. The OH groups present on maltose interact with OH groups of acrylic acid while the EGDMA provides support in form of polymerization to generate cavities within polymer matrix as shown in figure 4.26.

To enhance the sensor performance and sensitivity, the structure of imprinted polymer was optimized in such a way that recognition cavities should be situated in the close proximity and at the surface of polymer material. The surface area of receptors and interactions between the analyte and sensor receptors were enhanced by combining the MIPs with functionalized graphene.

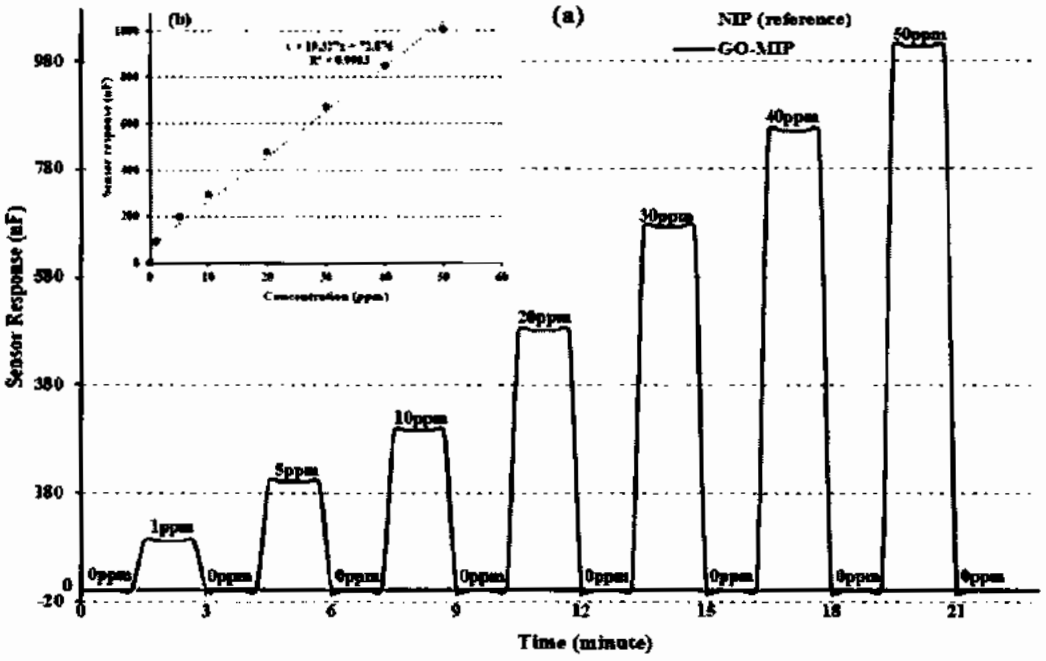

Figure 4.24: (a) Sensitivity response of NIP and GO-MIPs of methacrylic acid based maltose sensor at different concentration (0-50 ppm) (b) Linear regression analysis of GO-MIPs based maltose sensor.

For this purpose, functionalized graphene was added during polymerization. The sensitivity of graphene oxide based composite substantially enhanced towards analyte due to the excellent electrical and mechanical properties of functionalized graphene. Graphene oxide imprinted composite based sensor showed an improved sensor response when it was exposed to different concentrations of analyte i.e. 1 ppm, 5 ppm, 10 ppm, 20 ppm, 30 ppm, 40 ppm and 50 ppm and its sensor response was 92 nF, 201 nF, 295 nF, 482 nF, 674 nF, 851 nF and 1006 nF respectively. The GO-MIPs composite based sensor exhibited higher sensor response with increase in concentration which indicated the linear behavior of maltose sensor and linearity constant (R_2) was 0.99 shown in figure 4.24 (b). Functionalized graphene based sensor enhance the sensor response ~3 folds and limit of detection was also improved upto ~16 ppb to 600 ppm

calculated by signal to noise ratio (S/N= 3). The surface morphological studies showed availability of the high surface area as compared to other polymers which leads to the high sensor response because of maltose-MAA interactions which leads to the maximum adsorption of template molecules.

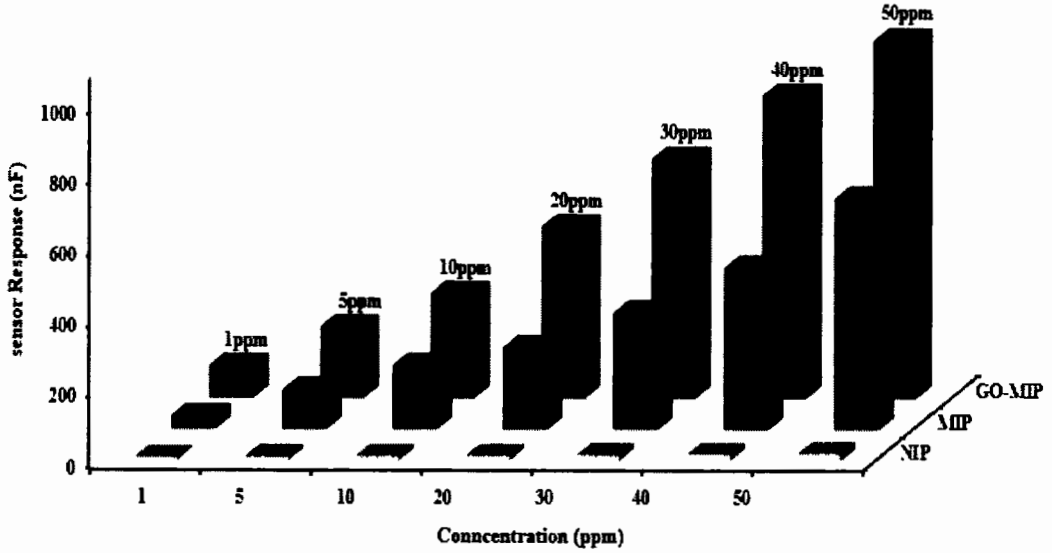

Figure 4.25: Comparison of sensor response of NIP, MIPs and GO-MIPs composite based maltose sensor at different concentrations (0-50 ppm).

GO-MIPs based sensor was found highly sensitive and reversible as can be seen from figure 4.24 (a). The bar graph in figure 4.25 shows the comparison of NIP, MIPs and GO-MIPs. The possible interactions between template molecules and polymer matrix where dipole-dipole force and hydrogen bonding cause the interaction between template molecule and imprinted cavities. It bears a lot of electroactive oxygen containing functional groups and has two-dimensional plane in its oxidation state. It is chemically stable and has a large surface area, its easily soluble in water that makes it an ideal material for the modification of electrodes and electrochemical detection.

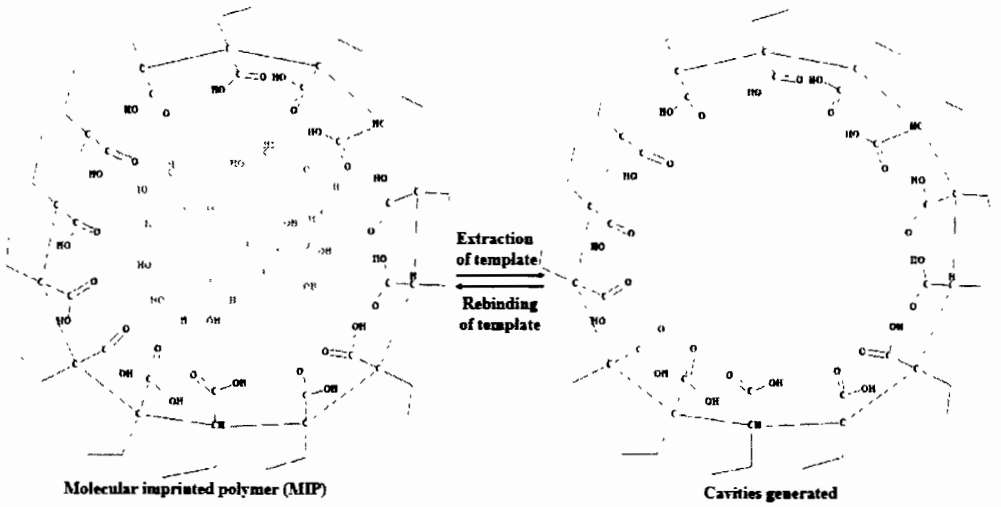

Figure 4.26: The rebinding and removal of template from methacrylic acid based maltose receptors.

4.3.4.4 Selectivity analysis of sensor

Selectivity is an important parameter of chemical sensor and sensitivity, alone is not sufficient, therefore, it is important to check the selectivity of MIP and GO-MIP composite based sensor by exposing it against different competing molecules based on structural and functional analogues. Sucrose, fructose, glucose and n-hexane were selected as interfering species to evaluate the selectivity performance of the sensor. At 50 ppm, conductance of maltose and other interfering molecules were checked and found that maltose MIP based sensor show signals (conductance) 610 nF whereas fructose, maltose, sucrose and n-hexane were 10, 9, 9 and 6 nF respectively. Selectivity co-efficient is far high for sucrose (61 times) as interfering molecule, for fructose and glucose, it was 68 folds, and also exhibits highly negligible response for n-hexane. Sensor response of GO-MIP composite based maltose sensor was 1006 nF and sensor signals of other competing molecules were 7, 3, 3 and 2 nF for sucrose, fructose, glucose, and n-hexane respectively. During polymerization, methacrylic acid and EGDMA rearrange themselves in a very effective way around the imprinted specie results in a high number of recognition sites which is highly selective towards the respective analyte. Selectivity co-efficient is highly increased for sucrose (143 times) as interfering molecule, for fructose and glucose, it was 335 folds, and also exhibits highly negligible response for n-hexane. This proves that GO-MIP (composite) sensor

is highly sensitive as well as selective against competing species. So these interfering molecular species might be entrapped in the cavities of MIP systems which are in fact generated for analyte molecules i.e. maltose molecules. The low response of these polymer based sensors for sucrose might be due to the fact that molecular geometry and molecular structure of interfering molecule do not resemble the molecular geometry and molecular structure of maltose.

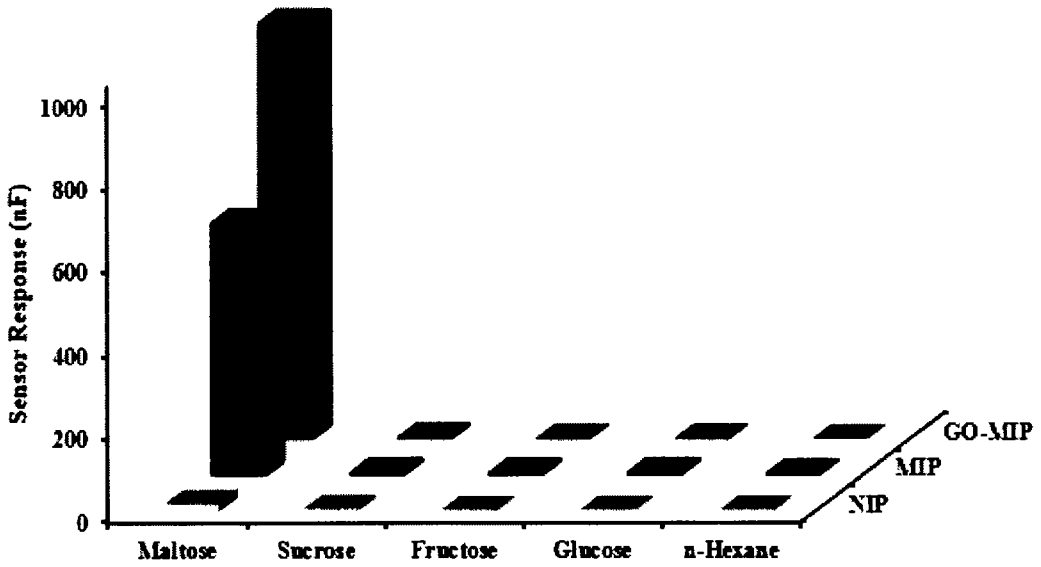

Figure 4.27: Selectivity analysis of methacrylic acid based maltose sensor against different competing molecules at 50 ppm.

This shows the achievement of molecular imprinted approach where sensor shows high selectivity. GO-MIP composite based sensor represented highly selective as compare to MIP based sensor response. The addition of functionalized graphene enhanced selectivity profile of fabricated sensor due to excellent surface area and electrical, mechanical properties. Therefore, GO-MIPs composite based sensors strongly prefer their template over all interfering molecules. The feature of selectivity makes a sensor to contribute in a different way towards different analytes. This property gives ability to sensor to work in complex environment.

4.3.4.5 Reproducibility, reusability and stability of sensor

To assess the reproducibility of GO-MIPs composite based sensor, three different sensors were synthesized using the same procedure. The fabricated sensors were store at room temperature and pressure for a period of one month. Graphene oxide composite based sensors were exposed to 50 ppm concentration of analyte and sensor response was measure thrice. From above mentioned measurements, it was found that sensor response was maintained upto 99.5 % with RSD ~0.27 % which indicated that the fabricated GO/MIP composite based sensor was excellently reproducible as shown in figure 4.28 (a). Furthermore, GO-MIPs composite based maltose sensor was stored under normal conditions of temperature and pressure for six months. This fabricated sensor was exposed to 50 ppm concentration of template molecule and sensor measurements were performed at regular intervals of one month for a period of six months under the same conditions. At zero month, the measured sensor response (conductance) was 1006 nF. At zero month, the sensor signals were 1006 nF, after one month, sensor showed signals of 1004 nF whereas after two months, it was 1003 nF, for third and fourth months, sensor signals were 1002 and 997 nF, at fifth months, the noted sensor signals were 995 nF as shown in figure 3.7 (a).

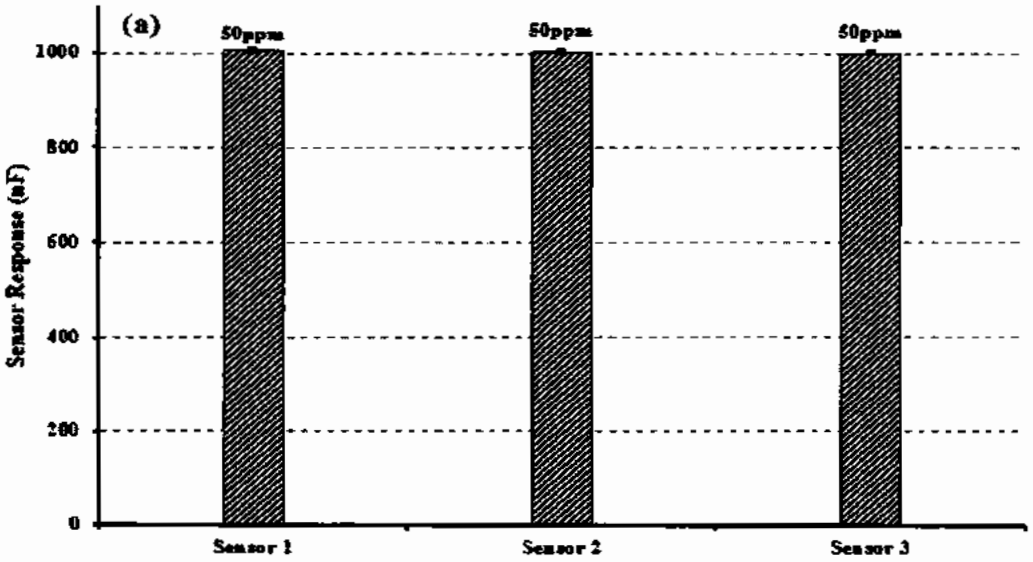

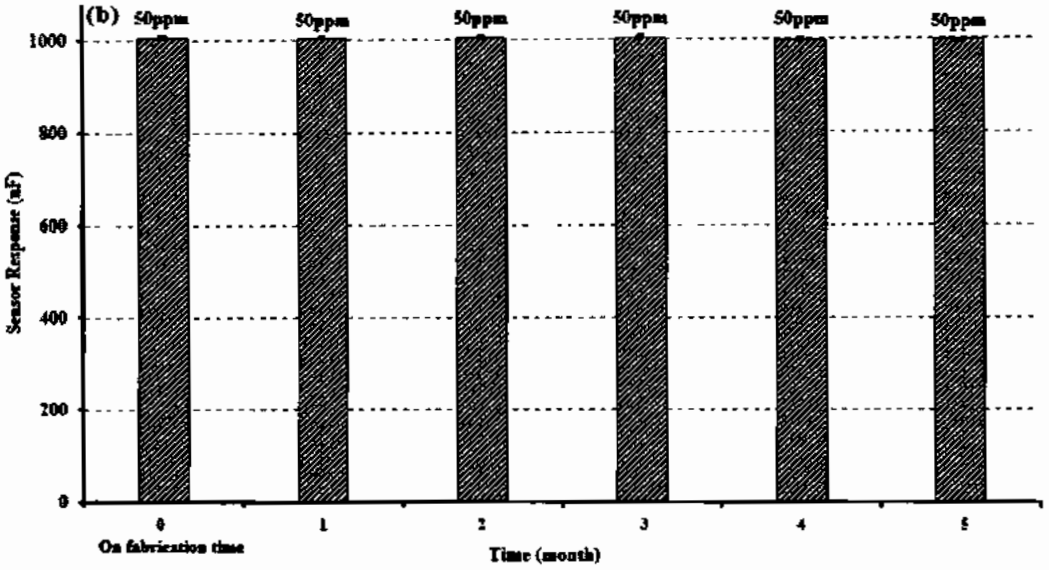

Figure 4.28: (a) Reproducibility and reusability a of three methacrylic acid based maltose sensors prepared in the same manner (b) Stability profile of maltose sensor over the period of six months.

After six months, these observations confirmed the stability of fabricated fructose sensor by 2 % RSD value (n=6) and maintained sensor response upto 97 of maltose sensor was also checked at 50ppm concentration with the same sensor shown in figure 4.28 (b) and relative standard deviation is less than ≥0.5 % and sensor response was maintained upto 99.5 % with continuous usage.

4.4 Comparison of sensor receptors (Imprinted polystyrene, polyurethane, polyvinyl pyrolidone and methacrylic acid)

Selection of functional monomer is of substantial importance for the detection of sugars by molecular imprinted polymer based sensors. Currently, different functional monomers were frequently used for molecular recognition i.e. styrene, DPDI, N-vinylpyrolidone and methacrylate. Styrene is a hydrophobic monomer and shows weak interactions with template molecule. DPDI as single functional monomer can be used for the preparation of stimuli-recognition element. DPDI can provide hydrogen binding sites to interact with analyte molecule. From figure 4.29, we can observe a lower response by polyurethane (monomer) might be due to lesser number of cavities on the

polymer surface matrix. When responses of urethane system against maltose was compared with response of polystyrene system it was revealed that response of urethane system was greater than polystyrene system. It may be possible that interaction of template with n-vinyl pyrolidone system is stronger than the interaction of polystyrene with template. As the structure and composition of n-VP are different from polystyrene so it might be assuming that cavities generated in n vinyl pyrolidone system are stronger which result in strong binding with template molecule i.e. maltose. The intermolecular attractive forces are possibly dipole-dipole interactions. As hydroxyl carries partial negative charge in maltose molecule. The extent of this dipole-dipole interaction is different for the two polymer system because of their structural and compositional differences.

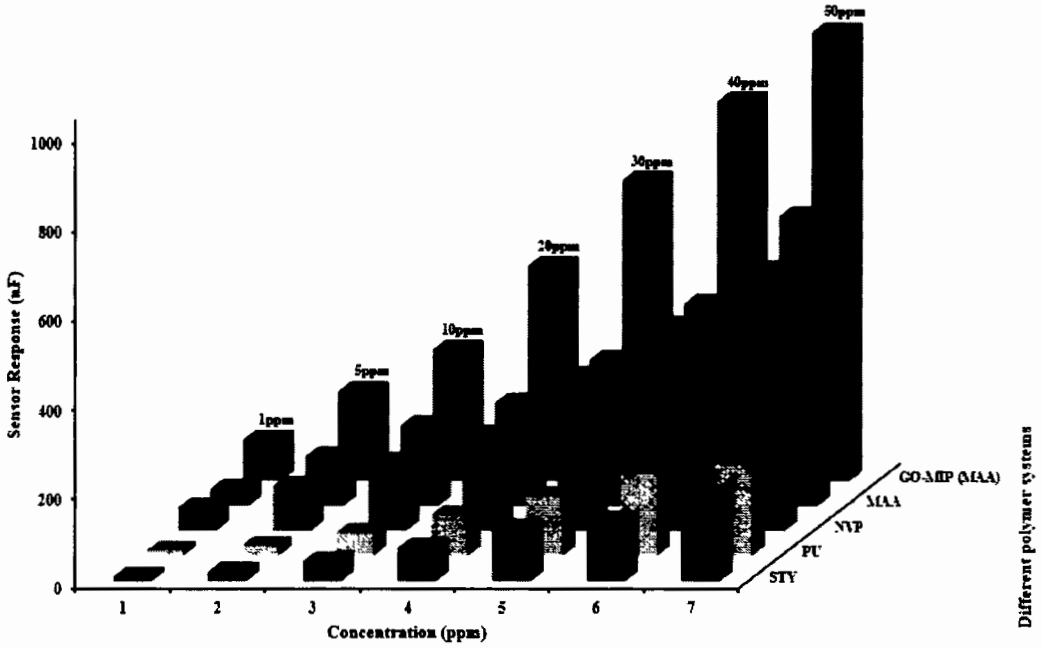

Figure 4.29: Comparison of different polymer systems used for the detection of maltose.

Sensor response was also measured by using Methacrylic acid as structural monomer. With Methacrylic acid as monomer, sensor showed the highest response. It may be due to the reason that binding sites generated by MAA were highly selective. The interactions between MAA and maltose were stronger than other monomers. GO-MIPs of methacrylate were also used to measure the sensor response for maltose and found

many folds' higher response than simple MIPs. The results obtained from different imprinted polymers were briefly reported in table 4.1 and compared these data with literature studies reporting fructose measurements using different electrochemical methods.

Table 4.1 : Comparison of previously reported work with recently designed sensors.

Analyte	**Detection method**	**Technique**	**Limit of detection**	**Range of detection**	**Reproducibility (RSD)**	**Reference**
Maltose	Non-enzymatic	Amperometry	1 µM (1000 ppb)	14 µM - 1.9 mM	-	(Emelyanova 2019)
Maltose	Non-enzymatic	Cyclic voltammetry (CV)	24.18 µM (24100 ppb)	0.18– 3.47 mM	0.823 %	(Xiaohong, Zhidong et al. 2017)
Maltose	Non-enzymatic (styrene as monomer)	Conductance	150 ppb	150 ppb to 507 ppm (~2 seconds)	0.8 % (97.8 % RSR)	Present work
Maltose	Non-enzymatic (urethane as monomer)	Conductance	115 ppb	115 ppb to 525 ppm (~2 seconds)	1.8 % (98 % RSR)	Present work
Maltose	Non-enzymatic (n-vinyl pyrolidone as monomer)	Conductance	68 ppb	68 ppb to 529 ppm (~2 seconds)	0.75 % (99 % RSR)	Present work
Maltose	Non-enzymatic (MAA as monomer)	Conductance	39 ppb	39 ppb to 530 ppm (~2 seconds)	0.48 % (99 % RSR)	Present work

Maltose	Non-enzymatic (MAA+ GO)	Conductance	16 ppb	16 ppb to 600 ppm (~2sec)	≥0.5 %	Present work

4.5 Conclusion

In this chapter, MIPs and GO-MIPs composites were used for the detection of maltose and polystyrene, n-vinylpyrolidone, polyurethane and methacrylate based receptors response was found in the following order: Styrene < Polyurethane < n-Vinylpyrolidone < Methacrylic acid. Furthermore, to enhance the sensor response, graphene oxide composites of acrylate based receptors are synthesized. It is found that graphene oxide composite based sensor responses are many folds higher as compared to that of imprinted polymers. We can conclude that methacrylate system is most suitable for the maltose imprinting and bears high sensitivity and selectivity. While the composite of imprinted acrylate with functionalized graphene induces higher incorporation and moieties for the template molecules and produced higher sensor response. The surface morphology of polyacrylate based maltose imprinted receptors depicts the uniform generation of template identical cavities as compared to other polymers. Hence the sensitivity, selectivity, limit of detection, reproducibility, reusability and stability of the fabricated sensor is improved by using GO-MIPs composite and it can have potential technological applications in field of chemical sensors and material science.

5 Chapter 5 FABRICATION OF MOLECULARLY IMPRINTED POLYMERS AND NANOCOMPOSITE BASED SENSORS FOR THE DETECTION OF SUCROSE

5.1 Introduction

Sucrose, commonly used as sweetener extracted from fruits, vegetables and sugarcane. The high content of sugar is sucrose (Pan, Yuan et al. 2016, Tuck, Ross et al. 2017) and animals maintain their energy level by the consumption of sucrose. It influences their lipid metabolism and insulin efficiency (Pérez-López, Mateos-Aparicio et al. 2016). Sucrose is a disaccharide composed of glucose and fructose subunits and both sub-units linked to each other through an oxygen atom (Head, Farbotko et al. 2013, Feng, Huang et al. 2017, Marques, Mans et al. 2017, Head, Klocker et al. 2018). Sucrose possesses eleven hydrogen bond acceptors and eight hydrogen bond donors with five rotatable bonds as can be seen in figure 5.1.

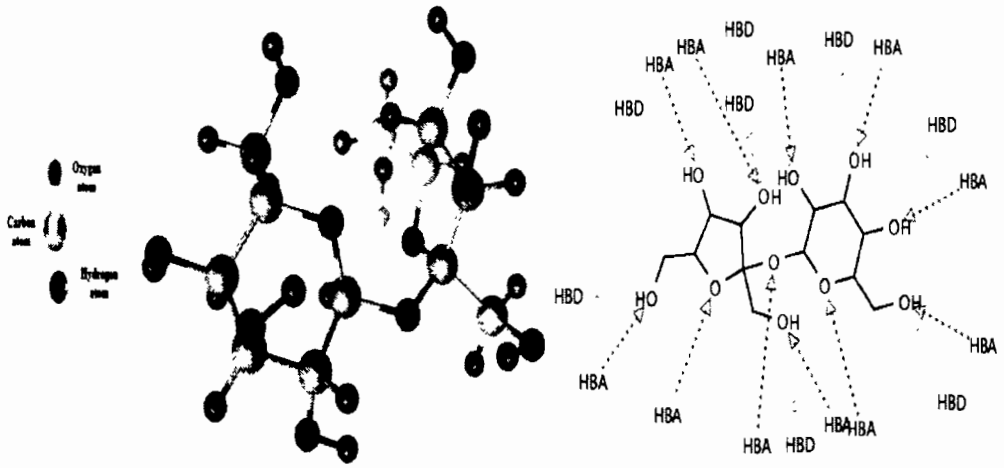

Figure 5.1 : 3D structure of sucrose (HBA = Hydrogen bond acceptor, HBD = Hydrogen bond donor)

Excessive intake of sucrose causes serious health issues to human beings such as genetic sucrose-isomaltase deficiency (GSID), heart diseases, obesity and diabetes mellitus (Sobrino-Gregorio, Vargas et al. 2017). Therefore, a rapid and efficient quantification of sucrose is of substantial importance. Various conventional methods and techniques are in use for the quantification of sucrose such as colorimetry (Gaddes, Demirel et al. 2015, Gaddes, Reeves et al. 2017, Alev-Tuzuner, Beyler-Cigil et al. 2018), reverse phase high performance liquid chromatography (RP-HPLC) (Wang, Chen et al. 2018), high performance liquid chromatography (HPLC) (Shanmugavelan, Kim et al. 2013, Dvorackova, Snoblova et al. 2014, Ma, Sun et al. 2014, Li, Wu et al. 2018, Wang, Chen et al. 2018), florometry (Seo, Jung et al. 2014, Liu, Ding et al. 2018),

polarimetry and near infrared spectroscopy (Pan, Zhu et al. 2015). These methods and techniques have some limitations like complex operation, high cost and time consumption. Therefore, there is a need for simple and low cost alternative methods, tools and electrochemical sensors have potential to be promising tools for the detection of sucrose contents. Chemical sensors are simple, low cost, highly stable, high sensitivity and specific to the specific analyte and number of efforts have been made to quantify sucrose contents by using electrochemical sensors (Kong, Pan et al. 2012, Tang, Zhang et al. 2017). Recently, molecular imprinted polymers (MIPs) based sensors got significant research interest to improve the analytical performance of electrochemical sensors. The MIPs are artificially synthesized receptors with selectivity and higher affinity in their size, shape, spatial arrangement of functional groups towards the targeted molecule (analyte). In this chapter, we reported the fabrication of MIPs and GO-MIPs (nanocomposite) based sensors using different polymeric systems (styrene, vinyl-pyrolidone, urethane and acrylate) and cross-linker ratios. The synthesized receptors were characterized by FT-IR, SEM and TGA. Furthermore, real-time sensor measurements have been performed to assess the various sensor parameters by exposing fabricated sensor to different concentrations of sucrose and other competing species.

5.2 Experimental section

5.2.1 Chemicals and materials

For the synthesis of NIP, MIPs and GO-MIPs composite based sucrose sensors, following chemicals such as glucose (99.5 %), sucrose (99 %), maltose (99 %), fructose (99 %), dimethyl sulphoxide (DMSO, 99.7 %), n-vinyl pyrolidone (99 %), 4, 4′diphenylmethanediioscyanate (DPDI; 98 %), phloroglucinol (PG; 99 %), bisphenol A (BPA; ≥99 %), chloroform, methacrylic acid (MAA; 99 %), styrene and 2,2′-azobisisobutyronitrile (AIBN; 99 %) and ethylene glycol dimethacrylate (EGDMA; 98%), acetone (≥ 99 %), methanol (99.8 %, anhydrous), ethanol (99.8 %, anhydrous) were purchased from Merck and Sigma Aldrich with the maximum available purity.

5.2.1.1 Synthesis of styrene based molecularly imprinted polymer (PS-MIP)

4.3×10^{-4} mM of styrene, 2.6×10^{-4} mM of ethylene glycol dimethacrylate (EGDMA), 2 mg of AIBN as free radical initiator were mixed into an eppendorf tube. To the above solution, 500µL of dimethyl sulfoxide (DMSO) as solvent and sucrose (2 mM) were added and vortex it to obtain homogenized solution. Then mixture was polymerized into water bath at 70 °C for 45 minutes till transparent gel point is reached.

5.2.2 Synthesis of non-imprinted polymer (PS-NIP)

Non-imprinted polymer (reference) was also synthesized exactly in the same way without adding template (sucrose). Styrene (4.3×10^{-4} mM), 2.6×10^{-4} mM of ethylene glycol dimethacrylate (EGDMA), 2 mg of AIBN as free radical initiator were mixed into an eppendorf tube. To the above solution, 500µL of dimethyl sulfoxide (DMSO) as solvent and vortex it to obtain homogenized solution. Then mixture was polymerized into water bath at 70 °C for 45 minutes till transparent gel point is reached.

5.2.3 Synthesis of n-vinyl pyrolidone based molecularly imprinted polymer (VP-MIP)

Poly(vinylpyrolidone) based MIP was synthesized by following this method. Vinyl pyrolidone (4.6×10^{-4}mM, 2.6×10^{-4} mM of EGDMA were mixed into an eppendorf having 500 µL (4 mmole sucrose solution in DMSO) of sucrose solution. After homogenizing, 4mg of AIBN was added to above mixture and vortex. The resultant solution was heated to 60 °C for 45minutes in water bath till a transparent gel point was attained.

5.2.4 Synthesis of non-imprinted polymer (NVP-NIP)

NVP-NIP was prepared without adding template (sucrose) molecule in the same way as MIP was synthesized. Poly(vinylpyrolidone) based MIP was synthesized by following this method. Vinyl pyrolidone (4.6×10^{-4} mM), 2.6×10^{-4} mM of EGDMA were mixed into an eppendorf having 500 µL of DMSO, 4 mg of AIBN was added to above mixture and vortex. The resultant solution was heated to 60 °C for 45 minutes in water bath till a transparent gel point was attained.

5.2.5 Synthesis of methacrylic acid based molecularly imprinted polymer (MAA-MIP)

Sucrose imprinted polymer was synthesized by mixing 5.8 $\times 10^{-4}$ mM of methacrylic acid (MAA) as functional monomer, 2.6×10^{-4} mM of EGDMA as cross linker, 4 mg of AIBN as free radical initiator and 500 µL of DMSO as solvent. 2 mg (2 mM) of sucrose was added to the above mixture as template. The mixture was vortex for 5 minutes to homogenize and then place in water bath at 60 °C for 45 minutes to polymerize.

5.2.6 Synthesis of non-imprinted polymer (MAA-NIP)

NIP was prepared in the same manner without adding the template (sucrose). Sucrose imprinted polymer was synthesized by mixing 5.8×10^{-4} mM of methacrylic acid (MAA) as functional monomer, 2.6×10^{-4} mM of EGDMA as cross linker, 4 mg of AIBN as free radical initiator and 500 µL of DMSO as solvent. The mixture was vortex for 5 minutes to homogenize and then place in water bath at 60 °C for 45 minutes to polymerize.

5.2.7 Synthesis of urethane based molecularly imprinted polymer (PU-MIP)

Polyurethane based maltose imprinted receptors were synthesized using 50 to 50 ratio between monomer and cross-linker. Urethane based receptors were synthesized by 1.9×10^{-6} mM of phloroglucinol (PG), 8 $\times 10^{-6}$ mM of bisphenol A and 3.6×10^{-6} mM of DPDI was vortexed in 1 mL of DMSO. Sucrose (2 mmole) was added and homogenized by vortex. The resultant solution was heated for 30 minutes at 45 °C in water bath till gel point was obtained which indicated the synthesis of maltose imprinted polymer.

5.2.8 Synthesis of non-imprinted polymer (PU-NIP)

PU-NIP was also prepared in the same way without adding sucrose as template molecule. Urethane based receptors were synthesized by 1.9×10^{-6} mM of phloroglucinol (PG), 8 $\times 10^{-6}$ mM of bisphenol A and 3.6×10^{-6} mM of DPDI was vortexed in 1 mL of DMSO The resultant solution was heated for 30 minutes at 45 °C in water bath till get point was obtained which indicated the synthesis of sucrose imprinted polymer.

5.2.9 Synthesis of polyurethane based graphene oxide (PU-GO-MIP) composite

Graphene oxide composite of molecularly imprinted urethane was synthesized by adding 0.5 mg of graphene oxide in 600 µL of imprinted DPDI, sonicate and a suspension of PU-GO-MIP composite was achieved.

5.2.10 Immobilization of NIPs, MIPs and GO-Composite onto IDEs

IDEs were washed with methanol and de-ionized water. 5 µL of polymer (MIP) was spin coated onto IDEs at a speed of 2000 rpm and dried in oven for 18hrs to completely adhere the polymer thin film on IDEs.

5.2.11 Removal of template from MIPs

To remove the template from imprinted polymer matrix, IDEs were placed into deionized water and constantly stirred by magnetic stirrer for 3 hours at room temperature.

5.3 Results and discussion

5.3.1 Characterization and sensor measurements of styrene system based receptors

5.3.1.1 Characterization of synthesized receptors by FTIR spectroscopy and scanning electron microscope (SEM)

To assess the functional group modification of synthesized NIP and MIPs, ATR-FTIR analysis was performed.

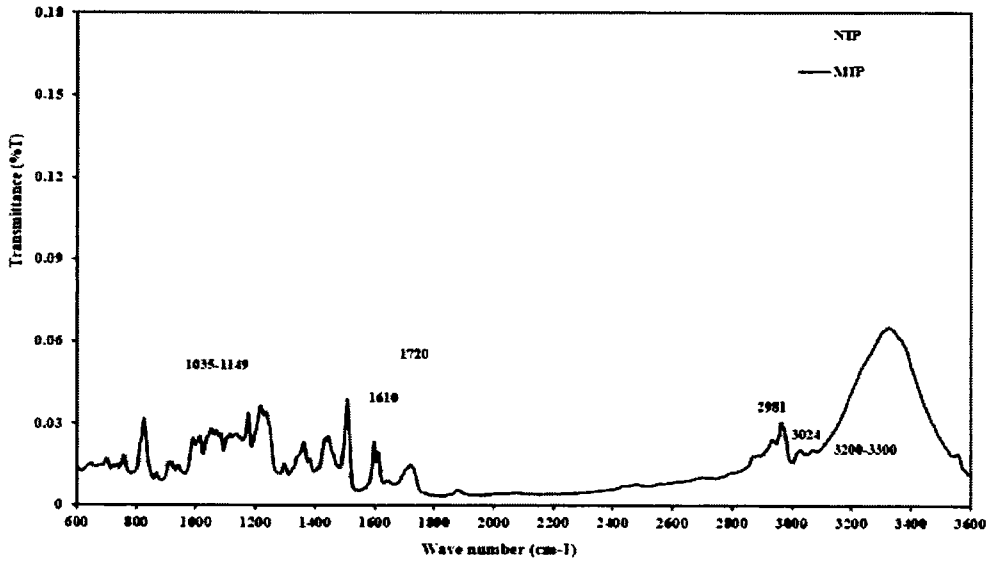

Figure 5.2: FT-IR spectra of non-imprinted and imprinted polystyrene based sucrose sensor.

FTIR spectra for polystyrene system was observed in the range from 600-4000 cm^{-1}. The characteristic peak at 900-1100 cm^{-1} indicates the presence of glucose in case of both MIP and GO-MIP whereas absence of this peak in NIP spectra confirms the removal of glucose. The absorption peak at 3000-3400 cm^{-1} was attributed to stretching vibrations of –OH of sucrose and confirms the hydrogen bond formation which is absent in NIP. The peak at 2800-2900 cm^{-1} were assigned to the sp^2 (CH) aromatic rings. By comparing the peaks present with MIP and GO-MIP, were found absent in NIP.

To study the surface morphology of NIP and MIP, scanning electron microscope was used. For thin films generation, receptors were coated onto a glassy substrate. Microscopic images showed that NIPs have very smooth surface while the images of imprinted polymers showed high surface roughness due to the swelling of polymer on the incorporation of template molecules within the polymeric matrix as shown in figure 5.3. The SEM images showed that micro and nanostructures have been produced in the imprinted polymer surface due to swelling of polymer surface and porogenic effect

during polymerization while such structures have not been observed in the micrographs of NIPs

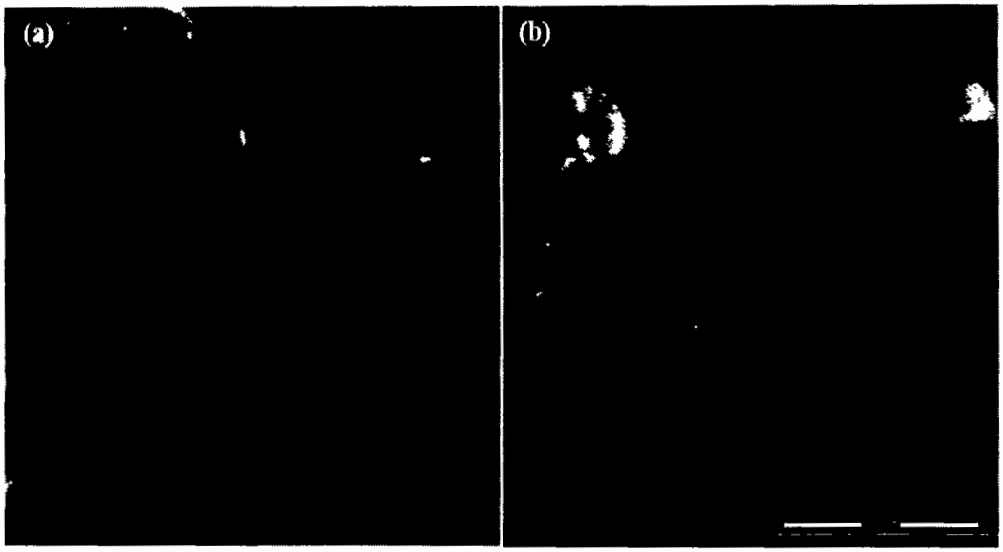

Figure 5.3: SEM images of (a) NIP and (b) MIP polystyrene based sucrose receptors.

5.3.1.2 Sensitivity measurements of fabricated sensor

To develop sucrose imprinted electrochemical sensor, the receptors were coated onto the IDEs and exposed to different concentrations of analyte ranging from 1 ppm to 50 ppm. At 0 ppm, the observed capacitance was 0 and at 1 ppm, 5 ppm, 10 ppm, 20 ppm, 30 ppm, 40 ppm and 50 ppm of sucrose, the sensor responses of 18 nF, 34 nF, 67 nF, 107 nF, 144 nF, 185 nF and 227 nF have been observed respectively with the lowest limit of detection ~83 ppb of sucrose. The obtained electrochemical results demonstrated that newly fabricated sensor was highly sensitive even at very low concentration of 1ppm as shown in figure 5.4 (a). The NIP was also exposed to the same concentrations of analyte and sensor signals were found very less. The linearity of sensor was also assessed by linear regression analysis of obtained sensor responses at different concentrations of analyte (0-50 ppm) and the sensor showed linear response with a linear co-efficient of regression (R^2) of value 0.99 as can be seen in figure 5.4 (b). The sensor showed a change in signals from 18 nF to 227 nF towards 1 ppm to 50 ppm concentrations of sucrose which indicates the concentration dependent linearity of sensor signals which is due to the change in number of sucrose molecules incorporated in sensor moieties.

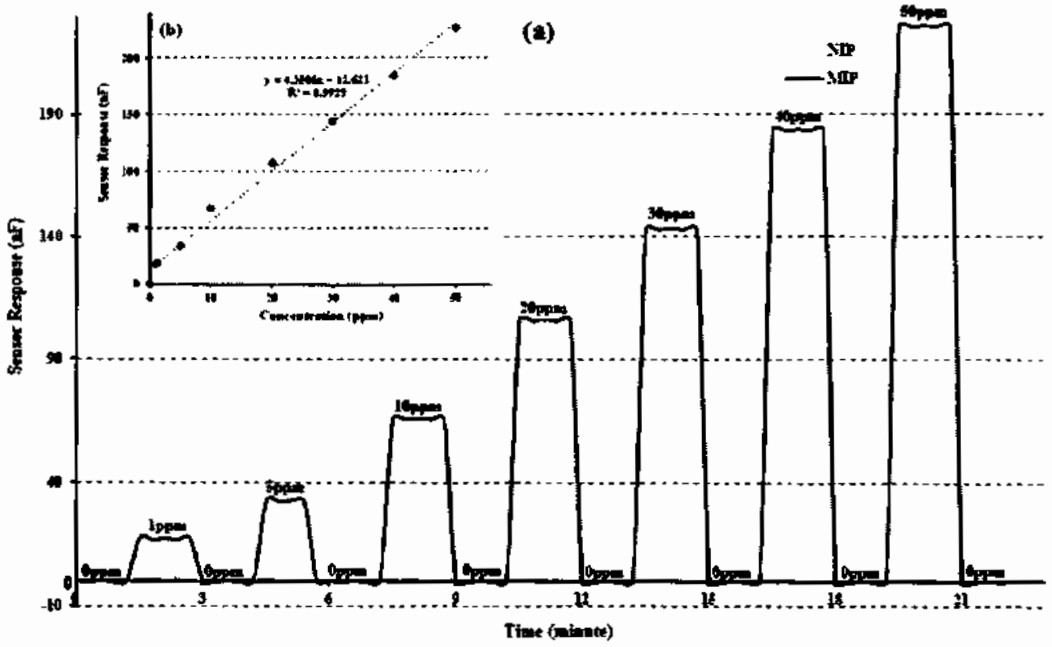

Figure 5.4: (a) Sensitivity response of NIP and MIPs based polystyrene sucrose sensor at different concentrations (0-50 ppm) and (b) Linear regression analysis of sucrose sensor.

The increase of capacitance might be due to the -OH (hydroxyl) group present in sucrose with upper detection limit of 520 ppm which was trapped within the molecular cavities present in polymeric matrix coated onto IDEs. The sensor exhibits an excellent reversibility when subjected to zero concentration of sucrose solution.

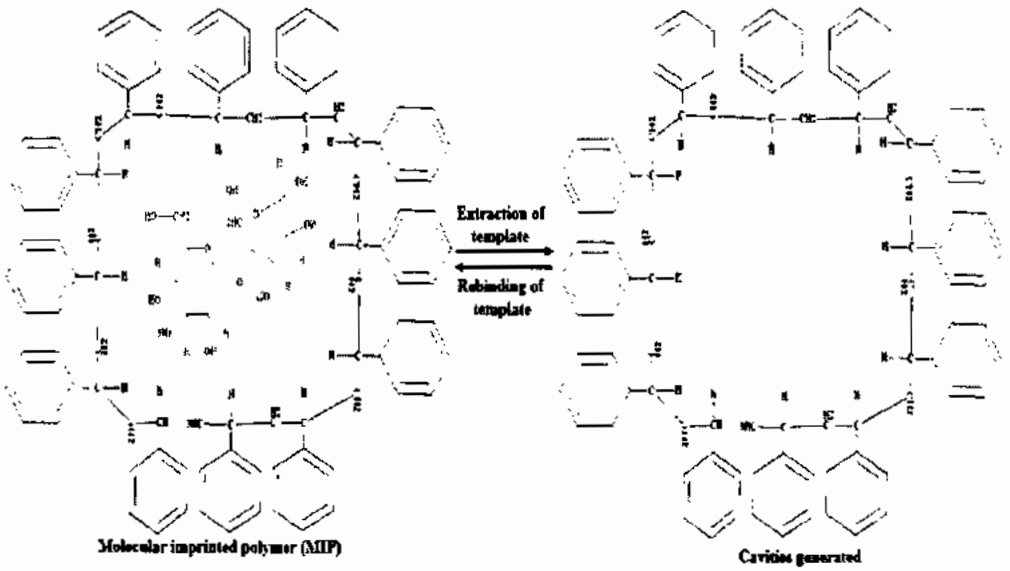

Figure 5.5: The extraction and rebinding of template into polystyrene based sucrose receptors.

Styrene monomer is hydrophobic in nature with no special functionality and the role it may assist in formation of sucrose imprint within polymer matrix where it could specifically fix and coordinate with the crosslinking agent, EGDMA. It thus makes the shape and geometrically fit sieves in MIPS that make it capable of selective incorporation of template molecules. While the behavior of sensor with NIPs as recognition materials is not influenced by the change in concentration. By employing the bulk imprinting technique, artificial receptors were synthesized by structuring the surface imprinted polymer of sucrose with particular template for the sucrose detection. Various non-covalent interactions such as hydrophobic interactions, dipole-dipole interactions, hydrogen bonds and π-π interactions are supporting the reversibility of sensor instead of strong covalent bonds. Figure 5.5 shows the non-covalent interactions between analyte (sucrose) and functional monomer (styrene). As a result, an appropriate polymer must have affinity counterparts with the analyte being able to develop an exact structure of template molecule which is more or less fixed by cross-linker. In this case polystyrene layer consisting of styrene and ethylene glycol dimethacrylate (EGDMA) turned into a feasible receptor layer for the detection of sucrose. The pattern produced on the sensitive layer is actually attained by bulk imprinting with sucrose molecule. In this way, receptor cavities are produced on the sensitive layer for reversible insertion of sucrose. For successful imprinting process, sensor response by selective analyte recognition is a proof, particularly comparing non-imprinted and imprinted thin film coating.

5.3.1.3 Selectivity analysis of sensor

To assess the quality of a sensor, selectivity is an important parameter. For this purpose, sucrose imprinted polymer based sensor was exposed to different competing species such as maltose, fructose, glucose and n-hexane at specific concentration i.e. 50 ppm. The sensor signals obtained with analyte was 227 nF whereas for maltose, fructose, glucose and n-hexane were 10 nF, 7 nF, 7 nF and 5 nF respectively. From these observations, we can say that each sensor exhibits the highest sensor response to its template molecule and very minute sensor response was found against different interfering molecules. Sensor measurements ensure the successful imprinting pattern

achieved by bulk imprinting technology. This technique in response might produce sterically and chemical induced fit cavities for the insertion of template molecule. The most prominent sensor response was observed by templated species i.e. sucrose whereas a very minute sensitivity was achieved for maltose and sucrose fabricated sensor retained insensitive to fructose, glucose and n-hexane. Selectivity studies to fabricated sensor were performed by styrene imprinted polymer with maltose (geometrical difference and specific spatial).

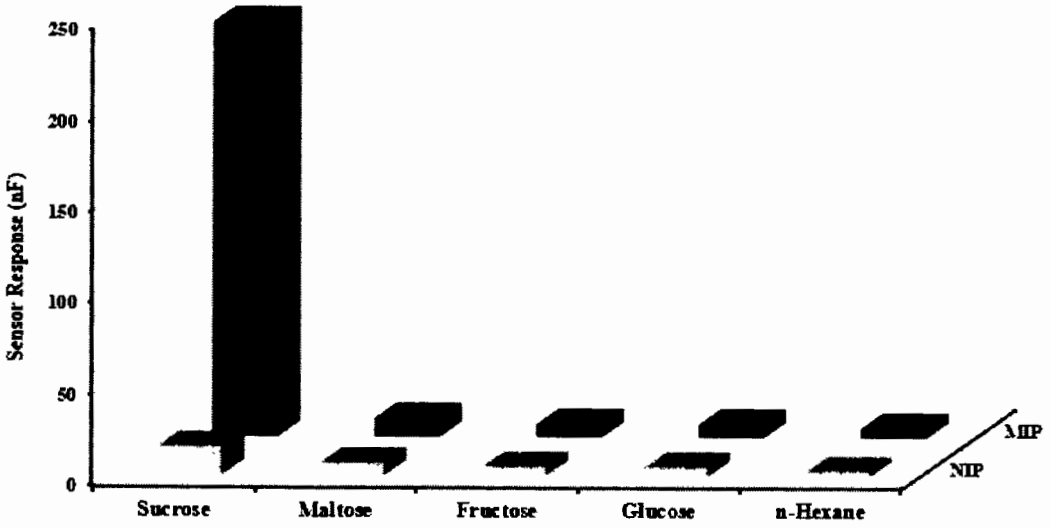

Figure 5.6: Selectivity analysis of polystyrene based sucrose sensor against different competing molecules at 50 ppm.

Selectivity analysis is an important feature of imprinting. The moieties developed after extractions of the template molecules are complementary identical to the imprinting species in size, shape and coordination geometries which leads to substantial selectivity of fabricated sensor. The sensor selectivity response demonstrates whether a fabricated sensor is suitable for the sample, in which number of competing molecules with highly identical mass, structure and chemical properties are present along with the analyte of interest. Therefore, it is important to analyze if the sensor is selective for the molecule of interest or not.

5.3.1.4 Reproducibility, reusability and stability

To investigate the reproducibility, three different sucrose imprinted sensors were synthesized at the same time using the same method of synthesis and stored at room temperature and pressure. After one month, the sensitivity was assessed by exposing the sensor to specific concentration i.e. 50 ppm of sucrose as shown by figure 5.7 (a). The obtained relative standard deviation (RSD) of 0.5 % signifies the effective reproducibility of fabricated sensor with continuous usage. In addition, 99 % of sensor response was maintained which also indicate that sucrose MIP based sensor possesses excellent reproducibility. To assess the stability of fabricated sensor, sucrose imprinted sensor was synthesized using the same procedure and stored under normal conditions of temperature and pressure. The fabricated sensor was exposed to specific concentration of template molecule every month for a period of six months and sensor response was noted. At zero month, the sensor response was 227 nF, after one month, it was 225 nF. For second, third, fourth and fifth months, the measured sensor responses were 224 nF, 220 nF, 218 nF and 216 nF respectively as shown in figure 5.7 (b). From these observations, the calculated RSD value of 1.9 % indicated that the fabricated sensor is highly stable under the above mentioned conditions. These measurements confirm the excellent reproducibility and stability of the fabricated sensor.

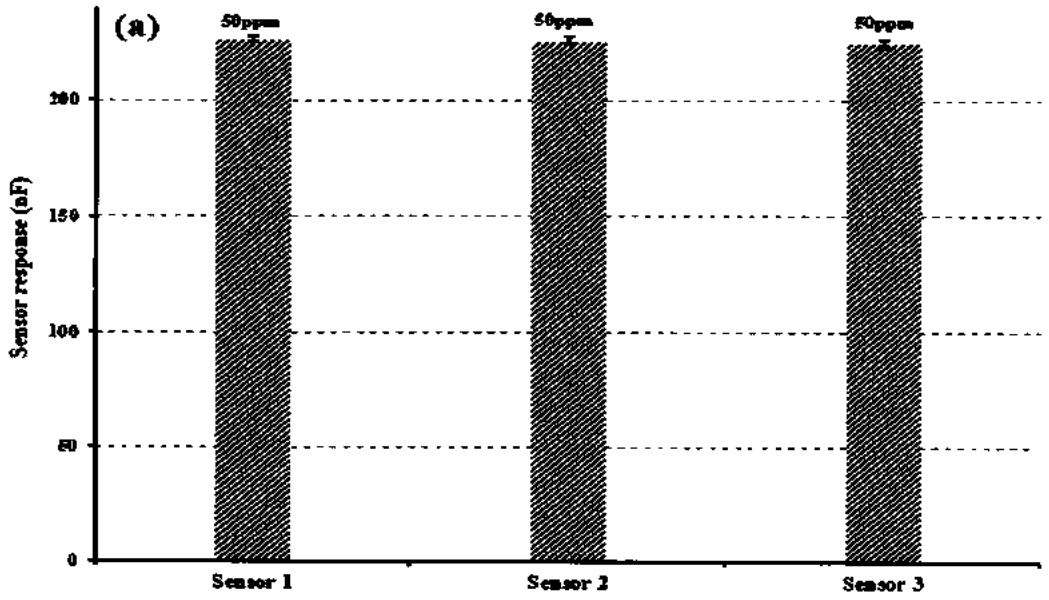

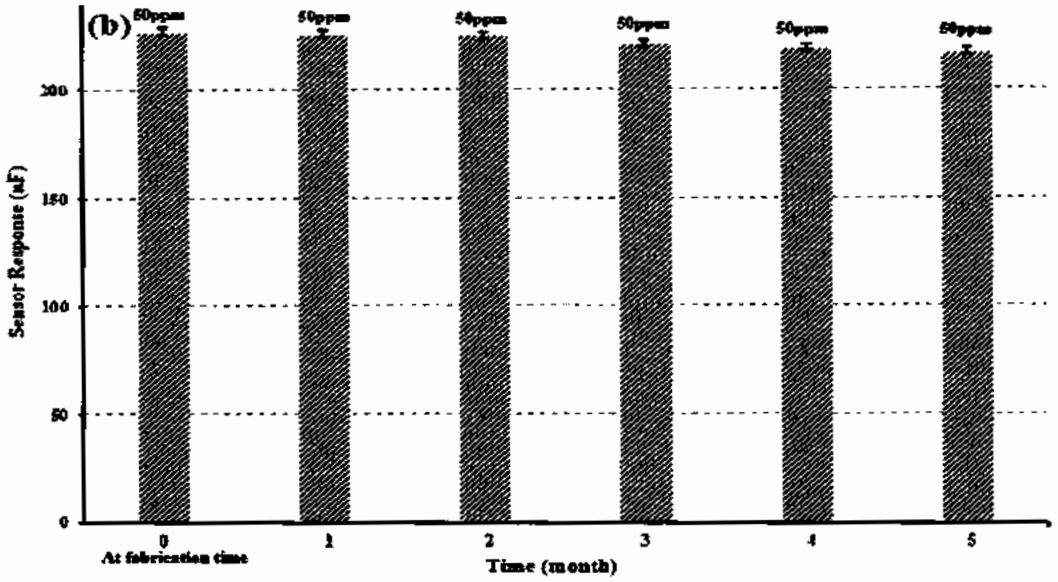

Figure 5.7: (a) Reproducibility and reusability of three polystyrene based sucrose sensors prepared in the same manner (b) Stability profile of sucrose sensor over the period of six months.

5.3.2 Characterization and sensor measurements of n-vinyl pyrolidone system based receptors

5.3.2.1 Characterization of synthesized receptors by FTIR spectroscopy and scanning electron microscope (SEM)

FTIR analysis was performed to study the functional group modification of n- vinyl pyrolidone based receptors (MIPs and NIPs) during polymerization. To study the chemical structure of thin films of imprinted and non-imprinted polymers, FTIR was plotted between wave number and % transmittance. A peak was observed at 2980 cm^{-1} as shown by figure 2.3, due to stretching vibrations of sp^3 (CH), while C-O-C stretching vibration was found at 1160 cm^{-1}. The ester group of EGDMA showed a characteristic stretching band at 1734 cm^{-1}. The peak at 1425 cm^{-1} was found a representative peak of C=N, C=C due to the stretching of pyridine group present in n-vinylpyrolidone. These major peaks in spectra showed that the polymerization occurred and imprinted polyvinyl pyrolidone were achieved by free radical polymerization of EGDMA and VP shown in figure 5.8.

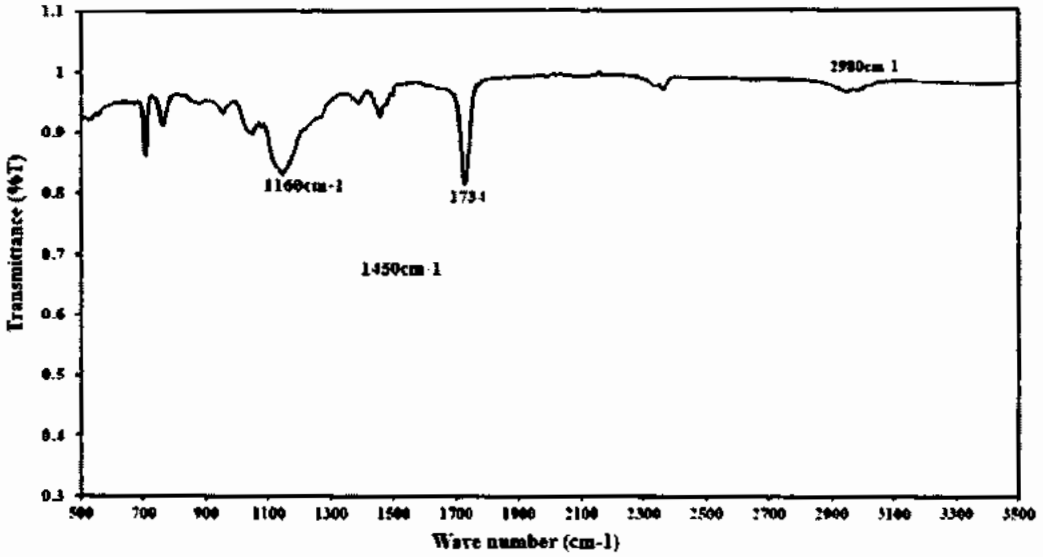

Figure 5.8: FT-IR spectra of non- imprinted and imprinted polyvinyl pyrolidone based sucrose receptors.

To assess the surface morphology of MIP and NIP receptors, scanning electron microscope was used. The synthesized receptors were coated onto the glass substrate to obtain the thin films of fabricated receptors. The MIPs based receptors showed highly porous and rough surface while non-imprinted polymer possess very smooth surface as shown in figure 5.9. The SEM images showed that microstructures present on the imprinted receptor surface were due to the swelling of polymer on the incorporation of template within polymer matrix. NIP has very smooth surface because such structures have not been seen on NIP thin film. Different morphology of both MIP and NIP indicated the successful polymerization of polymers.

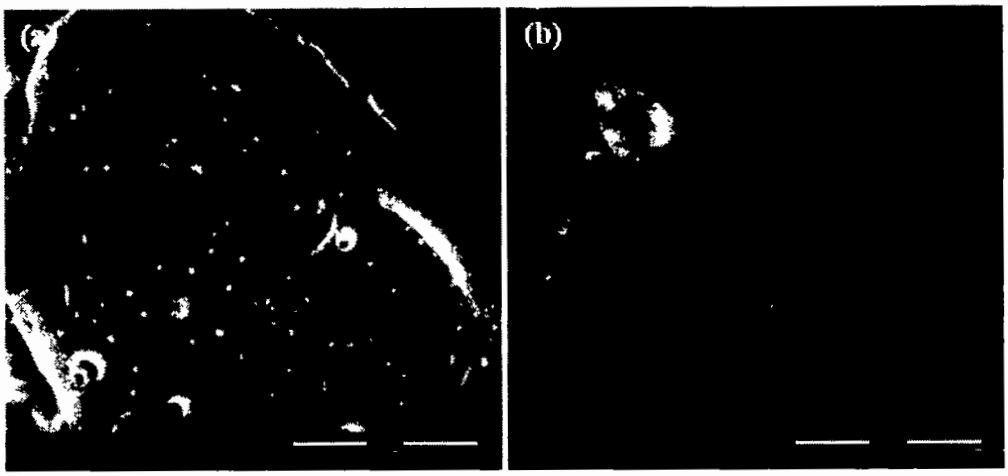

Figure 5.9: SEM images of (a) NIP and (b) MIPs of polyvinyl pyrolidone based sucrose receptors.

5.3.2.2 Sensitivity measurements of fabricated sensor

After the functional group and surface morphological characterization of both imprinted and non-imprinted polymer based receptors, these were immobilized onto transducer system for the sensing of sucrose. The fabricated sensor was exposed to the different concentrations (0 ppm, 1 ppm, 5 ppm, 10 ppm, 20 ppm, 30 ppm, 40 ppm and 50 ppm) of sucrose. At 1 ppm concentration of analyte, sensor response was 22 nF. Sucrose sensor exhibited sensor signals of 22 nF, 50 nF, 81 nF, 113 nF, 175 nF, 241 nF and 315 nF against different concentrations of 1-50 ppm respectively. While response of non-imprinted (NIP) was very low at the same concentrations and significant difference of sensor response was found between MIPs coated IDE and NIPs coated IDE because of availability of imprinted cavities/selective molecular imprints on the surface of imprinted polymer based receptors. As the concentration of sucrose increases, sensor response (conductance) also increases which means that sensor response is concentration dependent. The linear regression analysis of sensor responses at different concentrations of analyte (0-50 ppm) depicts the linearity of sensor with a co-efficient of regression (R^2) of value 0.99 as can be seen in figure 5.10 (a) and (b). Increase in the conductance upon increasing the template concentration leads to saturation point at a higher concentration due to complete filling of cavities in the domain of polymer via adsorption of template molecule and saturation limit of ~525 ppm was recorded from the sensor response of fabricated sucrose sensor.

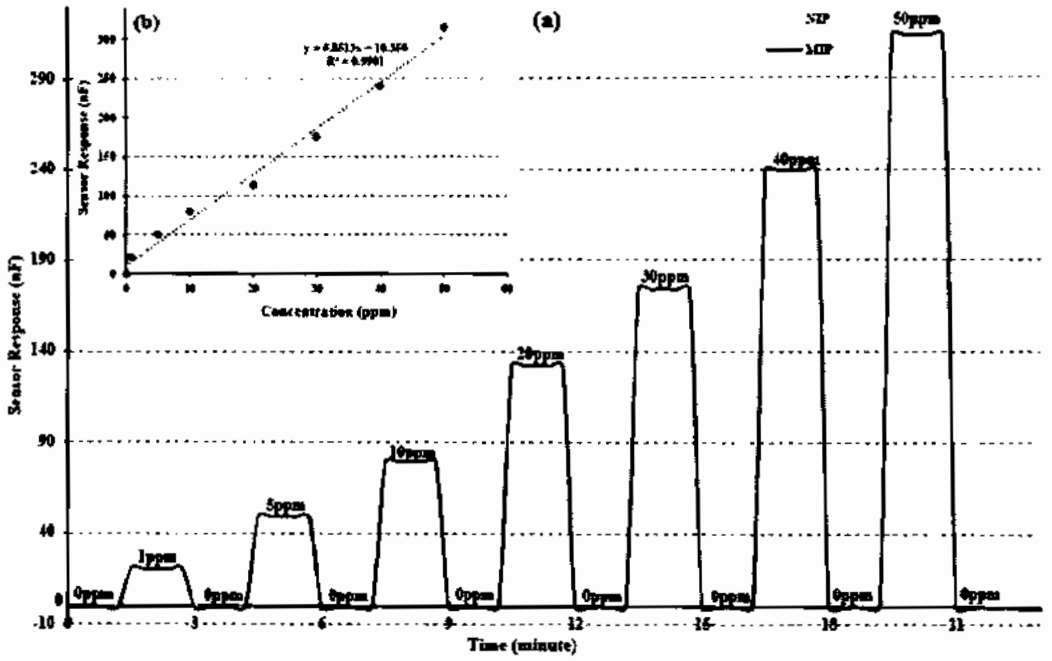

Figure 5.10: Sensitivity response of imprinted and non-imprinted polyvinyl pyrolidone based maltose sensor at different concentrations (0-50 ppm) and (b) Linear regression analysis of sucrose sensor.

While the sensor showed the lower limit of detection of ~68 ppb towards the sucrose. On the other hand, NIP does not show any significant change in its response due to lack of binding capacity towards analyte. The non-covalent interactions between the template molecules and polymeric matrix may base on the interaction of functional monomer and sucrose, the OH group present on sucrose interact with C=O group of vinyl pyrolidone while the EGDMA provides support in form of polymerization to generate cavities within polymer matrix. receptors. The possible interactions between template molecules and polymer matrix can be seen in figure 5.11 where dipole-dipole force and hydrogen bonding cause the interaction between template molecule and imprinted cavities.

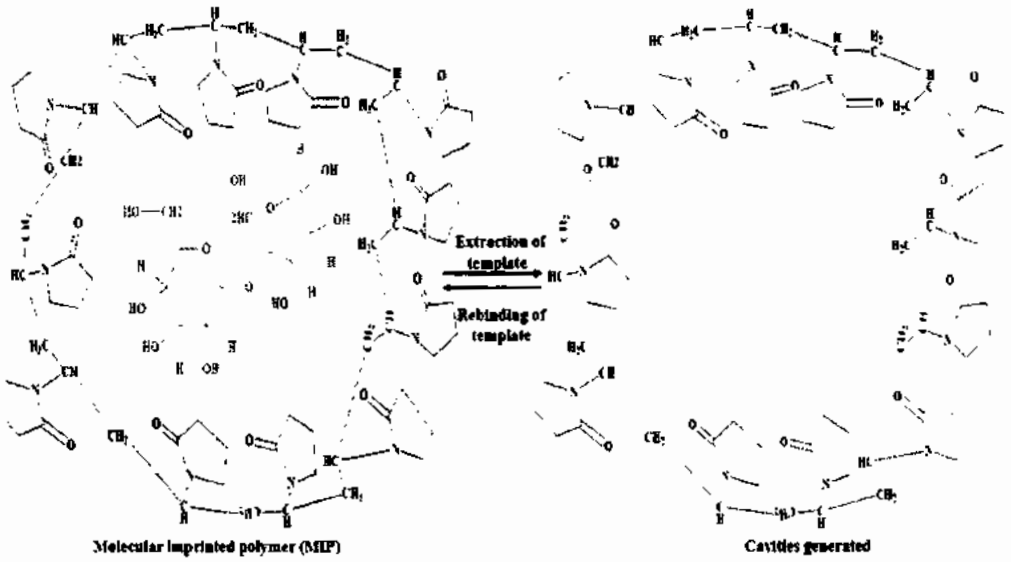

Figure 5.11: The extraction and rebinding of template into n-vinylpyrolidone imprinted sucrose

The capacity of an analyte to not recognize other interfering molecules is based on the same shape, same size and similar electro-activity of the designed sensor.

5.3.2.3 Selectivity analysis of sensor

Selectivity is a fundamental parameter of chemical sensor for its real-time application. Responses of fabricated sucrose sensor were recorded against different competing molecules such as maltose, fructose, glucose and n-hexane at 50 ppm concentration of analyte under similar conditions as shown in figure 5.12. The sensor response exhibited by specific analyte (sucrose) was 315 nF at 50 ppm concentration of template molecule while sensor showed a response of 9 nF, 8 nF and 3 nF for maltose, fructose, glucose and n-hexane respectively. The fabricated sensor showed a substantially higher response towards sucrose as compared to other structurally resembling molecules due to selective incorporation of sucrose molecules within polymeric receptors.

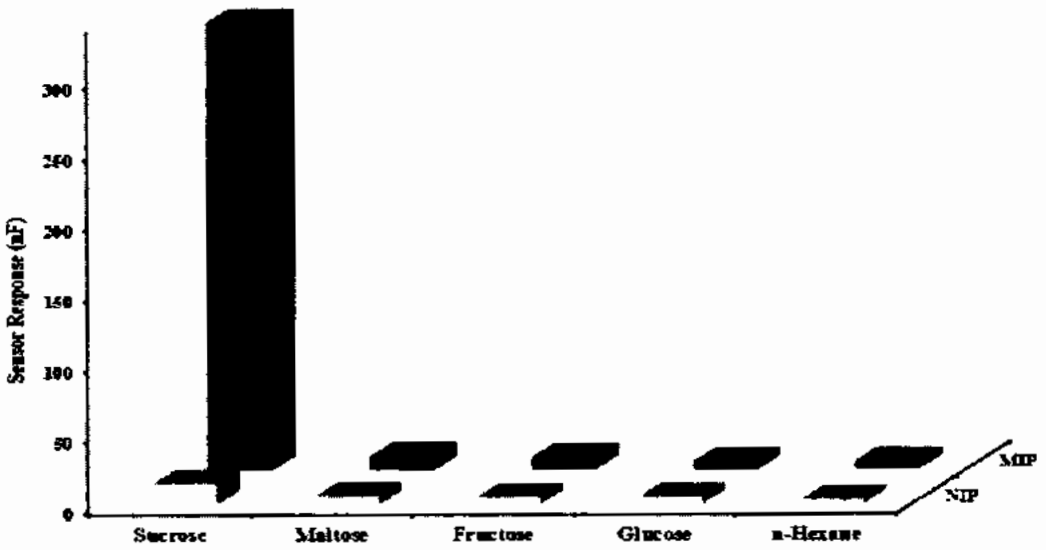

Figure 5.12: Selectivity analysis of sucrose sensor against different competing molecules at 50ppm

n-Hexane also has negligible selectivity response attributed by structural resemblance because hexane molecules may not be entrapped in the selective cavities of template i.e. sucrose due to geometrical difference.

5.3.2.4 Reproducibility, reusability and stability

Reproducibility and stability are the most important parameters for chemical sensor practical applications.

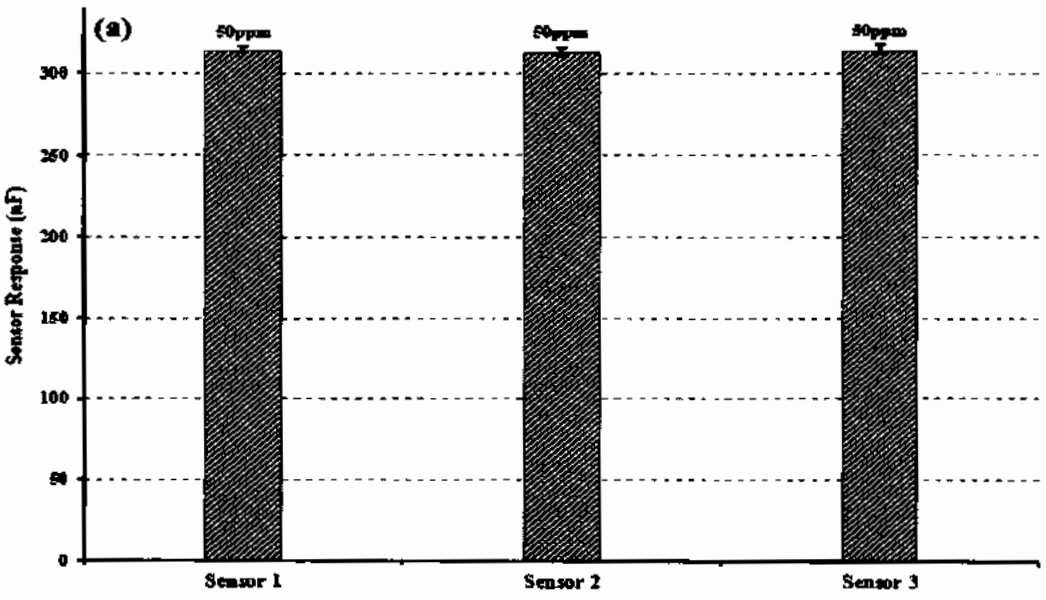

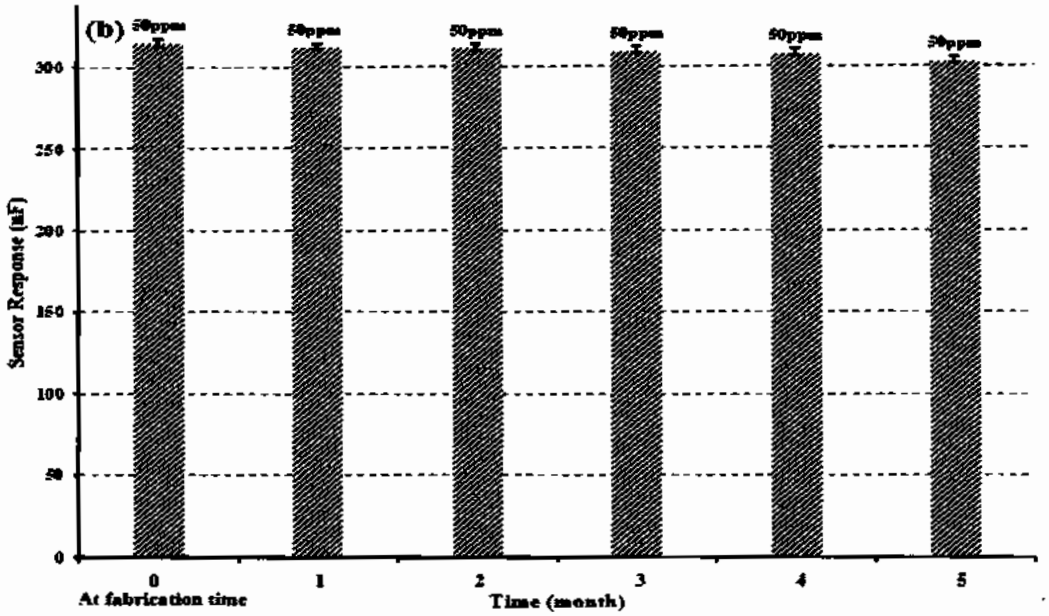

Figure 5.13: (a) Reproducibility and reusability a of three polyvinyl pyrolidone based sucrose sensors prepared in the same manner (b) Stability profile of sucrose sensor over the period of six months.

For reproducibility analysis, three different sensors were synthesized by following the same procedure and stored at room temperature and pressure for one month. After one month, these fabricated sensors were exposed to 50 ppm concentration of analyte and sensor response was measured as depicted from figure 5.13 (a). From the above observations, the RSD value of 0.3 % indicating a relatively good sensor reproducibility under above mentioned conditions and maintained its sensor response of 99 % after regular usage. Stability of sucrose sensor was also performed by storing the fabricated sensor at room temperature and pressure for six months. After each month, sensor response was measured and found a slight decrease in sensor response after every month and maintained sensor response upto 98 %as can be seen in figure 5.13 (b).

5.3.3 Characterization and sensor measurements of methacrylic acid based receptors

5.3.3.1 Characterization of synthesized receptors by FTIR spectroscopy and scanning electron microscope (SEM)

To examine the functional group modification of NIP and MIPs of methacrylate based receptors, FTIR analysis was performed. FTIR spectra was obtained in the range of 500-4000 cm^{-1}. FTIR spectra for acrylate based receptors was obtained in the range of 700-3900 cm^{-1} as shown in figure 5.14. Spectra of MAA and EGDMA showed –C=C

stretching frequency at 1650 cm^{-1}. The peaks at 1670-1515 cm^{-1} are vibrational peaks indicating C-H stretching and C-H bending of polymer chains. The characteristics peaks centered at 1035-1149 cm^{-1} indicated the presence of polysaccharides in MIP. The absorption peak at 3200-3400 cm^{-1} was attributed to stretching vibrations of -OH of glucose. The peak at 1702 cm^{-1} shows the presence of ester group in the matrix and the other extra peaks are attributed to free radicle polymerization.

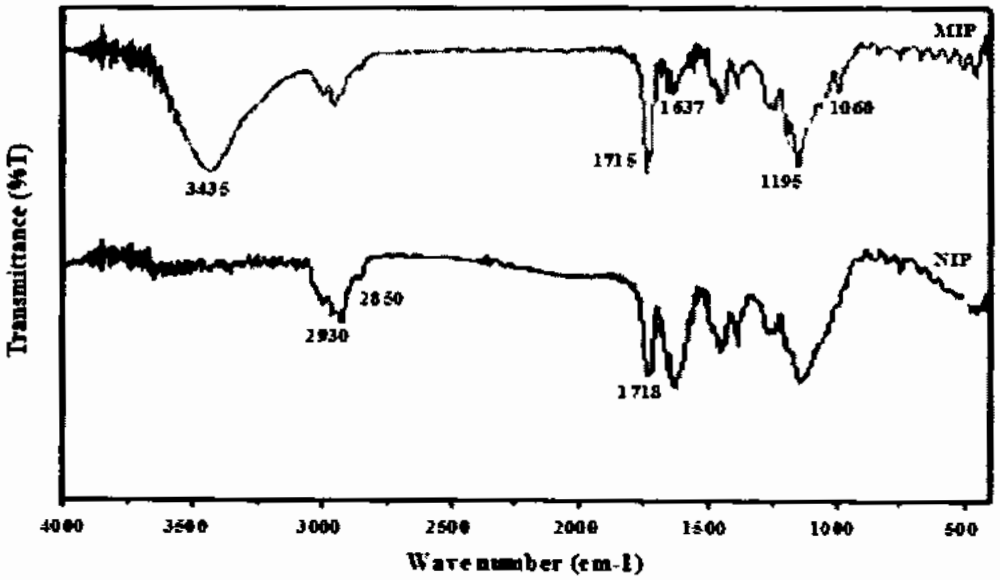

Figure 5.14: FT-IR spectra of imprinted and non-imprinted methacrylic acid based sucrose receptors

FTIR spectra provided confirmation for the successful preparation of non-imprinted and imprinted polymer based receptors.

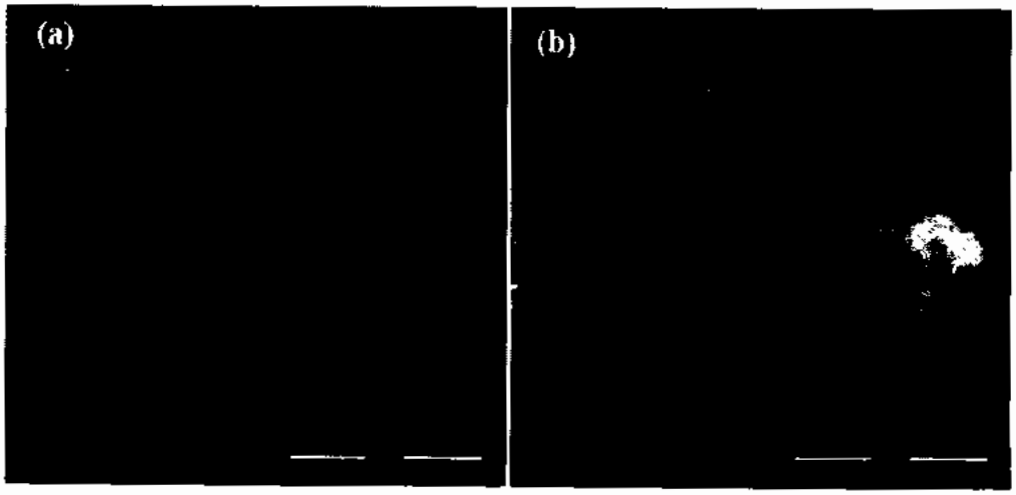

Figure 5.15 : SEM images of (a) NIP and (b) MIPs of methyacrylic acid based sucrose receptors.

To examine the surface morphology of polyvinyl pyrolidone based sucrose receptors, scanning electron microscope was used. These receptors were coated onto a glass substrate to obtain thin films of fabricated receptors and microscopic images of the molecular imprinted polymer and non-imprinted polymer (NIPs) showed in figure 5.15. The SEM images showed that micro and nanostructures have been produced in the imprinted polymer surface due the swelling of polymer on the incorporation of template within the polymer matrix while such structures have not been seen in NIP

5.3.3.2 Sensitivity measurements of fabricated sensor

To develop sucrose imprinted electrochemical sensor, the receptors were coated onto the IDEs and exposed to different concentrations of analyte ranging from 1 ppm to 50 ppm. At 0 ppm, the observed capacitance was 0 and at 1 ppm, 5 ppm, 10 ppm, 20 ppm, 30 ppm, 40 ppm and 50 ppm of sucrose the sensor responses of 38 nF, 99 nF, 139 nF, 212 nF, 298 nF, 397 nF and 505 nF have been observed respectively. The obtained electrochemical results demonstrated that newly fabricated sensor was highly sensitive even at very low concentration of 1 ppm as shown in figure 5. 16(a).

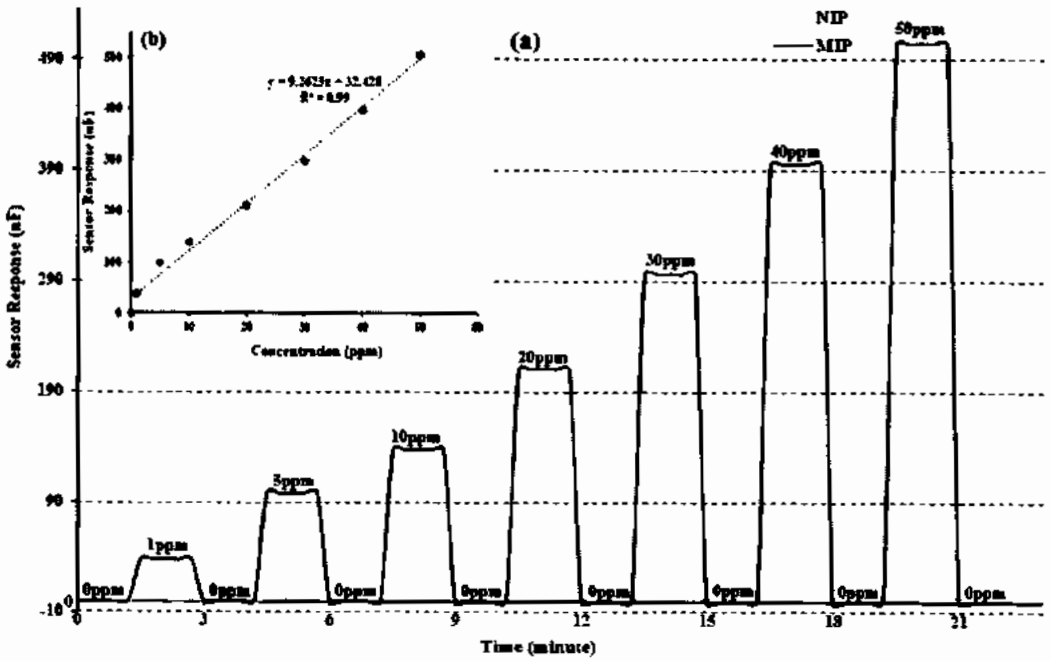

Figure 5.16: (a) Sensitivity response of NIP and MIP of methacrylic acid based sucrose sensor at different concentration (0-50 ppm) (b) Linear regression analysis of sucrose sensor.

The NIP was also exposed to the same concentrations of analyte and sensor signals were found very less. The linearity of sensor was also assessed by linear regression analysis of obtained sensor responses at different concentrations of analyte (0-50 ppm) and the sensor showed linear response with a linear co-efficient of regression (R^2) of value 0.99 as can be seen in figure 5.16 (b). The sensor showed a change in signals from 38 nF to 505 nF towards 1 ppm to 50 ppm concentrations of sucrose which indicates the concentration dependent linearity of sensor signals in the range of ~39 ppb to 520 ppm which is due to the change in number of sucrose molecules incorporated in sensor moieties. The increase of capacitance might be due to the -OH (hydroxyl) group present in sucrose which was trapped within the molecular cavities present in polymeric matrix coated onto IDEs. The sensor exhibits an excellent reversibility when subjected to zero concentration of sucrose solution. Increase in the conductance upon increasing the template concentration leads to saturation point at a higher concentration because of complete filling of cavities in the domain of polymer via adsorption of template molecule. For measuring sensitivity of molecular imprinted polymer, nanomolar (nM) concentrations can be detected.

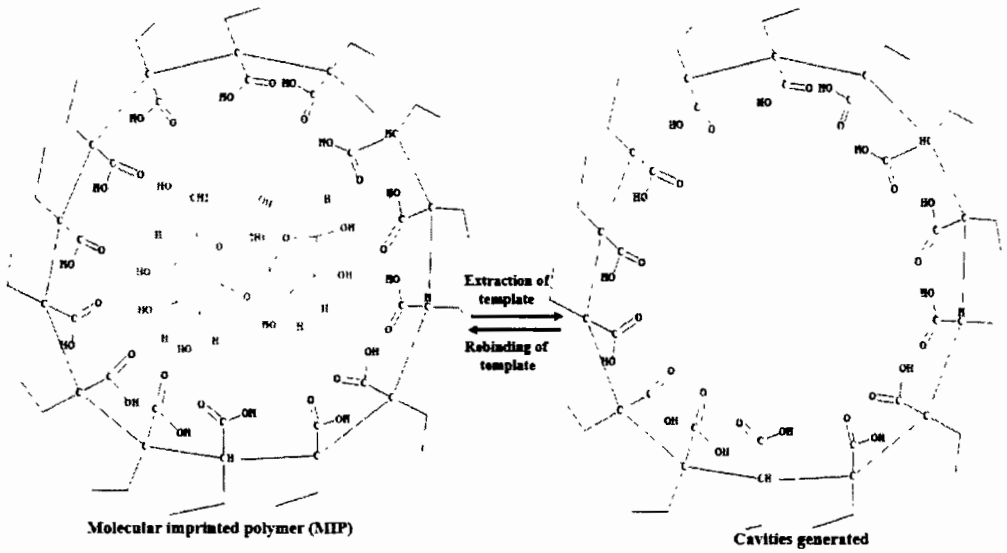

Figure 5.17: The rebinding and removal of template from methacrylic acid based sucrose receptors.

After washing the sensor with de-ionized water, its response again reaches to its initial value which means the sensor shows complete reversibility and regeneratability. While the sensor possesses the lower limit of detection of ~39 ppb towards the sucrose. On

the other hand, NIP does not show any significant change in its response due to lack of binding capacity towards analyte. Higher sensor response may be due to the key and lock mechanism. The non-covalent interactions between the template molecules and polymeric matrix may base on the interaction of crosslinking agent and sucrose and the OH group of sucrose may interact with –COOH group of methacrylic acid while cross-linker (EGDMA) the provides support in form of polymerization to generate cavities within polymer matrix. The possible interactions between template molecules and polymer matrix can be seen in figure 5.17 where dipole-dipole force and hydrogen bonding cause the interaction between template molecule and imprinted cavities.

5.3.3.3 Selectivity analysis of sensor

To assess the selectivity of polyacrylate based sucrose sensor, four different competing molecules were used which are functional and structural analogues of sucrose such as maltose, fructose, glucose and n-hexane. The sensor response was measured by monitoring the reduction in signals of MIP and NIP at 50 ppm concentration of templated molecule (sucrose) in the presence of these interfering species. The sucrose imprinted sensor was exposed to specific concentration of 50 ppm of template (sucrose) molecule and it showed the sensor response of 505 nF while maltose showed a response of 6n F, for fructose and glucose, it was 5 nF for both competing species. The observed sensor response for n-hexane, another competing molecule showed response of 2 nF as can be seen from figure 5.18. MIP based sensor showed at least twenty-four times more response for sucrose molecule than a non-imprinted polymer (NIP). It is evident from these measurements that in case of competing molecules, there is no significant difference in the sensor signals showed by MIP and NIP. It is fascinating to know that though maltose has probably similar structure as sucrose, the observed response is very negligible than for sucrose. This fabricated sensor exhibited eighty-four times lower response for maltose, one hundred and one times higher than fructose and glucose and one hundred and two hundred and fifty-two folds higher than n-hexane shown in figure 5.18. These mentioned results revealed the high selectivity response of proposed sensor.

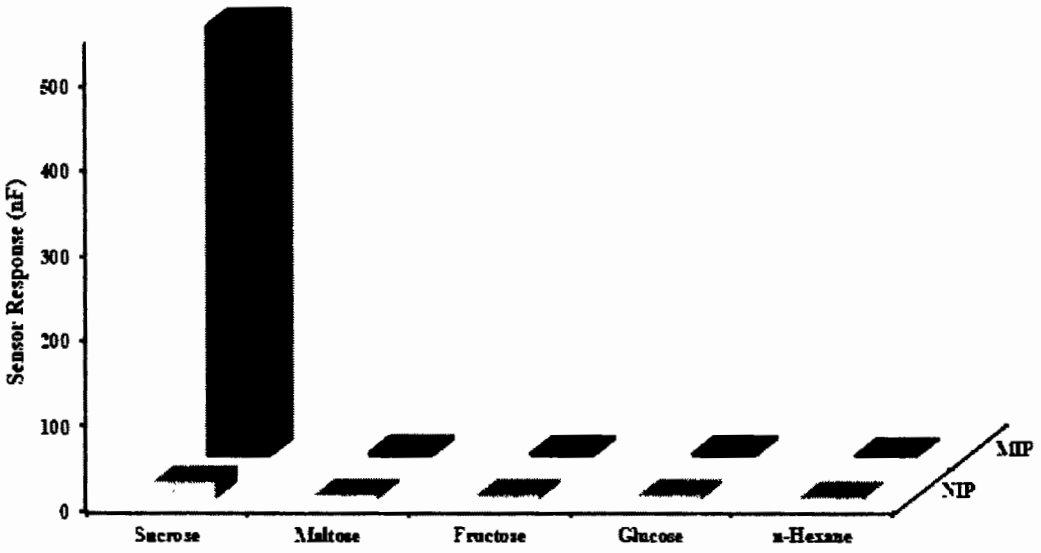

Figure 5.18: Selectivity analysis of methacrylic acid based sucrose sensor against different competing molecules at 50 ppm.

High specificity response of sensor mainly attributed by the selective recognition sites and not merely the cavities which reproduces the phenomenon of imprinting during the polymerization corresponding to size, shape, geometry and adjustment of functional groups.

5.3.3.4 Reproducibility, reusability and stability

To investigate the reproducibility of polyacrylate based sucrose sensor, three different sensors were synthesized thrice and kept at normal temperature and pressure for one month. After above mentioned time period, these sensors were exposed to 50 ppm concentration of analyte and sensor response was measured. From these observations, <0.4 % of RSD value indicated that sucrose sensor is highly reproducible under room temperature and pressure with retained sensor response of 99 % as shown in figure 5.19 (a). To access the stability of fabricated sensor, a sucrose senor was produced by following the similar method of synthesis and stored at normal conditions of temperature and pressure for a period of six months. The fabricated sensor was exposed to 50 ppm concentration of template molecule and sensor response was measure after every month for a period of six months as depicted in figure 5.19 (b).

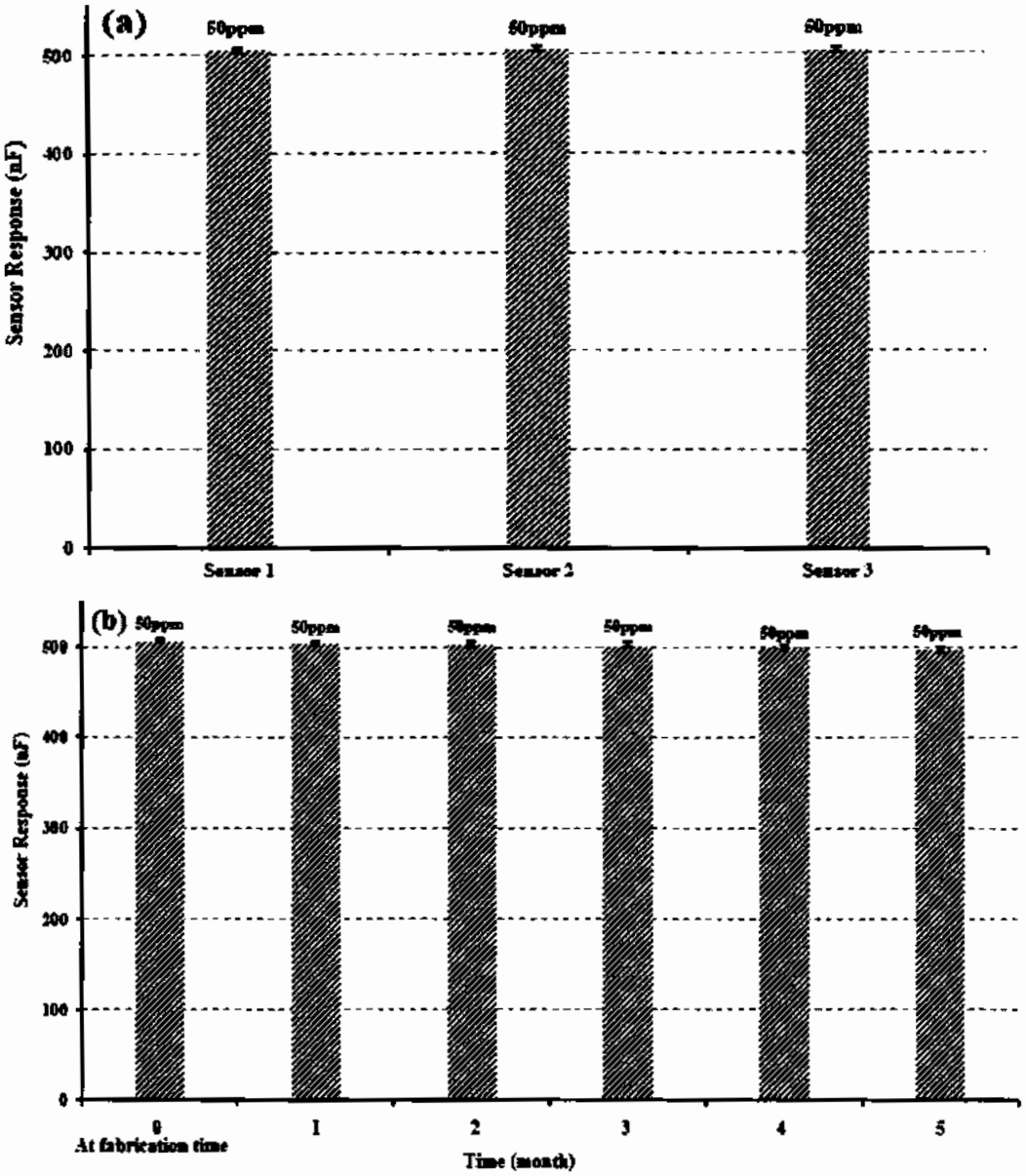

Figure 5.19: (a) Reproducibility and reusability a of three methacrylic acid based sucrose sensors prepared in the same manner (b) Stability profile of sucrose sensor over the period of six months.

The obtained relative standard deviation (RSD) of 0.75 % signified the effective stability of 50 ppm concentration with continuous usage. In addition, 99 % of sensor response was maintained which also indicated that sucrose sensor possesses excellent stability.

5.3.4 Characterization and sensor measurements of urethane system based receptors

5.3.4.1 Characterization of synthesized receptors by FTIR spectroscopy and scanning electron microscope (SEM)

To assess the functional group modifications for NIP, MIPs and GO/MIPs composite during polymerization, FTIR analysis was performed. FTIR spectra was obtained in the range of 500- 4000 cm^{-1}. In this polymer matrix, N-H characteristic absorption peak was found at 3328 cm^{-1} due to the presence of hydrogen bond in the urethane linkage and urea groups. Carbonyl group showed stretching vibrations at 1726 cm^{-1}. The stretching vibrations of ester (C(O)-C) was present at 1126 cm^{-1}. The carbonyl peak (C=O) around 1700 cm^{-1} due to ester-polyols and urethane.

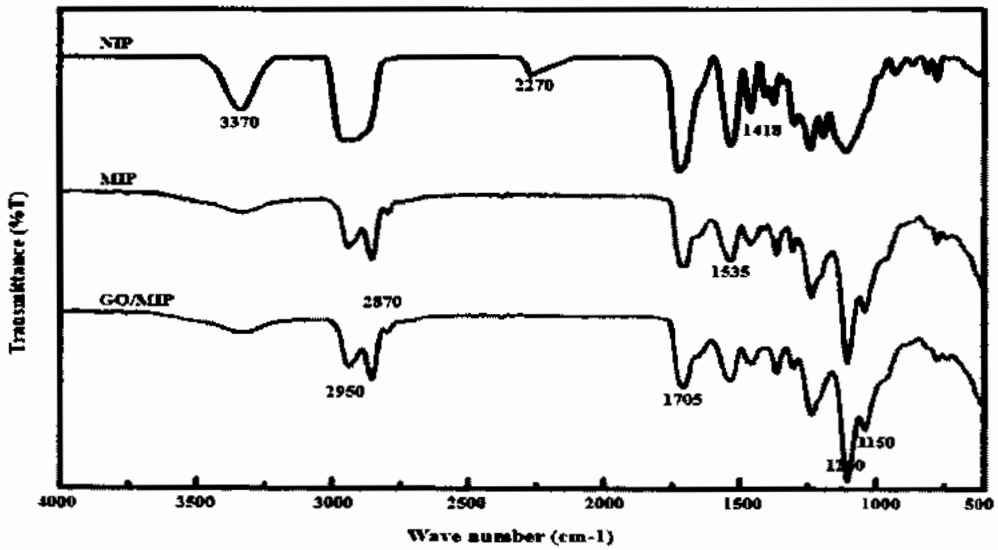

Figure 5.20: FT-IR spectra of imprinted, non-imprinted and GO-MIPs composite polyurethane based sucrose receptors.

To examine the surface morphology of NIP, MIPs and GO/MIPs composite, polyurethane based sucrose receptors were characterized by scanning electron microscope. Microscopic images showed that functionalized graphene composite based receptors were completely embedded to MIPs based receptors and also revealed that functionalized graphene adhered with PU/MIPs. Furthermore, micro-sized pores were present on the surface of MIPs due to swelling of polymer on the incorporation of template molecule within the polymer matrix whereas NIP exhibited non-porous and highly smooth surface. Therefore, topography of NIP, MIPs, and GO-MIPs composite

are extremely different from each other which indicates the effective polymerization of different polymers.

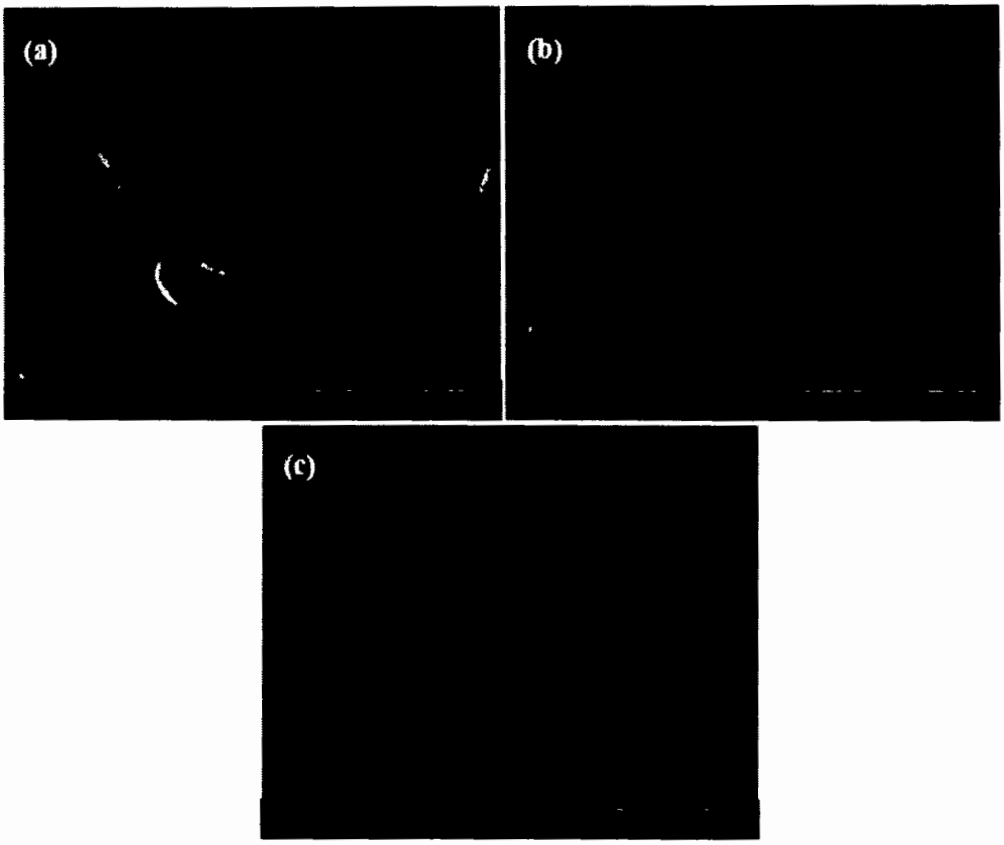

Figure 5.21: SEM images of (a) NIP (b) MIPs and (c) GO/MIPs composite of polyurethane based sucrose receptors.

5.3.4.2 Thermogravimetric (TGA/DTA) analysis

Thermogravimetric analysis was performed for the stability of non-imprinted, imprinted polymer and functionalized graphene based composite. TGA/ DTA profile was examined in the temperature range of 25-600 °C under nitrogen atmosphere. NIP shows an initial weight loss of -1.579/5.32 mg from 23.22 °C to 302.75 °C temperature which is due to the loss of solvent and water loss. The loss of mass between 125 °C and 400 °C is basically removal of water or -OH (hydroxyl group) condensation. The weight loss initiates from 400 °C is because of breakdown of imprinted polymer coatings (Li, Zhao et al. 2018).

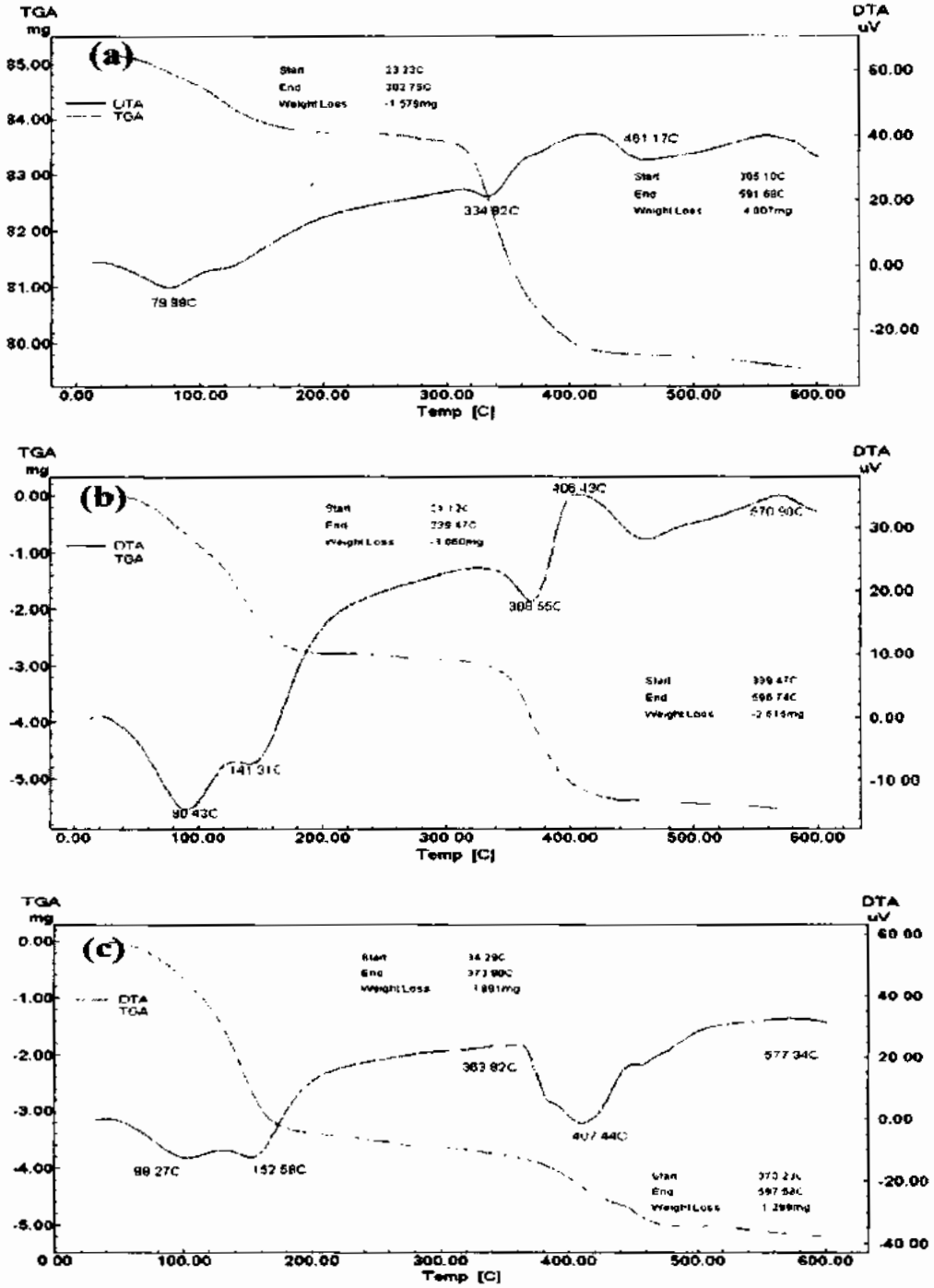

Figure 5.22: TGA and DTA curves of (a) NIP (b) MIPs and (c) GO-MIPs composite of polyurethane based sucrose receptors.

In the second phase, mass loss was -4.007 mg between a temperature of 305.10 °C and 591.69 °C shown in figure 5.22 (a) and total mass loss of NIP was -5.586/5.32 mg (-105 %). In case of molecular imprinted polymer, a very small weight loss was noted (-

3.060 mg) from temperature range of 21.12℃-339.47℃. In second shift, very minute mass loss of -2.515 mg was observed between a temperature of 339.47 ℃ - 596.74 ℃. The total mass loss of -5.189/5.75 mg (-3.891 - 1.298 mg= -90.24 %) as shown in figure 5.22 b. In case GO-MIP nanocomposite, first mass change starts from 34.28 ℃ and ends at 373.47 ℃ with mass loss of -3.891/5.86 mg. The second shift of mass change starts at 373.23 ℃ and stopped at 597.58 ℃ bears a weight loss of -1.289/5.86 mg. The overall weight loss of GO-MIP nanocomposite was -5.18 mg (-88.39 %). The presence of peaks in case of DTG curve at 25-600 ℃ is related to the weight losses of TG curves. The trend of mass loss in NIP and MIPs are related to GO/MIPs apart from the total loss is highly negligible in case of All NIP, MIPs and GO/MIPs composite. Furthermore, these results indicated that NIP, MIPs and GO/MIPs have been synthesized successfully with excellent thermal stability.

5.3.4.3 Sensitivity measurements of fabricated sensor

After coating of polyurethane based sucrose receptors onto IDEs and washed to generate cavities within polymeric matrix, the fabricated sensor was exposed to various concentrations of sucrose to assess its sensitivity profile.

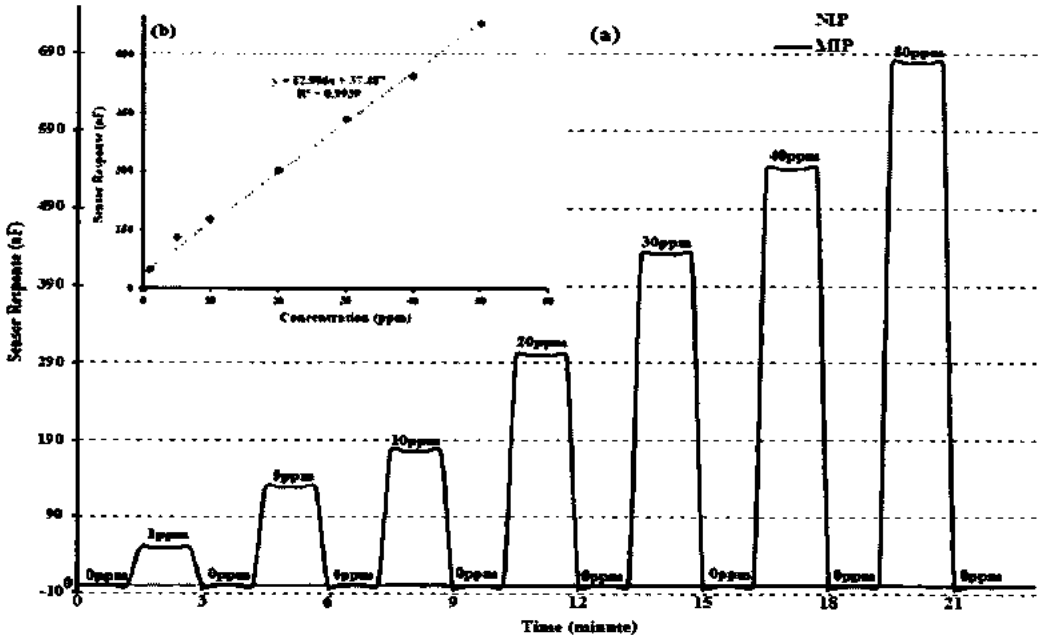

Figure 5.23: (a) Sensitivity response of MIP and NIPs of polyurethane based sucrose sensor at different concentration (0-50 ppm) (b) Linear regression analysis of sucrose sensor.

At 0ppm, the observed capacitance was 0 and at 1 ppm, 5 ppm, 10 ppm, 20 ppm, 30 ppm, 40 ppm and 50 ppm of sucrose the sensor responses of 49 nF, 129 nF, 178 nF, 302 nF, 432 nF, 542 nF and 679 nF have been observed respectively with the lowest limit of detection ~31 ppb of fabricated sensor. The obtained electrochemical results demonstrated that newly fabricated sensor was highly sensitive even at very low concentration of 1 ppm as shown in figure 5.23 (a). The NIP was also exposed to the same concentrations of analyte and sensor signals were found very less. The linearity of sensor was assessed by linear regression analysis of obtained sensor responses at different concentrations of analyte (0-50 ppm) and the sensor showed linear response in the range of ~31 ppb to 528 ppm with a linear co-efficient of regression (R^2) of value 0.99 as can be seen in figure 5.23 (b). The increase in sensor response (capacitance) might be due to the -OH (hydroxyl) groups present in sucrose which were trapped within the molecular cavities present in polymeric matrix coated onto IDEs. The MIPs coated sensor yields substantially higher response as compared to NIPs due to the presence of structurally related cavities present on the surface of MIP.

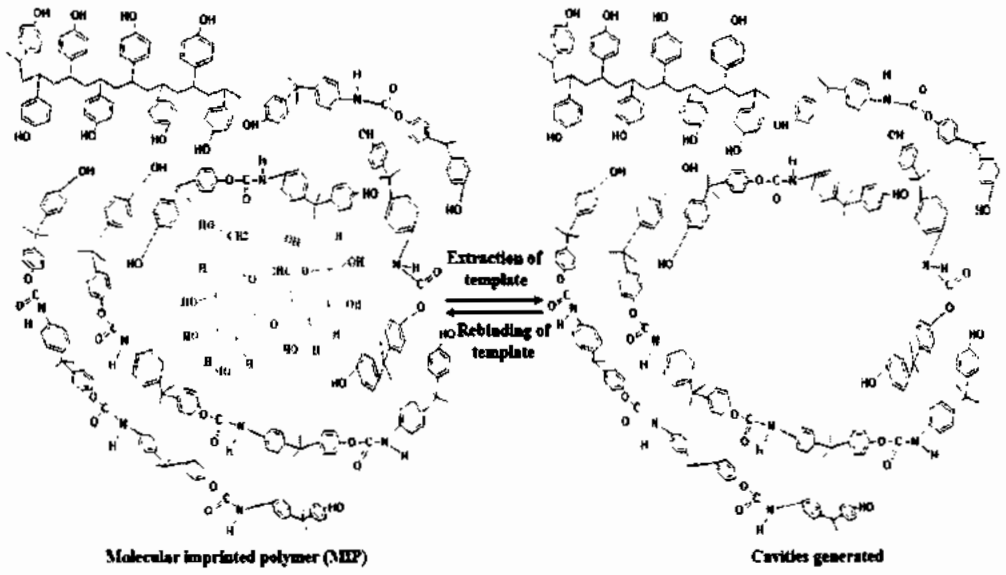

Figure 5.24: The rebinding and removal of template from polyurethane based sucrose receptors.

The non-covalent interactions play an important role in the removal of template molecule including electrostatic, Vander waals interactions, π-π stacking forces and

hydrogen bonding etc. These forces between the template molecules (sucrose) and polymeric matrix depends on the interaction of crosslinking agent and the -OH group present with sucrose interact with DPDI while the Bisphenol A provides support in polymerization to generate cavities within polymer matrix. The possible interactions between template molecules and polymer matrix can be seen in figure 5.24 where dipole-dipole force and hydrogen bonding (between N-H group of DPDI and -OH of fructose) cause the interaction between template molecule and imprinted cavities.

In order to enhance the sensor response, functionalized graphene was used due to its excellent mechanical and electrical properties. Graphene oxide also has a very large surface area and therefore, more chances for the successful collisions to increase the sensitivity behavior of the sensor. The use of functionalized graphene helped to develop a more homogeneous and accessible distribution of binding sites on the composite surface which increased the fast, rapid, regular and homogeneous adsorption dynamics. Furthermore, it eliminates interference and helps to improve the sensor response. Graphene oxide based imprinted composite was also exposed to different concentrations of analyte and exhibited a highly linear and improved sensor response as shown in figure 5.25 (a). The sensor was exposed against different concentrations i.e. 0-50ppm and obtained sensor response was 94 nF, 189 nF, 269 nF, 482 nF, 683 nF, 809 nF and 1107 nF respectively. By increasing the concentration of template molecule, sensor response also increases which proves the linearity of sensor with linear regression constant (R_2) = 0.99 as shown in figure 5.25 (b). The lowest limit of detection was ~16 ppb with upper detection point ~600 ppm for the fabricated sucrose sensor.

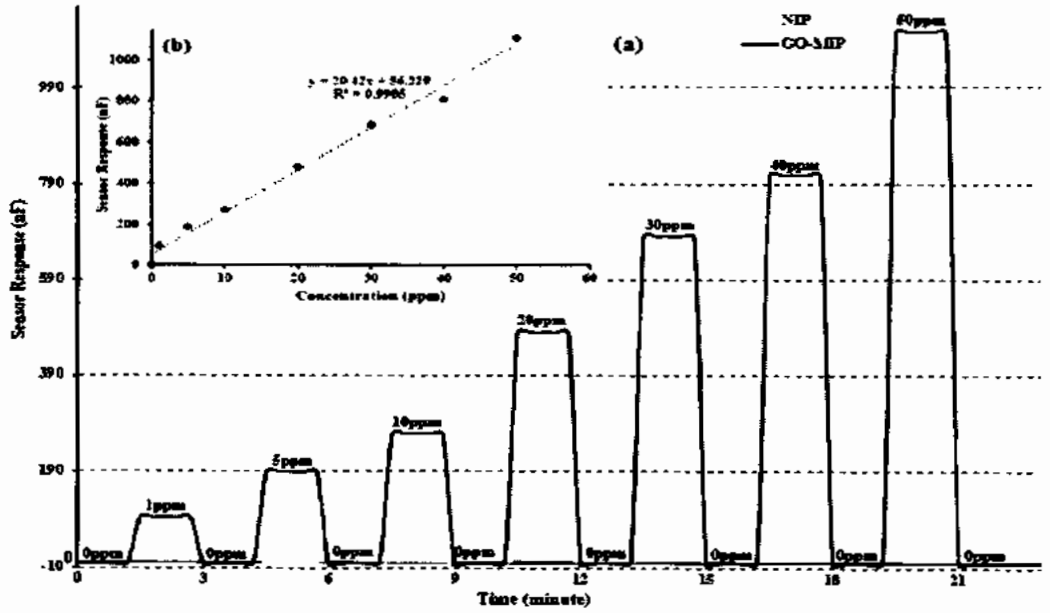

Figure 5.25: (a) Sensitivity response of GO-MIPs composite and NIP of polyurethane based sucrose sensor at different concentrations (0-50 ppm) (b) Linear regression analysis of sucrose sensor.

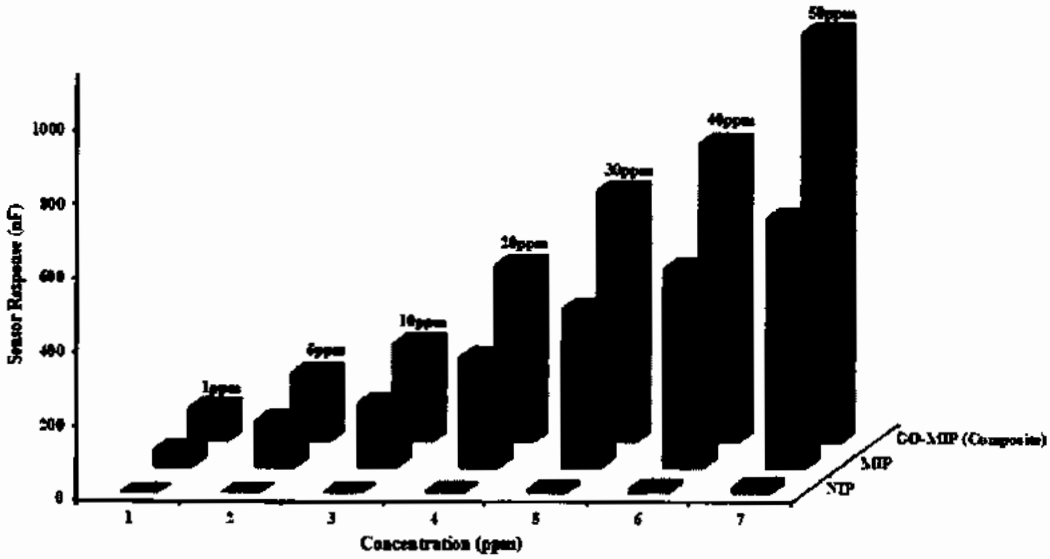

Figure 5.26: Comparison of sensor response of MIP, NIPs and GO-MIPs composite of polyurethane based sucrose sensor at different concentrations of sucrose (0-50 ppm).

The topographical studies of polyurethane based sucrose sensor showed the highest availability of surface area for the synthesis of template identical cavities as compared to the other polymers which played major contribute for the enhanced sensor response. Comparison of NIP, MIPs and GO-MIPs composite was shown in figure 5.26 by bar graph. This graph confirms the substantial worth of graphene sheets while comparing

the sensor signals of MIPs and GO-MIPs composite, the response of GO-MIPs composite based sucrose sensor was 1.9 folds higher than simple MIPs based sensor.

5.3.4.4 Selectivity analysis of sensor

To examine the selectivity of fabricated sensor, NIP, MIPs and GO/MIPs composite based sucrose sensor was exposed to different competing molecules (solution) at 50 ppm concentration. MIPs based sensor shows response of (conductance) 679 nF for sucrose whereas maltose, fructose, glucose and n-hexane exhibited the sensor response of 7 nF, 6 nF, 6 nF and 5 nF respectively. Furthermore, GO-MIPs composite based sucrose sensor was also exposed to different concentrations of sucrose and recorded sensor response was 1008 nF. The response of composite based sensor for other competing molecules was 6 nF, 5 nF, 5 nF and 2 nF for maltose, fructose, glucose and n-hexane respectively. Each molecule responds differently to its imprinted polymer being somewhat cross sensitive against same sensor due to substantial physicochemical resemblance in different molecules. Thus, bulk molecular imprinting approach supports the selective response for distinguishing them even very closely resembled molecules as shown in figure 5.27.

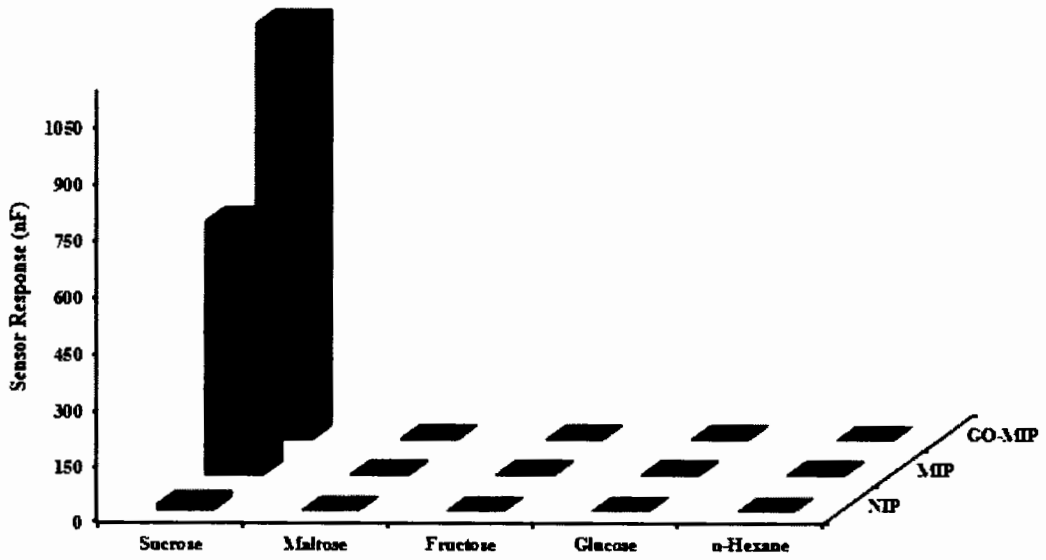

Figure 5.27: Selectivity analysis NIP, MIPs and GO-MIPs composite of polyurethane based sucrose sensor against different competing molecules at 50 ppm.

During polymerization, DPDI and Bisphenol A rearrange themselves in a very effective way around the imprinted specie results in a high number of recognition sites which is highly selective towards the respective analyte. Selectivity response was far high for maltose (168 times) as interfering molecule, for fructose and glucose, it was 201 folds, and also exhibits highly negligible response for n-hexane. This proves that GO-MIPs (composite) based sensor is highly specific as well as selective against competing species. High selectivity response of sensor mainly attributed by the selective recognition sites and is merely the cavities which reproduce the phenomenon of imprinting during the polymerization corresponding to size, shape, geometry and adjustment of functional groups.

5.3.4.5 Reproducibility, reusability and stability studies of fabricated sensor

Reproducibility and stability are important parameters for the application of sensors. To study the reproducibility of GO-MIPs composite based sensor, three different sensors were synthesized by using the same method and stored under similar conditions of temperature and pressure for one month.

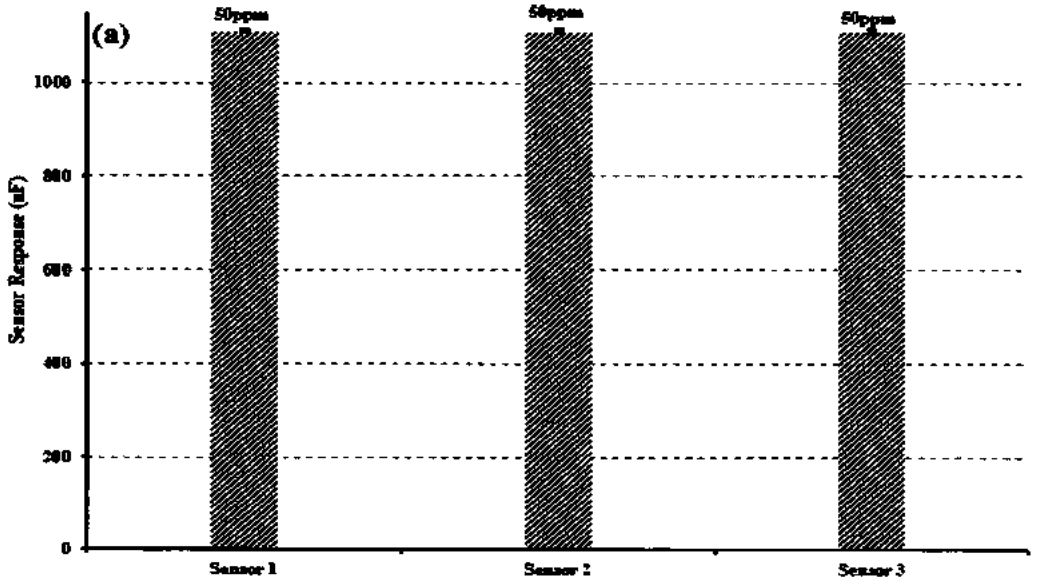

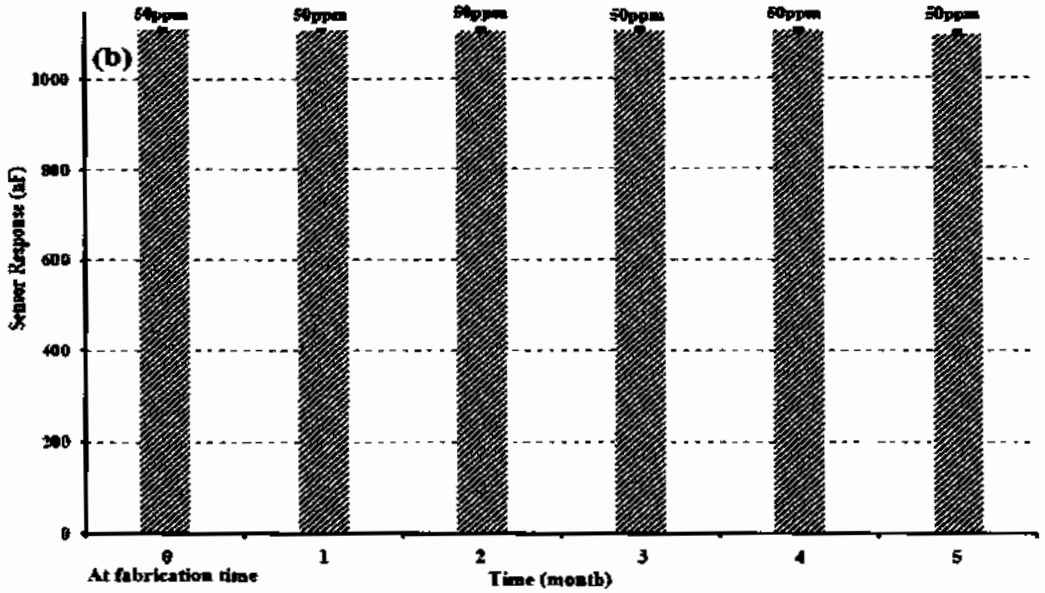

Figure 5.28: (a) Reproducibility and reusability of three GO-MIPs composite of polyurethane based sucrose sensors prepared in the same manner (b) stability profile of sucrose sensor over the period of six months.

After a month, these fabricated sensors were exposed to 50ppm concentration of sucrose and their sensor response was recorded as can be seen from figure 5.28 (a). The above mentioned observations indicated that GO/MIPs composite based sensor showed only a highly negligible decrease in sensor response with relative standard deviation (RSD) of ~0.42 %. Furthermore, for stability analysis of GO-MIPs based sucrose sensor, a sensor was designed following the same procedure of synthesis and stored for a period of six months under normal conditions. Senor response was measured on monthly basis at 50 ppm concentration of sucrose and RSD value of 0.9 % described that GO-MIPs composite based sucrose sensor possesses excellent stability under above mentioned conditions and maintained sensor response upto 99.5 % with continuous usage as shown in figure 5.28 (b). We considered that the excellent reproducibility and stability was described during the sensor preparation, which not only improved sensor response of the GO/MIP films, but also locked the size and shape of the recognition caves.

5.4 Comparison of sensor receptors (imprinted polystyrene, polyvinyl pyrolidone, methacrylic acid and polyurethane)

Different molecular imprinted polymers were synthesized by using various polymerization systems shown in figure 5.29. From this graph, in case of styrene as monomer, we can see a lower sensor response which might be due to the hydrophobic nature of styrene without any specific functionality.

In case of styrene, very weak interactions were found between monomer and template molecule. After the extraction of template, it might not adsorb efficiently the template molecule and tat the end, very small sensor response was found. It is notable from the above results that n-vinyl pyrolidone based polymer produces higher sensor effect due to its aromaticity and functionality. It can be seen from figure that efficient imprinting using a simple monomer (MAA) had a strong influence on adsorption of the template used to prepare hydrophobic polymer matrix. When template is a polyhydroxy molecule, then there might the possibility of stronger hydrogen bonding interactions with methacrylic acid as monomer which is the major reason for the increased sensor response.

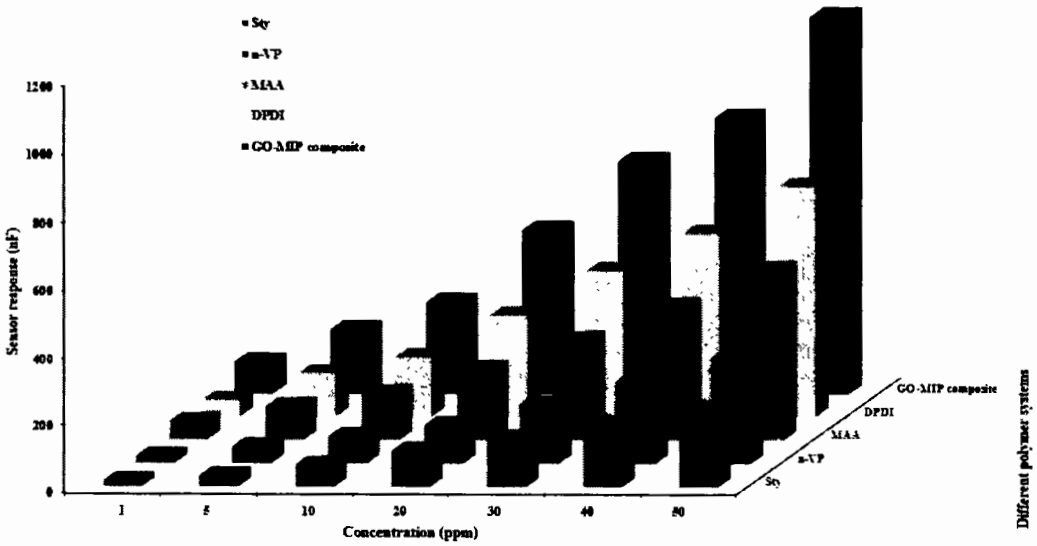

Figure 5.29: Comparison of sensor response of four different imprinted polymer systems.

Polyurethane system was assessed to enhance the sensor signals. 4, 4′-diisocyanatodiphenylmethane as monomer has proton donor groups (N-H or O-H) as well as the lone pair donor groups (C=O). The proton donor group in this polymer may interact with template molecule by forming H-bonding with electron donor groups (C=O). while the electron pair donor groups of polymer as well as template may interact with each other and as result enhances the sensor signals. The results obtained from different imprinted polymers and graphene oxide based composite were briefly reported in table 5.1 and compared this data with literature studies reporting sucrose measurements using different electrochemical methods.

Table 5.1: Comparison of previously reported work with recently designed sensors.

Analyte	**Technique**	**Limit of detection**	**Reproducibility (RSD)**	**Reference**
Sucrose	Cyclic voltammetry (CV)	3μ M/L^{-1} (3000 ppb)	2.6 %	(Shekarchizadeh, Ensafi et al. 2013)
Sucrose	FTIR	0.403 $\mu M/L^{-1}$ (403 ppb)	2.415 %	(Cengiz and Durak 2019)
Sucrose	HPLC	0.195 $\mu M/L^{-1}$ (195 ppb)	0.823 %	(Cengiz and Durak 2019)
Sucrose	HPLC-RI optimized method	3.21 $\mu M/mL^{-1}$ (3210 ppb)	4.01 %	(Filip, Vlassa et al. 2016)
Sucrose	Conductance	83 ppb (~83 ppb- 520 ppm)	1.5 % (97.8 % RSR)	Present work
Sucrose	Conductance	68 ppb (~68 ppb to 525 ppm)	1.42 % (98 % RSR)	Present work
Sucrose	Conductance	39 ppb (~39 ppb to 520 ppm)	0.75 % (99 % RSR)	Present work

Sucrose	Conductance	31 ppb (~31 ppb to 528 ppm)	0.48 % (99 % RSR)	Present work
Sucrose	Conductance	16 ppb (~16ppb to 600 ppm)	0.42 %	Present work

5.5 Conclusion

In this chapter, molecularly imprinted polymer based sensor receptors for the detection of sucrose were synthesized by using four monomers i.e. styrene, n-vinylpyrolidone, methacrylic acid and 4, 4′-diisocyanatodiphenylmethane. MIPs synthesis procedures were optimized and receptors were characterized by FTIR, SEM and TGAs. Various sensor parameters like sensitivity, linearity, selectivity, reproducibility, limit of detection, stability and response time of fabricated sensors were investigated by exposing them to different concentrations of its template molecule and competing molecules. Imprinted polystyrene based sensor has lower limit of detection of ~83 ppb of sucrose and imprinted n-vinyl pyrolidone based sucrose sensor showed lower limit of detection of ~68 ppb towards sucrose. While imprinted polyacrylate based sensor showed a lower limit of detection of ~39 ppb of sucrose and imprinted polyurethane based sensor bears a lowest limit of detection of ~31 ppb of sucrose. Overall, sensitivity and selectivity of imprinted polymers were in the following order: styrene < n-vinylpyrolidone < methacrylic acid < polyurethane. Furthermore, the sensitivity, selectivity and other sensor parameters improved by using functionalized graphene-MIPs (GO-MIPs) nanocomposite as sensor receptors. The composite based sensor showed higher sensitivity and selectivity and improved lower limit of detection of 16 ppb towards sucrose. The GO-MIPs sensor may have potential technological applications for the detection of sucrose in pharmaceutical industry, food industry and in other relevant fields. The topographical studies of urethane system based sucrose imprinted sensors depicts the uniform generation of template identical cavities as compared to other polymers.

6 CONCLUSION AND FUTURE ASPECTS

For mono and disaccharides detection, MIPs and composites have been synthesized by using different polymer systems (n-vinylpyrolidone, styrene, urethane and acrylate systems) by employing the optimized ratio between monomer and cross-linker. For glucose detection, sensitivity and selectivity of imprinted polymer was in the following order; n-Vinylpyrolidone < Acrylate < Urethane < Styrene < Sty-GO-MIPs composite. We can conclude that nanocomposite of functionalized graphene styrene based glucose sensor is most suitable for the imprinting of glucose and bears high sensitivity and selectivity. For fructose detection, sensitivity and selectivity of imprinted polymer was in the following order; n-Vinylpyrolidone < Urethane < Styrene < Acrylate < Acrylate-GO-MIPs composite. It is found from the results that GO-methacrylate nanocomposite based fructose sensor is the most suitable for the imprinting of fructose. Sensitivity and selectivity of maltose imprinted polymers were in the following order: Styrene < Polyurethane < n-Vinylpyrolidone < Methacrylic acid < Methacrylate-GO-MIPs composite. We can say that graphene oxide methacrylate nanocomposite based maltose sensor is the best option for the detection of maltose. Sensor response of sucrose imprinted sensors was in the following order: Styrene <n-Vinylpyrolidone < Methacrylic acid <Polyurethane <Polyurethane-GO-MIPs composite. On the basis of above mentioned results, we can say that GO-MIP nanocomposite sucrose sensor showed excellent sensor response towards sucrose. The GO-MIPs sensor may have potential technological applications for the detection of sucrose in pharmaceutical industry, food industry and in other relevant fields. The sensor response of a fabricated might be increased by using nanomaterial; Noble-metal nanoparticles i.e. Silver (Ag), gold (Au), Platinum (Pt), Rhudenium (Rh), Rhodium (Rd), Ruthenium (Ru), Iridium (Ir) and Palladium (Pd), metal oxide nanoparticles (CeO_2, CuO, ZnO, TiO_2, and MnO_2), Electroactive nanocomposites (Au NP/rGo, Ni NPs@MWCNTs, Gr-AuNPMnO_2-MWCNTs, Gr-Au NP-C-dots) for the modification of receptors. Different electrodes i.e. (GE, CE, GCE, QCM) and Magnetic electrode could also use to improve the sensor signals.

7 REFERENCES

Afzal, A., Feroz, S., Iqbal. N., Mujahid A., and Rehman, A., (2016). A collaborative effect imprinted polymers and Au nanoparticles on bioanalogous detection of organic vapours. Sensors and Actuators B: Chemical, 231, 431-439.

Alev-Tuzuner, B., Beyler-Cigil, A., Vezir Kahraman, M., and Yarat, A., (2018). PEG-based hydrogel-coated test strip for on-site urea determination. International Journal of Polymeric Materials and Polymeric Biomaterials, 5, 1-10.

Alexander, S., Baraneedharan. P., Balasubrahmanyan, S., and Ramaprabhu, S., (2017). Highly sensitive and selective non enzymatic electrochemical glucose sensors based on Graphene Oxide-Molecular Imprinted Polymer. Materials Science and Engineering, 78, 124-129.

Alexander, S., Baraneedharan, P., Balasubrahmanyan. S., and Ramaprabhu, S., (2017). Modified graphene based molecular imprinted polymer for electrochemical non-enzymatic cholesterol biosensor. European Polymer Journal, 86, 106-116.

Alexander, C., Andersson, H. S., Andersson, L. I., Ansell, Kirsch, R. J. N. I., Nicholls, A., O'Mahony, J., and Whitcombe, M. J., (2006). Molecular imprinting science and technology: a survey of the literature for the years up to and including 2003. Journal of Molecular Recognition: An Interdisciplinary Journal,19(2), 106-180.

Auriol, M., Filali-Meknassi, Y., Tyagi, R. D., Adams, C. D., and Surampalli, R. Y., (2011). Endocrine disrupting compounds removal from wastewater, a new challenge. Biochemistry, 41, 525-539.

Al-Zubaidi, A., Heldmann, M., Mertins, A., Jauch-Chara, K., and Münte, T. F., (2018). Influences of Hunger, Satiety and Oral Glucose on Functional Brain Connectivity: A Multimethod Resting-State fMRI Study. Neuroscience, 382, 80-92.

Alijanpour, S., Akhoondi, R., and Chaichi, M., (2017). 1-Ethyl-3-methylimidazolium ethylsulfate/copper (II) as catalyst for lucigenin chemiluminescence and its application to glucose detection. Journal of Analytical Chemistry, 72(1), 120-127.

Alduraywish, A., Fattah, D., Abd-Eltawab, A.A., Al-Ruwili, M., Alhassan, A., Alnafe N., and Alruwailly, F., (2017). Depression and Anxiety and Their Correlates in Patients with Diabetes Mellitus in Al-Jouf Region, Saudi Arabia. Clinical Medicine and Diagnostics. 7(2), 48-56.

Anunciacao, P. C., Morais Cardoso, L. de., Queiroz, V. A. V., Menezes, C. B. de., Carvalho, C. W. P. de., Pinheiro-Sant'Ana, H. M., and Alfenas, R. d. C. G., (2018). Consumption of a drink containing extruded sorghum reduces glycaemic response of the subsequent meal. European Journal of Nutrition, 57(1), 251-257.

Bajwa, S. Z., Mustafa, G., Samardzic, R., Wangchareansak, T., and Lieberzeit, P. A., (2012). Nanostructured materials with biomimetic recognition abilities for chemical sensing. Nanoscale Research Letters, 7(1), 1-7.

Behera, M., Rai, M., Mishra, P., Bhaduaria, D., Yadav, V., Agarwal, R., Karoli, N., Prasad, A., Gupta, S., and Sharma, R., (2018). Neutrophil Gelatinase-associated Lipocalin: As a Predictor of Early Diabetic Nephropathy in Type 2 Diabetes Mellitus.

Boobphahom, S., Rattanawaleedirojn, P., Boonyongmaneerat, Y., Rengpipat, S., Chailapakul, O., Rodthongkum, N., (2019). TiO_2 sol/graphene modified 3D porous Ni foam: A novel platform for enzymatic electrochemical biosensor. Journal of Sensors, 2, 23-30.

Bagheri, H., Pajooheshpour, N., Afkhami, A., and Khoshsafar, H., (2016). Fabrication of a novel electrochemical sensing platform based on a core-shell nano-structured/molecularly imprinted polymer for sensitive and selective determination of ephedrine. RSC Advances, 6(56), 51135-51145.

Braga, G. S., Lieberzeit, P. A., and Fonseca, F. J., (2017). Selective chemical sensor based on molecularly imprinted polymer to detect isoborneol in aqueous samples. Olfaction and Electronic Nose (ISOEN), 2017 ISOCS/IEEE International Symposium on, IEEE. 1-3.

Babu, K., Sheet, S., Lee, Y. S., and Kumar, G. G., (2018). Three-Dimensional Dendrite Cu-Co/Reduced Graphene Oxide Architectures on a Disposable Pencil Graphite

Electrode as an Electrochemical Sensor for Nonenzymatic Glucose Detection. Acs Sustainable Chemistry and Engineering, 6(2), 1909-1918.

Bangen, K. J., Werhane, M. L., Weigand, A. J., Edmonds, E. C., Delano-Wood, L., Thomas, K. R., Nation, D. A., Evangelista, N. D., Clark, A. L.,and Liu, T. T., (2018). Reduced regional cerebral blood flow relates to poorer cognition in older adults with type 2 diabetes. Frontiers in Aging Neuroscience, 10, 10-17.

Bennett, J., and Forster, T., (2009). IR Cards: Inquiry-Based Introduction to Infrared Spectroscopy. Journal of Chemical Education, 87(1), 73-77.

Berg, J. M., Stryer, L., and Tymoczko, J. L., (2015). Stryer Biochemie, Springer-Verlag.

Bossi, A., Bonini, F., Turner, A., and Piletsky, S., (2007). Molecularly imprinted polymers for the recognition of proteins: the state of the art. Biosensors and Bioelectronics, 22(6), 1131-1137.

Branger, C., Meouche, W. and Margaillan, A., (2013). Recent advances on ion-imprinted polymers. Reactive and Functional Polymers, 73(6), 859-875.

Barman, S. C., Hossain, M. F., and Park, J. Y., (2018). Soft surfactant-assisted uniformly dispersed platinum nanoparticles for high performance electrochemical non-enzymatic glucose sensing platform. Journal of Electroanalytical Chemistry, 824, 121-127.

Basabe-Desmonts, L., Reinhoudt, D. N., and Crego-Calama, M., (2007). Design of fluorescent materials for chemical sensing. Chemical Society Reviews, 36(6), 993-1017.

Bennett, J., Forster, T., and Cards, I. R. (2009). Inquiry-based introduction to infrared spectroscopy. Chemical Education, 87, 73-77.

Carvalho, C. T., Souza, Z. M., Arbex, N., Sa, D., de Sa, D. A. R., de Sa, L. B. P. C., and Arbex, A. K., (2018). The Role of Fructose in Public Health and Obesity. Health, 10(04), 434-441.

Coelho, M. K. L., Giarola, J. d. F.A., da Silva, T. M., Tarley, C. R. T., Borges, K. B., and Pereira, A. C., (2016). Development and Application of Electrochemical Sensor Based on Molecularly Imprinted Polymer and Carbon Nanotubes for the Determination of Carvedilol. Chemosensors, 4(4), 133-142.

Castedal, M., Skoglund, C., Axelson, C., and Bennet, W., (2018). Steroid-free immunosuppression with low-dose tacrolimus is safe and significantly reduces the incidence of new-onset diabetes mellitus following liver transplantation. Scandinavian journal of Gastroenterology, 1-7.

Cornelis, P., Givanoudi, S., Yongabi, D., Iken, H., Duwé, S., Deschaume, O., Robbens, J., Dedecker, P., Bartic, C., Wübbenhorst, M. and Schöning, M.J., 2019. Sensitive and Specific Detection of E. Coli using Biomimetic Receptors in Combination with a Modified Heat-Transfer Method. Biosensors and Bioelectronics, 136, 97-105.

Chen, G., Shu, H., Wang, L., Bashir, K., Wang, Q., Cui, X., Li, X., Luo, Z., Chang, C. and Fu, Q., 2020. Facile One-Step Targeted Immobilization of an Enzyme based on Silane Emulsion Self-Assembled Molecularly Imprinted Polymers for Visual Sensors. Analyst, 145(1), 268-276.

Chatterjee, T. N., Das, D., Roy, R. B., Tudu, B., Sabhapondit, S., Tamuly, P., Pramanik, P., and Bandyopadhyay, R., (2018). Molecular Imprinted Polymer Based Electrode for Sensing Catechin (+ C) in Green Tea. IEEE Sensors Journal, 18(6), 2236-2244.

Cho, S. J., Noh, H-B., Won, M-S., Cho, C-H., Kim, K. B., and Shim, Y-B., (2018). A selective glucose sensor based on direct oxidation on a bimetal catalyst with a molecular imprinted polymer. Biosensors and Bioelectronics, 99, 471-478.

Chung, J. S., and Hur, S. H., (2016). A highly sensitive enzyme-free glucose sensor based on Co_3O_4 nanoflowers and 3D graphene oxide hydrogel fabricated via hydrothermal synthesis. Sensors and Actuators B: Chemical, 223, 76-82.

Cao, W. K., Wu, L. T., Zhang, C., Song, G. Y., Ke, J. C., Cheng, Q., and Cui, T. J., (2018). Acoustic surface waves on three-dimensional groove gratings with sub-wavelength thickness. Applied Physics Express, 11(8), 873-901.

Cecchini, A., Raffa, V., Canfarotta, F., Signore, G., Piletsky, S., MacDonald, M. P., and Cuschieri, A., (2017). In Vivo Recognition of Human Vascular Endothelial Growth Factor by Molecularly Imprinted Polymers. Nano Letters, 17(4), 2307-2312.

Cengiz, M. F., and Durak, M. Z., (2019). Rapid detection of sucrose adulteration in honey using Fourier transform infrared spectroscopy. Spectroscopy Letters, 1-7.

Chaiyo, S., Mehmeti, E., Siangproh, W., Hoang, T. L., Nguyen, H. P., Chailapakul O., and Kalcher, K., (2018). Non-enzymatic electrochemical detection of glucose with a disposable paper-based sensor using a cobalt phthalocyanine-ionic liquid-graphene composite. Biosensors and Bioelectronics, 102, 113-120.

Chattopadhyay, S., George, A., John J., and Sathyapalan, T., (2018). Adjustment of the GRACE score by 2-hour post-load glucose improves prediction of long-term major adverse cardiac events in acute coronary syndrome in patients without known diabetes. European Heart Journal. 23-35

Chen, L., Wang, X., Lu, W., Wu, X., and Li, J., (2016). Molecular imprinting: perspectives and applications. Chemical Society Reviews, 45(8), 2137-2211.

Chen, T-L., Lo, Y-L., Liao C-C., and Phan Q-H., (2018). Noninvasive measurement of glucose concentration on human fingertip by optical coherence tomography. Journal of biomedical optics, 23(4), 47-51.

Chen, T-L., Lo, Y-L., and Phan, Q-H., (2018). Non-invasive glucose monitoring based on optical coherence tomography. Biomedical Imaging and Sensing Conference, International Society for Optics and Photonics. 107, 1-12.

Cheong, W. J., Yang, S. H., and. Ali, S., (2013). Molecular imprinted polymers for separation science: A review of reviews. Journal of Separation Science, 36(3), 609-628.

Choi, S.-H., Kozukue, N., Kim H.-J., and Friedman, M., (2016). Analysis of protein amino acids, non-protein amino acids and metabolites, dietary protein, glucose, fructose, sucrose, phenolic, and flavonoid content and antioxidative properties of potato tubers, peels, and cortexes (pulps). Journal of Food Composition and Analysis, 50, 77-78.

Chong, M. N., Jin, B., Chow, C. W., and Saint, C., (2010). Recent developments in photocatalytic water treatment technology: a review. Water Research, 44(10), 2997-3027.

Chung, J. S., and Hur, S. H., (2016). A highly sensitive enzyme-free glucose sensor based on Co_3O_4 nanoflowers and 3D graphene oxide hydrogel fabricated via hydrothermal synthesis. Sensors and Actuators B, 223, 76-82.

Chunta, S., R, Suedee., S, Singsanan., and P. A. Lieberzeit., (2019). Sensing Array based on Molecularly Imprinted Polymers for Simultaneous Assessment of Lipoproteins, Sensors and Actuators B: Chemical, 298. 1268-1272.

Ciuk, A. K., Gloe, T.-E., and Lindhorst, T. K., (2018). Carbohydrate-scaffolded thymine multimers: Scope and limitations of the allylation-hydroboration sequence. European Journal of Organic Chemistry, 48, 6971-6982.

Cote, G. L., Grunden, D. T., Malik, B. H., Pirnstill C., and Thomas, E., (2020). Dual Amplitude Modulation and Polarization Frequency Modulation as well as Compensation for Noninvasive Glucose Monitoring, Google Patents. U.S. Patent No. 10,702,197.

Dai, J., Zhou, Z., Zhao, C., Wei, X., Dai, X., Gao, L., Cao, Z., and Yan, Y., (2014). Versatile method to obtain homogeneous imprinted polymer thin film at surface of superparamagnetic nanoparticles for tetracycline binding. Industrial and Engineering Chemistry Research, 53(17), 7157-7166.

Dhara, K., Ramachandran, T., Nair, B. G., and Babu, T. S., (2016). Au nanoparticles decorated reduced graphene oxide for the fabrication of disposable nonenzymatic hydrogen peroxide sensor. Electroanalytical Chemistry, 764, 64-70.

Dhara, K., and Mahapatra, D. R., (2018). Electrochemical nonenzymatic sensing of glucose using advanced nanomaterials. Microchimica Acta, 185(1), 49-55.

Devkota, J., Ohodnicki, P. R., and Greve, D. W., (2017). SAW sensors for chemical vapors and gases. Sensors, 17(4), 801.

De Souza Costa, J. B., N. T. de Paula, P. A. da Silva, G. C. de Souza, A. P. S. Paim and Lavorante, A. F., (2019). A spectrophotometric procedure for sialic acid determination

in milk employing a flow-batch analysis system with direct heating. Microchemical Journal. 147, 782-788.

Da Silva, M. S., Viveiros, R., Bonifácio, V., Aguiar-Ricardo, A., and Casimiro, T., (2011). Novel semi-covalent synthesis of molecularly imprinted polymersin $SCCO_2$: MIP-supported hybrid membranes for sepsration based on molecular recognition Semant. Sech, 1-8.

G., Dimitriadis, P., Mitrou, V., Lambadiari, E., Maratou, and Raptis, S. A., (2011). Insulin effects in muscle and adipose tissue. Diabetes Research and Clinical Practice, 93, 52-59.

Dorkó, Z., Nagy-Szakolczai, A., Tóth, B., and Horvai, G., (2018). The Selectivity of Polymers Imprinted with Amines. Molecules, 23(6), 1298- 1307.

Dvorackova, E., Snoblova, M., and Hrdlicka, P., (2014). Carbohydrate analysis: From sample preparation to HPLC on different stationary phases coupled with evaporative light-scattering detection. Journal of Separation Science, 37(4), 323-337.

Dai, H., Cao, P., Chen, D., Li, Y., Wang, N., Ma, H., and Lin, M., (2018). Ni-Co-S/PPy core-shell nanohybrid on nickel foam as a non-enzymatic electrochemical glucose sensor. Synthetic Metals, 235, 97-102.

Dash, R. P., Babu, R. J., and Srinivas, N. R., (2018). Reappraisal and perspectives of clinical drug–drug interaction potential of α-glucosidase inhibitors such as acarbose, voglibose and miglitol in the treatment of type 2 diabetes mellitus. Xenobiotica, 48(1), 89-108.

Emran, M. Y., Khalifa, H., Gomaa, H., Shenashen, M. A., Akhtar, N., Mekawy, M., Faheem, A., and El-Safty, S. A., (2017). Hierarchical CN doped NiO with dual-head echinop flowers for ultrasensitive monitoring of epinephrine in human blood serum. Microchimica Acta, 184(11), 4553-4562.

Emelyanova, E. V., (2019). Biosensor for maltose quantification and estimation of maltase activity. Advances in Biochips, 1(1), 2-11.

Emran, M. Y., Shenashen, M. A., Morita, H., and El-Safty, S. A., (2018). 3D-Ridge Stocked Layers of Nitrogen-Doped Mesoporous Carbon Nanosheets for Ultrasensitive

Monitoring of Dopamine Released from PC12 Cells under K^+ Stimulation. Advanced Healthcare Materials, 17, 44-59.

Emran, M. Y., Mekawy, M. , Akhtar, N., Shenashen, M. A EL-Sewify, ., I. M., Faheem, A., and El-Safty, S. A., (2018). Broccoli-shaped biosensor hierarchy for electrochemical screening of noradrenaline in living cells. Biosensors and Bioelectronics, 100, 122-131.

Ertürk, G. and B. Mattiasson (2017). Molecular imprinting techniques used for the preparation of biosensors. Sensors, 17(2), 288-293.

Emir Diltemiz, S., Kecili, R., Ersoz, A., and Say, R., (2017). Molecular imprinting technology in quartz crystal microbalance (QCM) sensors. Sensors, 17(3), 454-461.

Elshaarawy, F. S., Mina, S. A., Gabr, N. M., Abdelkhalik, S. M., Kamel, R., Ibrahim, H. A., and Haggag, E. G., (2018). HPLC Investigation of Carbohydrates and Phenolic Constituents of Livistona decipiens and Livistona australis Leaves and Assessment of their Protective Activity against Ulcerative Colitis. Journal of Advanced Pharmaceutical Research, 2(3), 201-211.

Ensafi, A. A., Nasr-Esfahani, P., and Rezaei, B., (2018). Synthesis of molecularly imprinted polymer on carbon quantum dots as an optical sensor for selective fluorescent determination of promethazine hydrochloride. Sensors and Actuators B: Chemical, 257, 889-896.

Eersels, K., Dilien, H., Lowdon, J., Steen Redeker, E., Rogosic, R., Heidt, B., Peeters, M., Cornelis, P., Lux, P., Reutelingsperger, C., and Schurgers, L., 2018. A Novel Biomimetic Tool for Assessing Vitamin K Status Based on Molecularly Imprinted Polymers. Nutrients, 10(6), 751-763.

Falco, B., and Lanzotti, V., (2018). NMR spectroscopy and mass spectrometry in metabolomics analysis of Salvia. Phytochemistry Reviews, 17(5), 951-972.

Foltynski, P., Ladyzynski, P., Pankowska E., and Mazurczak, K., (2018). Efficacy of automatic bolus calculator with automatic speech recognition in patients with type 1 diabetes: A randomized cross-over trial. Journal of diabetes, 10(7), 600-608.

Farid, M. M., Goudini, L., Piri, F., Zamani, A., and Saadati, F., (2016). Molecular imprinting method for fabricating novel glucose sensor: Polyvinyl acetate electrode reinforced by MnO_2/CuO loaded on graphene oxide nanoparticles. Food Chemistry, 194, 61-67.

Feng, H., Huang, Z., Lou, X., Li J., and Hui, G., (2017). Study of a sucrose sensor by functional Cu foam material and its applications in commercial beverages. Food Analytical Methods, 10(2), 407-418.

Fareed, M., Salam, N., Khoja, A. T., Abdulrahman, M., and Ahamed, M., (2017). Life Style Related Risk Factors of Type 2 Diabetes Mellitus and Its Increased Prevalence in Saudi Arabia: A Brief Review. Health Sciences, 6(3), 125-132.

Fernández-Cori, R., Gomero, J. C. M., Huayhuas-Chipana, B. C., Sotomayor, M. d. P. T., and Montoya, J. G. R., (2015). Nanostructured Sensors for Determination of 3-(3, 4-Dichlorophenyl)-1, 1-Dimethylurea Based in Molecularly Imprinted Polymers (MIPs) Deposited in Screen Printed Carbon Nanotubes. ECS Transactions, 66(37), 33-41.

Filip, M., Vlassa, M., Coman, V., and Halmagyi, A., (2016). Simultaneous determination of glucose, fructose, sucrose and sorbitol in the leaf and fruit peel of different apple cultivars by the HPLC-RI optimized method. Food Chemistry, 199, 653-659.

Fraden, J. (2016). Chemical and Biological Sensors. Handbook of Modern Sensors, Springer: 645-697.

Frasco, M. F., Truta, L. A., Sales, M. G. F., and Moreira, F. T., (2017). Imprinting technology in electrochemical biomimetic sensors. Sensors 17(3), 523.

García, J. M., Pablos, J. L., García, F. C., and Serna F., (2016). Sensory polymers for detecting explosives and chemical warfare agents. Industrial Applications for Intelligent Polymers and Coatings, Springer, 553-576.

Gui, R., Jin, H., Guo, H., and Wang, Z. (2018). Recent advances and future prospects in molecularly imprinted polymers-based electrochemical biosensors. Biosensors and Bioelectronics, 100, 56-70.

Gaddes, D., Reeves, W. B., and Tadigadapa, S., (2017). Calorimetric biosensing system for quantification of urinary creatinine. ACS Sensors, 2(6), 796-802.

Griffin, T., Wall, D., Browne, G., Dennedy, M., and O'Shea, P., (2018). Associations between glycaemic control and activation of the renin-angiotensin-aldosterone system in participants with type 2 diabetes mellitus and hypertension. Annals of Clinical Biochemistry, 55(3), 373-384.

Gaddes, D. E., Demirel, M. C., Reeves, W. B., and Tadigadapa, S., (2015). Remote calorimetric detection of urea via flow injection analysis. Analyst, 140(23), 8033-8040.

He, G., Tian, L., Cai, Y., Wu, S., Su, Y., Yan, H., Pu, W., Zhang J., and Li, L., (2018). Sensitive nonenzymatic electrochemical glucose detection based on hollow porous NiO. Nanoscale Research Letters, 13(1), 3-14.

Haupt, K., and Mosbach, K., (2000). Molecularly imprinted polymers and their use in biomimetic sensors. Chemical Reviews, 100(7), 2495-2504.

Ho, P. M., Rumsfeld, J. S., Masoudi, F. A., McClure, D. L., Plomondon, M. E., Steiner, J. F. and Magid, D. J., (2006). Effect of medication nonadherence on hospitalization and mortality among patients with diabetes mellitus. Archives of Internal Medicine, 166(17), 1836-1841.

Huang, D., Guo, X., Peng, Z., Zeng, G., Xu, P., Gong, X., Deng, R., Xue, W., Wang, R., and Yi, H., (2018). White rot fungi and advanced combined biotechnology with nanomaterials: promising tools for endocrine-disrupting compounds biotransformation. Critical Reviews in Biotechnology, 38(5), 671-689.

Huang, D., Jiang, Q. S., Yang, J. Q., Cui, T., Wang, N. R., Du T. T., and Jiang, X. H., (2018). Simultaneous determination of nine analytes related to the pathogenesis of diabetic encephalopathy in diabetic rat cortex and hippocampus by HPLC-FLD. Biomedical Chromatography, 38-43.

Head, L., Klocker, N., and Aguirre-Bielschowsky, I., (2018). Environmental values, knowledge and behaviour: Contributions of an emergent literature on the role of ethnicity and migration. Progress in Human Geography, 43(3, 397-415.

Head, L. M., Farbotko, C., Gibson, C. R., Gill, N. J., and Waitt G. R., (2013). Environmental issues and household sustainability in Australia, 34, 211- 228.

Herrera, M., Segura, A., Sanchez, A., Sanchez, A., Vargas, M., Villalta, M., Harrison, R. A., Gutierrez, J., and Leon, G., (2017). Freeze-dried EchiTAb+ ICP antivenom formulated with sucrose is more resistant to thermal stress than the liquid formulation stabilized with sorbitol. Toxicon, 133, 123-126.

Hou, J., Li, H., Wang, L., Zhang, P., Zhou, T., Ding H., and Ding, L., (2016). Rapid microwave-assisted synthesis of molecularly imprinted polymers on carbon quantum dots for fluorescent sensing of tetracycline in milk. Talanta, 146, 34-40.

Hu, Y., Feng, S., Gao, F., Li-Chan, E. C., Grant, E., and Lu, X., (2015). Detection of melamine in milk using molecularly imprinted polymers-surface enhanced Raman spectroscopy. Food Chemistry, 176, 123-129.

Iacovazzo, D., Flanagan, S. E., Walker, E., Quezado, R., de Sousa Barros, F. A., Caswell, R., Johnson, M. B., Wakeling, M., Brandle M., and Guo, M., (2018). MAFA missense mutation causes familial insulinomatosis and diabetes mellitus. Proceedings of the National Academy of Sciences, 201-226.

Isaac, I. C., Wootton, S. A., Johnson, T. J., Baldwin, E. L., Gu, L., Karki, B., Williams, A., Halfmann, N. C., Zhu, H., and Vargas-Ramirez, J. M., (2017). Evaluating the efficacy of genetically engineered Escherichia coli W (ATCC 9637) to produce limonene from industrial sugar beets (Beta vulgaris L.). Industrial Crops and Products, 108, 248-256.

Iacob, B.-C., Bodoki, A. E., Oprean, L., and Bodoki, E., (2018). Metal-Ligand Interactions in Molecular Imprinting, 1, 11-23.

Jia, X., Tan, H., and Zhu, J., (2017). Responsive Photonic Crystals with Tunable Structural Color. Polymer-Engineered Nanostructures for Advanced Energy Applications, Springer, 151-172.

Joo, S., and Brown, R. B., (2008). Chemical sensors with integrated electronics. Chemical Reviews, 108, 638-643.

Kong, L-J., Pan, M-F., Fang, G-Z., Qian, K., and Wang, S., (2012). An electrochemical sensor for rapid determination of ractopamine based on a molecularly imprinted electrosynthesized o-aminothiophenol film. Analytical and Bioanalytical Chemistry, 404(6-7), 1653-1660.

Kirchert, S., and Morlock, G. E., (2018). Simultaneous determination of mono-, di-, oligo-and polysaccharides via planar chromatography in 4 different prebiotic foods and 60 naturally degraded insulin samples. Journal of Chromatography A, 1569, 212-221.

Kubo, T., Tachibana, K., Naito, T., Mukai, S., Akiyoshi, K., Balachandran, J., and Otsuka, K., (2018). Magnetic Field Stimuli-Sensitive Drug Release Using a Magnetic Thermal Seed Coated with Thermal-Responsive Molecularly Imprinted Polymer. ACS Biomaterials Science and Engineering, 5(2), 759-767.

Karst, S. G., Lammer, J., Radwan, S. H., Kwak, H., Silva, P. S., Burns, S. A., Aiello, L. P., and Sun, J. K. (2018). Characterization of In Vivo Retinal Lesions of Diabetic Retinopathy Using Adaptive Optics Scanning Laser Ophthalmoscopy. International Journal of Endocrinology, 20, 431-438.

Kajisa, T., Li, W., Michinobu, T., and Sakata, T., (2018). Well-designed dopamine-imprinted polymer interface for selective and quantitative dopamine detection among catecholamines using a potentiometric biosensor. Biosensors and Bioelectronics, 117, 810-817.

Kim, J., Yoo, H.-W., Kim, M., Kim, E.-J., Sung, C., Lee, P.-G., Park B. G., and Kim, B.G., (2018). Rewiring FadR regulon for the selective production of ω-hydroxy palmitic acid from glucose in Escherichia coli. Metabolic Engineering, 47,414-422.

Kryscio, D. R. and Peppas, N. A., (2012). Critical review and perspective of macromolecularly imprinted polymers. Acta Biomaterialia, 8(2), 461-473.

Latif, U., Najafi, B., Glanznig G., and Dickert, F. L., (2013). Quality assessment of automotive fuel and oil-improving environmental sustainability. Sensors and Actuators B: Chemical, 188, 584-589.

Leotério, D. M., Silva, P. A., Souza, G. C., Alves, A. d. A., Belian, M. F., Galembeck, A., and Lavorante A. F., (2015). Copper-4, 4′-dipyridyl coordination compound as solid

reagent for spectrophotometric determination of reducing sugar employing a multicommutation approach. Food Control, 57, 225-231.

Lee, Y. Y., Shibamoto, T., Ha, S. D., Ha, J., Lee, J., and Jang, H. W., (2019). Determination of glyoxal, methylglyoxal, and diacetyl in red ginseng products using dispersive liquid-liquid microextraction coupled with GC-MS. Journal of Separation Science. 42(6), 1230-1239.

Li, J., Chen, J., and Wang, S., (2011). In Risk Management of Supply and Cash Flows in Supply Chains, 1-48. Springer New York, 2, 45-60.

Liu, W., Ding, F., Wang, Y., Mao, L., Liang, R., Zou, P., Wang, X., Zhao, Q., and Rao, H., (2018). Fluorometric and colorimetric sensor array for discrimination of glucose using enzymatic-triggered dual-signal system consisting of Au@Ag nanoparticles and carbon nanodots. Sensors and Actuators B: Chemical, 265, 310-317.

Liu, W., Guo, Y., Luo, J., Kou, J., Zheng, H., Li, B., and Zhang, Z., (2015). A molecularly imprinted polymer based a lab-on-paper chemiluminescence device for the detection of dichlorvos. Spectrochimica Acta Part A: Molecular and Biomolecular Spectroscopy, 141, 51-57.

Liu, F., He, J., Zeng, M., Hao, J., Guo, Q., Song Y., and Wang, L., (2016). Cu–hemin metal-organic frameworks with peroxidase-like activity as peroxidase mimics for colorimetric sensing of glucose. Journal of Nanoparticle Research, 18(5), 106.

Liao, S.-H., Lu, S.-Y., Bao, S.-J., Yu Y.-N., and Wang, M-Q. (2016). $NiMoO_4$ nanofibres designed by electrospining technique for glucose electrocatalytic oxidation. Analytica Chimica Acta, 905, 72-78.

Li, R., Liu, X., Wang, H., Wu, Y., and Lu, Z., (2018). High-performance hybrid electrode decorated by well-aligned nanograss arrays for glucose sensing. Biosensors and Bioelectronics, 102, 288-295.

Lian, W., Liu, S., Yu, J., Xing, X., Li, J., Cui, M., and Huang, J., (2012). Electrochemical sensor based on gold nanoparticles fabricated molecularly imprinted polymer film at chitosan-platinum nanoparticles/graphene-gold nanoparticles double

nanocomposites modified electrode for detection of erythromycin. Biosensors and Bioelectronics, 38(1), 163-169.

Liang, S., Dai, Y., Helden, L., Schwarzkopf, J., and Wordenweber, R., (2018). Surface acoustic waves in strain-engineered K0. 7Na0. $3NbO_3$ thin films." Applied Physics Letters, 113(5), 52-60.

Lin, S., Feng, W., Miao, X., Zhang, X., Chen, S., Chen, Y., Wang, W., and Zhang Y., (2018). A flexible and highly sensitive nonenzymatic glucose sensor based on DVD-laser scribed graphene substrate. Biosensors and Bioelectronics, 110, 89-96.

Ling, W., Liew, G., Li, Y., Hao, Y., Pan, H., Wang, H., Ning, B., Xu, H., and Huang, X., (2018). Implantable Flexible Electronics: Materials and Techniques for Implantable Nutrient Sensing Using Flexible Sensors Integrated with Metal-Organic Frameworks (Adv. Mater. 23/2018). Advanced Materials, 30(23), 166-187.

Liu, J., Qian, T., Wang, M., Liu, X., Xu, N., You, Y., and Yan, C., (2017). Molecularly imprinted polymer enables high-efficiency recognition and trapping lithium polysulfides for stable lithium sulfur battery. Nano Letters, 17(8), 5064-5070.

Liu, T., M. Li, P. Dong, Y. Zhang and Guo, L., (2018). Design and facile synthesis of mesoporous cobalt nitride nanosheets modified by pyrolytic carbon for the nonenzymatic glucose detection. Sensors and Actuators B: Chemical 255: 1983-1994.

Liu, W-C., Lo Y-L., and Phan Q-H., (2018). Circular birefringence/dichroism measurement of optical scattering samples using amplitude-modulation polarimetry. Optics and Lasers in Engineering, 102, 45-51.

Li, H., Zhao, L., Xu, Y., Zhou, T., Liu, H., Huang, N., Ding, J., Li, Y., and Ding, L., (2018). Single-hole hollow molecularly imprinted polymer embedded carbon dot for fast detection of tetracycline in honey. Talanta, 185, 542-549.

Li, S., Wu, Q., Yin, F., Zhu, Z., He, J., and Barba, F. J., (2018). Development of a Combined Trifluoroacetic Acid Hydrolysis and HPLC-ELSD Method to Identify and Quantify Inulin Recovered from Jerusalem artichoke Assisted by Ultrasound Extraction. Applied Sciences, 8(5), 122-128.

Long, T., and Phong, H., (2018). Non-enzymatic electrochemical detection of glucose with a disposable paper-based sensor using a cobalt phthalocyanineâ ionic liquida graphene composite. Biosensors and Bioelectronics. 102, 113-120.

Martin, P. E., Shaughnessy, E. M. O, Wright, C. S., and Graham, A., (2018). The potential of human induced pluripotent stem cells for modelling diabetic wound healing in vitro. Clinical Science, 132(15), 1629-1643.

Malik, M. I., Shaikh, H., Mustafa, G., and Bhanger, M. I., (2018). Recent Applications of Molecularly Imprinted Polymers in Analytical Chemistry. Separation and Purification Reviews, 1-41.

Meng, H.B., Zhang, X.F., Pu, Y.L., Chen, X.L., Feng, J.J., Han, D.M. and Wang, A.J., 2019. One-pot Solvothermal Synthesis of Reduced Graphene Oxide-Supported Uniform PtCo Nanocrystals for Efficient and Robust Electrocatalysis. Journal of Colloid and Interface Science, 543, 17-24.

Marques, W. L., Mans, R., Marella, E. R., Cordeiro, R. L., Broek, M. van den, Daran, J.-M. G., Pronk, J. T., Gombert A. K., and van Maris, A. J., (2017). Elimination of sucrose transport and hydrolysis in Saccharomyces cerevisiae: a platform strain for engineering sucrose metabolism. FEMS Yeast Research, 17(1).

Maruo, S., Mori, K., Motoyama, K., Nakamura, M., Kawarabayashi, R., Kakutani, Y., Yamazaki, Y., Morioka, T., Shoji, T., and Inaba, M., (2018). Correlation analysis of monocyte subsets and insulin resistance considering fetuin-A involvement in patients with type 2 diabetes. Clinical and Translational Medicine, 7(1), 9.

Meier, F., Schott, B., Riedel, D., and Mizaikoff, B., (2012). Computational and experimental study on the influence of the porogen on the selectivity of 4-nitrophenol molecularly imprinted polymers. Analytica Chimica Acta, 744, 68-74.

Meng, W., Wen, Y., Dai, L., He, Z., and Wang, L., (2018). A novel electrochemical sensor for glucose detection based on Ag@ ZIF-67 nanocomposite. Sensors and Actuators B Chemical, 260, 852-860.

Micha, R., Shulkin, M. L., Penalvo, J. L., Khatibzadeh, S., Singh, G. M., Rao, M., Fahimi, S., Powles, J., and Mozaffarian, D., (2017). Etiologic effects and optimal

intakes of foods and nutrients for risk of cardiovascular diseases and diabetes: Systematic reviews and meta-analyses from the Nutrition and Chronic Diseases Expert Group (NutriCoDE). PLoS One, 12(4), 149-175.

Mielgo-Ayuso, J., Valtuena, J., Huybrechts, I., Breidenassel, C., Cuenca-Garcia, M., De Henauw, S., Stehle, P., Kafatos, A., Kersting, M., and Widhalm, K., (2017). Fruit and vegetables consumption is associated with higher vitamin intake and blood vitamin status among European adolescents. European Journal of Clinical Nutrition, 71(4), 458-467.

Munoz, M., Valdes, M., Munoz-Quezada, M., Lucero, B., Rubilar, P., Pino, P., and Iglesias, V., (2018). Urinary Inorganic Arsenic Concentration and Gestational Diabetes Mellitus in Pregnant Women from Arica, Chile. International Journal Of Environmental Research And Public Health, 15(7), 14-18.

Muhammad, P., Liu, J., Xing, R., Wen, Y., Wang, Y., and Liu, Z., (2017). Fast probing of glucose and fructose in plant tissues via plasmonic affinity sandwich assay with molecularly-imprinted extraction microprobes. Analytica Chimica Acta, 995, 34-42.

Ma, C., Sun, Z., Chen, C., Zhang, L., and Zhu, S., (2014). Simultaneous separation and determination of fructose, sorbitol, glucose and sucrose in fruits by HPLC-ELSD. Food Chemistry, 145, 784-788

Muscogiuri, G., Balercia, G., Barrea, L., Cignarelli, A., Giorgino, F., Holst, J. J., Laudisio, D., Orio, F., Tirabassi, G., and Colao, A., (2018). Gut: a key player in the pathogenesis of type 2 diabetes? Critical Reviews in Food Science and Nutrition, 58(8),1294-1309.

Mustafa, G., Hussain, M., Iqbal, N., Dickert, F. L., and Lieberzeit, P. A., (2012). Quartz crystal microbalance sensor based on affinity interactions between organic thiols and molybdenum disulfide nanoparticles. Sensors and Actuators B: Chemical, 162(1), 63-67.

Mujahid, A., and Dickert, F. L., (2017). Surface Acoustic Wave (SAW) for Chemical Sensing Applications of Recognition Layers. Sensors, 17(12), 27-36.

Nicolae, I., Miu, D., and Viespe, C., (2018). Sub-limit detection in SAW sensors by FFT spectral analysis of frequency time instability. Sensor Review, 4, 409-421.

Nikbakht, E., Khalesi, S., Singh, I., Williams, L. T., West N. P., and Colson, N., (2018). Effect of probiotics and synbiotics on blood glucose: a systematic review and meta-analysis of controlled trials. European Journal of Nutrition, 57(1), 95-106.

Nicholas, P., Pittson, R., and Hart, J. P., (2018). Development of a simple, low cost chronoamperometric assay for fructose based on a commercial graphite-nanoparticle modified screen-printed carbon electrode. Food Chemistry, 241, 122-126.

Pan, J., Yuan, F., Yu, L., Huang, L., Fei, H., Cheng, F., and Zhang, Q., (2016). Performance of organics and nitrogen removal in subsurface wastewater infiltration systems by intermittent aeration and shunt distributing wastewater. Bioresource Technology, 211, 774-778.

Pan, L., Zhu, Q., Lu, R., and McGrath, J. M., (2015). Determination of sucrose content in sugar beet by portable visible and near-infrared spectroscopy. Food Chemistry, 167, 264-271.

Pan, J., W. Chen, Ma, Y., and Pan, G., (2018). Molecularly imprinted polymers as receptor mimics for selective cell recognition. Chemical Society Reviews. 47(13), 5574-5588.

Perumal, J., Balasundaram, G., Mahyuddin, A. P., Choolani, M., and Olivo, M., (2015). SERS-based quantitative detection of ovarian cancer prognostic factor haptoglobin. International Journal of Nanomedicine, 10, 18-31.

Perez-Lopez, E., Mateos-Aparicio, I., and Ruperez, P., (2016). Low molecular weight carbohydrates released from Okara by enzymatic treatment under high hydrostatic pressure. Innovative Food Science and Emerging Technologies, 38, 76-82.

Perreault, L., (2018). Prevention of Type 2 Diabetes. Diabetes and Exercise, Springer, 17-29.

Pollo, L., Duarte, L., Anacleto, M., Habert, A., and Borges, C., (2012). Polymeric membranes containing silver salts for propylene/propane separation. Brazilian Journal of Chemical Engineering, 29(2), 307-314.

Poonthiyil, V., Lindhorst, T. K., Golovko, V. B., and Fairbanks, A. J., (2018). Recent applications of click chemistry for the functionalization of gold nanoparticles and their conversion to glyco-gold nanoparticles. Beilstein Journal of Organic Chemistry, 14, 11-21.

Protheroe, J., Rowlands, G., Bartlam, B., and Levin-Zamir, D., (2017). Health literacy, diabetes prevention, and self-management. Journal Of Diabetes Research, 3, 23-29.

Qian, Q., Hu, Q., Li, L., Shi, P., Zhou, J., Kong, J., Zhang, X., Sun, G., and Huang, W., (2018). Sensitive fiber microelectrode made of nickel hydroxide nanosheets embedded in highly-aligned carbon nanotube scaffold for nonenzymatic glucose determination. Sensors and Actuators B: Chemical, 257, 23-28.

Ramanavicius, A., Ramanavicienė, A., and Malinauskas, A., (2013). Electrochemical sensors based on conducting polymer-polypyrrole. Electrochimica Acta, 5, 6025-6037.

Ren, Z., Liu, G., Ding Y., and Yao, Q., (2018). Effect of flow velocity on the photoacoustic detection for glucose aqueous solutions. 2017 International Conference on Optical Instruments and Technology: Optoelectronic Measurement Technology and Systems, International Society for Optics and Photonics. 21-25.

Röckendorf, N., and Lindhorst T. K., (2004). Glucuronic acid derivatives as branching units for the synthesis of glycopeptide mimetics. The Journal of Organic Chemistry, 69(13), 4441-4445.

Radwan, H., Ballout, R. A., Hasan, H., Lessan, N., Karavetian, M., and Rizk, R., (2018). The Epidemiology and Economic Burden of Obesity and Related Cardiometabolic Disorders in the United Arab Emirates: A Systematic Review and Qualitative Synthesis. Journal of Obesity, 20, 54-64.

Rush, E. C., and Yan, M. R., (2017). Evolution not revolution: nutrition and obesity. Nutrients, 9(5), 519.

Saylan, Y., Akgönüllü, S., Yavuz, H., Ünal, S., and Denizli, A. (2019). Molecularly Imprinted Polymer based Sensors for Medical Applications. Sensors, 19(6), 1279.

Sharma, D., Kaur, J., Rani, M., Bansal, A., Malik, M., and Kulandaivelan, S., (2018). Efficacy of pilates based mat exercise on quality of life, quality of sleep and satisfaction

with life in type 2 diabetes mellitus. Romanian Journal of Diabetes Nutrition and Metabolic Diseases 25(2), 149-156.

Shendurse, A. and C. Khedkar (2016). Glucose: Properties and Analysis. The encyclopedia of food and health, Academic Press Oxford, 3, 239-247.

Satoshi, F., Malcolm, L., Heron, K., Lai, J. W., Lee, S. H., Wu, X., Lucy, R., and Yang, W. C., (2013). An overview of developments and applications of oceanographic radar networks in Asia and Oceania countries. Ocean Science, 48, 69-97.

Seo, D.-H., Jung, J.-H., Kim H.-Y., and Park, C.-S., (2014). Direct and simple detection of recombinant proteins from cell lysates using differential scanning fluorimetry. Analytical Biochemistry, 444, 75-80.

Singh, R., Verma, R., Kaushik, A., Sumana, G., Sood, S., Gupta, R. K., and Malhotra, B. D., (2011). Chitosan-iron oxide nano-composite platform for mismatch-discriminating DNA hybridization for Neisseria gonorrhoeae detection causing sexually transmitted disease. Biosensors and Bioelectronics, 26(6), 2967-2974.

Souza Costa, J. B., de Paula, N. T., da Silva, P. A., de Souza, G. C., Paim, A. P. S., and Lavorante, A. F., (2019). A spectrophotometric procedure for sialic acid determination in milk employing a flow-batch analysis system with direct heating. Microchemical Journal. 147, 782-788.

Sáenz-Pérez, M., Lizundia, E., Laza, J. M., García-Barrasa, J., Vilas, J. L., and León, L. M., (2016). Methylene diphenyl diisocyanate (MDI) and toluene diisocyanate (TDI) based polyurethanes: thermal, shape-memory and mechanical behavior. RSC Advances, 6(73), 69094-69102.

Sun, S., Wang, H., Xie, J., and Su, Y., (2016). Simultaneous determination of rhamnose, xylitol, arabitol, fructose, glucose, inositol, sucrose, maltose in jujube (Zizyphus jujube Mill.) extract: comparison of HPLC–ELSD, LC–ESI–MS/MS and GC–MS. Chemistry Central Journal, 10(1), 25-37.

Shanmugavelan, P., Kim, S. Y., Kim, J. B., Kim, H. W., Cho, S. M., Kim, S. N., Kim, S. Y., Cho, Y. S., and Kim H. R., (2013). Evaluation of sugar content and composition

in commonly consumed Korean vegetables, fruits, cereals, seed plants, and leaves by HPLC-ELSD. Carbohydrate Research, 380, 112-117.

Shekarchizadeh, H., Ensafi, A. A., and Kadivar, M., (2013). Selective determination of sucrose based on electropolymerized molecularly imprinted polymer modified multiwall carbon nanotubes/glassy carbon electrode. Materials Science and Engineering: C, 33(6), 3553-3561.

Sobrino-Gregorio, L., Vargas, M., Chiralt, A., and Escriche, I., (2017). Thermal properties of honey as affected by the addition of sugar syrup. Journal of Food Engineering. 213, 69-75.

Saraf, M., Natarajan, K., and Mobin, S. M., (2018). Emerging Robust Heterostructure of MoS_2-rGO for High-Performance Supercapacitors. ACS Applied Materials and Interfaces. 10(19), 16588-16595.

Sharma, D., Kaur, J., Rani, M., Bansal, A., Malik, M., and Kulandaivelan, S. (2018). Efficacy Of Pilates Based Mat Exercise On Quality Of Life, Quality Of Sleep And Satisfaction With Life In Type 2 Diabetes Mellitus. Romanian Journal of Diabetes Nutrition and Metabolic Diseases, 25(2), 149-156.

Shen, W., Sun, J., Seah, J. Y. H., Shi, L., Tang, S., and Lee, H. K., (2018). Needle-based sampling coupled with colorimetric reaction catalyzed by layered double hydroxide peroxidase mimic for rapid detection of the change of d-glucose levels with time in bananas. Analytica Chimica Acta, 1001, 32-39.

Steinarsson, A. O., Rawshani, A., Gudbjörnsdottir, S., Franzén, S., Svensson, A.-M., and Sattar, N., (2018). Short-term progression of cardiometabolic risk factors in relation to age at type 2 diabetes diagnosis: a longitudinal observational study of 100,606 individuals from the Swedish National Diabetes Register. Diabetologia, 61(3), 599-606.

Shan, J., Li, J., Chu, X., Xu, M., Jin, F., Wang, X., Ma, L., Fang, X., Wei, Z., and Wang, X., (2018). High sensitivity glucose detection at extremely low concentrations using a MoS_2-based field-effect transistor. RSC Advances, 8(15), 7942-7948.

Silva, T. A., Moraes, F. C., Janegitz, B. C., and Fatibello-Filho, O., (2017). Electrochemical biosensors based on nanostructured carbon black: A review. Journal of Nanomaterials. 20, 341-352.

Silveira, P. P., Pokhvisneva, I., Gaudreau, H., Rifkin-Graboi, A., Broekman, B. F., Steiner, M., Levitan, R., Parent, C., Diorio, J., and Meaney, M. J., (2018). Birth weight and catch up growth are associated with childhood impulsivity in two independent cohorts. Scientific Reports, 8(1), 1-10.

Sojic, N., Arbault, S., Bouffier L., and Kuhn, A., (2017). Applications of electrogenerated chemiluminescence in analytical chemistry. Luminescence in Electrochemistry, Springer, 257-291.

Söylemez, M. A., and Güven, O. (2018). The Radiation synthesis of molecularly imprinted hydroxyethylmethacrylate-based matrices for glucose recognition. Hacettepe Journal of Biology and Chemistry, 46(1), 53-60.

Speltini, A., Scalabrini, A., Maraschi, F., Sturini, M., and Profumo, A., (2017). Newest applications of molecularly imprinted polymers for extraction of contaminants from environmental and food matrices: A review. Analytica Chimica Acta, 974, 1-26.

Sun, Y., Li, Y., Wang, N., Xu, Q. Q., Xu, L., and Lin, M., (2018). Copper-based Metal-organic Framework for Non-enzymatic Electrochemical Detection of Glucose. Electroanalysis, 30(3), 474-478.

Tajima, T., Nakamura, M., Tanaka, Y., and Seyama, M. (2018). Advances in Noninvasive Glucose Sensing Enabled by Photonics, Acoustics, and Microwaves. International Journal of Automation Technology, 12(1), 64-72.

Tanaka, S., Kaneti, Y. V., Bhattacharjee, R., Islam, M. N., Nakahata, R., Abdullah, N., Yusa, S.-i., Nguyen, N.-T., Shiddiky, M. J., and Yamauchi, Y., (2017). Mesoporous Iron Oxide Synthesized Using Poly (styrene-b-acrylic acid-b-ethylene glycol) Block Copolymer Micelles as Templates for Colorimetric and Electrochemical Detection of Glucose. ACS Applied Materials and Interfaces, 10(1), 1039-1049.

Tanaka, Y., Tajima, T., and Seyama, M., (2018). Differential photoacoustic spectroscopy with continuous wave lasers for non-invasive blood glucose monitoring.

Photons Plus Ultrasound: Imaging and Sensing 2018, International Society for Optics and Photonics. 45-49.

Tatulashvili, S., Patois-Vergès, B., Nguyen, A., Blonde, M. C., and Vergès, B., (2018). Detection of glucose metabolism disorders in coronary patients enrolled in cardiac rehabilitation: Is glycated haemoglobin useful? Data from the prospective REHABDIAB study. European Journal of Preventive Cardiallogy, 25(5), 464-471.

Trautwein, E. A., Koppenol, W. P., Jong, A., Hiemstra, H., Vermeer, M. A., Noakes, M., and Luscombe-Marsh, N. D. (2018). Plant sterols lower LDL-cholesterol and triglycerides in dyslipidemic individuals with or at risk of developing type 2 diabetes; a randomized, double-blind, placebo-controlled study. Nutrition and Diabetes, 8(1), 1-30.

Tuladhar, E., Sharma, V., Sigdel, M., and Shrestha, L., (2012). Type 2 diabetes mellitus with early phase acute inflammatory protein on serum protein electrophoresis." Journal of Pathology of Nepal, 2(3), 211-214.

Tang, Y., Zhang, H., and Zhang, Y., (2017). Molecularly Imprinted Polymers-based Sensing in Food Safety and Quality Analysis. Sensing Techniques for Food Safety and Quality Control, 164-199.

Thiruppathi, M., Thiyagarajan, N., Gopinathan, M., Chang J.-L., and Zen J.-M., (2017). A dually functional 4-aminophenylboronic acid dimer for voltammetric detection of hypochlorite, glucose and fructose. Microchimica Acta, 184(10), 4073-4080.

Tuck, C., Ross, L., Gibson, P., Barrett, J., and Muir, J. (2017). Adding glucose to food and solutions to enhance fructose absorption is not effective in preventing fructose-induced functional gastrointestinal symptoms: randomised controlled trials in patients with fructose malabsorption. Journal of Human Nutrition and Dietetics, 30(1), 73-82.

Vasapollo, G., Sole, R. D., Mergola, L., Lazzoi, M. R., Scardino, A., Scorrano, S., and Mele, G., (2011). Molecularly imprinted polymers: present and future prospective. Molecular Sciences, 12(9), 5908-5945.

Vijaykumar, S., Prasannkumar, S., Sherigara, B., Shelke, N., Aminabhavi, T. M., and Reddy, B. (2009). Copolymerization ofN-vinyl pyrrolidone with functionalized vinyl

monomers: Synthesis, characterization and reactivity relationships. Macromolecular Research, 17(12), 1003-1009.

Viveiros, R., Rebocho, S., and Casimiro, T., (2018). Green strategies for molecularly imprinted polymer development. Polymers, 10(3), 306- 311.

Villegas, L. R., Rivard, C. J., Hunter, B., You, Z., Roncal, C., Joy, M. S., and Le, M. T., (2018). Effects of fructose-containing sweeteners on fructose intestinal, hepatic, and oral bioavailability in dual-catheterized rats. PloS one, 13(11), 207-224.

Vargas, E., Ruiz, M., Campuzano, S., Reviejo, A., and Pingarrón, J., (2016). Non-invasive determination of glucose directly in raw fruits using a continuous flow system based on microdialysis sampling and amperometric detection at an integrated enzymatic biosensor. Analytica Chimica Acta, 914, 53-61.

Wan, E. Y. F., Fung, C. S. C., Jiao, F. F., Yu, E. Y. T., Chin, W. Y., Fong, D. Y. T., Wong, C. K. H., Chan, A. K. C., Chan, K. H. Y., and Kwok, R. L. P., (2018). Five-year effectiveness of the multidisciplinary Risk Assessment and Management Programme-Diabetes Mellitus (RAMP-DM) on diabetes-related complications and health service uses- a population-based and propensity-matched cohort study. Diabetes Care, 41(1), 49-59.

Wang, Q., Yu, L., Qi, C.-B., Ding, J., He, X.-M., Wang, R.-Q.,and Feng, Y.-Q., (2018). Rapid and sensitive serum glucose determination using chemical labeling coupled with black phosphorus-assisted laser desorption/ionization time-of-flight mass spectrometry. Talanta, 176, 344-349.

Wackerlig, J., and Schirhagl, R., (2015). Applications of molecularly imprinted polymer nanoparticles and their advances toward industrial use: a review. Analytical Chemistry, 88(1), 250-261.

Xiaohong, Z., Zhidong, Z., Xiongwei, L., Jian, L., and Guohua, H., (2017). A maltose, L-rhamnose sensor based on porous Cu foam and electrochemical amperometric it scanning method. Journal of Food Measurement and Characterization, 11(2), 548-555.

Xu, D., Gu, S., Ding, Y., and Wang, B., (2015). Synthesis and Characterization of Electrospun Nickel Doped Cobalt (II, III) Nanofibers with Application to Maltose Determination. Analytical Letters, 48(2), 269-280.

Wang, W., Chen, F., Wang, Y., Wang, L., Fu, H., Zheng, F., and Beecher, L., (2018). Optimization of reactions between reducing sugars and 1-phenyl-3-methyl-5-pyrazolone (PMP) by response surface methodology. Food Chemistry, 254, 158-164.

Wu, H., Tian, Q., Zheng, W., Jiang, Y., Xu, J., Li, X., Zhang, W., and Qiu, F., (2019). Non-enzymatic glucose sensor based on molecularly imprinted polymer: a theoretical, strategy fabrication and application. Journal of Solid State Electrochemistry, 1-10.

Wang, Q., Paim, L. L., Zhang, X., Wang, S., and Stradiotto, N. R., (2014). An Electrochemical Sensor for Reducing Sugars Based on a Glassy Carbon Electrode Modified with Electropolymerized Molecularly Imprinted Poly-o-phenylenediamine Film. Electroanalysis, 26(7), 1612-1622.

Wang, H.-C., and Lee, A.-R., (2015). Recent developments in blood glucose sensors. Journal of Food and Drug Analysis, 23(2), 191-200.

Wang, Q., Yu, L., Qi, C.-B., Ding, J., He, X.-M., Wang, R.-Q., and Feng, Y.-Q. (2018). Rapid and sensitive serum glucose determination using chemical labeling coupled with black phosphorus-assisted laser desorption/ionization time-of-flight mass spectrometry. Talanta 176, 344-349.

Whitcombe, M. J., Chianella, I., Larcombe, L., Piletsky, S. A., Noble, J., Porter, R., and Horgan, A., (2011). The rational development of molecularly imprinted polymer-based sensors for protein detection. Chemical Society Reviews, 40(3),1547-1571.

Whitcombe, M. J., Kirsch, N.,. and Nicholls, I. A., (2014). Molecular imprinting science and technology: a survey of the literature for the years 2004-2011. Journal of Molecular Recognition, 27(6), 297-401.

Wu, H., Lee, C.-J., Wang, H., Hu, Y., Young, M., Han, Y., Xu, F.-J., Cong, H., and Cheng, G., (2018). Highly sensitive and stable zwitterionic poly (sulfobetaine-3, 4-ethylenedioxythiophene) (PSBEDOT) glucose biosensor. Chemical Science 9(9), 2540-2546.

Wulff, G. (2005). The covalent and other stoichiometric approaches. Molecularly Imprinted Materials: Science and Technology, Yan, M., Ramström, O.(Eds), Marcel Dekker: New York: 59-92.

Xing, R., Wang, S., Bie, Z., He, H., and Liu, Z., (2017). Preparation of molecularly imprinted polymers specific to glycoproteins, glycans and monosaccharides via boronate affinity controllable–oriented surface imprinting. Nature Protocols 12(5): 964-971.

Xu, W. Z., Zhou, W., Bian, L. H., Huang, W. H., and Wu, X. Y., (2011). Preparation of molecularly imprinted polymer by surface imprinting technique and its performance for adsorption of dibenzothiophene. Journal of Separation Science 34(14): 1746-1753.

Xu, X., Niu, X., Wu, S., Zou, X., and Pan, J., (2018). A detachable and recyclable electrochemical sensor for high-performance detection of glucose based on boronate affinity. Sensors and Actuators B: Chemical, 268, 430-437.

Xiong, Y., Zhang, Y., Rong, P., Yang, J., Wang, W., and Liu, D., (2015). A high-throughput colorimetric assay for glucose detection based on glucose oxidase-catalyzed enlargement of gold nanoparticles. Nanoscale, 7(38),15584-15588.

Wackerlig, J. and Schirhagl, R., (2015). Applications of molecularly imprinted polymer nanoparticles and their advances toward industrial use: a review. Analytical Chemistry, 88(1), 250-261.

Xiaohong, Z., Zhidong, Z., Xiongwei, L., Jian, L., and Guohua, H., (2017). A maltose, L-rhamnose sensor based on porous Cu foam and electrochemical amperometric it scanning method. Journal of Food Measurement and Characterization, 11(2), 548-555.

Xu, D., Gu, S., Ding, Y., and Wang, B., (2015). Synthesis and Characterization of Electrospun Nickel Doped Cobalt (II, III) Nanofibers with Application to Maltose Determination. Analytical Letters, 48(2), 269-280.

Xie, F., Cao, X., Qu, F., Asiri, A. M., and Sun, X., (2018). Cobalt nitride nanowire array as an efficient electrochemical sensor for glucose and H_2O_2 detection. Sensors and Actuators B: Chemical, 255, 1254-1261.

Xing, R., Wang, S., Bie, Z., He, H., and Liu, Z., (2017). Preparation of molecularly imprinted polymers specific to glycoproteins, glycans and monosaccharides via boronate affinity controllable-oriented surface imprinting. Nature Protocols, 12(5), 964 987.

Yaiyiam, C., and Suthutvoravut, S., (2018). Screening of Diabetes Mellitus in Pregnancy by Hemoglobin A1c and Fasting Plasma Glucose at Ramathibodi Hospital. Ramathibodi Medical Journal, 41(3), 73-81.

Yarman, A. (2018). Development of a Molecularly Imprinted Polymer-based Electrochemical Sensor for Tyrosinase. Turkish Journal of Chemistry, 42(2), 346-354.

Yasinzai, M., Mustafa, G., Asghar, N., Ullah, I., Zahid, M., Lieberzeit, P. A., Han, D., and Latif, U., (2018). Ion-Imprinted Polymer-Based Receptors for Sensitive and Selective Detection of Mercury Ions in Aqueous Environment. Journal of Sensors, 3, 14-20.

Yuan, R.-m., Li, H.-j., Yin, X.-m., Wang, H.-q., Lu J.-h., and Zhang, L.-l., (2018). Coral-like Cu-Co-mixed oxide for stable electro-properties of glucose determination. Electrochimica Acta, 273, 502-510.

Yan, H., Wang, M., Han, Y., Qiao, F, and Row, K. H., (2014). Hybrid molecularly imprinted polymers synthesized with 3-aminopropyltriethoxysilane-methacrylic acid monomer for miniaturized solid-phase extraction: A new and economical sample preparation strategy for determination of acyclovir in urine. Journal of Chromatography A, 1346, 16-24.

Yang, B., Fu, C., Li, J., and Xu, G., (2018). Frontiers in highly sensitive molecularly imprinted electrochemical sensors: Challenges and strategies. TrAC Trends in Analytical Chemistry. 105, 52-67.

Yang, Q., Li, J., Wang, X., Peng, H., Xiong, H., and Chen, L., (2018). Strategies of molecular imprinting-based fluorescence sensors for chemical and biological analysis. Biosensors and Bioelectronics. 112, 54-71.

Yarman, A., Jetzschmann, K. J., Neumann, B., Zhang, X., Wollenberger, U., Cordin, A., Haupt, K., and Scheller, F. W., (2017). Enzymes as Tools in MIP-Sensors. Chemosensors, 5(2), 11.

Yılmaz, E., Garipcan, B., Patra, H. K., and Uzun, L., (2017). Molecular imprinting applications in forensic science. Sensors, 17(4), 691-701.

Zamora-Gálvez, A., Morales-Narváez, E., Mayorga-Martinez, C. C., and Merkoci, A., (2017). Applied Materials Today. 9, 387-401.

Zhang, X., Luo, J., Tang, P., Morante, J. R., Arbiol, J., Xu, C., Li, Q., and Fransaer, J., (2018). Ultrasensitive binder-free glucose sensors based on the pyrolysis of in situ grown Cu MOF. Sensors and Actuators B: Chemical, 254, 272-281.

Zheng, W., Wu, H., Jiang, Y., Xu, J., Li, X., Zhang, W., and Qiu, F., (2018). A molecularly-imprinted-electrochemical-sensor modified with nano-carbon-dots with high sensitivity and selectivity for rapid determination of glucose. Analytical Biochemistry, 555, 42-49.

Zimmermann-Schlegel, V., Wild, B., Nawroth, P., Kopf, S., Herzog, W., and Hartmann, M., (2018). Impact of Depression and Psychosocial Treatment on Heart Rate Variability in Patients with Type 2 Diabetes Mellitus: An Exploratory Analysis Based on the HEIDIS Trial. Experimental and Clinical Endocrinology and Diabetes. 127, 367-376.

Zhang, L., Ye, C., Li, X., Ding, Y., Liang, H., Zhao, G., and Wang, Y., (2018). A CuNi/C nanosheet array based on a metal–organic framework derivate as a supersensitive non-enzymatic glucose sensor. Nano-Micro Letters, 10(2), 28.

Zhang, X., Wu, Z., Liu, F., Fu, Q., Chen, X., Xu, J., Zhang, Z., Huang, Y., Tang ,Y., and Guo, T., (2018). Hydrogen peroxide and glucose concentration measurement using optical fiber grating sensors with corrodible plasmonic nanocoatings. Biomedical Optics Express, 9(4), 1735-1744.

Zhu, J., Yin, H., Gong, J., Al-Furjan, M., and Nie, Q., (2018). In situ growth of Ni/NiO on N-doped carbon spheres with excellent electrocatalytic performance for non-enzymatic glucose detection. Journal of Alloys and Compounds, 748, 145-153.

Zhu, X., Suk, H.-I., Wang, L., Lee, S.-W., Shen D., and Initiative A. s. D. N., (2017). A novel relational regularization feature selection method for joint regression and classification in AD diagnosis. Medical Image Analysis, 38, 205-214.